A dissertation submitted for the degree of Doctor of Philosophy

Towards an understanding of the role of Ca^{2+} signalling in neural stem cell activation

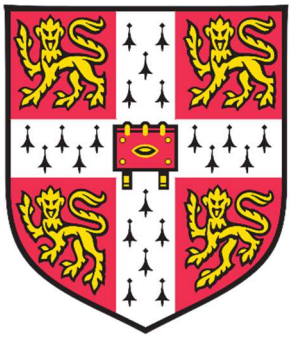

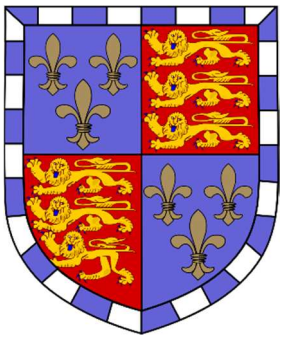

Mo Zhao

Supervisor: Professor Andrea H. Brand

--

Christ's College

University of Cambridge

Wellcome Trust / Cancer Research UK Gurdon Institute

Department of Physiology, Development and Neuroscience

September 2018

Declaration

This dissertation is the result of my own work and includes nothing which is the outcome of work done in collaboration except as declared in the Preface and specified in the text. It is not substantially the same as any that I have submitted, or, is being concurrently submitted for a degree or diploma or other qualification at the University of Cambridge or any other University or similar institution except as declared in the Preface and specified in the text. I further state that no substantial part of my dissertation has already been submitted, or, is being concurrently submitted for any such degree, diploma or other qualification at the University of Cambridge or any other University or similar institution except as declared in the Preface and specified in the text. It does not exceed the prescribed word limit for the relevant Degree Committee

Mo Zhao

Towards an understanding of the role of Ca^{2+} signalling in neural stem cell activation

Mo Zhao

PhD thesis summary

Regeneration of the adult human brain is a long time clinical challenge. The adult mammalian brain contains neural stem cells (NSCs) that are capable of brain repair, but they are mostly in a mitotically quiescent state. Identifying novel regulators of neural stem cell quiescence will provide more molecular targets for brain regeneration therapies.

Drosophila melanogaster is an excellent model for understanding NSC quiescence. The NSCs in *Drosophila* transit between quiescence and proliferation. The transcriptional profiles of quiescent and active NSCs have been determined, which reveal genes that are specifically expressed during quiescence. In this project, I analysed two quiescence-specific genes, *slowpoke* and *mulet*, in the context of NSC quiescence and activation. I also investigated if the adult *Drosophila* brain contained quiescent NSCs.

Slowpoke is the α subunit of Big-Potassium channel that is required in neurons for membrane potential repolarisation. I have shown that it is required for NSC activation. Loss of Slo in NSCs significantly extends the life span of neuroblasts, leading many of them to persist until adulthood. Slo acts largely independent of the insulin signalling pathway, a canonical pathway required for NSC activation. Since Slo is a negative regulator of Ca^{2+} signalling, I investigated Ca^{2+} levels in quiescent and active NSCs. I have found that quiescent NSCs have significantly higher intracellular Ca^{2+} compared to active NSCs. Upregulation of intracellular Ca^{2+} phenocopies loss of Slo, repressing NSC activation.

The second quiescence-specific gene I have assayed is *mulet*, a tubulin cofactor that destabilises microtubule. I have shown that in NSCs, *mulet* expresses exclusively at the quiescent stage. Loss of *mulet* results in growth defects at the whole organismal level, but does not affect NSC quiescence and activation. Therefore, *mulet* can be used as a marker for quiescent NSCs, although its function in regulating quiescence is yet unclear.

I hypothesised that astrocytes in the adult *Drosophila* brain were quiescent NSCs as some of them expressed the NSC marker, *deadpan*. In rodents, adult NSCs are astrocytes that can be triggered into proliferation by brain hyperactivation. I have found that hyperactivation of astrocytes, but not neurons, triggers cell cycle re-entry in the adult *Drosophila* brain. The cells that re-enter the cell cycle are mostly glia. However, these cells are arrested in the cell cycle and do not proceed to proliferate. Therefore, I have not found evidence that astrocytes function as NSCs in the adult *Drosophila* brain.

Acknowledgments

First I shall thank my supervisor Andrea for supporting my Ph.D study and organising a truly pleasant lab to work. I shall forever remember those inspiring discussions on science during lab meetings the retreats.

My sincere thanks also go to all the past and present members of the Brand lab, especially Dr Abhijit Das, Dr Takumi Suzuki, Dr Leo Otsuki and Dr Jelle van den Ameele, for their precious advice and encouragement. I would also like to thank our lab managers Catherine Davidson, Dr Rebecca Yakob and Melanie Cranston, for making everything run so smoothly. I shall also thank my fellow PhD students Benjemin Badger, Anna Hakes, Stephenie Norwood and Jocecyln Tang for going through the the PhD trial together.

I am indebted to the Chinese Scholarship Council for their generous financial support. Thank you to Dr Rick Liversay for being my advisor. I shall also thank the amazing people at the Gurdon Institute Imaging Facility, Alex Sossick, Dr Nichola Laurance and Dr Richard Butler, for all the valuable guide and support. And thank you, Leica SP8 confocal microscopes, upright or inverted, for generating 99% of the data for my PhD.

I would also like to thank my dear friends in Cambridge and foreign lands, for all the fun we have together. Special thanks to my partner Daniel, for being the most supporting and wonderful man I know of. Finally, I shall thank my parents and my extended family. Thank you for loving and believing in me since the very beginning of my life.

Table of Contents

List of figures

Chapter 1: Introduction

Chapter 2: Astrocytes Derived Seizures Induce Cell-Cycle Reentry In the Adult *Drosophila* Brain List of Tables

Chapter 3: Analysis of *slowpoke*, a Ca^{2+}-activated potassium channel gene required for neural stem cell reactivation

Chapter 4. Investigating calcium signalling: a possible downstream effector of *slowpoke* in neuroblast quiescence

Chapter 5: Analysis of *mulet*: a highly quiescence-specific microtubule regulator

Chapter 6. Conclusion and future directions

Chapter 7: Material and methods

List of tables

Glossary

aSC active stem cells
ALH after larval hatching
APF after pupa formation
AEL after egg laying
AE after eclosion
ATS after temperature shift
BBB blood brain barrier
BSA bovine serum albumin
BrdU bromodeoxyuridine
CNS central nervous system
CSF cerebrospinal fluid
DamID DNA adenine methyltransferase identification
DG dentate gyrus
EdU 5-ethynyl-2'-deoxyuridine
GEVI genetically-encoded voltage indicator
GMC ganglion mother cell
GPCR G protein-coupled receptors
GSLC glioblastoma stem-like cells
HSC hemopoietic stem cell
IPC intermediate progenitor cell
KA kainic acid
KD knockdown
PBS phosphate buffered saline
PBST 1X PBS, 0.3% Triton X-100
PBSW 1X PBS, 0.1% Tween-20
PFA paraformaldehyde
PKC Protein Kinase C
qSC quiescent stem cell
RT room temperature
MARCM mosaic analysis with a repressible cell marker
MT microtubule
MuSC muscle stem cell
NB neuroblasts
NGS normal goat serum
NSC neural stem cell
TaDa Targeted DamID
TAP transiently amplifying progenitor
TF transcription factor
TRK tyrosine receptor kinase
TRP transient receptor potential
SOCE store-operated Ca^{2+} entry
SPG subperineurial glia
SVZ subventricular zone
VDRC Vienne Drosophila Resouce Centre
VNC ventral nerve cord
VGCC voltage-gated calcium channel

1. Introduction

1.1 Quiescence and activation are critical for stem cell maintenance and functions

1.1.1 Stem cell quiescence and activation

Stem cells are defined as cells that are capable of both self-renewal and generating differentiated daughter cells. The concept of stem cells arose from studies in embyonic development as well as the adult hematopoietic system [Ramalho-Santos, M. and Willenbring, H., 2007]. Whereas embryonic stem cells are seen as continuously dividing cells, adult stem cells are mostly arrested in the cell cycle, a state described as quiescence [Cheung, T.H. and Rando, T.A., 2013]. Quiesence is crucial for the maintainace of stem cells. It has been shown in multiple tissues including the skin and bone marrow that loss of quiescence ultimately impairs regeneration [Iriuchishima, H et al, 2010][Lay, K *et al*, 2016]. Also, stem-like cells have been isolated from various types of tumour [Chen, W et al, 2016][Aulestia, FJ et al, 2018]. These cells are in a relatively quiescent state to evade killing and often associated with treatment failure [Chen, W *et al*, 2016][Aulestia, FJ *et al*, 2018]. Therefore, understanding stem cell quiescence addresses at least two major therapeutic challenges: tissue regeneration and cancer treatment.

Stem cell quiescence was first observed in mature mouse muscle that satellite cells (also known as muscle stem cells, MuSC) retained the DNA synthesis marker [^{3}H]thymidine for an extended period of time [Schultz, E *et al*, 1978]. These mitotically quiescent cells could be stimulated to proliferate by injury or growth factors [Schultz, E *et al*, 1985][Dodson, MV *et al*, 1985]. Since then, more stem cell types have been found to be in this reversible slow-cycling state, including hematopoietic stem cells (HSC), follicle stem cells and neural stem cells (NSC) [Cotsarelis, G *et al*, 1990][Rochat, A, *et al*, 1995][Morshead, C.M *et al*, 1994][Goodell, MA *et al*,1996].

More recent research reveals that qSCs differ from active stem cells (aSCs) in various aspects [reviewed in Cheung, H *et al*, 2013]. As expected, one common feature of qSCs is downregulation of genes that are involved in DNA synthesis and cell cycle

progression [Fukada, S *et al*, 2007][Forsberg, EC *et al*, 2010][Codega, P *et al*, 2014]. Overall protein synthesis is also reduced in qSCs via post-transcriptional control by miRNAs [Ji Z *et al*, 2009][Cheung, H *et al*, 2013]. Interestingly, despite a lower transcriptional output in qSCs, the chromatin of qSCs is in a more permissive state than the chromatin of active SCs (aSC) [Janina Ander and Andrea Brand, unpublished][Lien WH, *et al*, 2011][Cheung, H *et al*, 2013]. One explanation of this is that the permissive chromatin state marks genes that may be transcribed upon activation, rather than genes that are being actively transcribed. Metabolically, qSCs and aSCs also exhibit different profiles. qSCs normally reside in hypoxic niches and rely heavily on anaerobic glycolysis [Chen, CT *et al*, 2008][Suda, T *et al*, 2011][Takubo, K. *et al,* 2013][Ito, K *et al*, 2014]. Upon oxidative stress such as reactive oxygen species (ROS), HSCs, NSCs and MuSCs are forced into more proliferative states [Ito, K *et al*, 2006][Chen, CT *et al*, 2008][Le Belle, JE *et al*, 2011][Ito, K *et al*, 2014]. Interestingly, in both mouse and *Drosophila* quiescent NSCs, genes involved in cell-cell communication and signalling are enriched [Janinia Ander and Andrea Brand, unpublished][Codega, P *et al*, 2014]. These results suggest that qSCs are in a self-preserving state but are also poised to react to changes in the environment.

In adult mammals, stem cells are generally quiescent. For instance, without stimuli like injury, almost all satellite cells in mature mouse muscle do not divide [Schultz, E *et al*, 1978]. Also in adult mice, ~90% of NSCs and follicle stem cells are quiescent [Horsley, V *et al*, 2008][Lugert, S *et al*, 2010][Codega, P *et al*, 2014]. This predominantly quiescent behaviour is crucial for the maintenance of adult stem cells, as many studies have shown that the loss of quiescence depletes the stem cell pool and causes defects in tissue regeneration [Kippin, T *et al*, 2005][Miyamoto, K *et al*, 2007][Lay, K *et al*, 2016]. Also, stem cells gradually lose quiescence as animals age, which correlates with reduced proliferative capacity [Castilho, RM *et al*, 2009][Lugert, S *et al*, 2010][Chakkalakal, JV *et al*, 2012].

Understanding stem cell quiescence can potentially bring precious insights into many age-related diseases and stem cell therapies. For example, a very recent study shows that quiescence can be restored in MuSCs by the induction of Oncostatin M [Sampath, S *et al*, 2018]. This treatment significantly improves their regenerative capacity after serial transplantation [Sampath, S *et al*, 2018]. However, many questions remain to

be addressed in this rapidly evolving field. First, quiescent stem cells are currently identified by their label retaining abilities. The quiescent population of neural stem cells can be identified by the combination of GFAP expression and lack of CD133 [Codega, P et al, 2014]. However, GFAP is a NSC specific marker and having to use a combination of markers adds technical complexity [Codega, P *et al*, 2014]. The field yet awaits markers, or ideally a single marker, that label quiescent stem cells across different tissues. In my PhD project, I compared the transcriptomes of quiescent and cycling *Drosophila* NSCs to identify candidates for such markers. Second, it is becoming clear that quiescent stem cells form a heterogenous population. For instance, despite the dogma that stem cells arrest in G_0 state, it is recently discovered that the majority of *Drosophila* NSCs are G_2-arrested [Otsuki and Brand, 2018]. Also, quiescent mouse muscle stem cells display different sensitivities towards activation signals [Rodgers, JT et al, 2014]. How is this heterogeneity related to stem cell functions? Perhaps it is the case that rather than two distinct “quiescent” and “active” populations, there is a spectrum of stem cell activity? Advances in single cell technologies will provide insights to these questions. Third, stem cell quiescence has been shown to affect the result of transplantation [Iriuchishima, H *et al*, 2010][Sampath, S *et al*, 2018]. Thus, identifying novel regulators of stem cell quiescence would provide valuable therapeutic targets for stem cell treatments.

1.1.2 Neural stem cell activation and adult neurogenesis

Adult neural stem cells are predominantly quiescent in rodent models [Morshead, CM, 1994][Lugert, S *et al* 2010][Codega, P *et al*, 2014]. Adult NSCs cycle between quiescence and activation to generate proper numbers of neurons and glia [Bonaguidi, MA *et al*, 2011][Basak, O *et al*, 2018]. This regenerative capacity has implications in important brain functions including memory, injury repair and stress response [Goldman,S *et al* 1983][Liu, J *et al*, 1998][Kempermann and Gage, 2002][Snyder, JS *et al*, 2011][Mckenzie *et al*, 2014].

Many factors have been shown to change the balance between quiescent and active NSCs, thus affecting adult neurogenesis [reviewed in Ming and Song, 2005]. Enriched environmental input and exercise pose challenges to the brain and increase neurogenesis in adult rodents [van Praag, H *et al*, 1999][Rochefort, C *et al*, 2002][Brown, J *et al*, 2003]. On the other hand, rodent models of aging, depression

and drug abuse show reduced adult neurogenesis [Kuhn, HG *et al*, 1996][Eisch, AJ *et al*, 2000][Duman, RS *et al*, 2001]. Also, brains inflicted by pathological stimuli including ischemia, seizures and neurodegenerative diseases upregulate adult neurogenesis [Kokaia, Z and Lindvall, O, 2003][Parent, JM *et al* 1997][Jin, K *et al*, 2004][Magnusson, J *et al*, 2014][Sierra, A *et al*, 2015]. It has been shown with rodent models that seizures and ischemia cause adult neurogenesis by inducing astrocytes to divide [Magnusson, J *et al*, 2014][Sierra, A *et al*, 2015]. In particular, ischemia induces non-neurogenic astrocytes to divide and generate neurons [Magnusson, J *et al*, 2014]. It is intuitive to think that neurogenesis after brain injury acts as a compensatory mechanism. Indeed, after neonatal brain injury in mice (day 2 after birth), SVZ neuroblasts migrate toward the injured area, differentiate into mature interneurons and contribute to functional recovery [Jinnou, H *et al*, 2018]. However, no evidence has shown that pathological adult neurogenesis benefits brain function recovery [Hayashi, Y *et al*, 2018].

In rodent brains, adult NSCs reside in specialised niches in the subventricular zone (SVZ) and the hippocampal dentate gyrus (DG) [reviewed Ming, GL and Song, H, 2005]. However, in areas where neurogenesis is non-existent or extremely limited in normal conditions, new neurons can be produced in response to stress. For example, induced neuronal apoptosis is sufficient to cause neurogenesis in mouse neocortex [Magavi, SS *et al*, 2000]. Neuronal degeneration in a mouse Parkinson disease model leads to new neurons in the substantia nigra [Lie, DC *et al*, 2002]. In these cases, the identities of neural progenitors are not clearly defined. In 2014, Magnusson and colleagues found that astrocytes in the striatum, a region previously considered as non-neurogenic, could activate in response to stroke and produce neurons [Magnusson, JP *et al*, 2014]. These findings not only expand the concept of NSCs but also advance the therapeutic potential of NSC activation.

The existence of adult neurogenesis in rodents is well-established, what about human? Eriksson and colleagues examined postmortem samples of adult human hippocampi from patients who received BrdU (a S phase marker) infusion for cancer diagnosis [Eriksson, PS et al 1998]. They found BrdU-labelled neurons which they considered as adult-born neurons [Eriksson, PS et al 1998]. Spalding and colleagues used nuclear-bomb-test-derived ^{14}C to birthdate adult human hippocampal neurons and showed there were 700 neurons added to each hippocampus everyday [Spalding,

K.L *et al*, 2013]. However, when assaying adult-born neurons using 'young neuron' markers rather than DNA synthesis markers, controversy emerged [Boldrini, M et al, 2018][Sorrells, SF et al, 2018]. Sorrells and colleagues could not detect new-born neurons and dividing progenitors in the hippocampi from human over 13 years old [Sorrells, SF et al, 2018]. Using similar set of markers, Boldrini and colleagues examined hippocampi from human over 13 years old and detected both new-born neurons and dividing progenitors [Boldrini, M et al, 2018]. They also reported the decline of quiescent NSCs in the adult human hippocampus with age [Boldrini, M et al, 2018]. Further research is required to resolve the discrepancy, but neither of the results challenges the existence of quiescent NSCs in the adult human brain.

1.2 *Drosophila* central nervous system (CNS) as a model for studying neural stem cell quiescence and activation

1.2.1 Parallels between *Drosophila* and mammalian neural stem cells

Drosophila brains are much smaller and simpler compared to mammalian brains, but they also consist of neurons and glia that arise from neural/glial stem cells [Egger, B *et al*, 2002][Miller, F *et al*, 2007]. Like in mammals, neurons and glia in the *Drosophila* CNS exhibit huge morphological and functional diversity, which make the fly brain a valuable system to study fundamental principles of neurobiology [Strausfeld, NJ and Hirth, F, 2013][Freeman, M, 2015][Kaiser, M, 2015].

Drosophila melanogaster undergo complete metamorphosis during development. Although most larval neurons are conserved in the adult brain, the CNS undergoes a major remodeling during metamophosis. Among many changes that happen during this transition, two are most dramatic and relevant to this study. First, the larval brain contains hundreds of NSCs (also called neuroblasts (NBs), the two terms will be used interchangeably in this thesis) while the adult brain is considered to contain no neural stem cell. Second, the larval central brain is fused with the ventral nerve cord (VNC) while the adult central brain is connected to the VNC by a very fine, axon-rich structure called the cervical connetive [Figure 1.1].

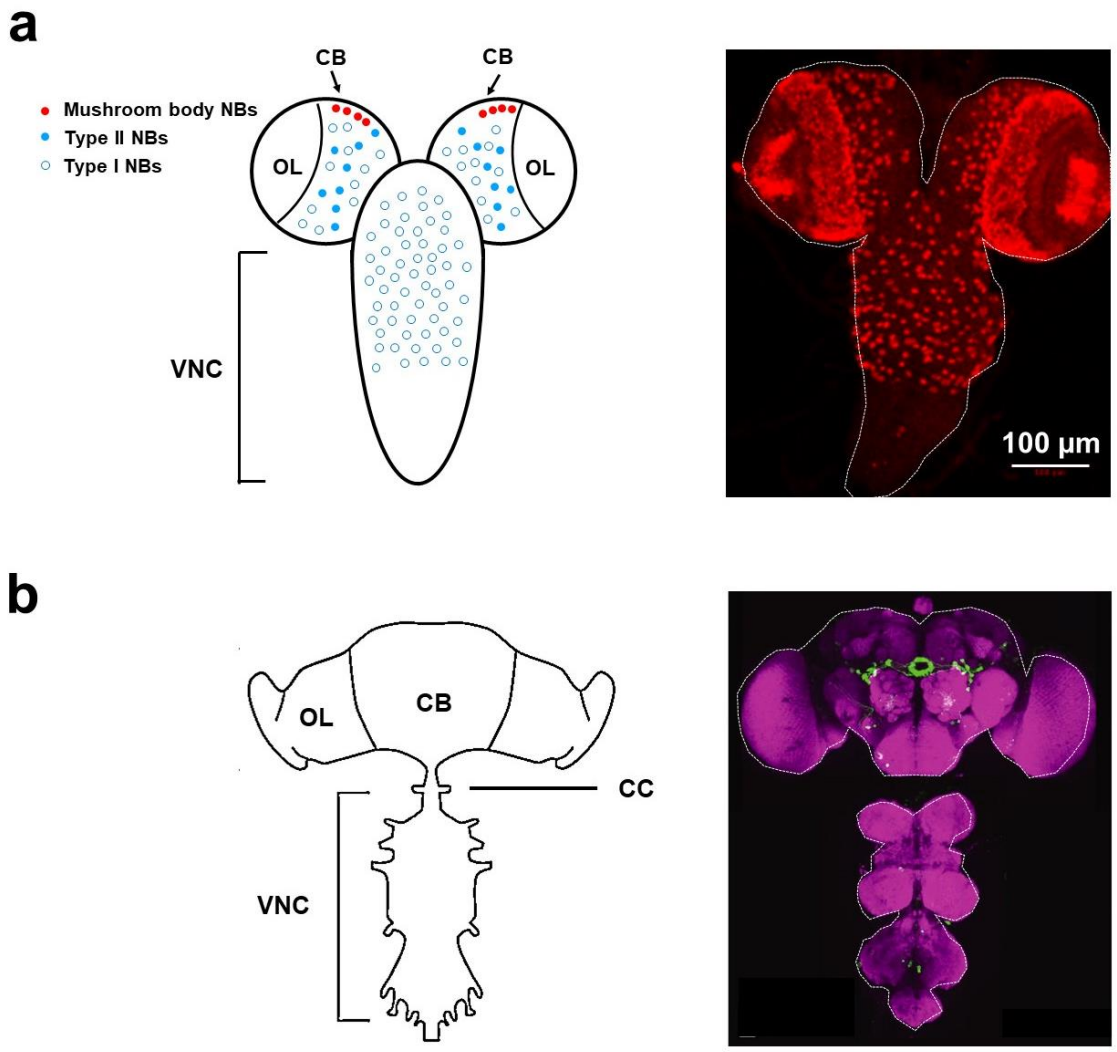

Figure 1.1 Anatomical structures of the larval and adult *Drosophila* CNS (a) Left: Illustration of L3 larval CNS (dorsal view). CB: central brain. OL: optic lobe. Right: A L3 larval CNS. Red: NB nuclei. **(b)** Left: Illustration of adult CNS. CC: cervical connect. Right: An adult CNS [Pfeiffer, B.D *et al*, 2007, scale bar not available]. Magenta: Neuropil. Green: octopamine receptor 2+ neurons.

Drosophila neural stem cells (also termed neuroblasts) have been proven to be a valuable tool for understanding neurodevelopment and stem cell biology [Doe, CQ *et al*, 1998][Reichert, H, 2009][Brand, AH and Livesey, FJ, 2011]. The behaviour of *Drosophila* and mammalian NSCs, as well as the pathways that control their behaviour, are found to be conserved in many ways. *Drosophila* and mammalian NSCs both originate from the neuroectoderm during embryonic development [Campos-Ortega, JA, 1993][Temple, S, 2001]. Neuroectoderm cells then acquire NSC properties through activation of a group of conserved bHLH transcription factors (TF)

called proneural genes, including *achete, scute* and *lethal-of-scute* in flies and Ascl1, Ngn1 and Ngn2 in mammals [Guillemot, F, 2007][Egger, B, 2008][Reichert, H, 2009]. Also, the highly evolutionarily conserved Notch pathway is known to suppress neural fate in both *Drosophila* and in the mammalian neuroectoderm [Cabrera, CV, 1990][Ishibashi, M *et al*, 1995][Wakeham, A *et al*,1997][Egger, B *et al*, 2008].

Following their generation, NSCs proliferate in either symmetric manner to replenish the stem cell pool or asymmetric manner to produce neural progeny. In developing mammalian cortex, the majority of NSCs (~80%) divide asymmetrically to generate a self-renewed stem cell and a more differentiated daughter cell [Noctor, SC, *et al*, 2004]. Until very recently, it was believed that stem cells in the adult mammalian brain also followed this pattern as they arised directly from the embryonic NSCs [Furutachi, S *et al*, 2015][Silva-Vargas, V *et al*, 2018]. However, using clonal lineage-tracing methods and *ex vivo* imaging, Obernier and collegues showed that the vast majority of adult mouse NSCs (~80%) in the SVZ divided symmetrically to generate either two neurons or two stem cells [Obernier, K *et al,* 2018]. Very interestingly, using *in vivo* imaging, Pilz, G.A and colleagues found that NSCs in the adult mouse hippocampus mostly divide assymetrcially (~80%) [Pilz, G.A *et al*, 2018]. However, neuronal hyperactivity can trigger the same group of NSCs to divide symmetrically and generate reactive astrocytes [Sierra, A *et al*, 2015]. These results demonstrate the complexity of cell division modes of rodent NSCs. In contrast, *Drosophila* NSCs divide in much more defined patterns. Once delaminated from the symmetrically dividing neuroepithelium, NSCs only divide assymetrically [Egger, B *et al*, 2008][Egger, B *et al*, 2010][Homem, CC and Knoblich, JA, 2012]. Therefore, *Drosophila* NSCs provide an excellent *in vivo* model to study asymmetric NSC division which excludes confusion from symmetric dividing cells in the same system.

Mammalian NSCs have three modes of asymmetric proliferation: 1) generating a daughter stem cell and a neuron 2) generating a daughter stem cell plus an intermediate progenitor cell (IPC), which symmetrically divides and produces two neurons 3) generating several intermediate progenitors (IPs) that can each generate multiple neural progeny [Götz, M. and Huttner, WB, 2005][Kriegstein, A et al, 2006][Reichert, H, 2009][Gonçalves, JT *et al*, 2016][Figure 1.2 (a)]. Fascinatingly, all three division modes are conserved in *Drosophila* neural development. In the

developing *Drosophila* brain, most neuroblasts self-renew and generate a ganglion mother cell (GMC) which gives rise to two neurons. NBs following this division pattern are called type 1 NBs [Homem, K and Knoblich, JA, 2012][Figure 1.2 (b)]. Some type 1 NBs can switch to a different division mode, generating a GMC that directly differentiates into a neuron. This mode of division is called “type 0” [Karcavich, R and Doe, CQ, 2005][Baumgardt, M *et al*, 2014] [Figure 1.2 (b)]. The third proliferation mode is found in only 8 neuroblasts per brain which are called type 2 NBs. They are defined by the expression of NB marker *worniu* but lack of *asense* (type 1 NBs express both) [Carney, T.D *et al*, 2011]. Type 2 NBs have a more complex lineage, producing intermediate neural progenitors (INPs) that have stem cell properties and divide in the type 1 mode [Boone and Doe, 2008] [Figure 1.2 (b)].

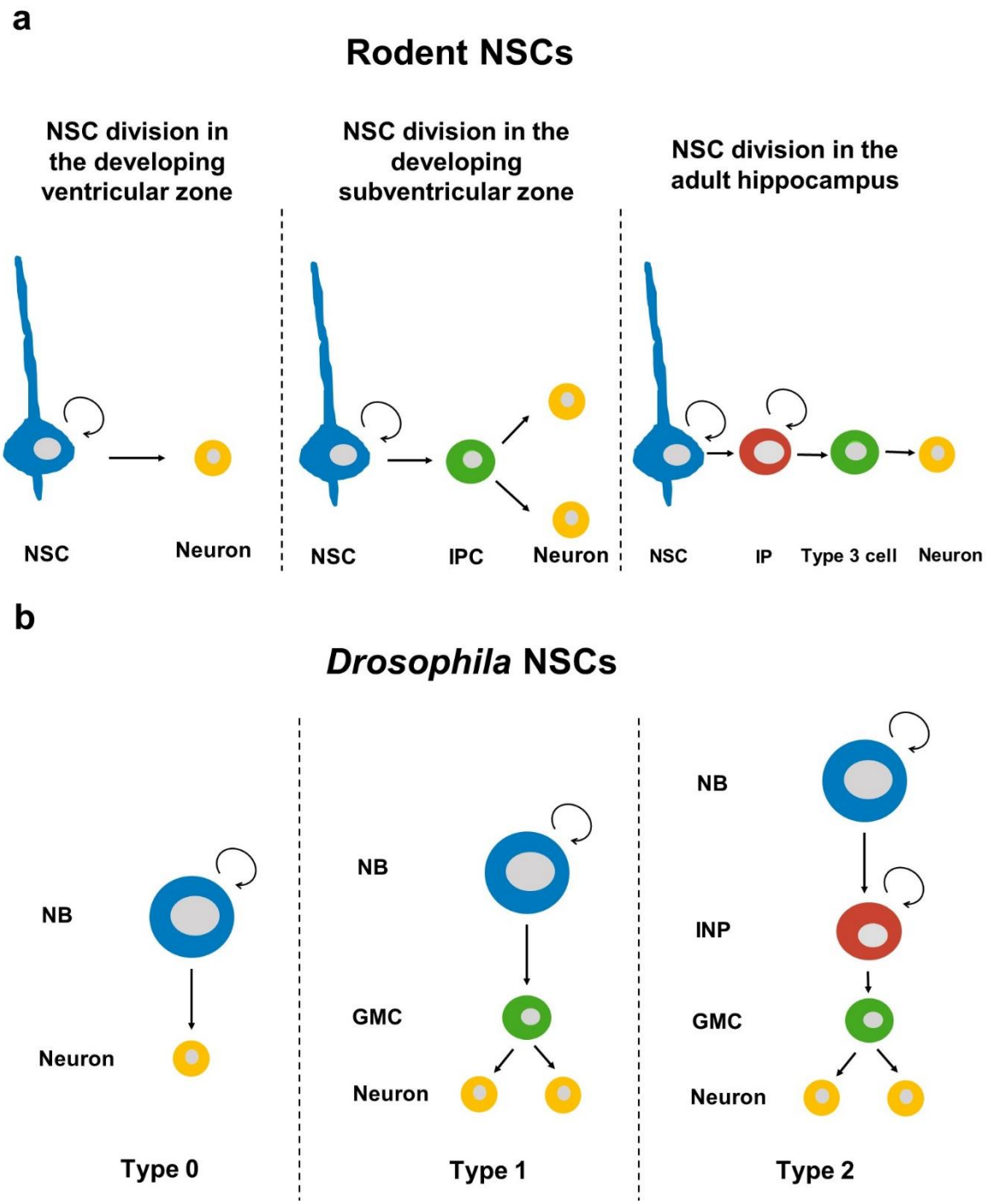

Figure 1.2 Comparable asymmetric division modes of mammalian and *Drosophila* NSCs
(a) Different asymmetric division modes of NSCs in rodents. IPC: intermediate progenitor cell. IP: Intermediate progenitor (also called type2a cells). **(b)** Different asymmetric division modes of NSCs in *Drosophila*. GMC: ganglion mother cell. INP: intermediate progenitor.

Like other stem cells, neural stem cells divide asymmetrically to self-renew and generate a more differentiated daughter cell [reviewed in Knoblich JA, 2008, Zhong, W and Chia, W, 2008]. The asymmetrical cell division is achieved by segregation of

fate determinants only to non-stem cell progeny. In *Drosophila* NSCs, asymmetrical distribution of proteins requires orientation of mitotic spindles along the basal-apical axis [Knoblich, JA, 2008]. The proteins that set up this polarity include the Par proteins, Inscuteable and Partner of Inscuteable (Pins), which are conserved in mammals [Goldstein, B and Macara, IG, 2007][Yu, F *et al* 2003][Postiglione, MP *et al*, 2011]. Moreover, many fate determinants segregated to the non-stem daughter cell are also conserved between *Drosophila* and mammals. For instance, *Drosophila* Numb has the mouse homologue Numb [Knoblich, JA, 2008], *Drosophila* Pros has homologue Prox1 which is highly conserved in all mammals [Torii, M *et al*, 1999][Elsir, T *et al*, 2012], *Drosophila* Brat has human homologue Trim3 [Mukherjee, S *et al*, 2013].

Furthermore, NSCs produce different types of progeny in a stereotyped order [Jacob, J *et al*, 2008][Okano, H and Temple, S, 2009]. This temporal sequence is most well-studied in *Drosophila*. During embryonic neurogenesis, NSCs express temporal factors in the following order: Hunchback (Hb)- Seven up (Svp) - Krüppel (Kr) - POU-domain TFs 1/2 (Pdm) - Castor (Cas) [Isshiki, T *et al*, 2001][Kanai, M *et al*, 2005][Kohwi, M and Doe, CQ, 2013][Figure 1.3]. Cas expression persists into larval stages. It is required, together with a transient pulse of Svp, for the temporal transition from Chinmo to Broad-Complex (Br-C) at the mid larval stage [Maurange, C *et al*, 2008][Figure1.3]. Interestingly, homologues of the abovementioned temporal factors are also found to shape NSC identities in vertebrates [Okano, H and Temple, S, 2009]. For example, the mouse homologue of Hb, Ikaros, is necessary and sufficient to confer early temporal competence on mouse retinal progenitors [Elliot, J *et al*, 2008]. Also, murine NSCs require two homologues of *Drosophila* Svp called Coup-TFI and Coup-TFII to acquire gliogenic competence [Naka, H *et al*, 2008].

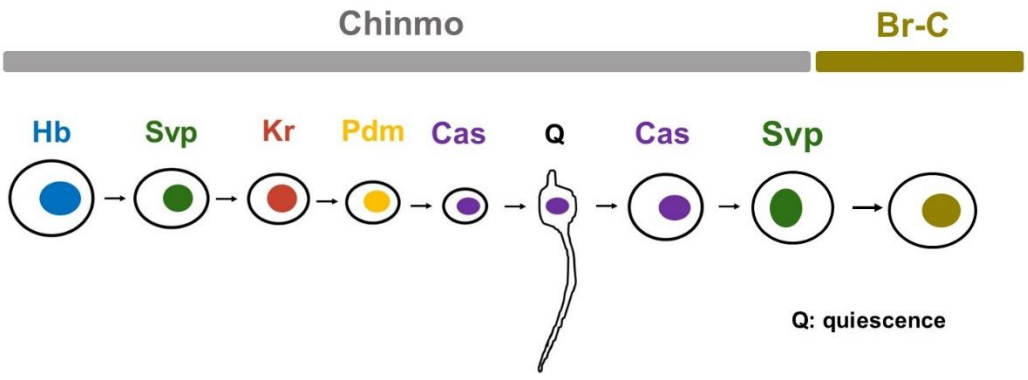

Figure 1.3 Temporal cascade of *Drosophila* neuroblasts: NBs express temporal factors in the order of Hb, Svp, Kr, Pdm, Cas and Svp. NBs also express Chinmo until mid-larval stage then transit into Br-C identity. Q: quiescent NBs.

Although *Drosophila* and mammalian NSCs share many similarities, one major difference between them is the timing of proliferation. In mammals, the majority of the CNS is generated prenatally. After the completion of prenatal neurogenesis, most NSCs transform into non-mitotic astrocytes [Kriegstein, A. and Alvarez-Buylla, A., 2009]. However, a small subset of NSCs acquire the astrocytic fate but also retain the capacity to proliferate in adult brains [Doetsch, F *et al*, 1999][Laywell, ED *et al*, 2000]. In contrast, all *Drosophila* NSCs terminate proliferation and disappear at pupal stages [White & Kenkel, 1978][Truman & Bate, 1988]. Fernandez-Hernandez and colleagues reported adult NSCs as well as adult-generated neurons in the optic lobe [Fernandez-Hernandez, I *et al*, 2013], but we could not reproduce their results in our lab. To date no adult neurogenesis has been reliably detected in flies under normal conditions [discussed in 2.1.1]. However, glial cells in adult *Drosophila* CNS are able to divide in response to injury [Kato, K *et al*, 2009][von Trotha *et al*, 2009]. Considering the glial nature of NSCs in mammals, it is interesting to explore if glia are also latent adult neural progenitors in *Drosophila*.

1.2.2 *Drosophila* NBs undergo quiescence and reactivation

The embryonic development of *Drosophila* lasts for about 22 hours and is divided into 17 stages [reviewed in Campos-Ortega, J.A. and Hartenstein, V., 1997]. From stage 9 to stage 11, about 500 NBs delaminate from the neuroepithelium to produce neurons and glia [Hartenstein and Campos- Ortega, 1984]. Wingless and Notch signalling are essential for NB delamination [Hartenstein, V *et al*, 1994][Egger, B *et al*, 2010]. Loss-of-function *wingless* mutants display defects in NB delamination timing and loss of a subset of NBs [Hartenstein, V *et al*, 1994]. Notch signaling, on the other hand, is required for suppressing the NB fate. In embryonic VNCs, expression of a Notch gain-of-function construct causes the absence of NB delamination while in larval optic lobes, loss of Notch causes NBs to delaminate prematurely [Hartenstein, V *et al*, 1994][Egger, B *et al*, 2010].

By stage 16, the majority of NBs in the abdominal segment of the ventral nerve cord (VNC) are then eliminated via apoptosis [White, K *et al*, 1994][Peterson, C *et al*, 2002][White, K *et al*, 1994][Rogulja-Ortmann, A, *et al*, 2007]. Near the end of stage 17, all but 10 surviving NBs become quiescent [Truman, JM and Bate, M, 1988][Prokop AN and Technau GM, 1991]. The 10 NBs that do not quiesce include 8 mushroom body NBs (4 per hemisphere) and 2 lateral NBs (1 per hemisphere) [Figure 1.4][Ito, K. and Hotta, Y., 1992].

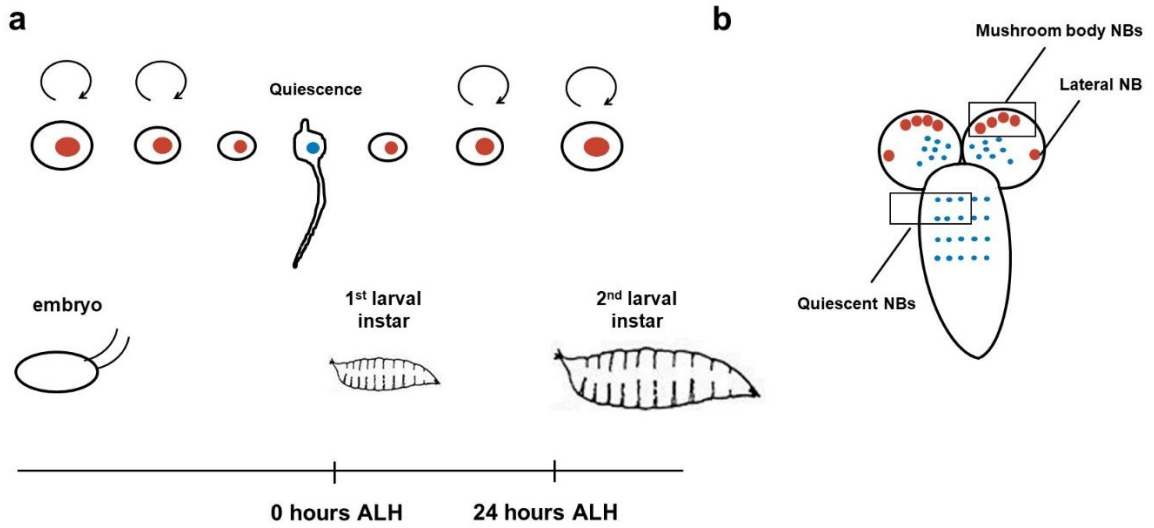

Figure 1.4 Neuroblasts quiesce and reactivate during embryonic and larval development (a) Neuroblast behaviour at different developmental stages. ALH: after larval hatching **(b)** Anatomy of L1 larval brain. Red: non-quiescent NBs. Blue: quiescent NBs.

Unlike larval NBs, embryonic NBs do not regrow after each division [Homem, K and Knoblich, JA, 2012]. When they enter quiescence, their cell bodies are no longer distinguishable in size from neurons. Quiescent NBs also extend long basal projections which resemble axons. These basal projections are conserved in mammalian NSCs, which receive signals from endothelial cells to maintain the quiescent state [Mirzadeh, Z *et al*., 2008][Ottone, C *et al*., 2014]. In *Drosophila*, the majority of quiescence projections make contact the synapse-dense neuropil [Chell, JM and Brand, AH, 2010][Leo Otsuki, Stephanie Norwood and Andrea Brand, unpublished]. Glia are well-established niche components for *Drosophila* NBs [Chell, JM and Brand, AH, 2010][Speder, P et al, 2014][Ding, R *et al*, 2016][Speder, P et al, 2018]. These observations point to a possibility that neurons are also niche

components for *Drosophila* NBs and the quiescent projections might receive signals from them.

In contrast to the widely accepted view that quiescent stem cells are G_0 cells, the majority of NBs (75%) arrest at G_2 phase [Otsuki, L and Brand, AH, 2018]. These G_2-arrested NBs reactivate earlier compared to G_0-arrested NBs [Otsuki, L and Brand, AH, 2018]. Moreover, whether a NB arrests at G_0 or G_2 phase is predetermined by its location [Otsuki, L and Brand, AH, 2018]. G_2-arrested NBs reactivate earlier than G_0-arrested NBs [Otsuki, L and Brand, AH, 2018], whether this difference affects post-embryonic neurogenesis is currently under investigation.

At 25°C, NBs stay quiescent for about 24 hours, approximately equal in duration to the first larval instar (L1) stage [Truman, J and Bate, M, 1988][Ito, K and Hotta, Y, 1992]. From late L1 to early L2 stage, NBs enlarge and reenter the cell cycle. In general, NBs in the brain lobes reactivate first, followed by the thoracic NBs and the abdominal NBs reactivate last [Leo Otsuki, PhD thesis, 2016]. Larval NBs regrow after each division and the length of average cycle cell is approximately 1 hour [Truman, J and Bate, M, 1988]. By the end of larval neurogenesis, each NB has produced about 100 progeny, and the total volume of the CNS expands by about 900%[Truman, J and Bate, M, 1988].

In summary, the adult *Drosophila* CNS is produced in two waves of neurogenesis. NBs proliferate during embryogenesis, transiently enter quiescence for ~24 hours, then reactivate to generate the majority of adult CNS. This clearly-defined, synchronised temporal pattern makes it very straightforward to monitor changes in quiescence and reactivation. Spatially, *Drosophila* NB quiescence and reactivation are also defined in a stereotyped pattern. In the thoracic segments of the VNC (tVNC), NBs are arranged in a repetitive, bilaterally symmetric pattern with 30 NBs per neuromere. This allows us to identity and name every single NB [Doe, CQ, 1992][Lacin, H and Truman, J, 2016]. In this thesis, analyses of NB behaviour are also focused on the tVNC unless specified otherwise. As a well-established model organism with a plethora of tools for genetic manipulation, *Drosophila* provides an excellent model for studying stem cell quiescence.

1.3 Known regulators of stem cell quiescence and activation

1.3.1 Regulators of quiescence and activation in *Drosophila* NBs

Entry into quiescence requires the correct temporal identity of NBs [Tsuji, T *et al*, 2008]. As described in 1.2.1, embryonic NBs sequentially express Hb, Svp, Kr, Pdm and Cas. In *pdm* mutant embryos, NBs enter quiescence prematurely [Tsuji, T *et al*., 2008]. Cas expression precedes quiescence entry and *cas* mutant NBs do not enter quiescence, suggesting *cas* is required for quiescence entry [Tsuji, T *et al*, 2008]. Transcription factors Nab and Squeeze are proposed to be the downstream targets of Cas/Pdm in controlling quiescence entry. [Tsuji, T *et al*, 2008].

Tsuji, T and colleagues also compared two defined NBs from the thorax and abdomen, named NB3-3T and NB3-3A. NB3-3T normally enters quiescence while NB3-3A is still dividing. Two Hox genes *antennapedia (*Antp*)* and *abdominal-A (abd-A)* are expressed in NB3-3T and NB3-3A, respectively [Hirth, F *et al*, 1998]. Removing *Antp* causes delayed quiescence entry in NB3-3T, while misexpression of *abd-A* in NB3-3T causes loss of *Antp* expression and defective quiescence entry [Tsuji, T *et al*, 2008]. Although the evidence is only gathered from one particular NB, these results suggest that Hox proteins are involved in setting the timing of quiescence entry.

G2-arrested NBs account for ~75% of total NBs in the thoracic VNC [Otsuki, L and Brand, AH, 2018]. An evolutionally conserved pseudo-kinase, Tribbles [Eyers, PA *et al*, 2017], is found to be required for G2-type quiescence entry [Otsuki, L and Brand, AH, 2018]. Tribbles promotes the G2 phase cell cycle arrest by promoting the degradation of $Cdc25^{String}$ protein [Mata, J *et al*, 2000][Otsuki, L and Brand, AH, 2018]. Tribbles also maintains quiescence via inhibiting the insulin signalling pathway, which is required for NB reactivation [Du, KY *et al*, 2003][Chell, JM and Brand, AH, 2010][Otsuki, L and Brand, AH, 2018].

Another intrinsic factor that has been reported to promote quiescence is the transcription factor Prospero (Pros) [Lai, SL and Doe, CQ, 2014]. Pros is a fate determinant that promotes the differentiation of GMCs by repressing stem cell genes as well as activating genes required for terminal differentiation [Spana, EP and Doe, CQ, 1995][Choksi, SP *et al*, 2006]. In NBs, Pros and *pros* mRNA are tethered to the

basal cortex by Miranda and Staufen respectively to prevent them from entering the nucleus as well as to ensure their segregation into the GMCs [Hirata, J *et al*, 1995][Knoblich, JA and Jan, YN, 1995][Ikeshima-Kataoka, H *et al*, 1997][Broadus, J *et al*, 1998][Schuldt, AJ *et al*, 1998]. High level of Pros in the NB nuclei induced by misexpression leads to cell cycle exit [Choksi, SP *et al*, 2006][Bayraktar, OA *et al*, 2010][Cabernard, C and Doe, CQ, 2010]. Lai and colleagues show that near the end of embryogenesis, a transient pulse of Prospero in the NB nuclei is required for quiescence entry [Lai, SL and Doe, CQ, 2014]. They also induce short pulse of Pros for 2 hours in proliferating L3 NSCs and show it is also sufficient to temporarily pause the cell cycle [Lai, SL and Doe, CQ, 2014]. Thus, they conclude that Pros acts in a dose-dependent manner. High levels of Pros causes permanent exit of cell cycle while low levels of Pro induce quiescence.

Earlier experiments have shown that nutrition is essential for NB reactivation. Under amino acid deprivation condition, NBs never reactivate [Britton and Edgar, 1998]. Yet when co-cultured with fat bodies from fed larvae, quiescent NBs enter the cell cycle [Britton and Edgar, 1998]. This work suggests that the fat body, the organ that performs many function of the mammalian liver and adipose tissue, acts as an amino acid sensor and sends interorgan signals to the brain [Søndergaard, L, 1993]. Further work illustrates that this unknown fat body derived signal is detected by the surface glia, a structure that encapsulates the brain and is comparable to the mammalian blood brain barrier (BBB) [Delvaso, MK *et al*, 2011][Chell, JM and Brand, AH, 2010][Sousa-Nunes *et al*., 2011][Figure 1.4]. The *Drosophila* BBB glia is comprised of perineural glia and subperineural glia [Delvaso, MK *et al*, 2011]. In the gap junction-connected subperineural glia, the fat body derived signal induces synchronised Ca^{2+} oscillations on the whole brain scale [Speder, P and Brand, AH, 2014]. The synchronised oscillations are required for the secretion of insulin like peptides (dILPs) by the subperineural glia [Speder, P and Brand, AH, 2014][Figure 1.5].

The insulin like peptides secreted by BBB glia activate the insulin signalling pathway in NBs, which is sufficient to trigger reactivation [Chell, JM and Brand, AH, 2010][Sousa-Nunes, R *et al* , 2011] [Figure 1.4]. The insulin signalling pathway is a conserved signalling pathway that is key to energy metabolism and growth [reviewed in Pollak, M, 2008]. Insulin-like growth factors have been shown to trigger proliferation

in mammalian stem cells including NSCs [Saka, VR *et al*, 2011][Bracko, O *et al*, 2012][Wang, G *et al*, 2018]. The *Drosophila* NB niche development is also dependent on nutrition and the insulin pathway. NBs and their progeny reside in cortex glial chambers that expand their membrane processes to form a complete sheath as the NBs reactivate [Pereanu, W *et al*, 2005]. This membrane expansion requires amino acids in the diet and activation of the insulin pathway in both cortex glia and NBs [Speder, P and Brand, AH, 2018] [Figure 1.5].

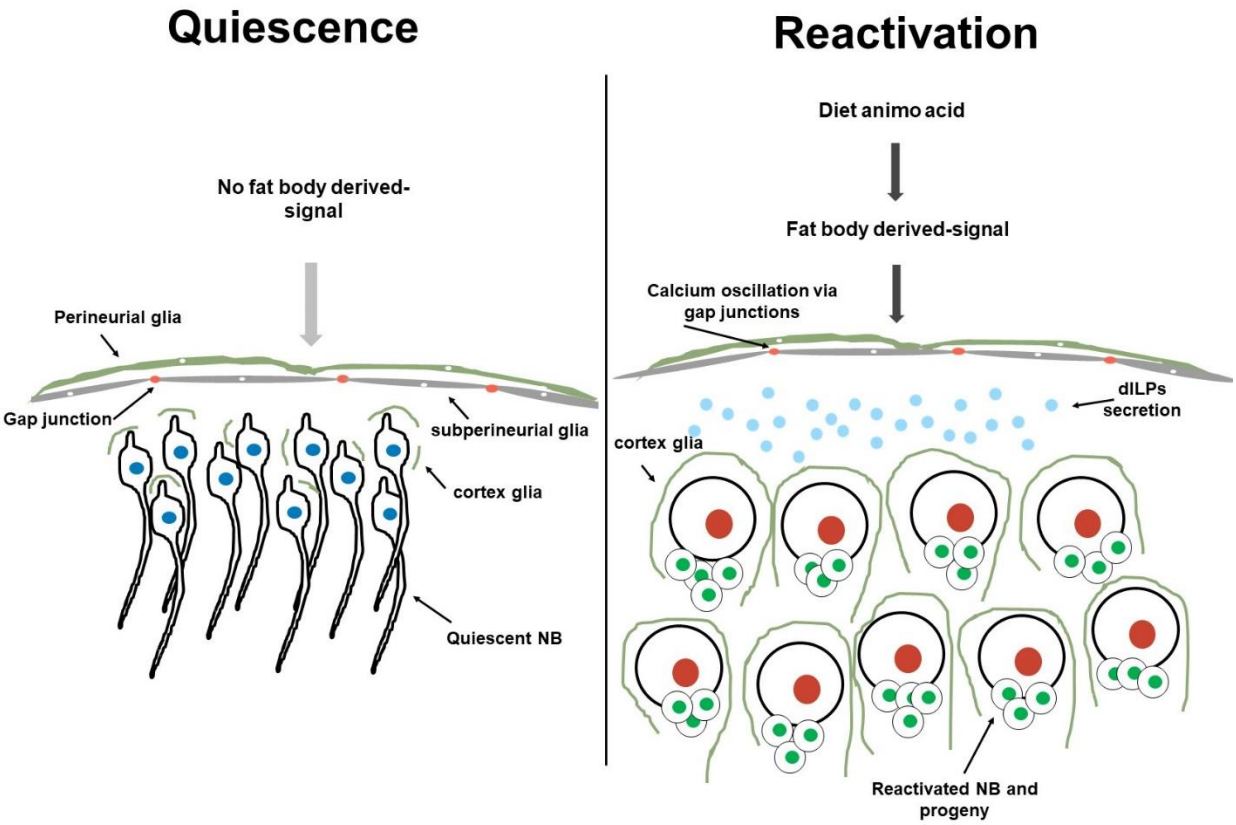

Figure 1.5 The glial niche is essential for neuroblast reactivation During quiescence, no dILPs are released by the surface glia and the cortex glial chamber do not conceal the NBs. As the larvae feed, the surface glia receive signals derived from the fat body and release dILPs, which trigger the NBs to enter the cell cycle and the cortex glial chamber to enclose the NBs and progeny.

Recently, the glial niche has been shown to modulate NB quiescence and activation via the Hippo signalling pathway [Poon, C.L *et al*, 2016][Ding, R *et al*, 2016]. The Hippo pathway is an evolutionarily conserved pathway that controls organ size and stem cell renewal in multiple organisms from fly to human [reviewed in Zhao, B *et al*,

2011]. In *Drosophila*, the core cascade of the Hippo pathway is as follows: the Hippo kinase phosphorylates Warts, which phosphorylates and inactivates the transcriptional coactivator Yorkie (Yki). Inactivated Yki is then excluded from the nucleus, which stops the transcription of Yki-regulated pro-proliferative genes [Huang, J *et al*, 2005]. This is consistent with Ding, R and colleagues' observation that Yki is not present in quiescent NB nucleus but gets translocated into the nucleus after reactivation [Ding, R *et al*, 2016]. Loss of Hippo signalling causes premature exit from quiescence and substantial overgrowth in overall brain size [Poon, C.L *et al*, 2016][Ding, R *et al*, 2016]. The NB Hippo signalling is regulated by transmembrane proteins Crumbs (Crb) and Echinoid (Ed) in both NBs and glia [Ding, R *et al*, 2016]. Either nutrition or activation of the insulin pathway is sufficient to downregulate Crb and Ed expression [Ding, R *et al*, 2016]. In summary, the Hippo pathway regulates NB quiescence in both cell-autonomous and niche-dependant manners.

NB activation is not only regulated by extrinsic signals but also intrinsic factors. Recently, Li, S and colleagues reported that the spindle matrix complex is required for the reactivation of NBs [Li, S *et al*, 2017]. Spindle matrix proteins co-locate with mitotic spindles during mitosis and facilitate spindle assembly [Zheng, Y., 2010][Schweizer, N, *et al*, 2014]. Interestingly, spindle matrix proteins are located in the nucleus during interphase and their nuclear functions are less well-established [Rath, U *et al*, 2004]. The *Drosophila* spindle matrix complex consists of four proteins: Chromator/Chriz (Chro), Megator (Mtor), Skeletor and enhanced adult sensory threshold (East) [Zheng, Y, 2010]. Li, S and colleagues show that the depletion of Chro is sufficient to prevent reactivation and causes reactivated NBs to reenter quiescence. Chro acts downstream of the insulin/PI3K/Akt pathway [Li, S *et al*, 2017]. Targeted DamID analysis of Chro reveals its binding to the regulatory region of grainyhead (*grh*) [Li, S *et al*, 2017], a temporal factor that is important for maintaining proliferation [Cenci, C and Gould, AP, 2005]. Depletion of Chro impairs *grh* expression In summary, *Drosophila* spindle matrix protein Chro functions as a transcription factor in the NB nucleus and is an intrinsic regulator of reactivation.

In summary, *Drosophila* NB quiescence entry is only regulated by intrinsic factors to our knowledge. Quiescence maintenance and reactivation is controlled by a

combination of intrinsic and extrinsic cues. The known factors involved in this quiescence-activation process are illustrated in Figure 1.6.

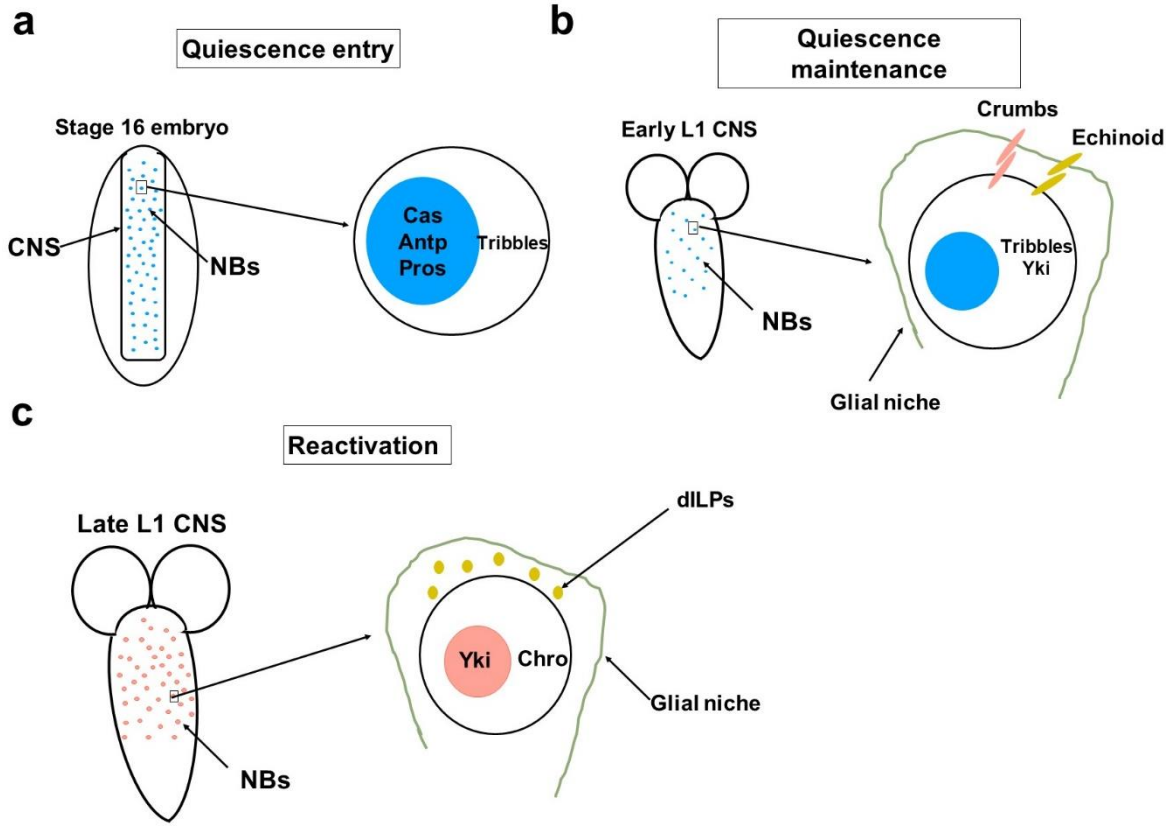

Figure 1.6 Extrinsic and intrinsic cues regulating NB quiescence and activation

1.3.2 Regulators of quiescence and activation in rodent adult NSCs

Mammalian adult NSCs reside in a specialised niche consisting of ependymal cells, cerebrospinal fluid (CSF), vasculature and neurons [Riquelme, PA, *et al*, 2008][Tong, CK, *et al*, 2014][Otsuki, L and Brand, AH 2017]. Signals from this microenvironment closely regulate the proliferation of adult NSCs. Adult NSCs in the subventriclar zone (SVZ) reside underneath a thin layer of ependymal cells, which lie between NSCs and the CSF that fills the ventricle [Del Bigio, MR, 1995][Mirzadeh, Z, *et al*, 2008][Figure 1.7]. Ependymal cells promote NSCs to exit quiescence via secreted factors such as the BMP pathway inhibitor Noggin [Lim, DA *et al*, 2000][Mira, H, *et al*, 2010]. NSCs also make direct contacts with the CSF by either penetrating the ependymal layer or extending a primary cilium to the CSF [Doetsch, F *et al*, 1999][Mirzadeh, Z, *et al*, 2008][Shen, Q *et al*, 2008]. Numerous growth factors in the CSF have been shown to promote neurogenesis, such as insulin-like growth factors (IGFs), vascular endothelial

growth factor (VEGF), basic fibroblast growth factor (bFGF) and GDF-11 [Lehtinen, MK, *et al*, 2011][Katsimpardi, L *et al*, 2014][Luo, Y *et al*, 2014]. Conversely, several CSF-borne ligands are known to promote NSC quiescence including Neurotrophin (NT)-3, chemokines and BMPs [Mira, H, *et al*, 2010][Delgado, AC, *et al*, 2014][Villeda, SA, *et al*, 2011]. CSF-borne soluble signals undergo significant changes throughout the life span, which could explain the decline of neurogenesis as the animals age [Silva-Vargas, V, 2016]. Apart from CSF-borne chemical signals, the physical properties of the CSF including flow speed also affect NSC proliferation [Petrik, D *et al*, 2018].

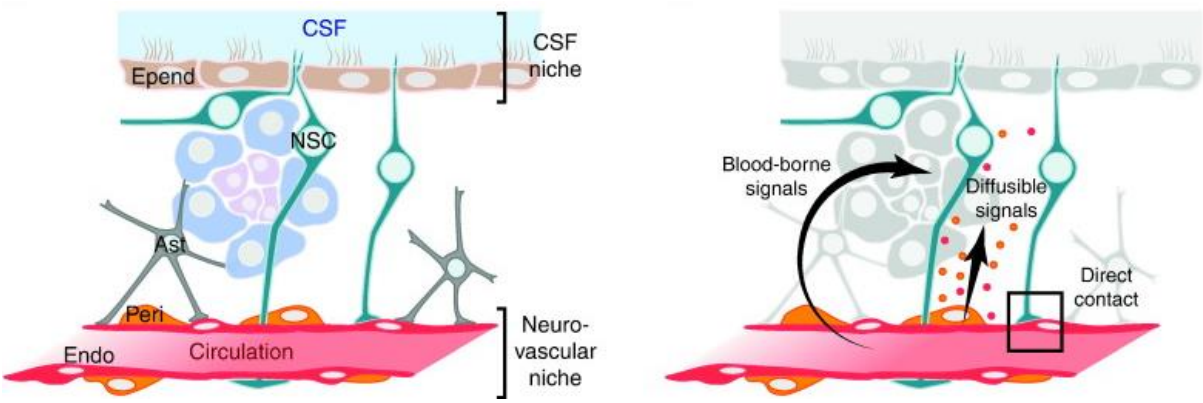

Figure 1.7 The adult mammalian SVZ niche. From Otsuki, L. and Brand, AH, 2017, with copyright permission from the publisher.

The neurovasculature in the ventricle wall is located basally in relation to the NSCs. This vascular niche regulates NSC quiescence and activation via diffusible signals as well as direct contacts [Otsuki, L and Brand, AH 2017]. NT3, amyloid precursor protein (APP) and transforming growth factor β1 (TGFβ1) are among the endothelial-derived factors that promote NSC quiescence [Pineda, JR *et al*, 2013][Delgado, AC, *et al*, 2014][Sato, Y *et al*, 2017]. On the other hand, endothelial cells also secret factors that stimulate proliferation, including brain-derived neurotrophic factor (BDNF), pigment epithelium-derived factor (PEDF) and epithelium growth factor (EGF) [Leventhal, C *et al*, 1999][Ramírez-Castillejo, C,2006][Gómez-Gaviro, MV *et al*, 2012]. Like quiescent *Drosophila* NSCs, adult mammalian NSCs extend long basal processes that terminate on blood vessels [Mirzadeh, Z *et al*, 2008][Shen, Q *et al*, 2008]. This direct contact is

important for maintaining quiescence via the Eph and Notch signalling pathways [Ottone, C *et al*, 2014].

Various neurotransmitters have been shown to regulate adult NSC proliferation [reviewed in Berg, DA *et al*, 2013]. The neurotransmitters are either produced by distant neurons or the immediate progeny of NSCs [Liu, X *et al*, 2005][Tong, CK *et al*, 2014][Bao, H *et al*, 2017]. Also, different neurotransmitters have different effects on NSC proliferation. GABA and serotonin inhibit proliferation, while glutamate, dopamine and acetylcholine promote proliferation [Banasr, M *et al*, 2004][Zhou, C *et al*, 2004][Song *et al*, 2012][Berg, DA *et al*, 2013][Hedlund, E *et al*, 2016]. More detailed discussion on neurotransmitter-regulated quiescence can be found in 3.1.4. Although many neurotransmitter regulate NSC activation, the downstream mechanisms remain very poorly understood [Berg, DA *et al*, 2013].

Nuclear factors work synergistically with niche signals to regulate adult NSC proliferation. The Sox family members Sox1 and Sox2 are among the extensively-studied TFs that promote NSC division. In the hippocampus, Sox1 marks active NSCs but is absent in quiescent NSCs [Venere, M *et al*, 2012]. Sox2 is expressed in adult NSCs and is essential for the maintenance of stem cell identity [Favaro, R *et al*, 2009]. Deletion of Sox2 in the adult NSC causes loss of the neurogenic signalling molecule Sonic hedgehog (Shh) [Lai, K *et al*, 2003][Ahn, S and Joyner, AL, 2005][Favaro, R *et al*, 2009]. Sox2 also positively regulates the expression of the nuclear orphan receptor tailless, which promotes NSC proliferation [Qu, Q *et al*, 2009][Shimozaki, K *et al*. 2011]. Ascl is another pro-activation TF in NSCs [Andersen, J *et al*, 2014]. In adult hippocampal NSCs, Ascl protein is degraded by the E3 ubiquitin ligase Huwe1, which indirectly inhibits activation [Urbán, N *et al*, 2016]. On the other hand, various nuclear factors negatively regulate NSC proliferation. For instance, FoxO3, a TF that is inactivated by the insulin signalling pathway, induces a program of genes that preserve quiescence [Renault, VM *et al*, 2009]. Similarly, NFIX from the nuclear factor one family is required for induction of quiescence by modulating the expression of cell adhesion and extracellular matrix proteins [Martynoga, B *et al,* 2013]. More recently, a chromatin remodelling factor CHD7 (chromodomain-helicase-DNA-binding protein 7) has recently been shown to maintain quiescence by repressing a group of positive regulators of cell cycle progression [Jones, KM *et al*, 2015].

Very recently, the importance of Ca^{2+} signalling in NSC quiescence has been addressed in three different studies in mammals [Aulestia, FJ *et al*, 2018][Domenichini, F *et al*, 2018][Petrik, D *et al*, 2018]. Adult SVZ NSCs possess functional store-operated Ca^{2+} entry (SOCE) [Domenichini, F *et al*, 2018]. SOCE is external Ca^{2+} entry triggered by Ca^{2+} depletion in the ER lumen [Venkatachalam, K *et al*, 2002]. In flies and mammals, SOCE is mediated by the coupling of ER Ca^{2+} sensor Stim and the plasma membrane Ca^{2+} channel Orai [Zhang, SL *et al*, 2005][Zhang, SL *et al*, 2006][Prakriya, M *et al*, 2006]. Inhibition of SOCE in cultured NSCs significantly impaired symmetrical self-renewal division while promoting asymmetrical cell division [Domenichini, F *et al*, 2018]. Petrik, D and colleagues also reported that in whole mount SVZ, blocking SOCE abrogated NSC activation caused by increased CSF flow [Petrik, D *et al*, 2018]. However, they did not specify whether it was symmetrical or asymmetrical proliferation that was affected [Petrik, D *et al*, 2018]. Moreover, in proliferating human glioblastoma stem-like cells which have many NSC properties, inhibition of SOCE was sufficient to drive them into quiescence [Galli, R *et al*, 2004][Aulestia, FJ *et al*, 2018]. Quiescent glioblastoma stem-like cells showed reduced SOCE and more efficient Ca^{2+} uptake by mitochondria [Aulestia, FJ *et al*, 2018]. These early results on the role of Ca^{2+} reveal a new prospect for understanding NSC quiescence and activation, which is very intriguing as the Ca^{2+} signaling is involved in the activation of stem cells including intestine stem cells, HSCs, MuSCs and follicle stem cells [Horsley, V et al, 2008][Tatsumi, R et al, 2009][Deng, HS et al, 2015][Umemoto, T et al, 2018], Moreover, Ca^{2+} influx is closely connected with cell excitability and is elicited by neurotransmitters which regulate NSC quiescence such as glutamate [MacDermott, AB *et al*, 1986][Berg, DA *et al*, 2013]. Thus, the Ca^{2+} signaling pathway is an intriguing candidate to investigate in *Drosophila* NB quiescence.

1.4 Project aims

The main objectives of my PhD are to find novel regulators of *Drosophila* neural stem cell quiescence and activation. The project is divided into two parts.

(i) Attempts to activate potential adult neural stem cells in *Drosophila* by neuronal/glial hyperactivity (chapter 2)

(ii) Validation and functional testing of genes that are enriched during quiescence in larval neural stem cells, with a focus on genes involved in cell excitability (chapter 3, 4 and 5)

2. Astrocytes Derived Seizures Induce Cell-Cycle Re-entry In the Adult *Drosophila* Brain

2.1 Introduction

2.1.1 Brain Plasticity in Adult *Drosophila*

Cell proliferation in mature brains was first described in rats more than 50 years ago [Altman,1962, 1963]. Since then, adult neurogenesis and gliogenesis have been found in many vertebrate and invertebrate species including humans [Sullivan *et al*, 2007][Eriksson *et al*, 1998]. Adult-born neurons and glia are involved in many important functions, including learning, memory and brain repair (also see 1.1.2)[Goldman. S *et al* 1983][Magavi. S*, et al*, 2005][Mckenzie *et al*, 2014].

In adult *Drosophila* brains, cell proliferation is present albeit in a very limited manner. In the wild type brain, S phase marker BrdU (Bromodeoxyuridine) incorporation is only found in 2-4 cells after 10 days of continuously labelling [von Trotha, J *et al*, 2009][Kato, K *et al*, 2009]. Those BrdU+ cells are found almost exclusively around the root of the antennal nerve [von Trotha *et al*, 2009][Kato, K *et al*, 2009]. Ectopic BrdU+ cells are induced by neural injury using needle poking, suggesting the mitotically dormant cells in the adult brain reactivate upon injury [Kato, K *et al*, 2009]. Moreover, the great majority of BrdU+ cells in adult brains co-stain with a glial marker, Repo, but never with the neuron marker Elav [von Trotha *et al*, 2009] [Kato *et al*, 2009]. This suggests only glia are born in the adult, although we cannot exclude the possibility that adult-born neurons do not express Elav, or the Repo positive cells are like the rodent radial glia which function as adult neural progenitors [Merkle, FT *et al*, 2004]. Using the clonal labelling technique Perma-Twin, Fernandez-Hernandez and colleagues claimed they found adult NSCs as well as adult-generated neurons in the optic lobe [Fernandez-Hernandez, I *et al*, 2013]. However, their results could not be reproduced in our lab by Dr Abhijit Das. Therefore, the question of adult neurogenesis in *Drosophila* remains open for further investigation.

2.1.2 A NSC-specific gene *deadpan* is active in a sub-population of adult astrocytes

In order to identify potential adult NSCs, Abhijit Das (Andrea Brand lab) investigated the expression of known NSC specific genes in the adult brain. Surprisingly, a ~3.5kb fragment of the *deadpan (dpn)* enhancer was found consistently to drive GAL4 expression in a fraction of adult astrocytes, which are charaterised by their unique position and morphology as large, multi-branched cells enwrapping the neuropil [Figure 2.1(a)(b)]. In the larval brain, this -GAL4 driver showed the same expression pattern as Deadpan protein, suggesting it is indeed a reporter of *deadpan* gene transcription [Abhijit Das and Andrea Brand, unpublished]. *Drosophila* astrocytes express the *astrocytic leucine-rich repeat molecule* (*alrm*) gene, the promoter of this gene was fused upstream of the GAL4 sequence to create the *alrm*-GAL4, a driver in most astrocytes [Doherty, J *et al*, 2009]. Interestingly, although astrocytes are present in the optic lobes, the *dpn*-GAL4 is expressed predominantly in central brain astrocytes.

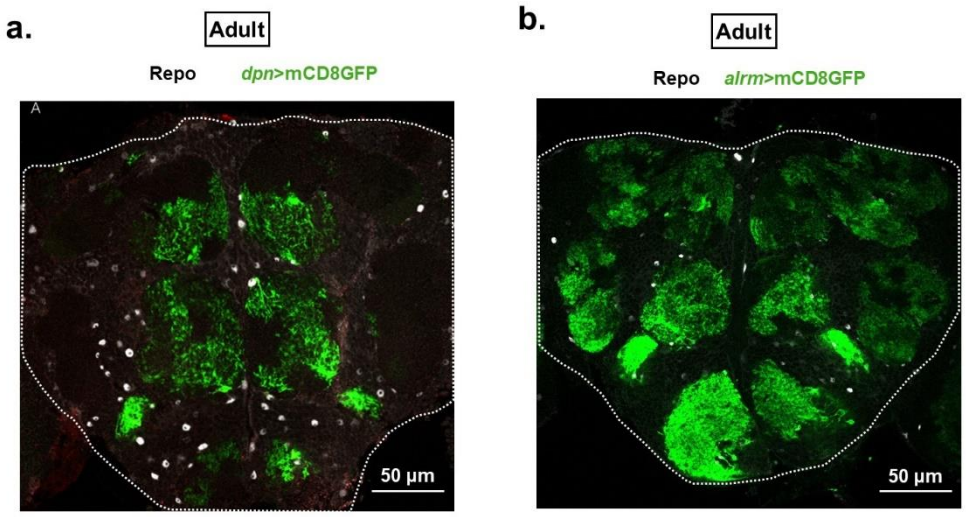

Figure 2.1 *deadpan*-GAL4 is expressed in a subpopulation of adult astrocytes (a) *dpn*-GAL4 is expressed in a subset of adult astrocytes. White: glia. Green: *dpn*-GAL4>mCD8GFP. White line outlines the central brain. **(b)** Distribution and morphology of astrocytes in the adult brain. White: glia. Green: *alrm*-GAL4> mCD8GFP. White line outlines the central brain.

Although the *dpn*-GAL4 driver showed a stable expression pattern in adult astrocytes, the protein itself was very elusive. Antibody staining against Deadpan shows weak staining in a small proportion of *dpn*-GAL4+ astrocytes [Abhijit Das and Andrea Brand, unpublished]. However, most *dpn*-GAL4+ astrocytes did not show any Deadpan staining at all [Abhijit Das and Andrea Brand, unpublished]. We therefore hypothesised

that Deadpan protein is only transiently expressed in a sub-population of adult astrocytes. Interestingly, in adult rodent brains, a sub-population of astrocytes also function as neural stem cells [Doetsch, F *et al*, 1999][Johansson, C.B *et al*, 1999], or have neurogenic potential when stimulated [Magnusson, JP *et al*, 2014].

2.1.3 Astrocytes are NSCs in adult mammalian brains

In rodents, adult NSCs are predominantly found in two neurogenic regions: the subgranular zone of the dentate gyrus (DG) in the hippocampus, and the subventricular zone (SVZ) lining the lateral ventricle [Altman, J & Das, GD, 1965][Altman, J, 1969]. The neural progenitors in the DG and SVZ derive from radial glial cells during prenatal development and continuously give rise to neurons and glia throughout adult life [Palmer, T *et al*, 1997][Merkle, FT *et al*, 2004][Su, H *et al*, 2007]. Interestingly, adult neural progenitors share many markers with astrocytes, such as GLAST (EAAT1), S100beta and GFAP [Doetsch, F *et al*, 1999][Seri, B *et al*, 2001][Kriegstein, A *et al*, 2009]. In particular, neurogenic astrocytes in the DG show similar electrophysiological properties to other astrocytes, which suggests they may retain the classical astrocytic functions such as supporting neurons and synaptic activities [Fukuda, S *et al*, 2003]

Neurogenic astrocytes in the DG and SVZ represent only a small subpopulation of astrocytes in the adult brain. The majority of astrocytes do not proliferate under normal conditions [Frison, J, 2016]. However, it has been shown in the adult mouse brain that upon experimentally induced stroke, astrocytes in the parenchyma, a normally non-neurogenic region, enter the cell cycle and give rise to new neurons [Magnusson, JP *et al*, 2014]. This finding suggests that mammalian astrocytes are capable of adopting the neural stem cell fate when stimulated. This leads to an interesting question: do *Drosophila* astrocytes have the same potential?

Drosophila astrocytes share remarkable similarities with their mammalian counterparts [Awasaki, T *et al*, 2008][Stork, T, *et al*, 2014]. Morphologically, they both extend several main branches, which further branch many times into a dense meshwork of processes. *Drosophila* and mammalian astrocytes both heavily infiltrate the surrounding neuropil and their fine processes are closely associated with synapses [Stork, T *et al*, 2014][Allen, NJ and Eroglu, C, 2017]. Functionally, *Drosophila*

astrocytes are able to uptake GABA via the GABA transporter and modulate synaptic activity, a function that is conserved in mammalian astrocytes [Stork, T *et al*, 2014][Boddum, K *et al*, 2016]. As in mammals, the astrocytic glutamate transporter EAAT1 is expressed in *Drosophila* astrocytes and the astroglial membrane responds to local synaptic glutamate release [Stork, T *et al*, 2014].

Taken together, the expression of a NSC specific gene in the astrocytes of adult *Drosophila* raises intriguing possibilities. We hypothesised that the *dpn*-GAL4+ astrocytes, or even the entire astroglial population in adult *Drosophila* brains might be quiescent neural progenitors. We therefore tested if we could stimulate them to divide and give rise to new neurons.

2.1.4 Brain hyperactivity triggers neurogenesis in the adult mammalian brain

As previously reviewed in 1.1.2, adult neurogenesis in mammals can be enhanced by many factors. One of those neurogenic stimuli is neuronal hyperactivation, which is the direct cause of seizures [Parent, J *et al*, 1997][Scott, B *et al*, 2000]. In experimental animals, there are three ways of modelling seizures: 1) electroconvulsive shock using earclip electrodes 2) systemic administration of kainic acid (KA), a glutamate receptor agonist 3) systemic administration of pilocarpine, a muscarinic acetylcholine receptor agonist [Ben-Ari, Y, 1985][Vaidya, V *et al*, 1999]. All three treatments activate quiescent NSCs in the adult rodent hippocampus, leading to new neurons and glia [Segi-Nishida, E *et al*, 2007][Lugert, S, 2010][Covolan, L *et al*, 2000]. In particular, KA-induced seizures at high dose causes the NSCs to divide symmetrically [Sierra, A *et al*, 2015]. This led to the generation of reactive astrocytes rather than neurons, as well as depletion of the NSC pool [Sierra, A *et al*, 2015].

Interestingly, although most studies on seizures and neurogenesis focused on NSCs in the hippocampus, it was reported that electroconvulsive seizures increase the number of newborn glia in the frontal cortex [Madsen, T *et al*, 2005]. This result suggests that non-neurogenic glia cells can also respond to neuronal hyperactivity with increased proliferation, presumably to repair the damaged brain tissue.

2.1.5 A glial basis of seizures in mammals and *Drosophila*

Although neuronal hyperactivation is the direct cause of seizures, the role of glia in the genesis and propagation of seizures has been gradually revealed in recent years [Robel, S & Sontheimer, H, 2016]. In particular, the roles astrocytes play in seizures attracted most interest due to their function in modulating synapses and coordinating neuronal activities [Haydon, P & Camignoto, G, 2006][Gomez-Gonzalo, M *et al*, 2010][Chever, O *et al*, 2016]. Ample experimental evidence has shown that astrocytes buffer extracellular neurotransmitters via a Ca^{2+} dependent mechanism. Increasing intracellular Ca^{2+} in astrocytes induces glutamate release, which leads to synchronised firing in neighboring neurons [Parpura, V *et al*, 1994][Tian, G *et al*, 2005]. Also, Ca^{2+} influx via the transient receptor channel A (TrpA) is responsible for the localised, near-membrane Ca^{2+} microdomains in rat astrocytes [Shigetomi, E *et al*, 2011]. Reducing this influx reduces GABA transport via GAT3, which consequently up-regulates the extracellular GABA and enhances the inhibitory synapses [Shigetomi, E *et al*, 2011].

In summary, astrocytes are excitable cells that respond to Ca^{2+} influx. Elevation of astrocytic Ca^{2+} promotes neuronal firing by releasing the excitatory neurotransmitter glutamate as well as uptaking the inhibitory neurotransmitter GABA. It is worth noticing that all the above-mentioned data were gathered in either cell culture, brain slices or isolated brains. Therefore, it was unclear if astrocytic hyperactivity was sufficient to cause seizures in freely behaving animals.

Although *Drosophila* glia exhibit morphological and functional similarities to their mammalian counterparts, the relationship between glia and seizures in flies is less well-studied. *Drosophila* cortex glia display near-membrane Ca^{2+} oscillations similar to what has been observed in mammalian astrocytes [Shigetomi, E *et al*, 2011][Melom, J & Littleton, J, 2013]. Disrupting these oscillations by mutating the glial specific $Na^{+}/Ca^{2+},K^{+}$ exchanger *zydeco* increases the animals' susceptibility to seizures [Melom, J & Littleton, J, 2013]. Also in the same paper, the authors induce pan-glial Ca^{2+} influx by activating ectopically expressed the *Drosophila* homolog of TrpA channel (dTrpA1) [Melom, J & Littleton, J, 2013]. This immediately induces severe seizures and paralyses the animals. The authors speculate the reason to be the impairment of BBB glia. Two more recent publications discuss the role of the glial

K^+/Cl^- cotransporter and Na^+/K^+ pump in *Drosophila*, suggesting the importance of glial K^+ homeostasis to avoid seizures [Rusan, Z *et al*, 2014][Hope, K *et al*, 2017].

In summary, we have found a subset of *Drosophila* adult astrocytes that possibly express the NSC marker *deadpan,* although no protein level evidence was found. Since a subset of astrocytes in rodents are adult NSCs which can be activated by seizures to proliferate, I decided to test whether inducing seizures in the adult fly brain could trigger astrocytes to divide.

2.2 Neuronal/Glial misexpression of dTrpA1 induces seizures and death in adult *Drosophila*

In order to investigate if seizures are sufficient to induce neurogenesis in the adult fly brain, I designed a reliable paradigm to produce seizures. As described in 2.1.4, in mammalian epilepsy models, seizures are induced by either electro-shocking the animals using earclip electrodes or systemic injection of neurotransmitter receptor agonists, neither are feasible in flies. More importantly, both treatments affect neurons and glia at the same time, which makes it impossible to dissect the origin of seizures. The cell-type specific expression tools available in *Drosophila* allowed me to induce seizures by directly hyperactivating neurons or glia using ectopically expressed cation channels. The cation channel I selected was dTrpA1 for the following reasons. First, it is regulated by temperature change, which allows rapid activation and inactivation. Second, its activation threshold is 26°C, which allows activation and inactivation within the temperature range for long term survival (18°C-29°C) [Pulver, S *et al*, 2009]. Third, Melom & Littleton (2013) have described that the pan-glial activation of dTrpA1 is sufficient to cause seizures.

The GAL4/UAS system was used for cell-type-specific hyperactivation of neurons and glia [Brand & Perrimon, 1993]. The drivers I used to overexpress dTrpA1 in neuron and different glial subtypes are listed in Table 1. Although the dTrpA1 channel activates at 26°C, the animals only developed immobilising seizures quickly at 32°C. Therefore, I used 32°C as the experimental condition for inducing seizures in all following experiments.

Table 2.1 Seizures induction in the adult brain when dTrpA1 is driven by cell-type specific drivers

GAL4 Driver	Expression	Seizures (32°C for 2 hours)
***nSyb*-GAL4**	mature neurons	yes
***repo*-GAL4**	all glia	yes
***alrm*-GAL4**	astrocytes	yes
NP6293-GAL4	perineurial glia	no
***moody*-GAL4,*mdr65*-GAL4**	sub-perineurial glia	no
cyg4g15-GAL4	cortex glia	yes

When dTrpA1 was activated in all mature neurons using *nSyb*-GAL4 as the driver, the animals experienced immobilising seizures within 30 minutes [Figure 2.2(a)]. Males were paralysed much more quickly than females (~10 minutes vs ~30 minutes). The animals were kept in 32°C for 2 hours, the maximum time they could resume mobility after induction of seizures. 7 days after induction of seizures, no lethality was observed in either males or females [Figure 2.2 (b)].

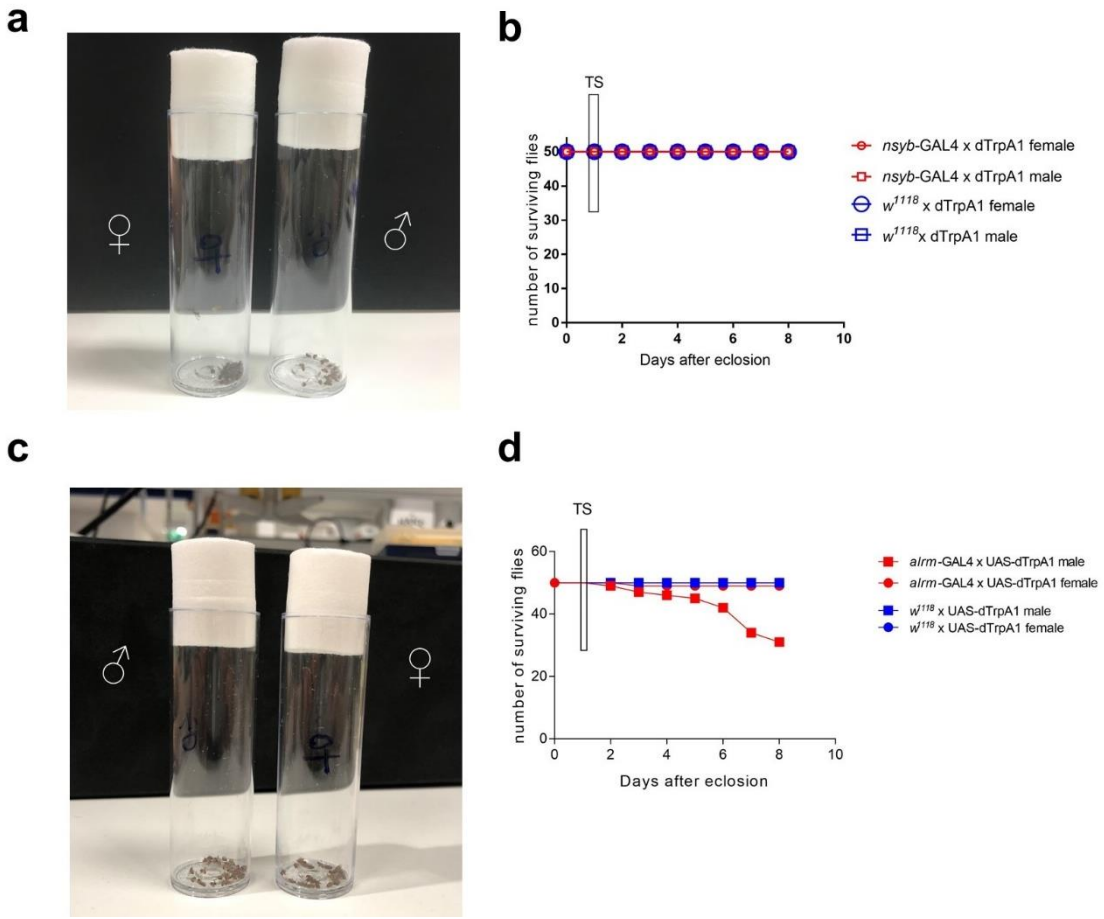

Figure 2.2 Activation of ectopically-expressed dTrpA1 in neurons and astrocytes (a) Activation of dTrpA1 in neurons caused seizures in both male (right) and female (left) adult flies. **(b)** Activation of dTrpA1 in neurons did not cause death in either male or female adult flies. n=50 flies per group. TS: temperature shift **(c)** Activation of dTrpA1 in astrocytes causes seizures in both male (left) and female (right) adult flies. **(d)** Activation of dTrpA1 in astrocytes is more lethal to males than females. n=50 flies per group. TS: temperature shift

As described in Melom & Littleton, 2013, pan-glial activation of dTrpA1 lead to acute seizures and paralysis of adult flies. This result was recapitulated under my experimental conditions. However, 30 minute induction of pan-glial seizures was enough to kill all animals [data not shown]. Therefore, I looked to hyperactivate different glial sub-types instead. As anticipated, activation of cortex glia caused immobilising seizures in adult flies with high lethality (similar to pan-glial induction, data not shown). Astrocytic hyperactivation also caused seizures and death [Figure 2.2 (c)(d)]. As with neuronal hyperactivation, male flies were paralysed more quickly than females. This difference between males and females was consistently observed

and not surprisingly, more male flies died than female flies 7 days after seizure induction [Figure 2.2 (d)].

Hyperactivating either the perineural or the sub-perineural glia did not lead to seizures at 32°C and no death was observed afterwards. These results suggest that seizures caused by pan-glial hyperactivation are not a result of disrupted BBB glia, contrary to what Melom & Littleton had predicted [Melom & Littleton, 2013].

2.3 Astrocyte-derived, but not neuron-derived seizures, induce EdU incorporation in the adult *Drosophila* brain

After I established a reproducible way to induce seizures in adult *Drosophila*, the next step was to investigate if seizures were sufficient to trigger cell proliferation in the brain. I used the nucleotide analog 5-ethynyl-2'-deoxyuridine (EdU) as a marker to trace adult-born cells. In vivo labelling of EdU was achieved by feeding the animals with food containing EdU (see Material and Methods). Adults that eclosed within 24 hours were collected and fed on EdU for another 24 hours, then they received a 2 hours temperature shift. In order to mark every adult-born cell, I continuously fed the animals with food containing EdU until the day of sacrifice.

I tested if hyperactivating neurons were sufficient to induce cell proliferation in the adult brain. The animals were sacrificed 7 days after the temperature shift (ATS) and continuously fed on EdU-containing food. As shown in Figure 2.3 (a), in both control and test brains, EdU+ cells were only found around the roots of the antennal nerves, consistent with what von Trotha, J *et al* (2009) and Kato, K *et al*, (2009) reported. No EdU+ cells above baseline were found in either sex [Figure 2.3 (b)]. No elevation of EdU+ cells was observed 7 days ATS. Therefore, although hyperactivation of neurons induces severe seizures in adult flies, it is not sufficient to cause EdU incorporation.

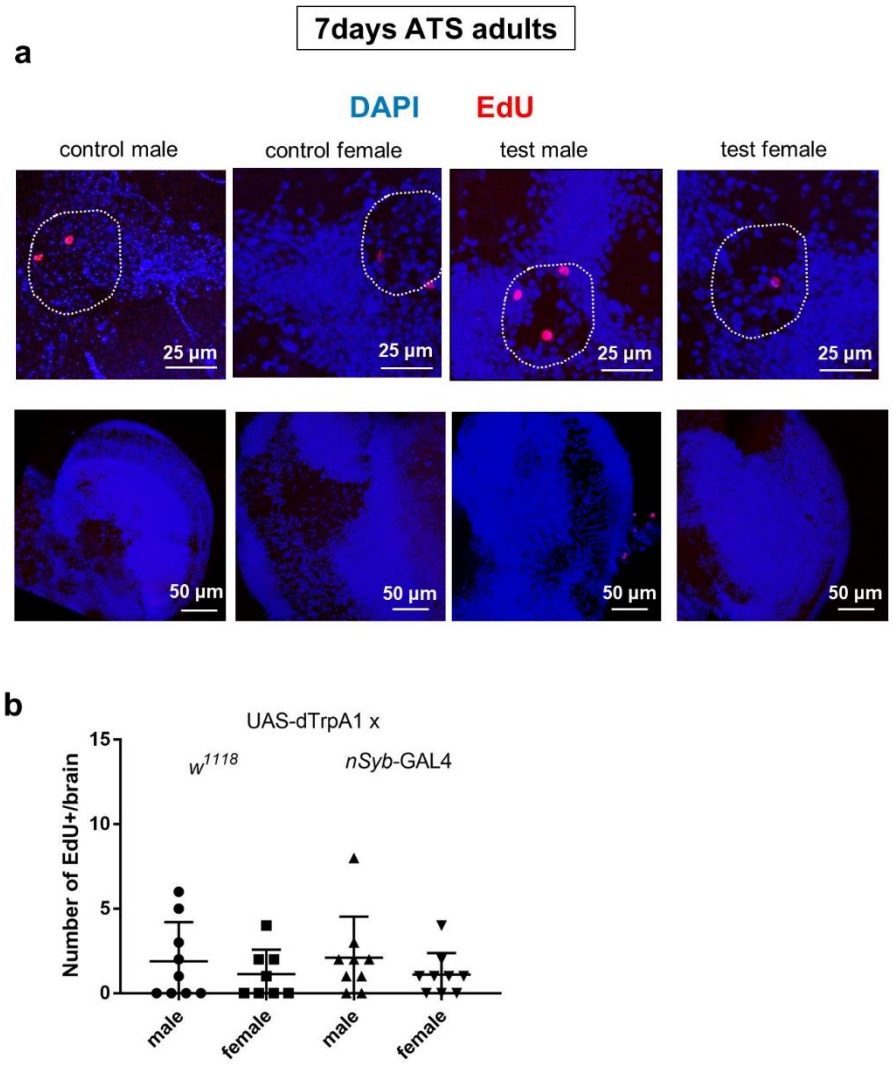

Figure 2.3 Induction of seizures by hyperactivating neurons does not lead to EdU incorporation in the adult brain (a) EdU+ cells (red) were found near roots of antennal nerve (marked by white dash) and the surrounding area. No EdU+ cells were ever observed in the optic lobe. Blue: nuclei stained with DAPI, all images were z-projections **(b)** Quantification of total EdU+ cell number per brain in (a), n=8-9 brains per genotype; p=0.70, Kruskal–Wallis H-test. Horizontal bar indicates median. Error bar indicates SD.

I next conducted hyperactivation of different glial subtypes to see if cell proliferation could be induced. Hyperactivating BBB glia did not cause seizures in adult flies. It was not surprising that no EdU incorporation above the baseline was observed after BBB glia hyperactivation [Figure 2.4]. As described in 2.2, hyperactivation of cortex glia for a very short period led to ~100% lethality within a day. Therefore, I could not obtain EdU incorporation data from the cortex glia-derived seizure group.

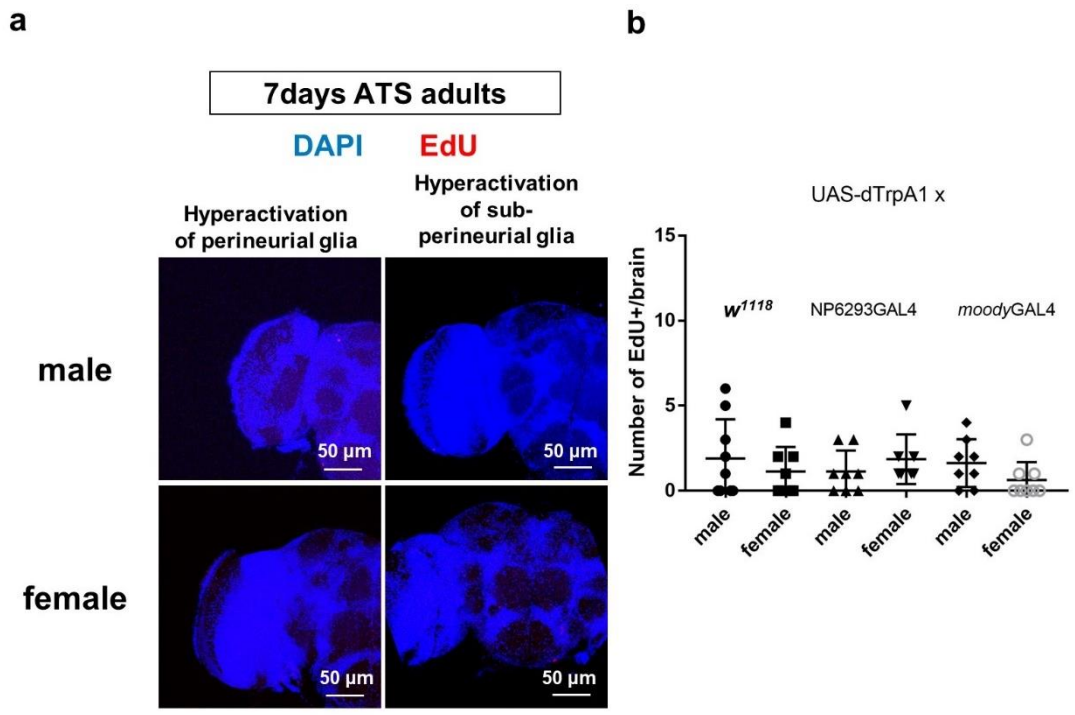

Figure 2.4 Hyperactivating BBB glia does not lead to EdU incorporation in the adult brain (a) Optic lobes and parts of the central brain (z-projection) from flies of corresponding genotype and sex. Blue: nuclei stained with DAPI. Red: EdU. **(b)** Quantification of total EdU+ cells per brain in (a), n=7-8 brains per genotype; p=0.43, Kruskal–Wallis H-test. Horizontal bar indicated mean. Error bar indicates SD.

Hyperactivating the astrocytes led to seizures in adult *Drosophila* and the severity of seizures depended on the sex of animals. The reason is not known but could be attributed to 1) the GAL4 driver is more strongly expressed in males or 2) male flies are naturally more susceptible to seizures [discussed in 2.7]. Therefore, I analysed EdU incorporation 7 days after astrocyte hyperactivation in male and female brains, respectively. Strikingly, in male brains and male brains only, there were a very large number of EdU+ cells compared to controls [Figure 2.6]. Moreover, while in the control brains no EdU+ cells were ever seen in places other than the antennal nerve root, the EdU+ cells induced by astrocytic seizures could be found anywhere in the brain, especially in the optic lobe. The penetrance of this phenotype was around 65% and the number of EdU+ cells vary from 5 cells per brain to 62 cells per brain [Figure 2.5 (a)(b)]. This finding suggests that many cells in the adult brain that never divide under physiological conditions maintain their ability to reenter the cell cycle. I confirmed that this phenotype was indeed the result of seizure induction, as astrocytic expression of

dTrpA1 without temperature shift did not induce EdU incorporation in male brains [Figure 2.5 (c)].

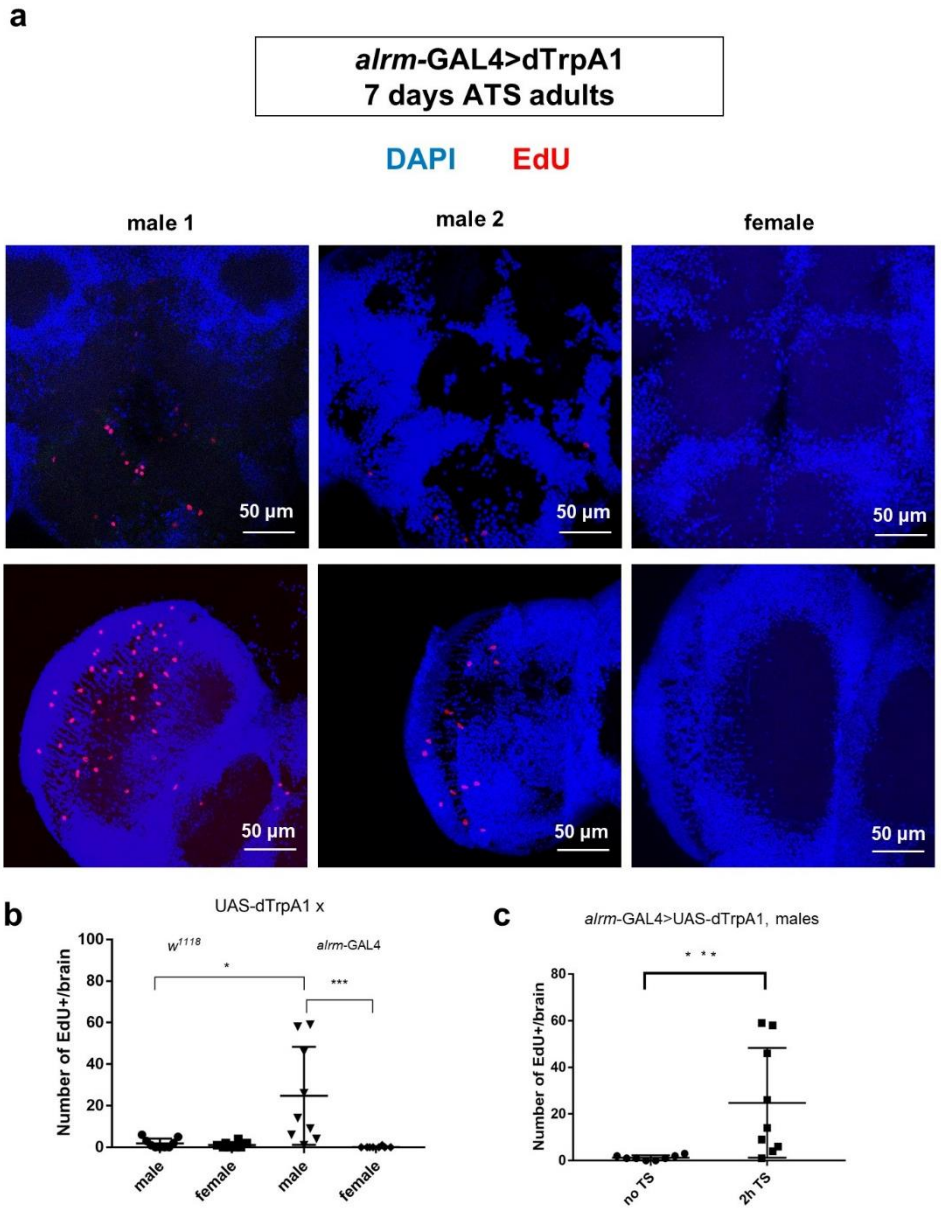

Figure 2.5 Hyperactivating astrocytes lead to significant EdU incorporation in male adult brains. (a) Brains (z-projection) of adult flies 7 days after astrocytic seizure induction. Top lane, left and middle: two male brains (showing central brain area) with different numbers of ectopic EdU+ (red) cells, right: a female brain (showing central brain area) showing no extopic EdU+ cells. **(b)** Quantification of EdU+ cells per brain in control and test groups subjected to 2 hour temperature shift. n=8-9 brains per genotype. Kolmogorov-Smirnov test. *:p<0.05, ***:p<0.001. Horizontal bar indicated mean. Error bar indicates SD. **(c)** Comparison of the total number of EdU+ cells in astrocytic dTrpA1 expression brains, with or without temperature shifts. p=0.0007, Kolmogorov-Smirnov test. Horizontal bar indicated mean. Error bar indicates SD.

2.4 Identity of EdU+ cells induced by astrocytic hyperactivation

2.4.1 EdU+ cells induced by astrocyte derived seizures have both astrocytic and non-astrocytic identities

I started this project hypothesising that astrocytes are the quiescent NSCs in adult *Drosophila* brains. Therefore, the next step was to find out if the EdU+ cells induced by astrocytic seizures were astrocytes or derived from astrocytes. Intriguingly, although astrocytes with EdU incorporation were occasionally found [Figure 2.6 (a)], most EdU+ cells did not express the astrocyte marker *alrm*-GAL4. Instead, they located in close proximity to the soma of EdU- astrocytes [Figure 2.6 (b)]. Whether these cells were astrocytes that had lost astrocytic identity or non-astrocytes stimulated by hyperactivation of neighboring astrocytes was not known.

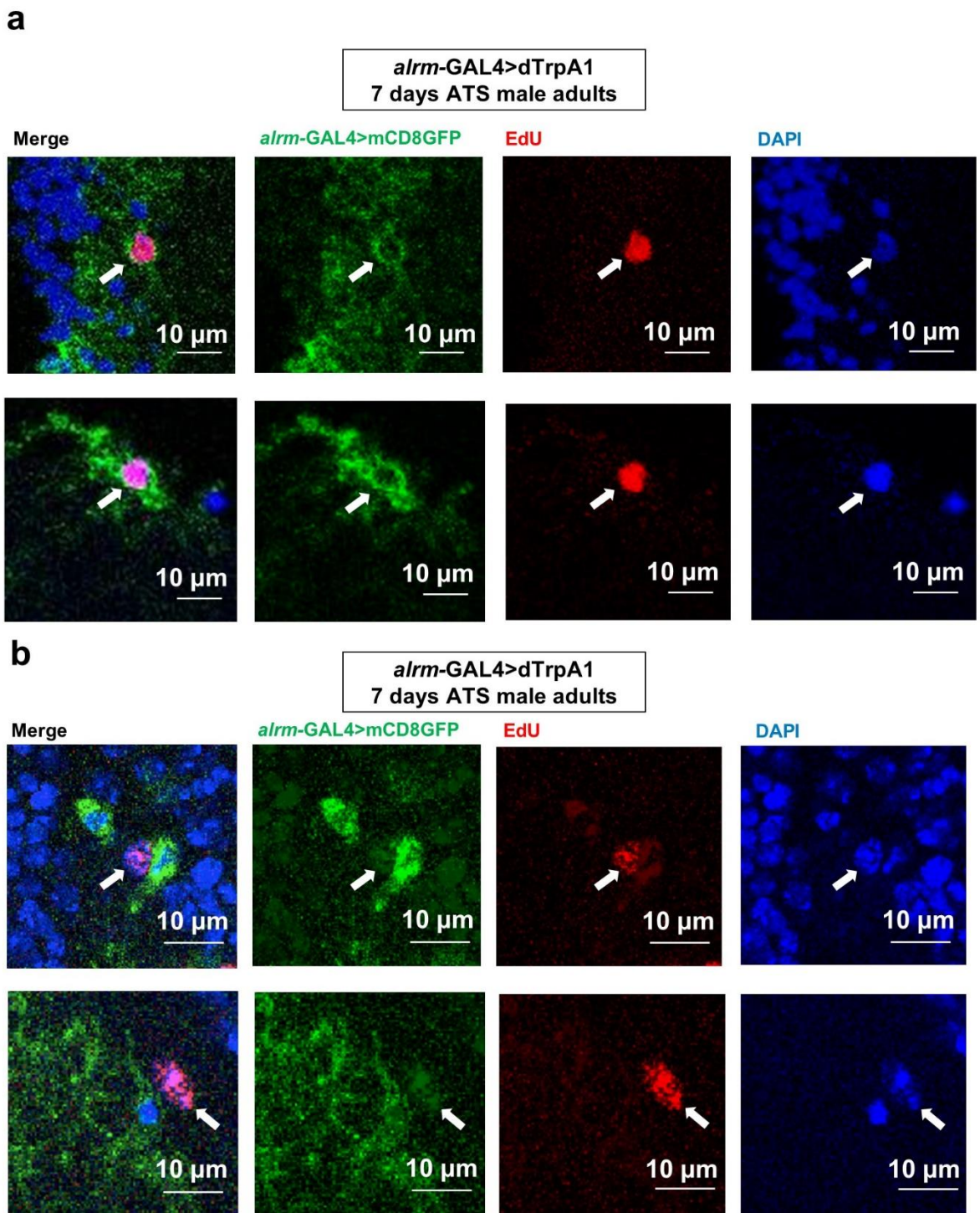

Figure 2.6 EdU+ cells induced by astrocyte derived seizures have both astrocytic and non-astrocytic identities. (a) EdU+ cells (red) that express the astrocytic marker *alrm*-GAL4 (reported by membrane GFP shown in green). **(b)** EdU+ cells (red) that do not express the astrocytic marker *alrm*-GAL4 (reported by membrane GFP shown in green), but are located next to the soma of EdU- astrocytes.

2.4.2 The majority of EdU positive cells in the adult brain express glial but not neuronal markers

To determine if adult neurogenesis occured after hyperactivation of astrocytes, I checked the identity of EdU+ cells by costaining with the glial marker Repo and the neuronal marker Elav. As shown in Figure 2.7, the majority of EdU+ cells (~80%) expressed Repo, while no EdU+ cells were ever found to express Elav. Therefore astrocytic hyperactivation is not sufficient to induce adult neurogenesis. Interestingly, the naturally occurring EdU+ cells in the adult brain showed almost exactly the same ratio, i.e, ~80% Repo+ and ~20% Repo/Elav double negative [von Trotha, J *et al*, 2009][Kato, K *et al*, 2009]. This coincidence might imply similar origins/fates of cells that undergo S phase in the adult brain under physiological and pathological conditions.

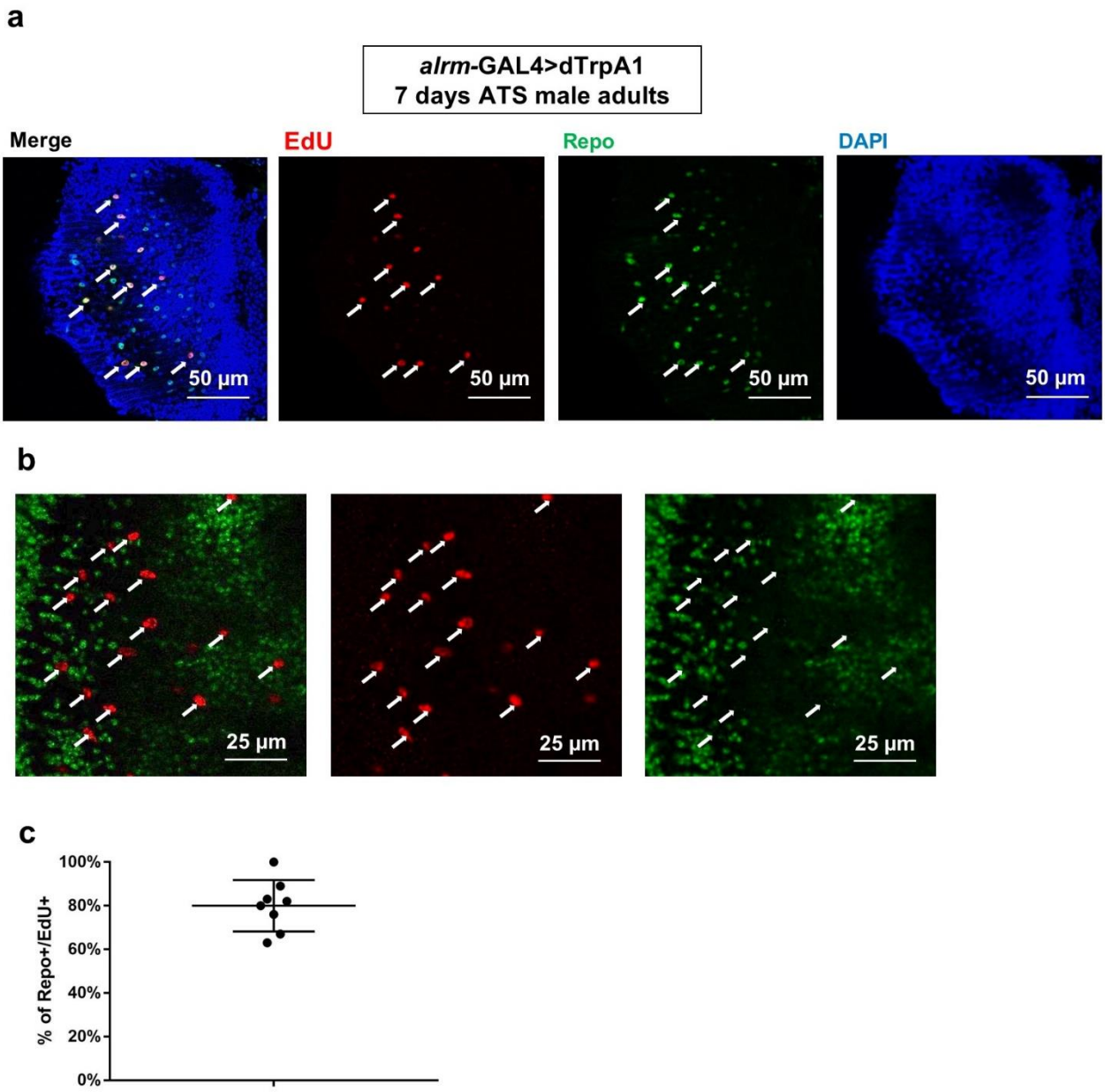

Figure 2.7 Identity of ectopic EdU+ cells induced by astrocyte hyperactivation. (a) The optic lobe (z-projection) of an 8 day old adult male (7 days after seizure induction). White arrow: cells that are positive for both Repo (green) and EdU (red) **(b)** The optic lobe of an 8 days old adult male (7 days after seizure induction, z-projection). No EdU+ (red) cell is also Elav+ (green) White arrow: cells that are positive for Elav. **(c)** Quantification of the percentage of Repo+ cells among EdU+ cells. n=8 brains. Horizontal bar indicates mean. Error bar indicates SD. Horizontal bar indicates mean.

2.4.3 The EdU positive cells in the adult brain lack the M-phase marker pH3

Although EdU is often used as a cell proliferation marker, cells that incorporate EdU could have gone through endoreplication or DNA repair rather than cell division. A

more direct indication of cell division is the M-phase marker phosphorylated Histone H3 (pH3). pH3 staining is reported to be completely absent in the adult brain, presumably because of the extreme low frequency of cell division (2-4 EdU+ cells per brain) [von Trothan, J *et al*, 2009][Kato, K *et al*, 2009]. However, although a large number (up to 130) EdU+ cells could be induced by astrocytic hyperactivation, no pH3 staining was ever detected in my experiments [Figure 2.8]. Moreover, if cell division happened on a large scale, nuclei 'couplets' that had not finished telophase should be observed. However, the EdU+ nuclei I observed in the adult brain had a very scattered pattern [Figure 2.7, 2.8]. Taken together, it seems unlikely that the EdU+ cells induced by astrocytic hyperactivation had actually undergone mitosis.

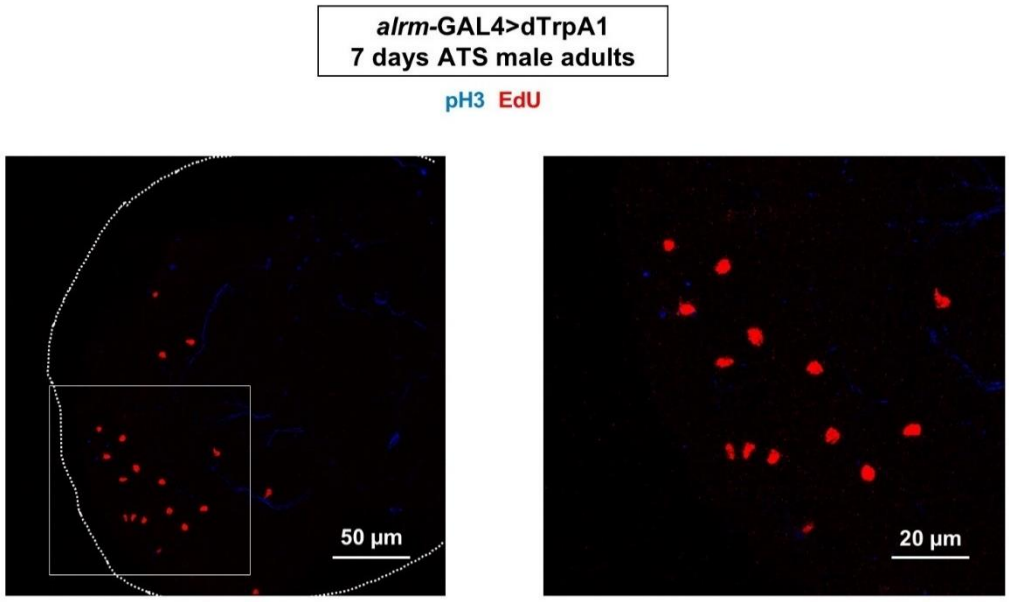

Figure 2.8 Ectopic EdU+ cells induced by astrocytes hyperactivation are not in M-phase
Left: Optic lobe from a male fly 7 days after astrocytic hyperactivation. White dash: Outline of the optic lobe. Right: Magnified image of the white framed area. Notice that no EdU+ cells co-stain with the M-phase marker pH3.

2.4.4 DNA contents of EdU positive cells in the adult brain do not exceed 4N

The fact that cells in the adult brain incorporate EdU but do not divide, points to the possibility of endoreplication, where cells undergo only the S-phase but not the rest of the cell cycle. Endoreplication occurs in the *Drosophila* subperineurial glia (SPG) during larval development [Unhavaithaya, Y and Orr-weaver, TL, 2012]. In order to wrap the rapidly expanding brain of 3rd instar larvae, SPG endoreplicate to increase in size [Unhavaithaya, Y and Orr-weaver, TL, 2012]. The average DNA content of a 3rd

instar larval SPG range from 5C to 22C, depending on their location in the brain (C value represents the haploid genome content), while the DNA content of a non-endoreplicating cell should not exceed 4C [Unhavaithaya, Y and Orr-weaver, TL, 2012].

In order to test if endoreplication occured in the EdU+ cells induced by astrocytic seizures, I used the same method Unhavaithaya, & Orr-weaver used to measure DNA content [Unhavaithaya, Y and Orr-weaver, TL, 2012]. The DAPI intensity of EdU+ nuclei was measured using the image processing software Volocity and normalized against the adjacent Elav-positive neurons, which are supposed to be post-mitotic and diploid. The result is plotted in Figure 2.9 (a). Three conclusions could be drawn immediately from the data. First, most cells had DNA content above 2C and many were above 3C, which suggested DNA replication had occurred rather than just DNA repair. Second, the DNA content of all the cells I measured never exceeded 4C, which excluded the possibility of endoreplication. Third, although the DNA content in EdU+ cells did not exceed 4C, there were cells that had DNA content very close to 4C, suggesting they were at the S/G_2 transition phase.

It has been reported in various cell types that cell cycle can be arrested at G_2 phase [Agarwal, M *et al*, 1995][Jowett, JBM *et al*, 1995][Galvin, KE *et al*, 2008]. In particular, quiescent NBs in *Drosophila* larval brains are predominantly G_2-arrested [Otsuki, L and Brand, AH, 2018]. Interestingly, some EdU+ cells induced by astrocytic seizures have DNA content close to 4C but do not divide, suggesting they could also be G_2-arrested cells. In order to test this hypothesis, I used Cyclin A as a marker for cells in the G_2 phase [Figure 2.9 (b)][Hayashi, S. and Yamaguchi, M., 1999]. As expected, I found both Cyc A+ and Cyc A- EdU+ cells induced by astrocyte-derived seizures [Figure 2.9 (b)]. The DNA content of those Cyc A+ cells was unknown due to lack of DAPI staining in the same sample. However, the expression of Cyc A in a subset of EdU+ cells suggests these cells have re-entered the cell cycle and were arrested at the G_2 phase for unknown reasons.

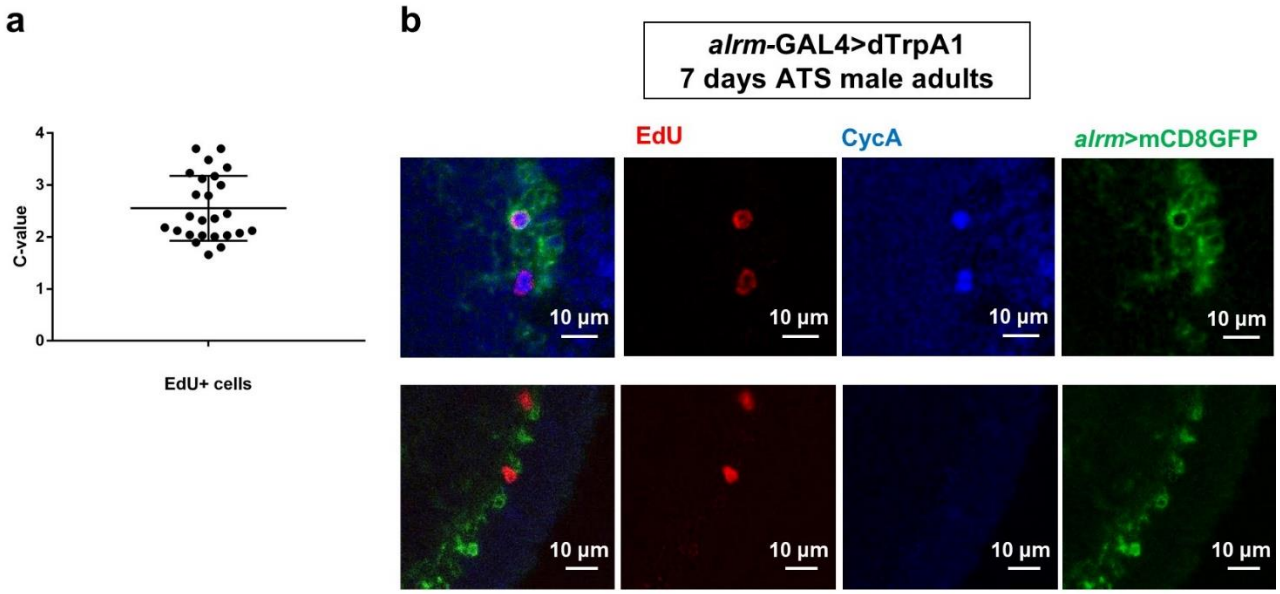

Figure 2.9 Analysis of cell cycle stages of EdU+ cells induced by astrocytic seizures. (a) Quantification of DNA content of EdU+ cells in adult central brains and optic lobes. Each data point represents DNA content from a single cell. Data are gathered from 2 brains. Error bar indicates SD **(b)** Top lane: EdU+ cells (red) induced by astrocytic seizures that expressed Cyclin A (blue). Bottom lane: EdU+ cells (red) induced by astrocytic seizures that did not express Cyclin A (blue).

2.5 The number of EdU+ cells increases over time after astrocytic seizure induction

In order to capture as many adult-born cells as possible, all experiments I have done so far were on brains dissected 7 days after seizure induction, with continuous EdU labelling. To understand how seizures-induced EdU incorporation changes over time, I conducted a time-course experiment, examining male adult brains 1,2,3,7 days after astrocytic hyperactivation with continuous EdU labelling. As shown in Figure 2.10 (b), there was a gradual increase of EdU+ cells after seizure induction.

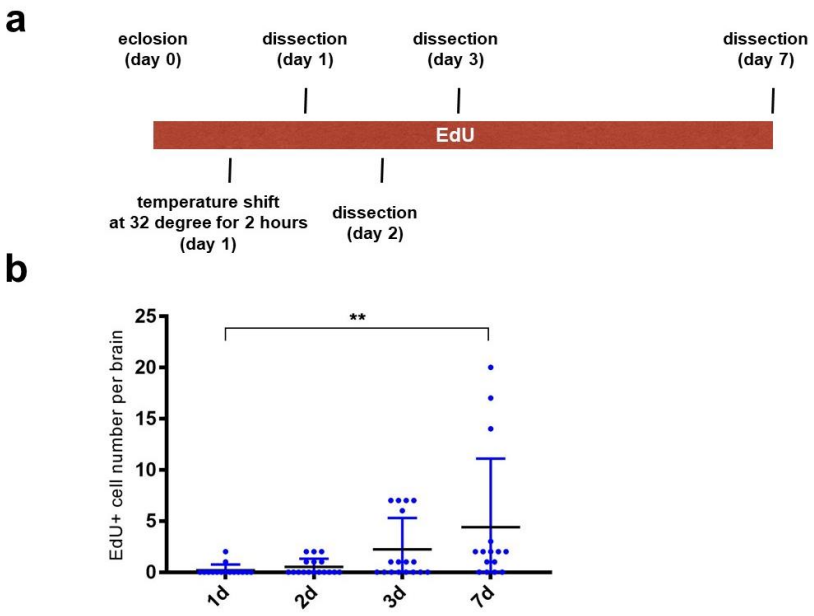

Figure 2.10 The number of EdU+ cells increases over time following astrocytic seizure induction with continuous EdU labeling (a) Experimental timeline of EdU feeding, seizure induction and sacrifice. **(b)** Quantification of EdU+ cells in male adult brains after astrocytic depolarization. n=15-17 brains per time point. Dunn's non-parametric multiple comparison, 1d vs 7d, p=0.0013, 1d vs 2d, 3d, not significant. Error bar indicates SD. Horizontal bar indicates mean.

Continuous EdU labelling showed a significant increase in EdU+ cells over time after astrocyte-derived seizures. There could be two reasons behind this: 1) more cells in the adult brain re-entered the cell cycle over time after seizures induction, but no cell division happened. 2) cells that incorporated EdU divided. One way of testing the two hypotheses is a pulse-chase experiment. If cells incorporated EdU had divided, the number of EdU+ cells should increase after the animals stopped feeding on EdU. Otherwise the number of EdU+ cells should stay the same. The animals were given EdU for 4 days, and their brains were dissected immediately or after another 4 days without EdU. As shown in Figure 2.11 (b), although there was an increase in average EdU+ cell number (2.2 vs 4.8), the possibility this increase was caused by chance could not be rejected (p=0.22, Mann-Whitney test). This observation was in agreement with the absence of pH3 staining as well as the very scattered distribution of EdU+ cells. So far, all evidence pointed to the absence of cell division in the adult brain after astrocytic hyperactivation, despite the appearance of many ectopic EdU+ cells.

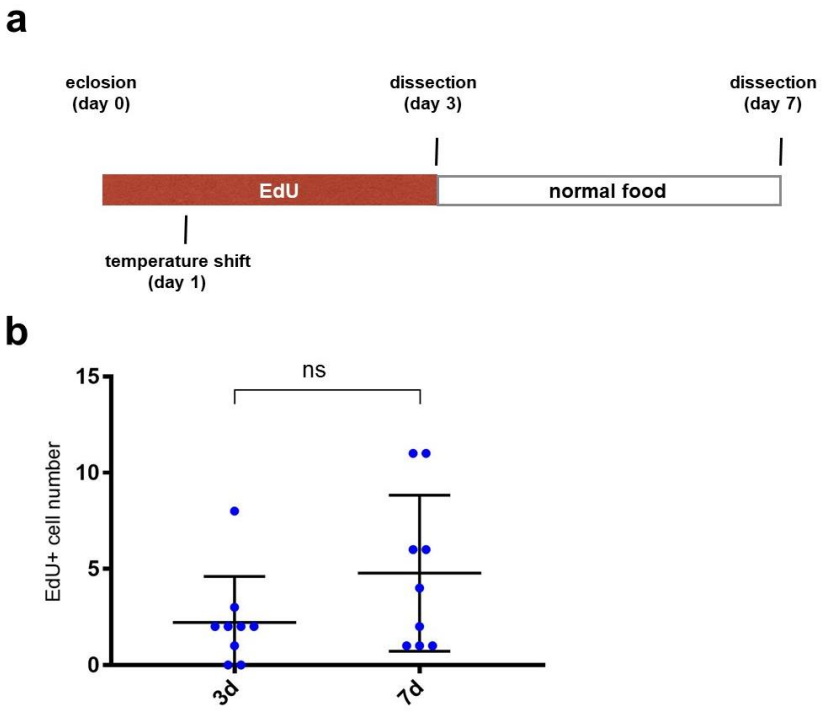

Figure 2.11 The number of EdU+ cells does not increase over time following astrocytic seizure induction with pulse-chase EdU labelling (a) Experimental timeline of EdU feeding, seizure induction and sacrifice. **(b)** Quantification of EdU+ cells in male adult brains after astrocytic depolarization. n=9 brains per time point. p=0.22, Mann-Whitney non-parametric test. Error bar indicates SD. Horizontal bar indicates mean.

2.6 Depolarisation of astrocytes using other cation channels also induces seizures and cell cycle reentry

I have confirmed that activation of dTrpA1 in astrocytes is sufficient to cause seizures and cell cycle reentry in male adult brains. Although dTrpA1 is widely used as a depolarisation tool in neurons [Berni, J *et al*, 2010][Doulea, J *et al*, 2011][Bidaye, S *et al*, 2014], more evidence is needed to conclude that astrocytic depolarisation is sufficient to drive seizures and EdU incorporation in the adult brain. Also, dTrpA1 is a non-selective cation channel that is permeable to monovalent and bivalent cations [Clapham, DE *et al*, 2001]. It would be interesting to dissect which cation is responsible for the phenotypes caused by dTrpA1.

I expressed two selective cation channels, NaChBac and dOrai/Stim complex in adult astrocytes, respectively. NaChBac is a Na^+ selective bacterial channel and dOrai/Stim

complex allows Ca^{2+} flux into the cytoplasm [Hewavitharana, T *et al*, 2007] [Charalambous, K and Wallace, BA, 2011]. The ubiquitously-expressed, temperature-sensitive GAL4 suppressor $GAL80^{TS}$ was used to restrict NaChBac and Orai/Stim misexpression only to adults [McGuire, S.E *et al*, 2003][also see 7.5.2].

2.6.1 Astrocytic misexpression of NaChBac causes seizures and cell cycle re-entry in adult fly brains

As shown in Figure 2.12 (a), after 24 hours of NaChBac misexpression in astrocytes, adult flies developed seizure-like behaviour. Unlike the immobilising seizures induced by dTrpA1 activation, seizures induced by astrocytic expression of NaChBac did not restrict movement. The animals were able to walk, climb on the wall or fly, but frequently fell over because of uncontrolled leg and wing movement, which resembled generalized tonic-clonic epilepsy in human [Theodore, WH *et al*, 1994]. Up to 7 days after temperature shift (to activate NaChBac misexpression), no lethality was observed in either sex [Figure 2.12 (b)]. Although interestingly, like the immobilising seizures induced by dTrpA1, male flies were more susceptible to seizures induced by NaChBac, displaying much higher frequency of epileptic fits [Figure 2.12 (a)].

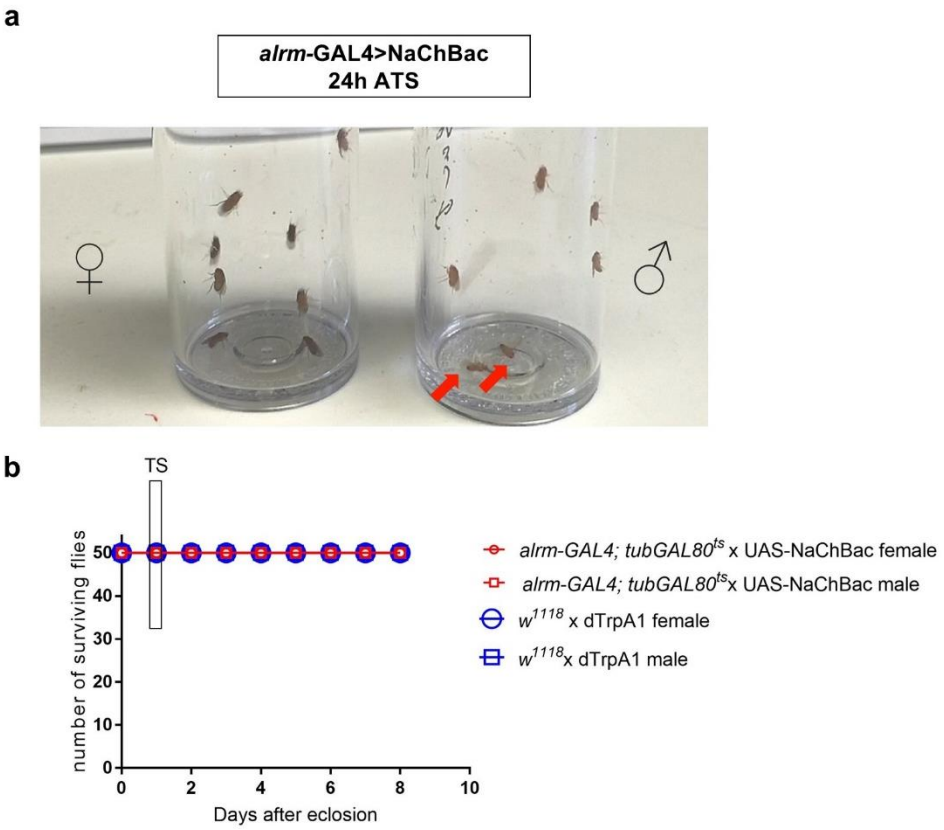

Figure 2.12 Misexpression of NaChBac in astrocytes causes seizures but not death in adult flies (a) Female flies (left) and male flies (right) after 24h of astrocytic expression of NaChBac. Red arrows: flies having epileptic fit. (b) Survival curves of flies with astrocytic expression of NaChBac and controls.

In order to test if NaChBac misexpression in astrocytes was sufficient to induce cell cycle reentry, I fed the animals with EdU containing food continuously and dissected the brains 7 days after temperature shift. No EdU+ cells were seen outside the root of antennal nerves. However, a small albeit significant increase of EdU+ cells (5.4 ± 2.0 vs 1.4 ± 1.2, n=8 brains per group) was observed in male adult brains, which was consistent with results obtained from dTrpA1 activation in astrocytes [Figure 2.13].

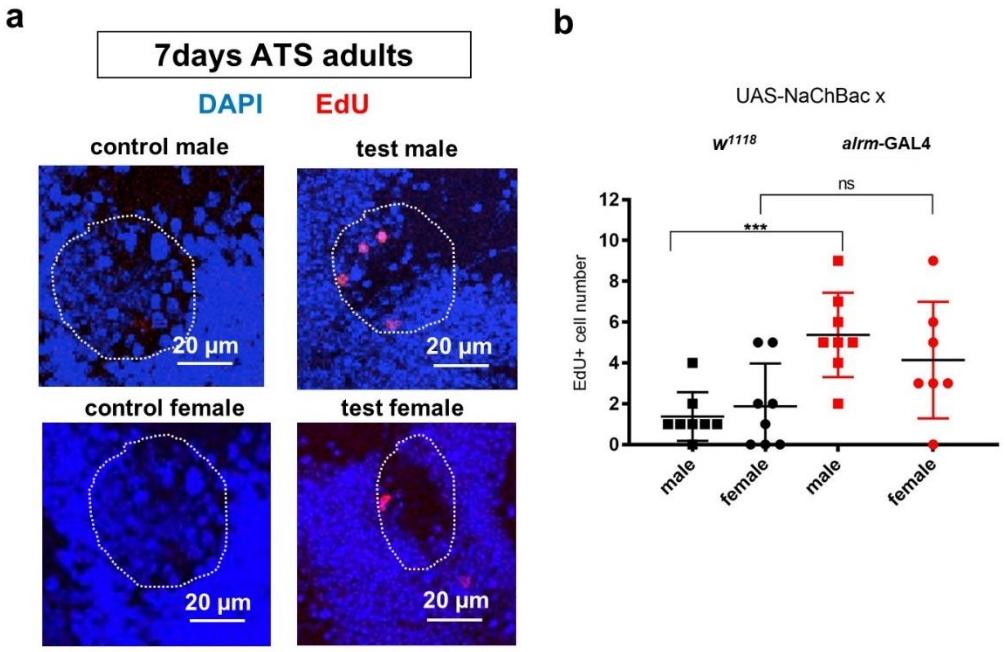

Figure 2.13 Misexpression of NaChBac in astrocytes induces an increase in EdU incorporation in male adult brains (a) Number of EdU+ cells (red) increases in male animals after misexpression of NaChBac in astrocytes. All EdU+ cells are found near the roots of antennal nerves (marked by white dash) **(b)** Quantification of EdU+ cells per brain. n=8 brains per group. ns: $p>0.05$. ***: $p<0.001$, Student's t-test, error bars indicate SD. Horizontal bar indicates mean.

2.6.2 Astrocytic misexpression of Orai/Stim complex causes seizures and cell cycle re-entry in adult fly brains, as well as death

Due to its high Ca^{2+} permeability, TRPA1 channels allow Ca^{2+} influx through the plasma membrane when activated [Clapham, DE *et al*, 2001][Karashima, Y *et al*, 2010]. As described in 2.1.5, Ca^{2+} influx into astrocytes has been shown to perturb neurotransmitter release and cause synchronised neuronal firing. I therefore misexpressed the Ca^{2+} specific dOrai/dStim complex in adults astrocytes to see if they recapitulate the phenotypes caused by dTrpA1 misexpression.

Drosophila Orai and Stim work synergistically as core regulators of store-operated Ca^{2+} entry (SOCE) [Hewavitharana, T *et al*, 2007][Venkiteswaran, G. and Hasan, G., 2009]. dStim is the ER store sensor located on the ER membrane[Hewavitharana, T *et al*, 2007][Venkiteswaran, G. and Hasan, G., 2009]. When the ER store is depleted, dStim couples with the plasma membrane Ca^{2+} specific channel dOrai to induce Ca^{2+} influx [Hewavitharana, T *et al*, 2007][Venkiteswaran, G. and Hasan, G., 2009]. They increase intracellular Ca^{2+} when co-misexpressed in *Drosophila* intestinal stem cells [Deng, HS *et al*, 2015]. Using the same UAS constructs that Deng, HS and colleagues used, I misexpressed the dOrai/dStim complex in adult astrocytes.

As shown in Figure 2.14 (a), 24 hours after astrocytic dOrai/dStim overexpression, the adult flies developed seizures. Unlike the NaChBac misexpression group, adult flies with astrocytic dOrai/Stim overexpression were immobilised with intermittent epileptic fits. dOrai/Stim overexpression was more lethal to male flies than female flies, consistent with previous results. Three days of astrocytic dOrai/Stim overexpression killed the majority of male flies and near 40% of female flies [Figure 2.14 (b)]. Therefore, I dissected the adult flies 3 days after temperature shift (to activate dOrai/Stim overexpression), with continuous EdU feeding. EdU assay showed significant increase of EdU+ cells appearing near the antennal nerve roots only in test male brains (8 ± 1.445 vs 0.75 ± 0.31, n=8-10 brains per group)[Figure 2.16 (b)]. In female brains, a small increase was observed but was not statistically significant [Figure 2.15 (b)].

Table 2.2 Numbers of EdU+ cells induced by astrocytic expression of different cation channels

	EdU feeding time	Test male	Test female	Control male	Control female
dTrpA1(non-selective)	7d	24.78 ± 7.85	1.13 ± 0.52	1.89±0.77	1.25±0.51
dOrai/Stim (Ca^{2+} only)	3d	8.00 ± 1.45	4.25 ± 1.16	0.88±0.31	2.13±0.75
NaChBac (Na^{+} only)	7d	5.40 ± 2.0	4.75 ± 1.01	1.38±0.74	1.88±0.42

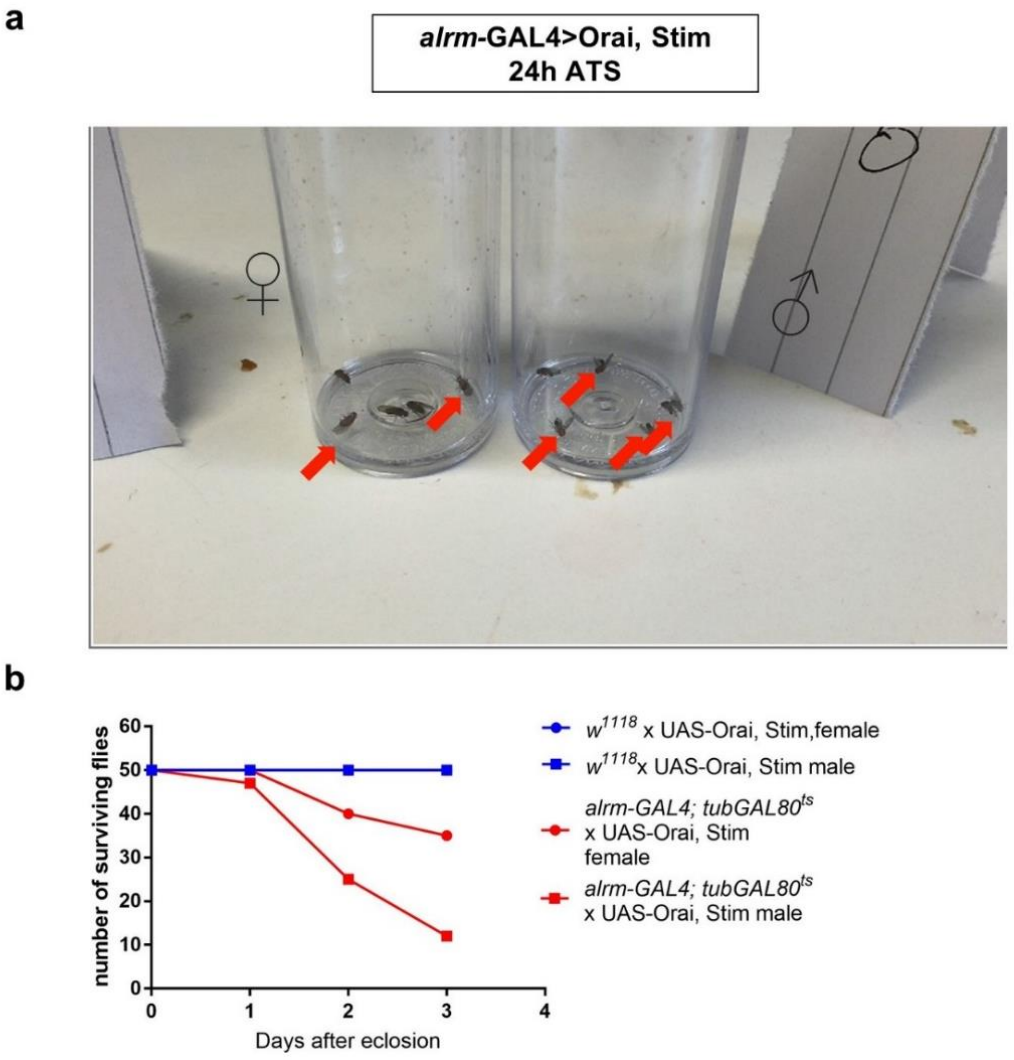

Figure 2.14 Misexpression of Orai &Stim in astrocytes causes seizures and death in adult flies (a) Female flies (left) and male flies (right) after 24h of astrocytic expression of Orai

and Stim. Red arrows: flies having epileptic fit. (b) Survival curves of flies with astrocytic expression of Orai and Stim compared to controls.

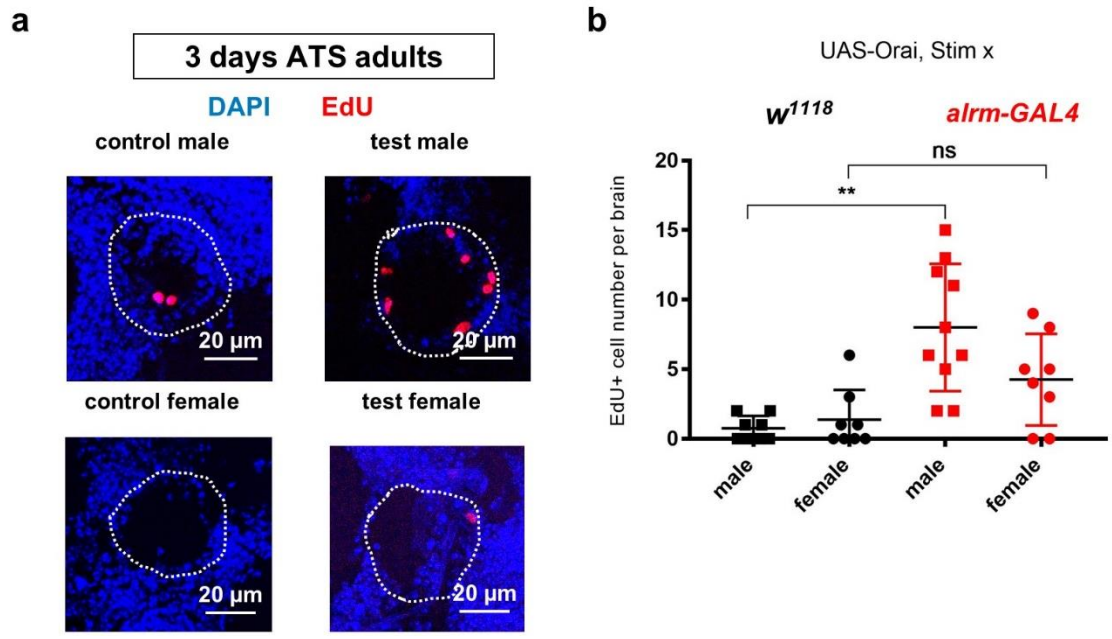

Figure 2.15 Misexpression of Orai &Stim in astrocytes induces an increase of EdU incorporation in male adult brains (a) Number of EdU+ cells (red) increased in male animals by misexpression of Orai and Stim in astrocytes. All EdU+ cells were found near the roots of antennal nerves (marked by white dash) and surrounding areas. **(b)** Quantifications of the number of EdU+ cells per brain. n=8-10 brains per group. ns: $p>0.05$. **: $p<0.01$, Student's t-test, error bars indicate SD. Horizontal bar indicates mean.

2.7 Chapter summary and discussion

In mammals, a subset of astrocytes function as adult NSCs. We found that in *Drosophila*, a subset of adult astrocytes express *dpn*GAL4, which could indicate the activity of the NSC marker gene *deadpan*. In this chapter, I tested the hypothesis that astrocytes are quiescent neural progenitors in the adult fly brain. In mammals, hyperactivating the brain activates adult NSCs and leads to the generation of new neurons and glia [Segi-Nishida, E *et al*, 2007][Covolan, L *et al*, 2000][Lugert, S, 2010][Sierra, A *et al*, 2015]. My results show that in the adult *Drosophila* brain, hyperactivation of astrocytes but not neurons causes cell cycle re-entry, but no evidence of new adult-born cells was found.

In mammals, seizure models all involve hyperactivating neurons and glia at the same time [Ben-Ari, Y, 1985][Pearce, B *et al*, 1986][Vaidya, V *et al*, 1999]. Using the cell type specific GAL4/UAS system, I was able to hyperactivate neurons and glia respectively. Surprisingly, I found that seizures induced by pan-neuronal hyperactivation caused much less lethality compared to seizures induced by pan-glial hyperactivation (no lethality after 2 hours seizures induction versus complete lethality after 30 minutes hyperactivation). This result agrees with previous findings that loss of cation equilibrium in glia cause seizures in flies [Melom, JE and Littleton,JT, 2013][Hope, K *et al*, 2017]. Moreover, in mammalian astrocytes, Ca^{2+} influx causes increased glutamate release, which leads to synchronised firing in neighbouring neurons [Tian, GF *et al*, 2005]. This could explain the fact that glial hyperactivation causes more severe phenotypes. When neurons are hyperactivated by forced cation influx, excitatory neurotransmitters like glutamate are released but then cleared by astrocytes [Anderson, CM. and Swanson, RA, 2000]. However, when astrocytes are hyperactivated, they release possibly higher level of glutamate and become less sufficient in uptaking extracellular glutamate [Tavares, RG *et al*, 2002][Tian, GF *et al*, 2005]. Taken together, my results provide new evidence for the debated theory that it is the excitability of glia (especially astrocytes) rather than neurons that underlies seizure initiation and propagation [Haydon, PG and Carmignoto, G, 2006][Carmignoto, G. and Haydon, PG, 2012].

It is well established in mammalian seizure models that hyperactivating the brain by chemical agents or electroconvulsive shock causes astrocytes to divide [Segi-Nishida, E *et al*, 2007][Covolan, L *et al*, 2000][Lugert, S, 2010][Sierra, A *et al*, 2015]. My results show that it is astrocytic rather than neuronal hyperactivation that cause cell cycle re-entry in the adult *Drosophila* brain. There are two possible explanations for this phenomenon. Astrocytic hyperactivation caused death in adult flies while neuronal hyperactivation did not. Thus we could speculate that astrocytic hyperactivation caused more damage to the brain, which might have triggered the cells to re-enter the cell cycle. On the other hand, hyperactivation in astrocytes *per se* might be required for cell cycle re-entry. I do not have any evidence to distinguish between the two possibilities and but both are supported by previous findings. On the one hand, apoptosis or mechanical lesions such as needle stabbing can also trigger glial proliferation in the adult fly brain [K, Kato *et al*, 2009]. On the other hand, sustained

Ca^{2+} elevation is a mitogenic signal in many cell types [Kojima, I *et al*, 1988][Failli, P *et al*, 1995][Deng, HS *et al*, 2015]. Also very recently, store-operated Ca^{2+} influx in mammalian NSCs have been shown to promote symmetrical division at the cost of asymmetrical division [Aulestia, FJ *et al*, 2018][Domenichini, F *et al*, 2018][Petrik, D *et al*, 2018][also see 1.3.2].

The majority of EdU+ cells induced by astrocytic hyperactivation express the glial marker Repo (~80%). The rest, 20% EdU+ cells, express neither the glial marker nor the neuronal marker Elav. It would be very interesting to see if the neuroblast marker Dpn is expressed by any of these EdU+ cells. Kato, K and colleagues report that glia incorporate the DNA synthesis marker BrdU in response to acute brain injury [Kato, K *et al*, 2009]. However, they could not find direct evidence of cell division such as the M phase marker pH3 [Kato, K *et al*, 2009]. They conclude that the lack of M phase makrer is due to the extreme low frequency of BrdU+ cells (<10 cells per brain). However, although the number of EdU+ cells induced by astrocytic hyperactivation was significantly higher (up to 130 cells per brain), I could not find evidence for mitosis, either. The DNA content of EdU+ cells induced by astrocytic hyperactivation is mostly between 2C-4C, which suggests they undergo DNA synthesis but are arrested at the S/G_2 phase. This is supported by the fact that some EdU+ cells also express the G_2 phase marker Cyclin A. Thus evidence points to the conclusion that glia in the adult fly brain enter the cell cycle upon brain injury but do not progress further than G_2 phase. This behaviour is different from neurogenic astrocytes in mammals. which proliferate in response to seizures and other types of injury [Segi-Nishida, E *et al*, 2007][Covolan, L *et al*, 2000][Lugert, S, 2010][Sierra, A *et al*, 2015].

The original purpose of my project was to test if astrocytes in adult fly brains are quiescent progenitors that can be activated by seizures and produce new cells. The answer is most likely to be no. Why would seizures induce cell cycle re-entry without proliferation? In mammalian brains, acute trauma triggers reactive astrogliosis [Sofroniew, MV, 2014][Liddelow, SA and Barres, BA, 2017]. Reactive astrogliosis reflects a spectrum of changes astrocytes undergo, including cellular upregulation of certain molecular markers, hypertrophy, and eventually proliferation to form glia scars [Sofroniew, MV, 2014][Liddelow, SA and Barres, BA, 2017]. Collectively, reactive astrogliosis acts as a double-edged sword. It counteracts acute stress and provides

neuroprotection [Pekny, M *et al*, 2014]. However, the formation of glia scars also prevents regeneration and therefore contributes to further tissue loss [Pekny, M *et al*, 2014]. Inhibition of cell cycle progression has been shown to reduce astrocytic scar in the adult mammalian brain and reduce neuron death [Di Giovanni *et al*, 2005]. Therefore, the cell-cycle arrest I observed might be a protective mechanism against further lesions to the adult brain.

One intriguing observation from my results is the difference between males and females in response to seizures. Males are significantly more sensitive to seizures induction and only the male brains incorporate significantly more EdU in response to astrocytic seizures. It is possible that the GAL4 driven expression of cation channels was stronger in males. Although all GAL4 drivers and UAS-misexpression constructs I used are located on auto-chromosomes, it is frequently observed that males carring mini-*white* markers on the autochromosome have deeper eye colouration compared to females of the same genotype. This possibility can be tested by doing qPCR of dTrpA1 in test animals.

Interestingly, studies in rodents and humans show that males are more susceptible to seizures than females and this difference might be due to sex hormones [Velíšková, J and DeSantis, KA, 2013]. However, my data shows that this sex dimorphism is conserved in flies which unlike mammals, do not have sex hormones. Therefore, the difference in neuronal excitability might reflect something more fundamental in the sex dimorphism of brains.

3. Analysis of *slowpoke*, a Ca^{2+}-activated potassium channel gene required for neural stem cell reactivation

3.1 Introduction

3.1.1 Quiescent neuroblasts extend an axon-like structure

Drosophila neuroblasts extend a conspicuous basal projection during quiescence [Chell, JM and Brand, AH, 2010][Leo Otsuki, Stephanie Norwood and Andrea Brand, unpublished]. This striking structure closely resembles axons [Figure 3.1]. To date, almost nothing is known about the function of this projection. However, its resemblance to axons suggests it could be communicating with other cell types in the brain.

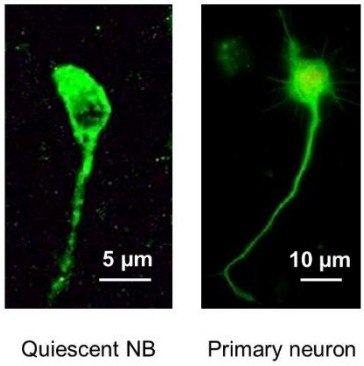

Figure 3.1 Quiescent neuroblasts extend an axon-like structure Left: a quiescent NB labelled with membrane GFP. Right: a cultured *Drosophila* primary neuron labelled with GFP [image adapted from Lu, W *et al*, 2013].

3.1.2 Mammalian neural stem cells respond to neuronal signals

Mammalian adult neural stem cells sit in a complex niche which consists of vasculature, ependymal cells, glia and neurons [Doetsch, F *et al*, 1997][Song, H *et al*, 2002][Riquelme, P *et al*, 2006] [Tavazoie,M *et al*, 2008]. Notably, adult neurogenesis in both hippocampus and subventricular zone is regulated by neurotransmitters. In mouse SVZ, neural precursors receive dopamine from axonal input which promotes proliferation [Hoglinger G.U *et al*, 2004]. In contrast, GABA produced locally in the SVZ negatively regulates neurogenesis [Liu, X *et al*, 2005]. Similarly, neural progenitors in mouse hippocampus receive GABA which inhibits their proliferation [Tozuka, T *et al*, 2005]. Further study shows that this GABA signaling comes from interneurons in the

dentate gyrus, which reinforces the concept that proliferation of neural stem cells is partly regulated by their neuronal niche [Song, J *et al*, 2012].

The fact that mammalian NSCs respond to neurotransmitters raises a fascinating possibility that NSCs may have neuronal-like electric activities. Indeed, spontaneous postsynaptic-like current is recorded in adult neural progenitors, which could be enhanced or subdued by GABA receptor agonists or antagonists [Tozuka, T *et al*, 2005]. It has also been shown in cultured rat adult neural progenitors that electric excitation is sufficient to promote neurogenesis, whether it is induced by electrophysiological stimuli or excitatory neurotransmitters such as glutamine [Deisseroth, K *et al*, 2004]. This is particularly interesting as it fits with my results that depolarisation of adult astrocytes is sufficient to trigger cell cycle reentry [Chapter 2].

In summary, abundant evidence has demonstrated that mammalian NSC proliferation is partially controlled by neuronal signals. Also, as discussed in 3.1.1, quiescent *Drosophila* neuroblasts share lots of similarities with neurons. This leads to an interesting hypothesis that quiescent *Drosophila* neuroblasts are excitable cells and their excitability affects quiescence and/or reactivation.

3.2 BK channel protein Slowpoke is expressed in quiescent neuroblasts

In order to assess neuronal activities in quiescent neuroblasts, I searched the quiescence-enriched gene list for genes that directly regulate neuronal excitability [Leo Otsuki, Janina Ander and Andrea Brand, unpublished]. I selected the gene *slowpoke (slo)* for further analysis. *slo* encodes the alpha-subunit of big-conductance Ca^{2+}-activated potassium channel (BK channel). In *Drosophila*, it is expressed in neurons, muscle, trachea and the midgut [Becker, M *et al*, 1995][Thomas, T *et al*, 1997]. However, no previous literature has described its expression or function in NBs. Therefore, it is a novel candidate in the context of neuroblast quiescence and reactivation.

3.2.1 Structure and known function of *slowpoke*

The gene *slowpoke* was first identified in a genetic screen as a mutation that abolished the Ca^{2+} dependent potassium current in flight muscles [Elkins, T *et al*, 1986]. Following genetic mapping and cloning it was revealed that it occupies a ~40 kb locus on the right arm of the 3rd chromosome [Atkinson, NS *et al*, 1991]. The *slo* gene has 24 transcripts generated by alternative splicing [Figure 3.2 (a)][Flybase] [Lagrutta, A *et al*, 1994]. These variants show a high degree of variability in Ca^{2+} sensitivity, unit conductance and kinetics of activation [Adelman, J *et al*, 1992][Lagrutta, A *et al*, 1994]. However, they all contain the featured structures of integral membrane voltage sensor, cytoplasmic Ca^{2+} sensor, K^+ conductance regulator and pore-forming domain [Figure 3.2 (b)][Schreiber, M *et al*, 1997][Jiang, Y *et al*, 2002][Wang, L *et al*, 2009][Yuan P *et al*, 2010]. The sequence of Slo differs extensively from other types of potassium channel, but it shares over 50% amino acid identities with mouse and human Ca^{2+} activated potassium channels [Atkinson, NS *et al*, 1991][Panllank, L *et al*, 1994].

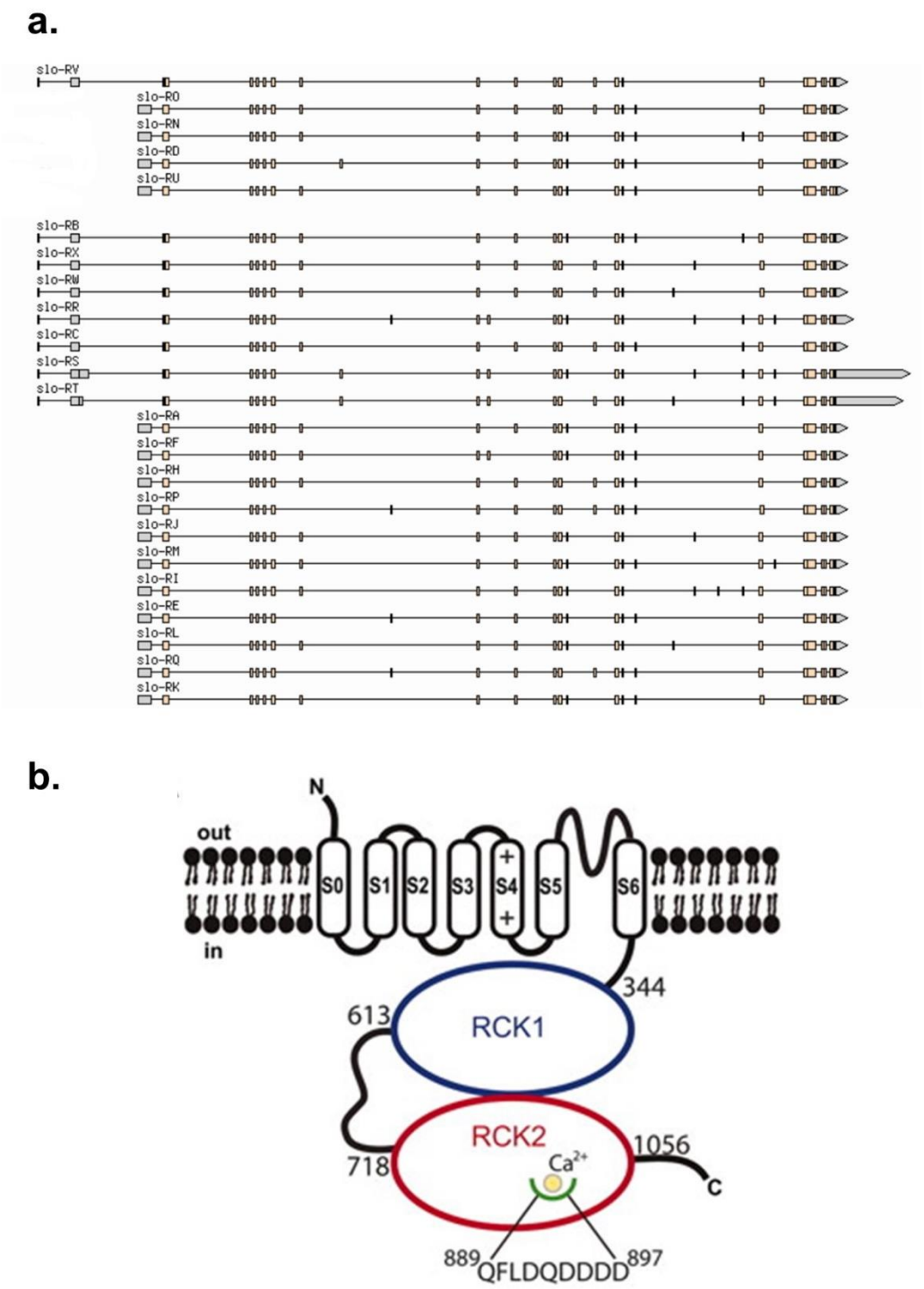

Figure 3.2 Structure of the *slo* locus and the Slo protein (a) Transcripts of the *slo* gene (Adapted from Flybase genome browser). Grey boxes: UTRs. Orange boxes: coding sequences. **(b)** Topology of the human Slo protein (adapted from Yuan P *et al*, 2010). The protein has seven transmembrane segments and one large cytoplasmic domain, which contains two regulators of K^+ conductance (RCKs) and one Ca^{2+} binding domain.

Slowpoke is a high-conductance potassium channel with dual gating mechanism. It is activated synergistically by membrane depolarisation and increased intracellular Ca^{2+}

concentration [Vergara, C *et al*, 1998][Magleby, K. L. 2003.][Cui, J *et al*, 2009]. Upon activation, it yields a rapid and large K^+ efflux current, which repolarises the membrane potential and closes voltage-gated channels, including Ca^{2+} channels. Thus, Slo negatively feeds back onto electric excitation and many cellular pathways that use Ca^{2+} as the secondary messenger.

From *C. elegans* to rodents, Slo is involved in many important physiological functions including neuronal activity, muscle contraction, blood pressure control and hearing [Fettiplace, R & Fuchs, P A, 1999] [Hu, H *et al*, 2001][Shao, L. *et al*, 2004][Sausbier, M *et al*, 2005][Carre-Pierrat, M.*et al*, 2006]. In neurons, Slo is a major repolarising force that negatively regulates neurotransmitter release [Wang, Z. *et al*, 2001][Raffaelli, G *et al*, 2004][Lee, J, *et al*, 2008][Ford, JK *et al*, 2014]. Loss of Slo increases the number of presynaptic boutons at the *Drosophila* NMJ [Lee, J & Wu, CF, 2010]. Also, suppression of Slo increases the spike broadening induced by frequent stimuli [Hu, H *et al*, 2001].

In summary, Slo is a major negative regulator of cell excitability in many different cell types including neurons. However, to my knowledge, no report to date has discussed the role of Slo or its homologues in neural stem cells.

3.2.2 *slo* is up-regulated in neuroblasts after quiescence entry

Targeted DamID analysis [generated by Janina Ander, PhD thesis, unpublished] indicates that *slo* is up-regulated in neuroblasts after quiescence entry. To verify this expression pattern, I used RNA *in situ* probes targeting a region shared by all *slo* transcripts. At pre-quiescence stage 14, no signal is detected in the CNS [Figure 3.3]. At stage 17 when all neuroblasts have become quiescent, clear signal of *slo* mRNA is detected in the entire CNS [Figure 3.3]. These results fit well with the Targeted DamID data and previous *in situ* hybridisations reported in Becker, M *et al* (1995). However, due to its pan-CNS expression pattern, the identity of cells expressing *slo* cannot be determined using this method.

Slo is an essential gene for balancing neuronal activity. Thus, it is not surprising that *slo* expression stays on in early L2 brains, when all neuroblasts are reactivated. The

expression is ubiquitous in the larval brain excluding the abdominal segments of VNC, which again makes it difficult to decide the identity of *slo* expressing cells [Figure 3.3].

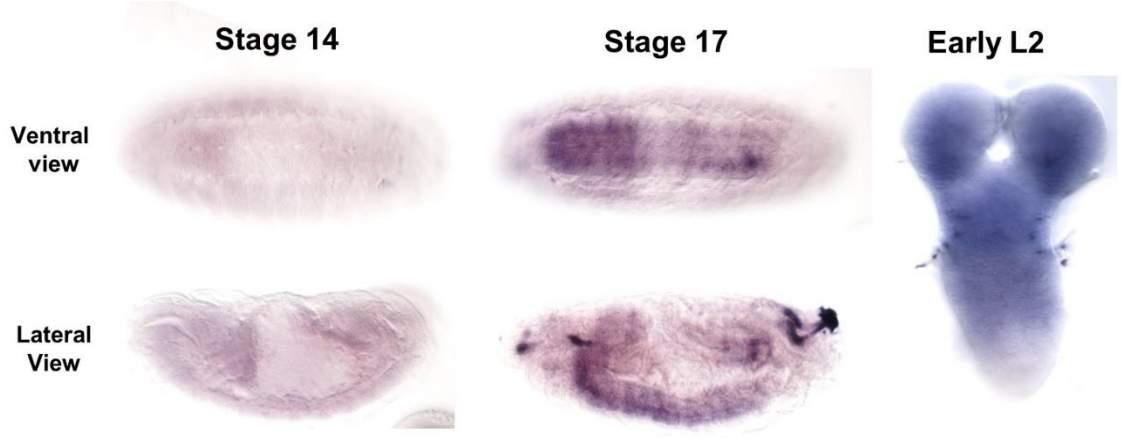

Figure 3.3 : *slo* starts to express in the CNS as neuroblasts become quiescent RNA *in situ* hybridisations against *slo* at different developmental stages.

3.3 RNAi mediated knockdown of *slo* leads to a near-complete loss of reactivation

In situ hybridisation revealed *slo* to be expressed after neuroblasts become quiescent (stage 17 vs late stage 14). Therefore, *slo* is unlikely to be required for quiescence entry. To test if *slo* is involved in reactivation, I knocked down *slo* using two RNAi lines from Vienne Drosophila Resource Centre (VDRC) (construct ID: GD 244, and KK 108671) using NB driver *wor*-GAL4. Both RNAi constructs caused significant reduction of reactivation at 24h ALH [Figure 3.4 (a)(b)]. To minimalise the chance of off-targets, I tested a non-overlapping TriP line (construct ID: JF02146), which also caused reactivation defects at 24 ALH [Figure 3.4 (a)(b)]. I also used *in silico* methods to check the specificity of the three RNAi constructs I used, which predicted no off-targets [Naito, Y *et al*, 2005]. Also, the line GD244 has been validated as causing a ~30% reduction of *slo* mRNA, which correlates with the more minor phenotype I obtained with this construct [Lee J and Wu CF, 2010][Scheckel, S *et al*, 2011].

Among the three *slo* RNAi lines I tested in neuroblasts, the line KK108671 caused the strongest effect. It resulted in a near-complete loss of reactivation at the beginning of L2 [Figure 3.4 (a)(b)]. More strikingly, most *slo* KD neuroblasts were still quiescent at the end of larval development (featured by quiescence projection or lack of progeny) [Figure 3.4 (c)]. Therefore, I decided to use KK108671 for further experiments. I will discuss the differences of the three RNAi constructs below.

For all three RNAi constructs I used（GD244, JF02146 and KK108671), they encode long hairpin RNAi. KK108671 and GD244 both target an coding-exon that is shared by all *slo* isoforms. The target sequence of KK108671 partially overlaps with that of GD244 by 174 bp, but KK108671 is longer (352 bp vs 291 bp) [Source: VDRC]. This could explain the why KK108671 is more efficient compared to GD244. JF02146 is 419 bp long and does not overlap with KK108671 and GD244. It targets the 3'UTR of all *slo* isoforms rather than the coding region. No published data regarding the efficiency of this construct is available to date.

KK108671 has been reported to cause significant reduction of Slo-specific current in *Drosophila* neurons [Kadas, D *et al*, 2015]. It belongs to the VDRC KK RNAi collection. 25% of the VDRC KK collection has been reported to ectopically enhance the Hippo signalling pathway due to a secondary landing site of the UAS-RNAi construct [Vissers, JH *et al*, 2016]. I have not verified if KK108671 carries this secondary landing site. However, in *Drosophila* NBs, activation of the Hippo pathway actually leads to premature reactivation [Ding, R *et al*, 2016]. Thus the strong reactivation delay phenotype KK108671 cause is unlikely to be the artefact of Hippo pathway enhancement.

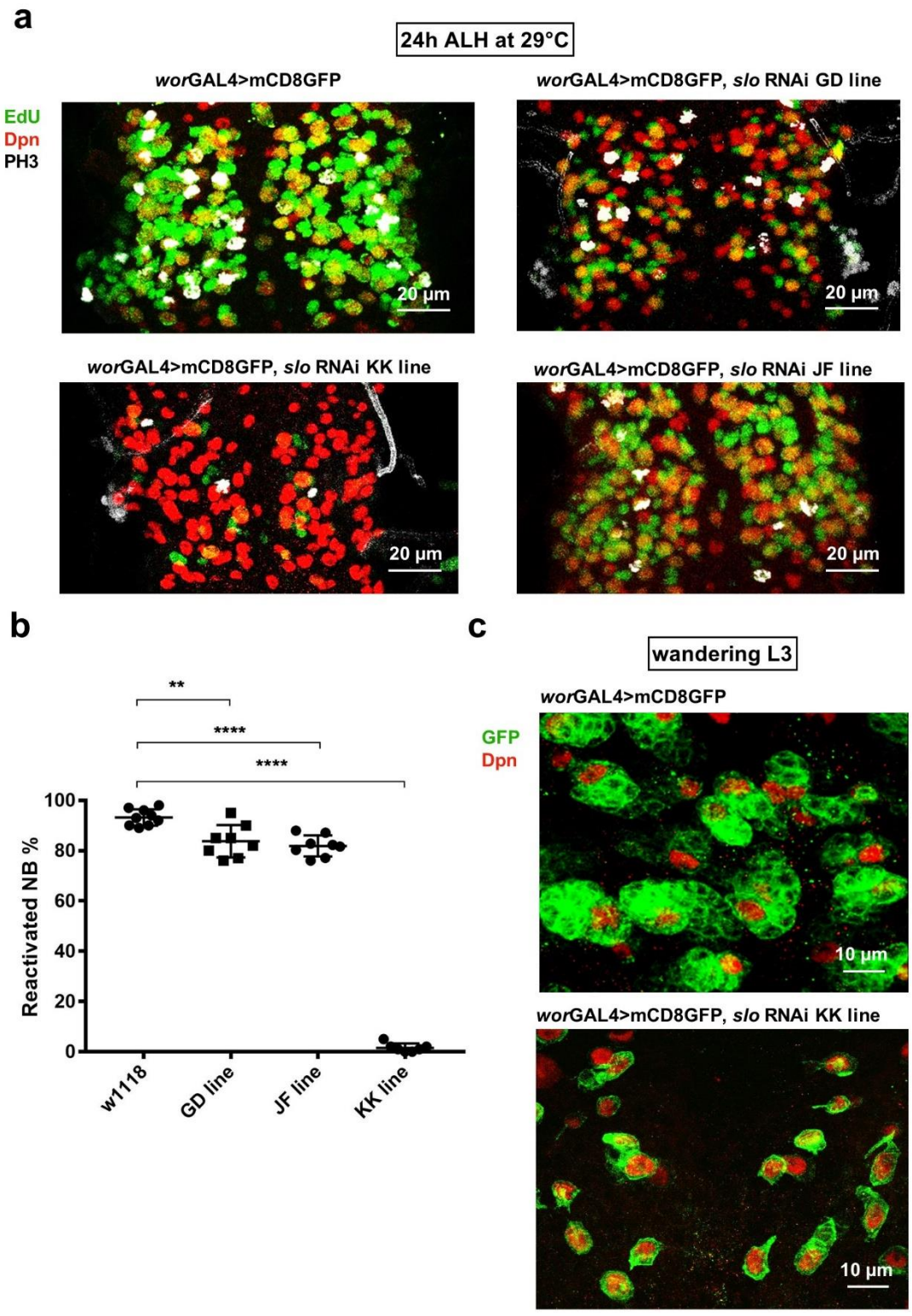

Figure 3.4 RNAi mediated knockdown of *slo* leads to a near-complete loss of reactivation (a) Reactivation in control brains (top left) and three *slowpoke* KD brains (top right: GD244, bottom left: KK108671, bottom right: JF02146). Assayed for EdU (green) incorporation and pH3 (white) staining in NB nuclei (red) **(b)** Quantification of the percentage of reactivated (pH3 and/or EdU-positive) NBs in each genotype (**, p<0.01, ****: p<1.0x10-4, n=8-9 brains per genotype, Student's T-test, error bars indicate SD. Horizontal bar indicates

mean. **(c)** NB lineages in control (left) and *slo* KD brains (KK 108671)(right) from wandering L3 larvae. Red: NBs. Green: membrane of NBs and their progeny.

To verify knockdown efficiency of KK108671, I conducted *in situ* hybridisations on brains of *wor*-GAL4>*slo* RNAi (KK108671) and controls (same probes as used in Figure 3.3). As shown in Figure 3.5, knocking down *slo* in NBs caused strong reduction of *slo* mRNA in the entire brain. This could be explained by the fact that GAL4 driver and siRNA in stem cells would inevitably be inherited by their progeny.

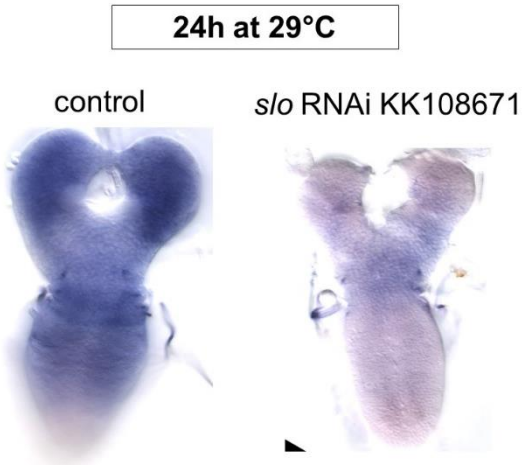

Figure 3.5 *slo* RNAi (KK 108671) causes significant knockdown of *slo* expression: *wor*-GAL4 was used to drive *slo* RNAi expression. Control (left) and KD brains (right) were dissected, fixed, hybridised at the same time to avoid variation between experiments. Both control and KD brains were allowed same amount of time for colour development.

It is well established that *slo* is expressed in mature neurons. It is important for the repolarisation of the membrane potential and release of neurotransmitters at the synapses [Lee, J. Wu, CF, 2010][Jepson JE *et al*, 2012][Jepson JE *et al*, 2014]. Since neuroblasts potentially make contact with neurons, I knocked down *slo* in mature neurons and assayed for neuroblast reactivation. No difference was observed in terms of reactivation timing [Figure 3.6]. Also, losing *slo* in mature neurons did not have apparent effect on the survival, development and behaviour at larval stage. No obvious abnormality in the test adults' behaviour was observed either, although their life span shortened significantly (50% died within a week after eclosion). The life span of *slo* mutant adults has not been described before. In terms of locomotor behaviour, slo^4 (a loss of function mutant) adults show reduced flying ability and defective leg movement [Aktinson, NS *et al*, 2000][Aktinson, NS *et al*, 2006]. However, *slo* is also functionally expressed in muscles [Aktinson, NS *et al*, 2000]. Thus it is not surprising that knocking down *slo* in neurons alone does not recapitulate the mutant phenotype.

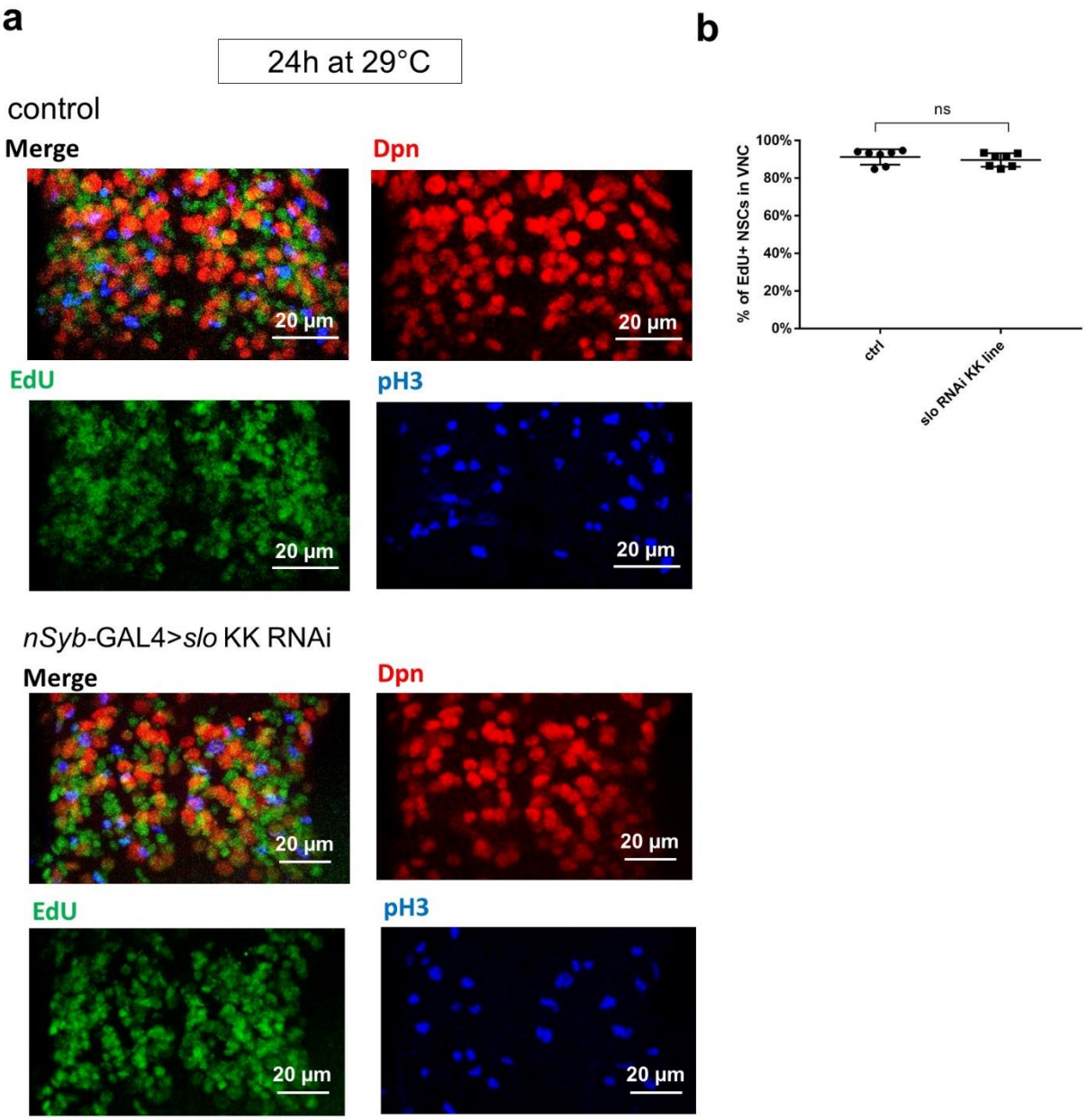

Figure 3.6 Knocking down *slo* in mature neurons does not affect reactivation (a) Reactivation in control brains (top) and neuron-specific *slo* KD brains (bottom). Assayed for the EdU (green) incorporation and pH3 (blue) staining in NBs nuclei (red) **(b)** Quantification of the percentage of reactivated NBs in each genotype ($p > 0.05$, n=7 brains per genotype, Student's T-test, error bars indicate SD, horizontal bar indicated mean.

So far, we have demonstrated that RNAi induced knockdown of *slo* in NBs is sufficient to prevent reactivation. Positive results from three different RNAi and *in silico* prediction suggest the chance of off-targets is minimal. In particular, *slo* RNAi KK108671 caused a near-complete loss of reactivation without affecting systemic

development. At any stage of larval development, the size of *slo* KD larvae was indistinguishable from controls [data not shown]. Also, Slo in mature neurons is not required for reactivation.

3.4 Reactivated neuroblasts do not return to quiescence after RNAi-mediated knockdown of *slo*

In mammalian glioma cells, blockage of Slo is reported to supress proliferation [Basrai, D *et al*, 2002][Weaver, AK *et al*, 2004]. The near complete loss of proliferation in NBs with *slo* knockdown thus raised an interesting question: is Slo required for NB reactivation, or proliferation *per se*? To answer this question, I knocked down *slo* after reactivation using the temperature sensitive GAL4/GAL80 system. The larvae were kept at 18°C (RNAi off) until 72 hours ALH, a time point when around 95% NBs were reactivated. [Figure 3.7 (a)(b)] The RNAi targeting *slo* was then turned-on by shifting the larvae to 29°C. After 45 hours of RNAi induction, proliferation of NBs was not affected [Figure 3.7 (c)(d)]. This result suggests that Slo is required for reactivation of NBs rather than proliferation in general. One possible caveat of this experiment is that *slo* is not sufficiently knocked down after 45 hour RNAi induction. However, it is not possible to extend the time of RNAi induction as the larvae reach pupation after 72 hours at 18°C plus 45h at 29°C. Also, my data show RNAi induction throughout development until 24h ALH causes significant knockdown of *slo,* which equals to ~24 hours of slo KD (since *slo* starts to express in the CNS near larval hatching) [Figure 3.4][Figure 3.5]. Therefore 45 hours of *slo* RNAi induction is likely to cause an efficient knockdown.

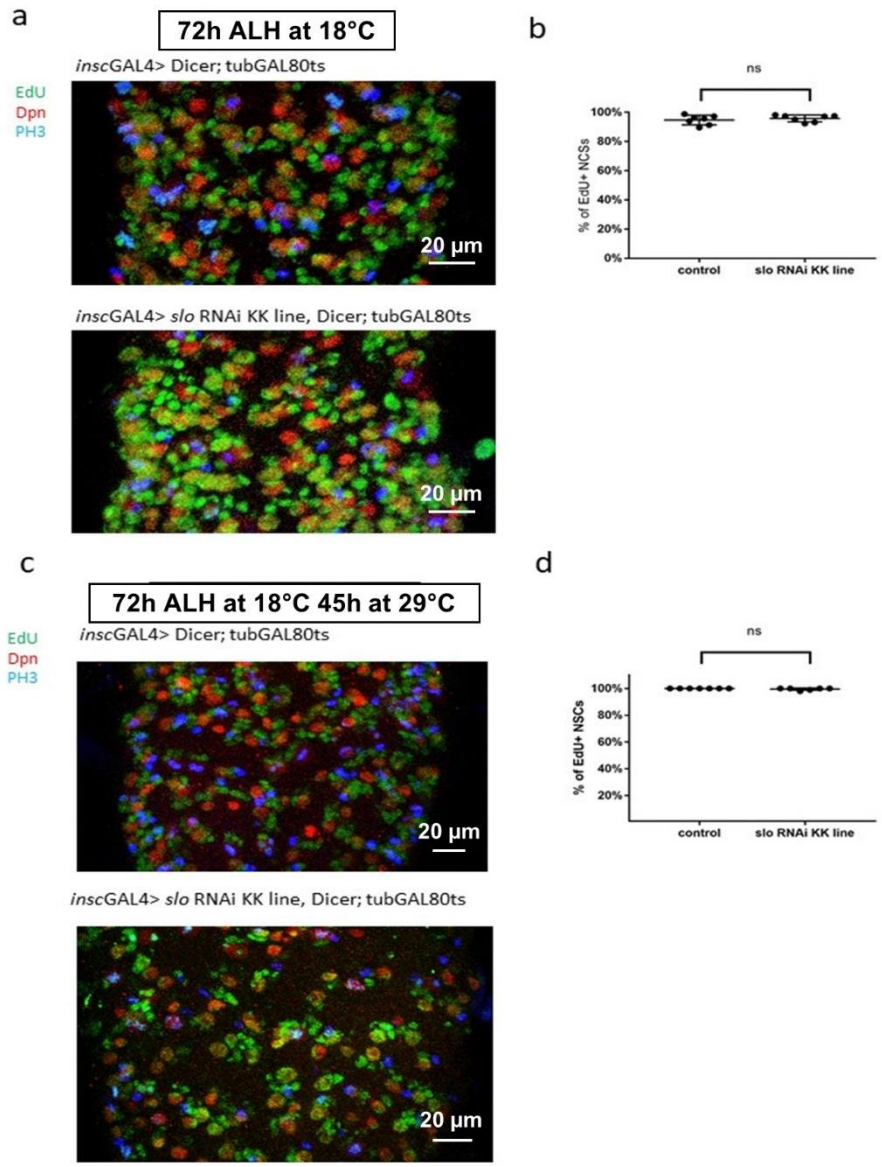

Figure 3.7: Post-reactivation knockdown of *slo* does not cause NBs to return to quiescence. (a) Expression of *slo* RNAi was effectively inhibited by *tublin*GAL80^{ts} until 72h ALH at 18°C. Red: NB, Green: EdU, Blue: PH3 **(b)** Quantification of the percentage of reactivated NBs (either EdU+ or PH3+, or both) in control and test VNCs. (n=7 brains per genotype, Student's T-test, p>0.05, error bars indicate SD, horizontal bar indicates mean) **(c)** Post-reactivation NBs cannot be driven back to quiescence by knocking down *slo*. The larvae were reared at 18°C until 72 hours ALH and shifted to 29°C to turn on RNAi expression. Brains were dissected 45h after temperature shift. (d) Quantification of the percentage of reactivated NBs (either EdU+ or PH3+, or both) in control and test brains. (n=6-7 brains per genotype, Student's T-test, p>0.05, error bars indicate SD, horizontal bar indicates mean)

3.5 Loss of *slo* in neuroblasts leads to reduced brain volume and early adult death

RNAi mediated knockdown of *slo* in NBs causes a near-complete loss of reactivation. It is not surprising that it also causes a strong reduction of brain volume [Figure 3.8 (a)]. I did not quantify the brain volume but the reduction was obvious and consistent between brains. I also quantified the number of neuroblasts in the thoracic segment of VNC in wandering L3 larvae, and no difference was found between control and test [Figure 3.8 (b)]. This result suggests *slo* is not required for the survival of neuroblasts.

Noticeably, NB-specific knockdown of *slo* seems to only affect neuroblasts in the central brain and the VNC. As shown in 3.8 (a), the size of optic lobes is mostly unchanged. It is known that *wor*-GAL4 is weakly expressed in optic lobe NBs. However, unlike NBs in the VNC and central brain, optic lobe NSCs only become neurogenic during larval phase and do not undergo quiescence [Ceron, J *et al*, 2001], which could explain why optic lobes are unaffected by *slo* KD.

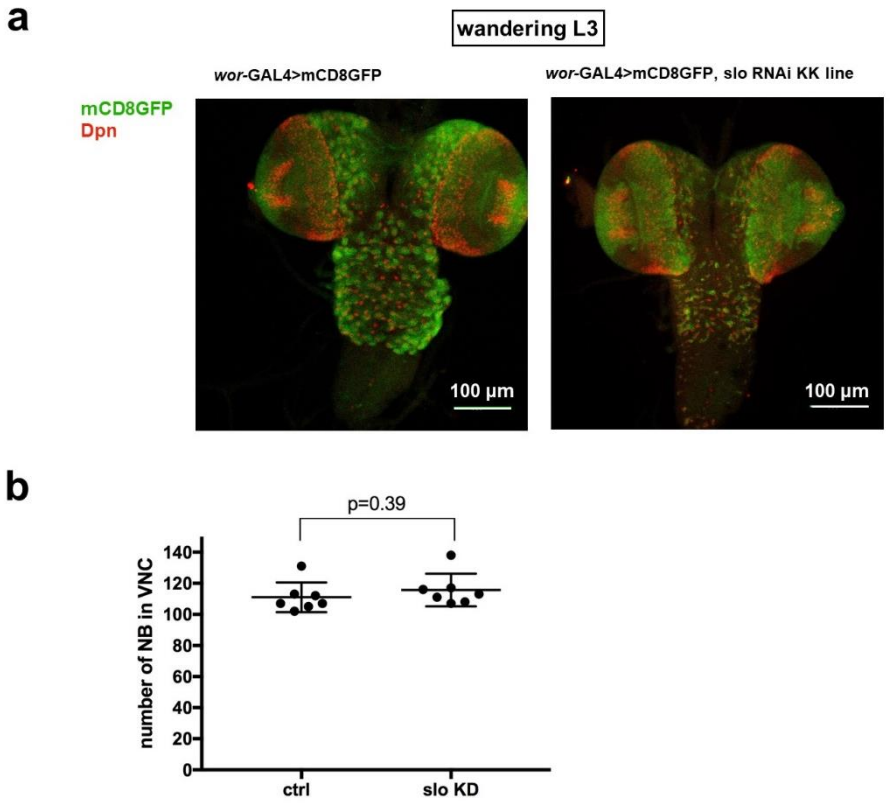

Figure 3.8 NB specific knockdown of *slo* causes reduced brain volume without affecting the number of neuroblasts (a) At the wandering L3 stage, control brains (left) were larger than brains with NB-specific knockdown of *slo* (right). Red: NB nuclei. Green: membrane GFP

labelling NB and progeny **(b)** Number of neuroblasts in the thoracic segment of VNC in control and *slo* KD brains. n=7 brains per genotype, Student's T-test, p>0.05, error bars indicate SD, horizontal bar indicates mean.

The larvae with NB-specific knockdown of *slo* did not show any abnormality in behaviour. No differences in survival, feeding and crawling were observed between test and control larvae. Also, at any stage of larval development, the size of test larvae was indistinguishable from controls, although they started wandering and pupating ~5 hours later. These results are not surprising given that the reactivated NSCs contribute primarily towards the adult CNS. Interestingly, with almost no secondary neurogenesis, all test adults were able to eclose from the pupae and expand their wings. This is very surprising given eclosion and wing expansion require ~ 300 motor neurons in the VNC, where reactivation was almost completely abolished by NB-specific *slo* knockdown [Kimura and Truman, 1990] [Robinow *et al*. 1993]. However, after eclosion, the adults were not able to move or feed, and all died within a day [Figure 3.9]. Dissection of these adult CNS showed significant reduction in size, which explained the immobility and death.

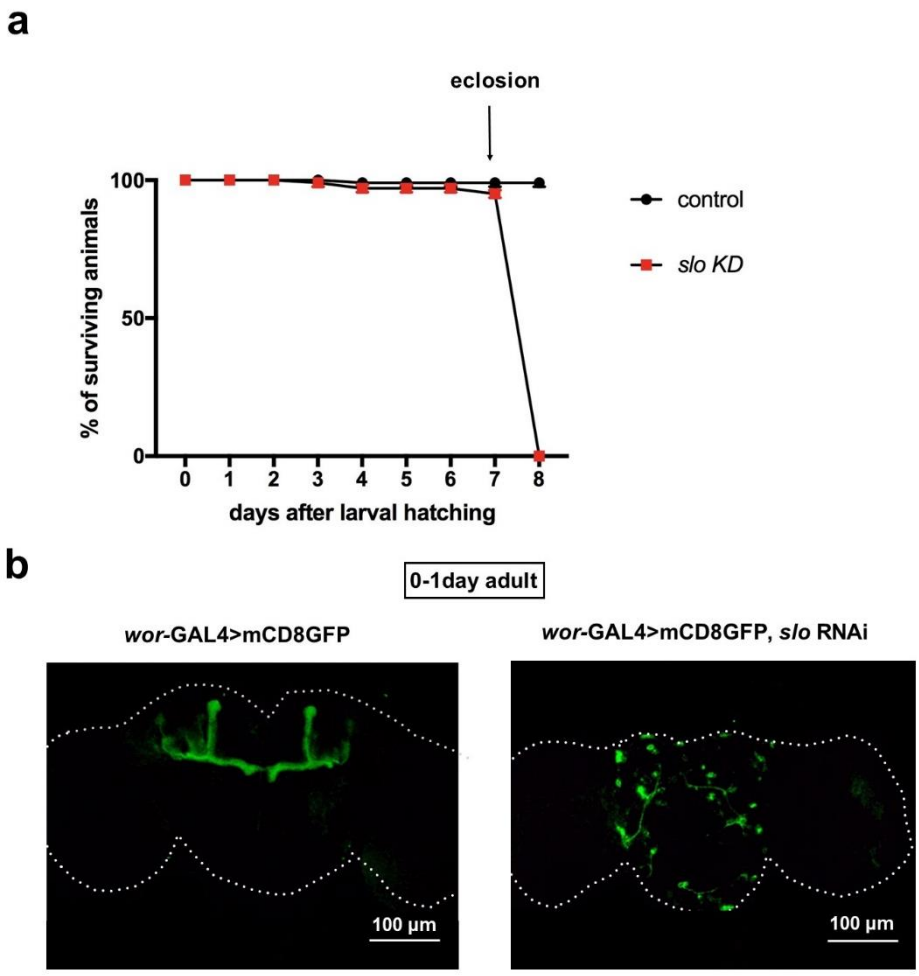

Figure 3.9 NB-specific *slo* KD larvae survive to adulthood but die soon after eclosion **(a)** Lethal phase of NB-specific *slo* KD animals and controls **(b)** Brains from NB-specific *slo* KD adults and controls. Scale bar: 100 µm. White dash: outline of the brain. Notice the mushroom body (labelled by mCD8GFP in the control brain) is absent in the test brain.

3.6 Loss of *slo* causes neuroblasts to persist until adulthood

All *Drosophila* neuroblasts terminate proliferation and disappear at pupal stage [White & Kenkel, 1978][Truman & Bate, 1988]. Different subsets of neuroblasts disappear via different mechanisms. In the abdominal VNC, neuroblasts are lost via programmed cell death before pupal formation [Bello, B *et al*, 2003]. In contrast, neuroblasts in the thoracic VNC and central brain undergo a terminal symmetric differentiation and lose stem cell properties before 30 hours after pupa formation (APF) [Maurange, C *et al*, 2008][Siegrist, S *et al*, 2010][Homem, K *et al*, 2014]. Mushroom body neuroblasts are the longest living neuroblasts that terminate proliferation at ~80h APF and are eliminated by apoptosis by 96h APF [Siegrist, S *et al*, 2010]. However, at the time of

adult emergence, no neuroblast (marked by stable expression of *deadpan*) could be detected in the CNS [described in Chapter 2].

Normally, all neuroblast are reactivated by 48h ALH, many hours before their elimination [Chell & Brand, 2010]. However, knocking down *slo* causes most NBs to stay quiescent at the end of larval development. It is then intriguing to know whether those long-quiescent NBs will still be eliminated on time. Since no NBs should be present in adult brains, I checked the *slo* KD brain and VNC from adults for the NB marker Deadpan. Very strikingly, there were large number (31.20 ± 4.50 in the VNC, 14.00 ± 4.14 in the central brain) of *wor*>mGFP cells/lineages in the test brain and VNC, while in controls the only GFP labelled structure was the mushroom body (due to the late disappearance of mushroom body neuroblasts) [Figure 3.10 (a)]. Moreover, many of these *wor*>mGFP cells/lineages contained a neuroblast [~40% in the central brain, ~60% in the VNC]. On average, the adult CNS of *slo* KD animals contained ~45 neuroblasts, plus many more *wor*>mGFP cells/lineages that had harboured a NB which disappeared shortly before eclosion [Figure 3.10]. Therefore, I conclude that knocking down *slo* significantly extends the life span of NBs, which could be the secondary effect of sustained quiescence.

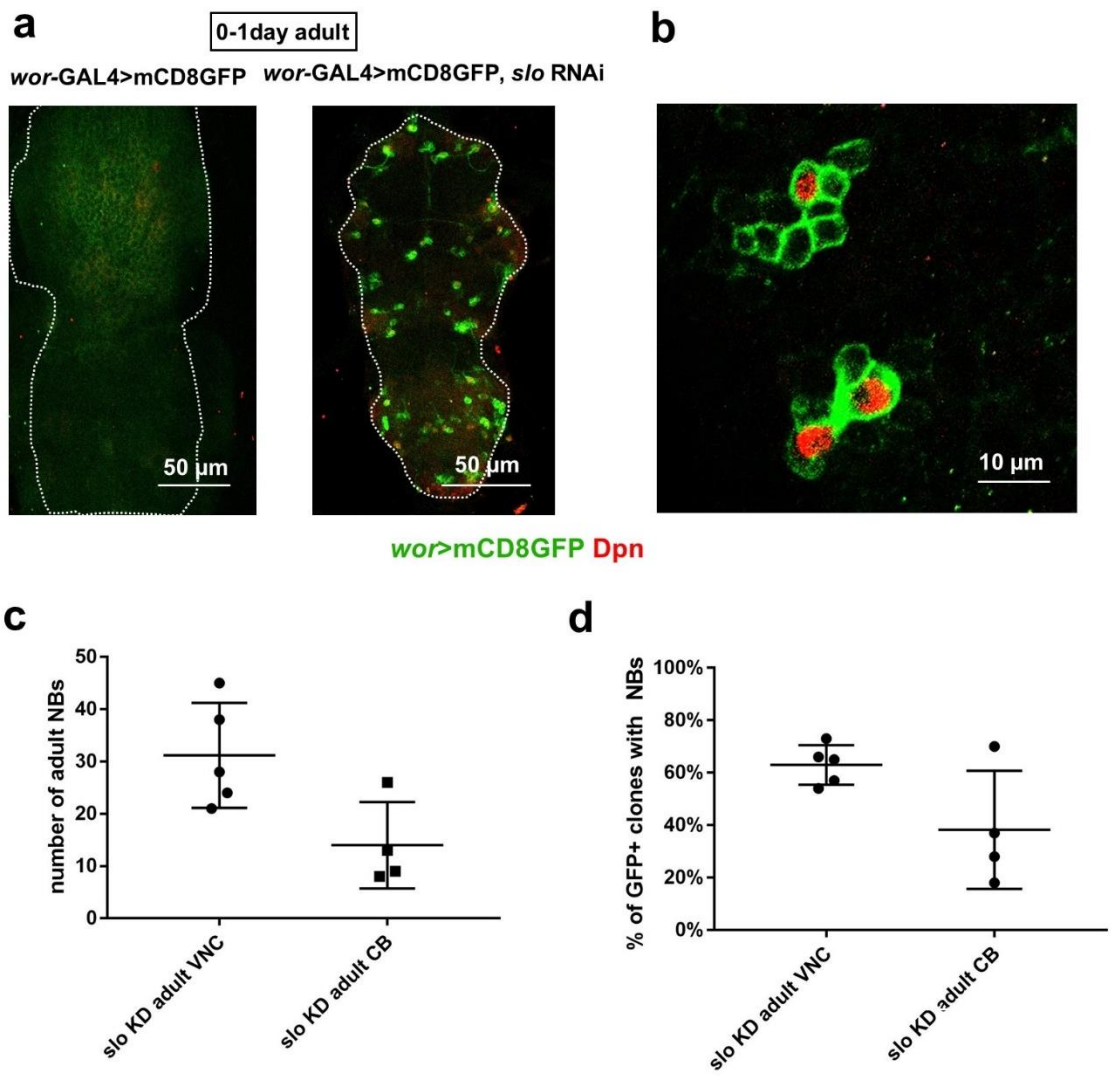

Figure 3.10 Loss of *slo* causes neuroblasts to persist until adulthood (a) Large number of Deadpan+ cells (red) and *wor*>mGFP+ (green) cells are present in adult brains with NB-specific KD of *slo*, in both VNCs (right) and central brains (Figure 3.9 (b)) **(b)** Neuroblasts in the adult VNC at higher magnification **(c)** Numbers of NBs in adult VNC (n=5 VNCs) and adult CB (n=4 brains). Error bar indicates SD, horizontal bar indicates mean.**(d)** Quantification of percentage of *wor*>mGFP+ cells/lineages that contain a neuroblast (VNC: n=5. CB: n=4). Error bar indicates SD, horizontal bar indicates mean.

Interestingly, the adult NBs appeared to be in different mitotic states. Some were labelled with the M phase marker phosphorylated histone H3, which suggests adult neurogenesis could exist in these brains [Figure 3.11]. Some still possessed the quiescent projection, maintaining their quiescence for 6 days longer than normal [Figure 3.11]. This is a truly striking phenotype as in wild type condition, NBs only stay

quiescent for around 24 hours. Unfortunately, I could not trace the fate of these quiescent adult NBs as the animals died within a day after eclosion.

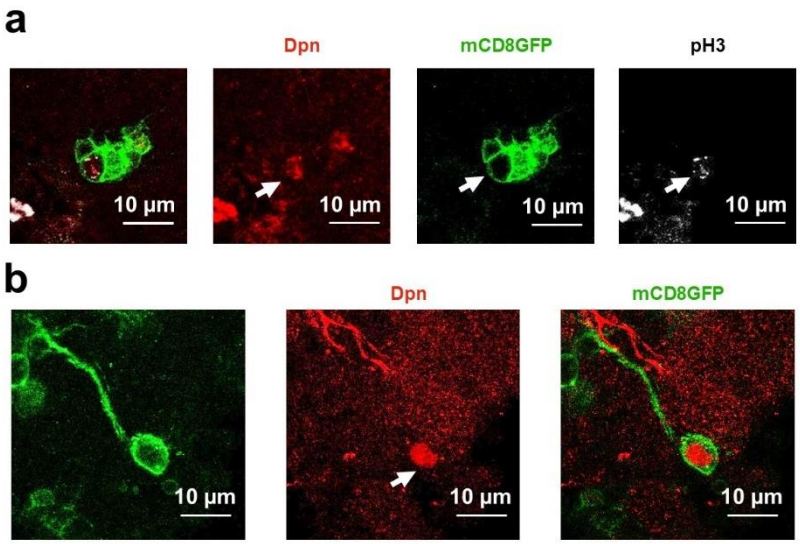

Figure 3.11 *slo* KD neuroblasts that persist until adulthood are in different mitotic states **(a)** A proliferating adult neuroblast. It had already generated a number of progeny labelled with mCD8GFP **(b)** A quiescent adult neuroblast, which still had the long quiescent projection.

3.7 *slo* KD NBs lose early temporal identity while remaining quiescent

Larval neuroblasts make several molecular transitions that switch the fates of progeny they produce [reviewed in C. Doe, 2017]. The most well-studied transitions are the Chinmo to Broad Complex (Br-C) transition and Imp to Syncrip (Syp) transition [Liu, Z *et al*, 2015][Narbonne-Reveau *et al*., 2016]. Both transitions happen at roughly the same time (~60h ALH), which marks the division between early and late temporal identities [Figure 3.12 (a)]. As we know, the majority of NBs are reactivated by 24h ALH, well before this mid-larval transition. This difference in timing leads me to ask whether reactivation is required for this temporal progression, which to my knowledge had never been addressed before.

I used anti-Chinmo and anti-Br-C antibodies to mark the temporal identity of tVNC NBs. At 0h hours ALH, both control and *slo* KD NBs expressed high level of Chinmo. At wandering 3rd larval stage, control NBs had completely lost Chinmo expression and Broad expression was below detectable level, which agreed with previous reports [Figure 3.12 (b)][Syed, HM *et al*, 2017]. Most *slo* KD NBs were had also significantly downregulated Chinmo. No Br-C+ NB could be detected at this stage either [Figure 3.12 (c)].

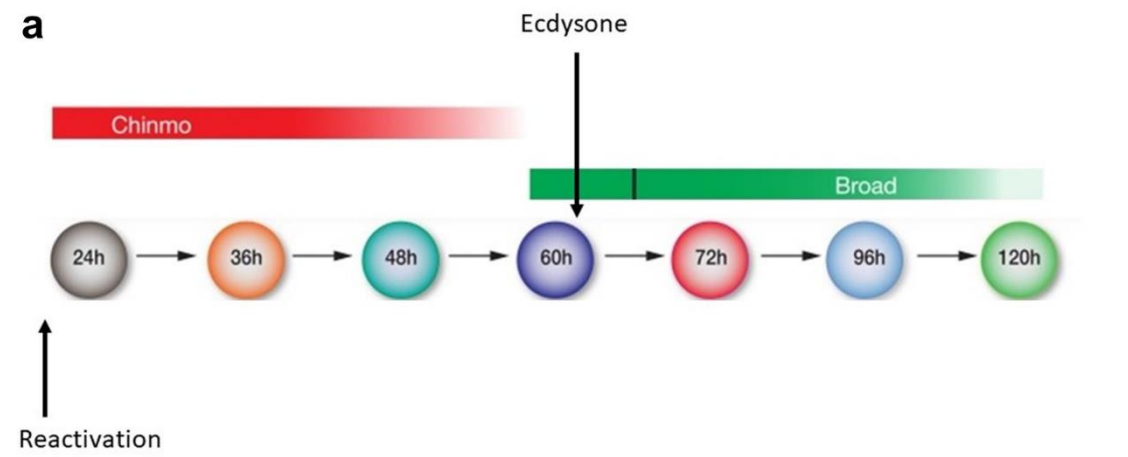
a
Ecdysone
Chinmo
Broad
24h
36h
48h
60h
72h
96h
120h
Reactivation

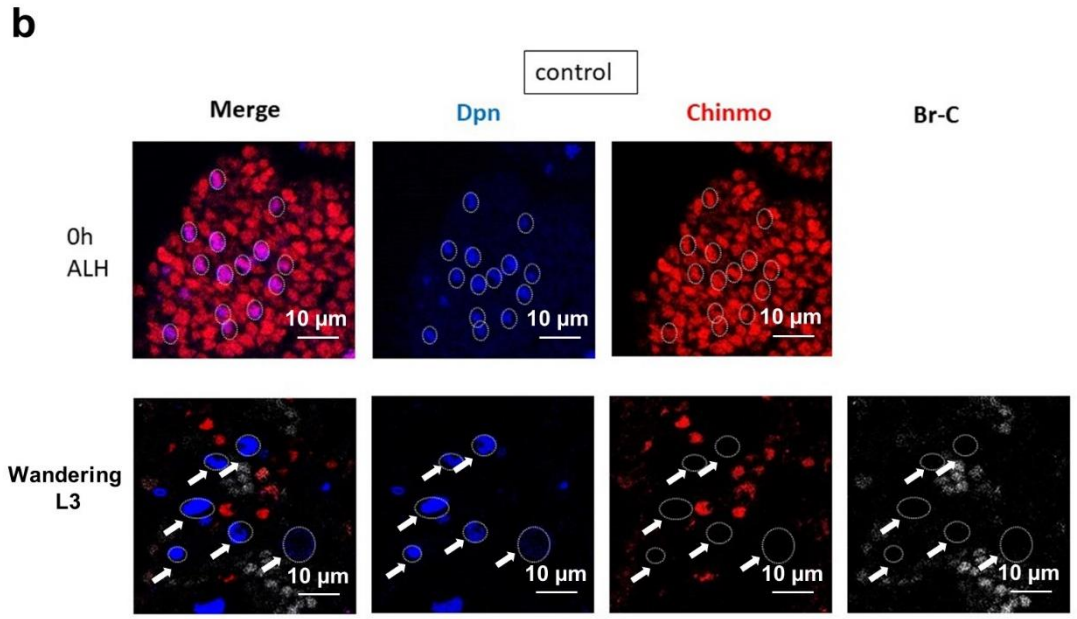
b
control
Merge
Dpn
Chinmo
Br-C
0h
ALH
Wandering
L3
10 µm

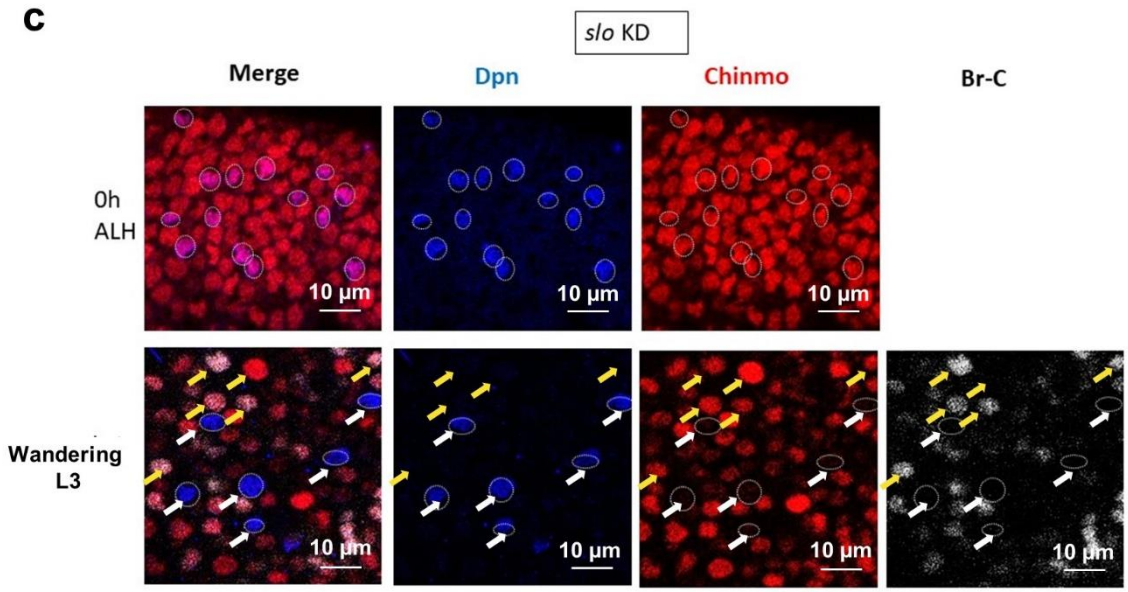
c
slo KD
Merge
Dpn
Chinmo
Br-C
0h
ALH
Wandering
L3
10 µm

Figure 3.12 *slo* KD NBs downregulate early temporal factor Chinmo while remaining quiescent (a) Expression window of Chinmo and Broad. Adapted from Syed, HM *et al*, 2017. **(b)** Expression of Chinmo (red) and Br-C (white) in control NBs (blue) at the beginning and end of larval life. White circles and arrows mark the NBs.**(c)** Expression of Chinmo (red) and Br-C (white) in *slo* KD NBs (blue) at the beginning and end of larval life. White circles and arrows mark the NBs. Yellow arrows mark neurons that co-express Chinmo and Br-C.

Chinmo+ and Br-C+ NBs generate large Chinmo+ and small Br-C+ neurons, respectively [Maurange, C *et al*, 2008]. These two types of neurons are distributed in a complementary pattern and hardly overlap [Figure 3.12 (b)][Maurange, C *et al*, 2008]. However, in the VNC of NB-specific *slo* KD animals, many cells co-expressed high level of Chinmo and Br-C [Figure 3.12 (c), bottom panel]. Although I did not use the neuronal marker in this experiment, based on the cell size and distribution, they are most likely to be neurons. This observation could be interesting for people who *wor*k on temporal identities of neurons.

In summary, my result suggests reactivation is not necessary for the downregulation of Chinmo. Whether it is required for NBs to turn on Br-C cannot be concluded from this experiment. It would also be interesting to test other pairs of early-late temporal factors such as Imp/Syp, Cas/Svp and see if reactivation is necessary for the transition.

3.8 Can *slo* knockdown neuroblasts be reactivated?

I have shown that RNAi-mediated knockdown of *slo* in NBs causes a very severe defect in reactivation. Most NBs stay quiescent throughout the entire larval life, I then asked if this phenotype could be rescued.

I used the temperature sensitive GAL4/GAL80 system to control the expression of *slo* RNAi. The animals were kept at 29°C (RNAi on) throughout embryonic development until 24 hours ALH, when around 80% NBs were reactivated in control brains and virtually no reactivation in test brains [Figure 3.13 (a)(c)]. The RNAi targeting *slowpoke* was then turned off by shifting the larvae to 18°C for 117 hours when the larvae reached the wandering stage. As shown in Figure 3.13 (b)(c), ~50% NBs were

reactivated in test brains. In contrast, if *slo* RNAi was present the whole time, almost all NBs stayed quiescent at wandering L3 stage [Figure 3.4]. Therefore, this experiment suggests that rather than have permanently lost the capacity to divide, NBs lacking Slo can be activated at a later stage once Slo expression is restored.

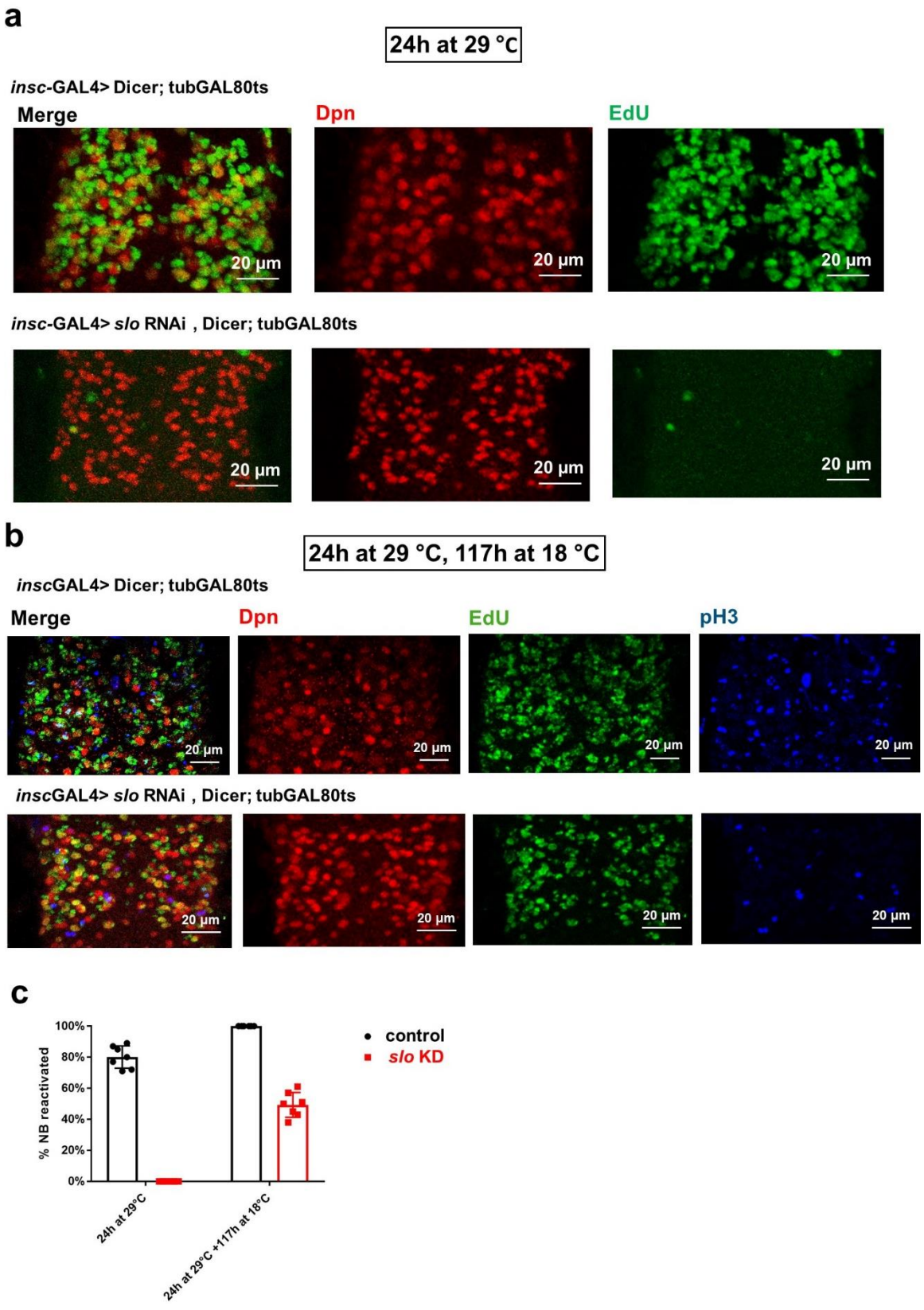

Figure 3.13 *slo* knockdown NBs can be reactivated once the RNAi is removed (a) *slo* KD causes complete loss of reactivation at 24 h ALH. The larvae were reared at 29°C throughout development. Red: NB; Green: EdU **(b)** NBs reactivate after *slo* RNAi is removed. The larvae were reared at 29°C until 24 hours ALH and shifted to 18°C to turn off the RNAi. Brains were dissected 117 h after the temperature shift**.** Red: NB; Green: EdU; Blue: pH3 **(c)** Quantification of the percentage of reactivated NBs in each genotype and condition. N=6-7 brains per group. Error bars indicate SD.

The insulin signaling pathway has been shown to be required and sufficient for neuroblast reactivation [Chell and Brand, 2010][Sousa-Nunes, R *et al*, 2011]. I then asked if activating the insulin signaling pathway would be sufficient to reactivate NBs in the absence of Slo. I co-expressed *slo* RNAi and a constitutively active form of Akt (myr-Akt, Britton, JS *et al*, 2002) and assayed reactivation at 48h ALH. NBs with myr-Akt overexpression and *slo* KD had a higher rate of reactivation compared to NBs with *slo* KD only [Figure 3.14]. However, Chell & Brand, 2010 showed that NBs lacking insulin input could be fully reactivated by myr-Akt at 24h ALH. While in the *slo* KD background, only ~30% NBs were reactivated at 48h ALH [Figure 3.14 (b)]. This result suggests that activation of the insulin pathway is not sufficient to rescue the *slo* KD phenotype. Therefore, Slo acts largely independently of the insulin signalling pathway.

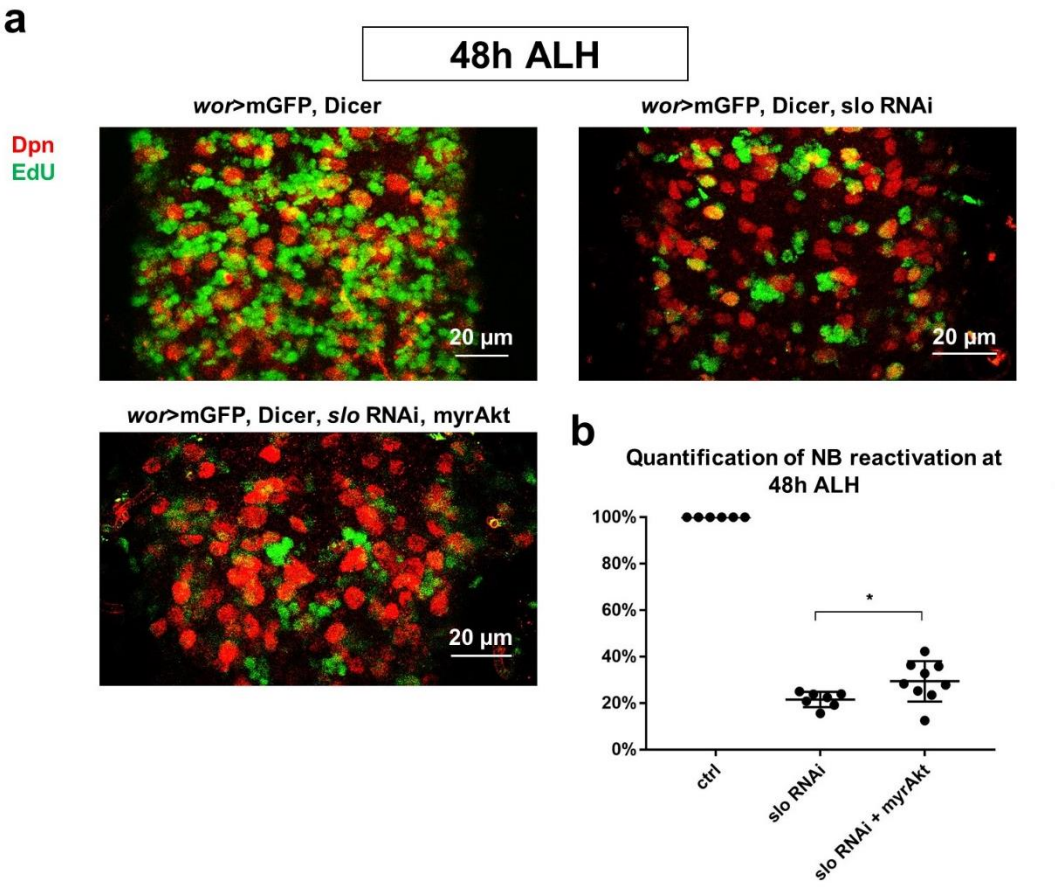

Figure 3.14 Overexpression of constitutively-active Akt in NBs partially rescues the *slo* KD phenotype (a) Epistasis experiment between *slo* KD and Akt. The *wor*-GAL4 driver was used to drive expression of indicated transgenes in NBs throughout development. Reactivation was assayed by EdU (green) incorporation in NB nuclei (red). **(b)** Quantification of reactivated NBs in each genotype. N=6-8 brains per genotype. *: $p<0.05$, Student's T-test, error bars indicate SD, horizontal bar indicates mean.

3.9 Chapter summary and discussion

In this chapter, I have described the gene *slo* which is required for neuroblast reactivation. NB-specific knocking down of *slo* causes near-complete loss of reactivation during larval life. Slo is not required for cell division *per se* as knocking down *slo* after reactivation does not impede proliferation. Also, although *slo* is expressed in both neurons and neuroblasts, knocking down *slo* in mature neurons does not affect reactivation.

After reactivation, neuroblasts proliferate extensively and produce around 90% of neurons in adult brains [reviewed in Homem and Knoblich, 2012]. Interestingly, my

results show that larval development, pupation and eclosion are completely independent of this round of neurogenesis. After eclosion, however, animals without NB reactivation are not able to walk, fly or feed and die within 24 hours, presumably due to a severe lack of neurons.

Neuroblasts terminate proliferation at pupal stage. After that, they either undergo programmed cell death or terminal differentiation. Would the same rule apply to NBs that do not reactivate? Intrigued by this question, I examined adult brains and VNCs with NB-specific *slo* KD. Very strikingly, I found many NBs in the adult CNS, some of them were still quiescent. This result suggests quiescence significantly extends the life span of stem cells. Similarly, in mammalian follicle stem cells and hematopoietic stem cells, loss of quiescence by ablating Foxo has been reported to accelerate the depletion of stem cell pool [Mayamoto, K *et al*, 2007][Lay, K *et al*, 2016]. Taken together, these findings suggest quiescence is both sufficient and necessary for stem cell maintenance.

Termination of NB proliferation is controlled by the temporal progression [Maurange, C *et al*, 2008][Chai, P *et al*, 2013]. It has been shown that stalled Chinmo to Br-C transition correlates with neuroblast division in adult thoracic VNC [Maurange, C *et al*, 2008]. My result shows that under *slo* KD condition, thoracic NBs downregulate Chinmo but still persist until adulthood. This suggests downregulation of Chinmo is not sufficient for NBs to terminate proliferation in time. Also, reactivation is not necessary for the temporal progression in thoracic NBs, at least not for the Chinmo to Br-C transition. This result is somewhat surprising as quiescence suspends the embryonic NSCs switching their temporal identity [Tsuji, T *et al*, 2008]

Although Slo/BK channels are extensively studied in neurons, their roles in neural stem cells have not been described before either in flies or in mammals. However, in mammalian CNS, *slo* is expressed in astrocytes and glioma cells, which are cells that divide in the adult brain and have stem cell properties [Zahradnikova, A. and Zahradnik, I.,1992][Liu, X *et al*, 2002][Gebremedhin, D, *et al*, 2003][Ou, J *et al*, 2009][Maugeri-Saccà, M *et al*, 2013]. More interestingly, in human glioma cells, a specific splice isoform of Slo/BK is highly enriched compared to non-malignant astrocytes [Liu, X *et al*, 2002]. Similarly, *slo* is overexpressed in rat glioma cells,

although the specific isoform is unknown [Ningaraj *et al*., 2002]. Weaver, A *et al*, 2004 reported that inhibition of Slo channel using a selective pharmacological inhibitor arrested glioma cells in S phase. However, this effect is only present when the glioma cells were cultured under serum deprivation condition. Knocking down *slo* using siRNA in culture medium with serum also did not affect glioma cell proliferation [Abdullaev, I.F, *et al*, 2010]. In summary, Slo/BK channels are functionally expressed in mammalian glioma cells, but their roles in regulating cell division remain largely unclear.

The canonical function of Slo is to carry out a large outward rectifying K^+ current when activated by membrane depolarisation and/or Ca^{2+} influx [Aktinson, NS *et al*, 1991][Schreiber, M, & Salkoff, L, 1997][Yuan, P *et al*, 2010]. By doing so it repolarises the cell membrane and negatively feeds back onto the Ca^{2+} influx [Robitaille, R *et al*, 1993][Atkinson, N.S *et al*, 2000][Hu, H *et al*, 2001][Raffaelli, G *et al*, 2004]. Therefore, loss of Slo in NBs could in theory results in membrane depolarisation as well as increased intracellular Ca^{2+}. Ca^{2+} signaling pathway is pivotal to many cellular functions and has recently been shown to regulate stem cell quiescence [Clapham, DE *et al*, 2007][Deng, HS *et al*, 2015][Xu *et al*, 2017][He, L *et al*, 2018][Petrik, D *et al*, 2018]. Therefore, I decided to further investigate the role of Ca^{2+} signaling in neuroblast and whether Slo affects reactivation via the Ca^{2+} signaling pathway.

Chapter 4. Investigating calcium signalling: a possible downstream effector of *slowpoke* in neuroblast quiescence

4.1 Introduction

4.1.1 Slowpoke regulates Ca^{2+} influx and membrane potential

Slowpoke is a large conductance K^+ channel that is activated synergistically by membrane depolarisation and cytoplasmic Ca^{2+} [Vergara, C *et al*, 1998][Magleby, K. L. 2003.][Cui, J *et al*, 2009]. In neurons and muscles, activation of Slo leads to large K^+ efflux that repolarises the cell membrane, which in turn deactivates the voltage gated Ca^{2+} channels (VGCCs), limiting further Ca^{2+} influx [Wang, Z. *et al*, 2001][Raffaelli, G *et al*, 2004][Lee, J, *et al*, 2008][Ford, JK *et al*, 2014]. Therefore, Slo acts as a negative feedback onto Ca^{2+} influx in excitable cells that express VGCCs. Interestingly, RNA-seq data reveal that two VGCC channel genes, *cacophony* (*cac*) and *Dmca1D*, are substantially expressed in reactivated *Drosophila* NBs [Berger, C et al, 2012]. Therefore, one possible mechanism of Slo regulating neuroblast activation is that it acts as a negative regulator of intracellular Ca^{2+} and moderates NB behaviour via Ca^{2+} signalling.

4.1.2 Brief introduction to Ca^{2+} signalling

Ca^{2+} signalling impacts nearly all aspects of cell life from mitosis to apoptosis [Clapham, DE, 2007]. In living cells, there is a 20,000-fold difference between cytoplasmic [Ca^{2+}] and extracellular [Ca^{2+}] (100 nM vs mMs) [Clapham, DE, 2007]. Intracellular Ca^{2+} stores such as the ER also store mM level of Ca^{2+} [Clapham, DE, 2007]. Therefore, Ca^{2+} influx into the cytoplasm can rapidly increase the $[Ca^{2+}]_{cyto}$ by several folds, which triggers a series of signal transductions [Clapham, DE, 2007].

Cells invest much of their energy in extruding Ca^{2+} from the cytoplasm into intracellular Ca^{2+} stores and the extracellular space. The main intracellular Ca^{2+} stores include the ER, mitochondria and Golgi apparatus [Clapham, DE, 2007] [Li, L.H *et al,* 2013]. Cytoplasmic Ca^{2+} is constantly transported into the ER and Golgi apparatus by the

Sarcoendoplasmic reticular Ca^{2+} ATPases (SERCA) [Clapham, DE, 2007][Li, L.H *et al,* 2013]. Similarly, ATPases located on the plasma membrane (PMCA) pump Ca^{2+} out of the cell [Clapham, DE, 2007]. The second mechanism of extruding Ca^{2+} from the cell is via the Na^{+}/Ca^{2+} exchangers and the Na^{+}/Ca^{2+}-K^{+} exchangers. When operating in the forward mode, these cation exchangers export Ca^{2+}/K^{+} in exchange for Na^{+} [Clapham, DE, 2007]. Mitochondria also uptake Ca^{2+} from the cytoplasm via the Ca^{2+}/H^{+} exchangers located on the inner mitochondrial membrane [Santo-Domingo, J. and Demaurex, N., 2010].

Ca^{2+} signalling is activated following Ca^{2+} influx into the cytoplasm from either the intracellular Ca^{2+} stores and/or the extracellular space. One universal mechanism is activation of phospholipase Cs (PLCs) by G protein-coupled receptors (GPCRs) and Tyrosine Kinase Receptors (TKRs) [Kadamur, G. and Ross, EM, 2013]. Activated PLCs cleave phosphatidylinositol 4, 5 bisphosphate (PIP_2) into 1,4,5-inositol trisphosphate (IP_3) and diacylglycerol (DAG) [Kadamur, G. and Ross, EM, 2013]. IP_3 binds to IP_3 receptor channels on the ER and Golgi apparatus membrane, allowing Ca^{2+} to diffuse from the these Ca^{2+} store into the cytoplasm [Mikoshiba, K., 2007]. DAG and increased $[Ca^{2+}]_{cyto}$ co-activate Protein Kinase Cs (PKCs) [Mochly-Rosen, D et al ,2012]. PKCs are a large family of kinases that regulate many cell functions including proliferation, cell death, gene transcription and cell motility [Mochly-Rosen, D et al ,2012]. Another mechanism for Ca^{2+} influx is direct entry via plasma Ca^{2+} channels including the VGCCs and TRP channels [Clapham, DE, 2007]. The Ca^{2+} influx from extracellular space also triggers the opening of RyR receptor on the ER and Golgi apparatus, which leads to more Ca^{2+} to flow into the cytoplasm [Van Petegem, F, 2012]. The fourth mechanism for Ca^{2+} entry is the store operated calcium entry (SOCE). Upon depletion of the ER Ca^{2+} store, ER-located Ca^{2+} sensor Stim couples with plasma membrane-located Ca^{2+} channel Orai, which allows Ca^{2+} to flux into the cell [Hewavitharana, T et al, 2007].

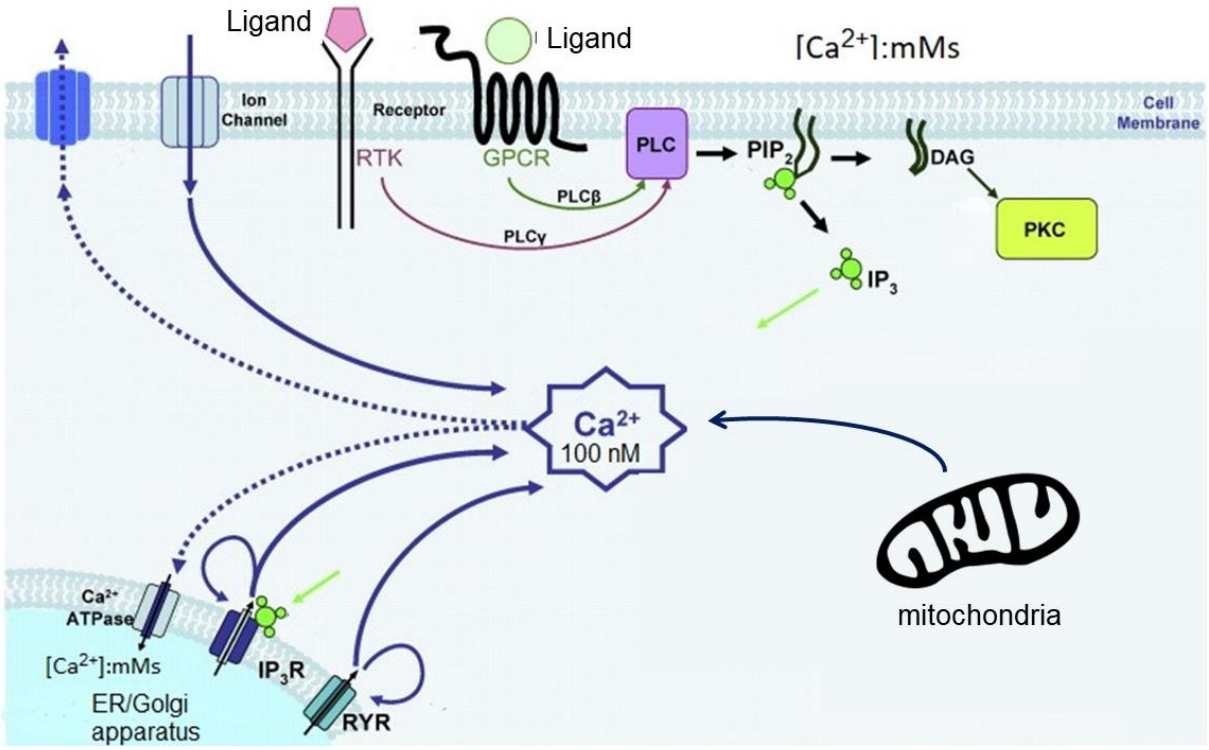

Figure 4.1 Summary of intracellular [Ca^{2+}] regulation [Figure adapted from Slusarski, D.C. and Pelegri, F., 2007]

Hundreds of proteins react to increased $[Ca^{2+}]_{cyto}$ by changing their conformation [Yap, KL et al, 1999]. Among all Ca^{2+} binding proteins, Calmodulin (Cam) is considered to be a central regulator of Ca^{2+}-dependant signalling [Clapham, DE, 2007][Berchtold, MW and Villalobo, A, 2014]. Calmodulin is ubiquitously expressed and very well-conserved across the Eukarya kingdom [Berchtold, MW and Villalobo, A, 2014]. It regulates cellular processes including but not limited to cell motility, proliferation, apoptosis, autophagy and gene expression. [Berchtold, MW and Villalobo, A, 2014]. The diversity of Calmodulin functions comes from its numerous target proteins. Calmodulin recruitment sites are present in hundreds of proteins, many of which are kinases (such as CamKs) and phosphatase (such as Calcineurin), which in turn regulate many signalling pathways via phosphorylation/dephosphorylation [Berchtold, MW and Villalobo, A, 2014][Takemoto-Kimura, S *et al*, 2017]. Therefore, Calmodulin lies at the heart of numerous Ca^{2+}-dependant pathways that affect nearly all aspects of cell life.

4.1.3 The dual role of Ca^{2+} signalling in stem cell quiescence

As a central regulator of cell physiology, Ca^{2+} signalling has significant impact on the behaviour of many different types of stem cells. Curiously, the role Ca^{2+} signalling plays in stem cell quiescence seems to be entirely context-dependant. Adult *Drosophila* intestine stem cells rarely divide under physiological conditions [Deng, HS et al, 2015]. Increasing cytosolic Ca^{2+} level in intestine stem cells significantly increased the frequency of cell division [Deng, HS et al, 2015][Xu, C et al, 2017][He, L et al, 2018]. Similarly, increasing cytosolic Ca^{2+} activates muscle satellite cells and this effect is dependant on Calmodulin [Tatsumi, R et al, 2009][Hara, M et al, 2012]. Very recently, it has been shown in quiescent hematopoietic stem cells that Ca^{2+} influx is required for initiating cell division, although suppression of the Ca^{2+} signalling after cell cycle entry is essential for maintaining the HSC population [Umemoto, T et al, 2018]. In some other stem cell types, however, Ca^{2+} signalling is required for maintaining quiescence. For instance, loss of Nuclear factor of activated T cells (NFAT), a transcription factor that responses to sustained elevation of Ca^{2+}, causes follicle stem cells to activate prematurely [Horsley, V *et al*, 2008].

Very recently, the role of Ca^{2+} signalling in NSC quiescence has been addressed in the mammalian system. Adult SVZ NSCs possess functional store-operated Ca^{2+} entry (SOCE) [Domenichini, F *et al*, 2018]. Inhibition of SOCE in cultured NSCs significantly impairs proliferation as well as shifts symmetrical self-renewal division to asymmetrical differentiative cell division [Domenichini, F *et al*, 2018]. Similarly, in proliferating human glioblastoma stem-like cells (GSLC) which have many NSC properties, inhibition of SOCE is sufficient to drive them into quiescence [Galli, R *et al*, 2004][Aulestia, FJ *et al*, 2018]. These results suggest SOCE is required for proliferation in NSCs or NSC-like cells. However, Aulestia, FJ and colleagues also show that resting $[Ca^{2+}]_{cyto}$ is higher in quiescent GSLCs compared to cycling GSLCs. In summary, these early results suggest Ca^{2+} signalling plays important roles in NSC quiescence, although more work needs to be done to decide the regulatory relationship as well as the downstream pathways.

It is well established that *Drosophila* NB reactivation is dependant on the insulin signalling pathway [Chell, JM and Brand, AH, 2010][Sousa-Nunes *et al*., 2011]. How does Ca^{2+} signalling interact with the insulin pathway, then? In mouse embryonic cells, insulin-like growth factor-I and -II elicit Ca^{2+} influx which is required for subsequent mitosis [Nishimoto, I et al, 1987][Kojima, I et al, 1988]. *In vitro* studies also show that activated PKC phosphorylates insulin receptors and reduces the kinase activity of insulin receptors by 65% [Bollag, G.E et al, 1986]. These data suggest Ca^{2+} signalling might act as a secondary messenger as well as a negative feedback on the insulin signalling pathway. However, whether this regulatory relationship is conserved in *Drosophila* NBs remains to be explored. Since Slo is known to regulate Ca^{2+} level, it would be interesting to test the role of Ca^{2+} signalling in NB quiescence and whether it could explain why Slo is required for NB reactivation.

4.2 Intracellular Ca^{2+} in quiescent NBs is significantly higher compared to reactivated NBs

To understand the role of Ca^{2+} in NB quiescence, I first compared $[Ca^{2+}]_{cyto}$ between quiescent and reactivated NBs. I deployed two tools of assaying $[Ca^{2+}]_{cyto}$. One is an activity-dependant transcriptional reporter that reports sustained elevation of $[Ca^{2+}]_{cyto}$ beyond basal level [Masuyama, K et al, 2012]. The other is a Ca^{2+} sensor that reports real-time $[Ca^{2+}]_{cyto}$ by changing its fluoresce intensity [Chen, TM et al, 2013][Gao, XJ et al, 2015].

The transcriptional Ca^{2+} reporter CaLexA was first developed to detect neuron activities in the fly brain [Masuyama, K et al, 2012]. It is based on the mammalian NFAT protein [Masuyama, K et al, 2012]. In mammalian cells, NFAT is imported in the nucleus upon sustained Ca^{2+} elevation [Putney, JW, 2012]. In the CaLexA system, the DNA binding C-terminal of NFAT is replaced by the transcription driver LexA [Venken, KJ et al, 2011][Masuyama, K et al, 2012][Figure 4.1 (a)]. Upon sustained $[Ca^{2+}]_{cyto}$ elevation, the modified NFAT is imported to the nucleus, driving the expression of membrane-targeted GFP controlled by the LexOP element [Venken, KJ et al, 2011][Masuyama, K et al, 2012][Figure 4.1 (a)]. The modified NFAT gene is downstream of UAS binding sites and thus can be specifically expressed in desired

cell types by the GAL4/UAS system [Brand, AH and Perrimon, N, 1993]. The fly CaLexA system is verified in olfactory neurons. Only flies that have been exposed to particular odours show GFP labelling in certain olfactory neurons, while in unstimulated flies these olfactory neurons remain unlabelled [Masuyama, K et al, 2012]. These results suggest the CaLexA system is unresponsive to low basal level neuronal activity.

I expressed the CaLexA constructs in neuroblasts using *wor*-GAL4 as the driver. I assayed brains at 0 hours and 72h ALH. At 0 hours ALH, almost all tVNC NBs were unlabelled [Figure 4.2 (b)]. In some brains (2 out of 6), a few NBs were brightly labelled (1-2 NBs per brain) [Figure 4.2 (b)]. However, this number is too few to draw any meaningful conclusion from. At 72 hours ALH, tVNC NBs were either not labelled at all or very weakly labelled [Figure 4.2 (c)]. Their progeny which presumably had inherited the CaLexA reporters were clearly labelled, suggesting the CaLexA system is functional in my experimental conditions [Figure 4.2 (c)].

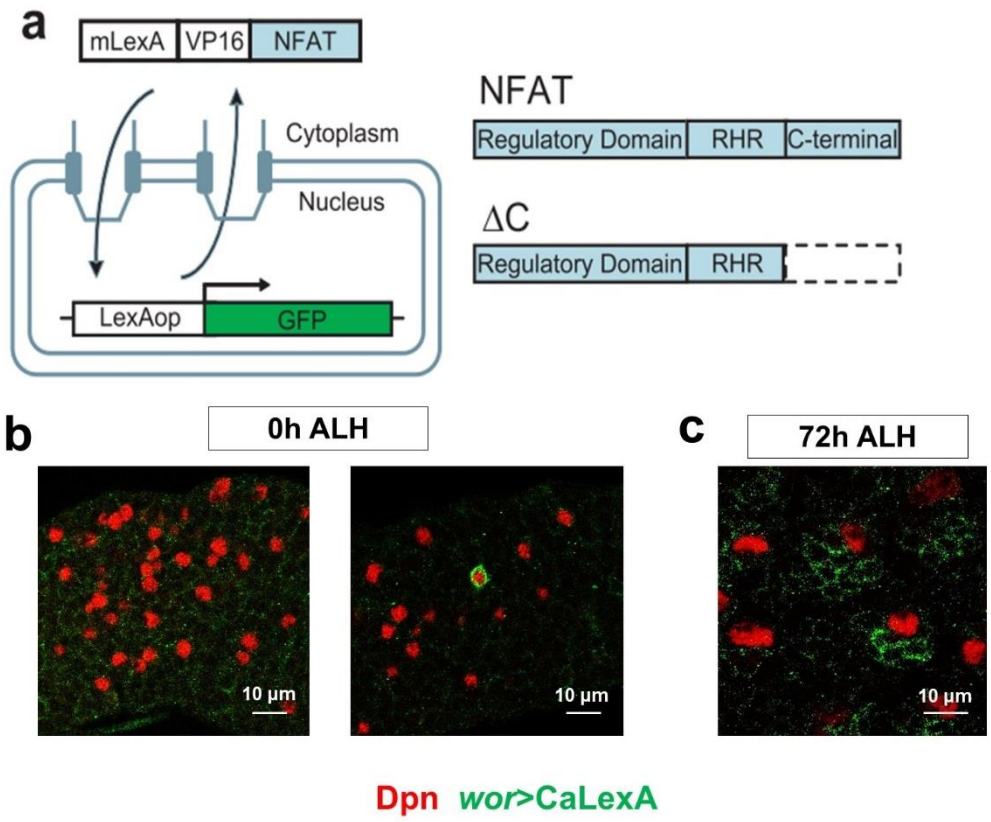

Figure 4.2 Assaying $[Ca^{2+}]_{in}$ in NBs using the transcriptional reporter CaLexA (a) Illustration of the CaLexA system (from Masuyama, K et al, 2012) **(b)** Left: quiescent NBs (red)

are mostly not labelled by the CaLexA reporter (green) Right: Example of a quiesnent NB labelled by the CaLexA reporter **(c)** Neuronal progeny but not reactivated NBs (red) are labelled by the CaLexA reporter (green)

The CaLexA reporter did not yield useful comparison of the intracellular Ca^{2+} level between quiescent and reactivated NBs. However, we know that CaLexA can only detect Ca^{2+} activity above a certain threshold, It is possible that the intracellular Ca^{2+} level in both quiescent and reactivated NBs are below the threshold. Therefore, I used GCaMP, a genetically encoded Ca^{2+} indicator which is based on the fusion between Calmodulin and GFP [Nakai, J et al, 2001]. When Ca^{2+} binds to the Calmodulin sequence, the conformational changes induce a subsequent conformational change in the GFP, which changes its fluorescence intensity [Nakai, J et al, 2001]. GCaMPs have been widely studied and improved since it was first introduced [Ye, L et al, 2017]. In this experiment I used GCaMP6m, the latest generation of GCaMPs [Chen, TW et al, 2013][Barnett, LM et al, 2017]. Its fluorescent intensity changes sharply and almost linearly between 0.02-1.5 μM free Ca^{2+}, which comprises the range of $[Ca^{2+}]_{cyto}$ change when Ca^{2+} signalling is activated (from 0.1μM to 1μM) [Clapham, DE et al, 2007][Chen, TW et al, 2013][Barnett, LM et al, 2017]. Therefore, GCaMP6m is in theory a suitable tool for measuring intracellular Ca^{2+} in living cells.

I monitored GCaMP6m signals in neuroblasts using live imaging. Imaging in live larvae is proven difficult due to the movements of the animal. Loss of signal through the body wall is another major concern. Therefore, I imaged freshly dissected *ex vivo* brains mounted in insect Schneider medium, a medium that closely mimics the composition of haemolymph and used in various *ex vivo* organ culture conditions [Tsao, CK et al, 2016][Neville, KE et al, 2018][Figure 4.3 (a)][see Materials and Methods].

I imaged quiescent and reactivated NBs at 0h ALH and 72h ALH, respectively. One technical difficulty of live imaging NBs is to distinguish NBs from their recent progeny, which still express markers they inherit from the NB. At 72h ALH, NBs are significantly larger than any other cell types in the brain and can be easily distinguished [Figure 4.3 (c)]. Therefore, for imaging at 72h ALH, I used the conventional NB driver *wor*-GAL4

to drive the expression of GCaMP6m constructs and membrane-targeted RFP. However, at 0h ALH, NBs are not distinguishable from their progeny by size. Therefore, I used a novel driver, *mlt*-GAL4, which specifically drives in quiescent NBs. Detailed description of this driver can be found in Chapter 5 [Figure 5.6]. In brief, at 0h ALH, *mlt*-GAL4 is exclusively expressed in NBs and midline glia. Since the midline glia are located dorsal to the NB layer and has very different morphology, *mlt*-GAL4 can be used as a NB-specific driver for live imaging purpose [Figure 4.3 (b)].

Using the selected NB drivers, I expressed GCaMP6m and membrane-targeted RFP. In both conditions, GCaMP6m signal is normalised to membrane-targeted RFP signal to control for variables including the GAL4 driver expression level, tissue depth and movements during imaging [Speder, P and Brand AH, 2014][Deng, HS et al, 2015]. All videos were taken using the same microscope and imaging settings, including laser intensity, objective, scanning speed and resolution [see Material and Methods]

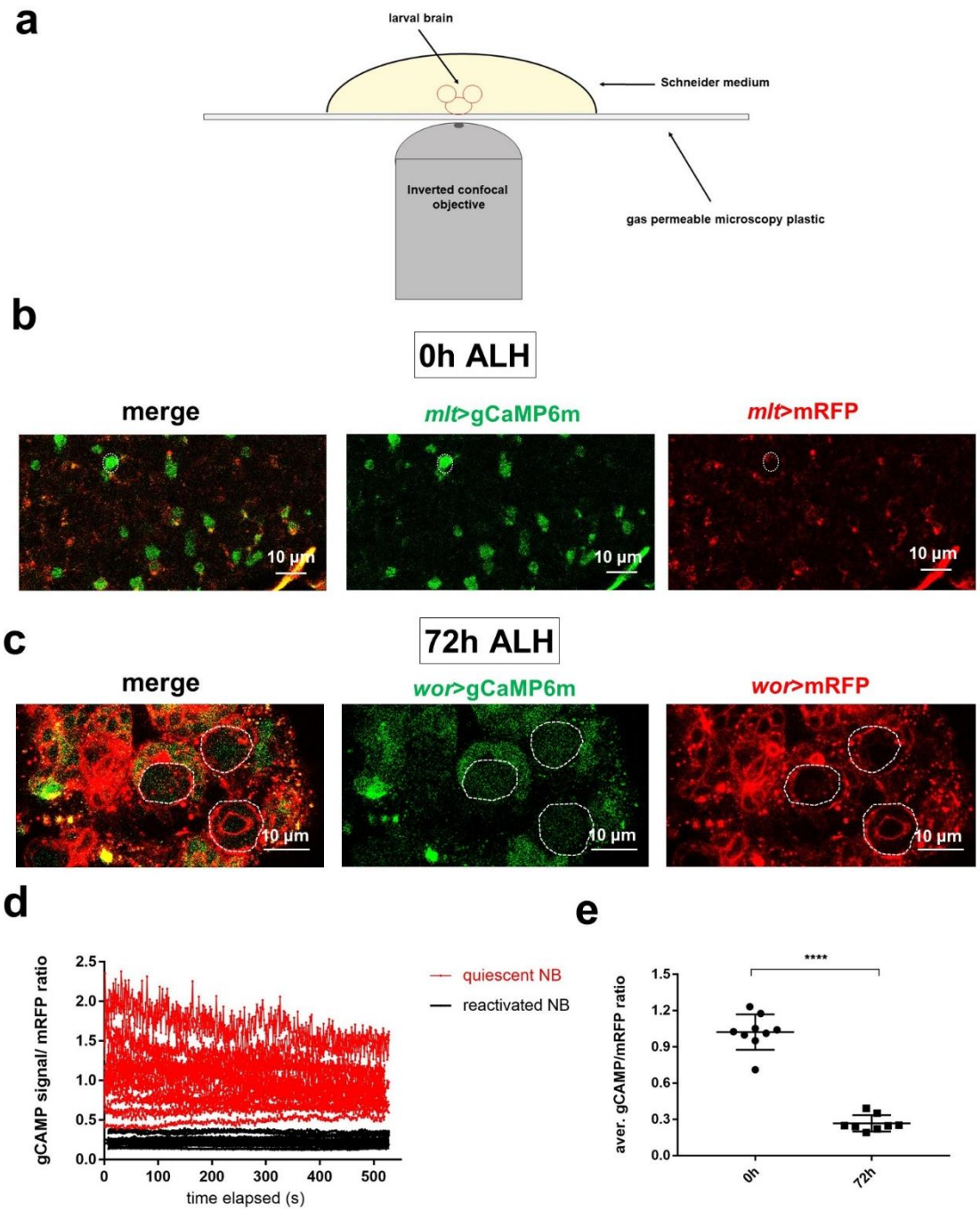

Figure 4.3 Live recording using GCaMP6m reveals higher $[Ca^{2+}]_{in}$ in quiescent NBs compared to reactivated NBs (a) Experimental setup of live imaging *ex vivo* cultured larval brains **(b)** A snapshot of the thoracic VNC at 0 hours ALH from live imaging. Green: GCaMP6m. Red: membrane targeted RFP. White circle: one particularly bright NB **(c)** A snapshot of thoracic VNC at 72 hours ALH from live imaging. Green: GCaMP6m. Red: membrane targeted RFP. White circles: NBs **(d)** Real-time normalised GCaMP6m signal in quiescent (red) and reactivated NBs (black). n=20 NBs per group, randomly selected from all measured NBs. **(e)** Quantification of average normalised GCaMP6m signal in 0h ALH and 72h ALH brains (4-5

NBs per brain, 8-9 brains per group, each dot represents a brain). Student t-test, ****: p<0.0001. Error bar represents SD.

At 0h ALH, bright GCaMP6m signals were detected in the tVNC and their pattern suggested they were NBs [Figure 4.3 (b)]. RFP signal at this stage was weak but detectable [Figure 4.3 (b)]. Interestingly, NBs with unusually high GCaMP6m signal intensity were recorded at very low frequency (1 or 2 NB per brain) [Figure 4.3 (c)]. This is consistent with the CaLexA results showing very few NBs labelled at 0h ALH. At 72h ALH, reactivated NBs, together with their progeny, were clearly labelled by the membrane-targeted RFP [Figure 4.3 (c)]. Interestingly, compared to their progeny, GCaMP6m signal in reactivated NBs was significantly weaker [Figure 4.3 (c)].

To capture changes in Ca^{2+} intensity, I imaged each brain for 8 min 40 sec. During this time, normalised GCaMP6m fluorescence in most NBs remained stable or declined slightly [Figure 4.3 (d)]. Clearly, quiescent NBs had higher normalised GCaMP6m florescence (~0.5-2) compared to reactivated NBs (~0.2-0.4) [Figure 4.3 (d)]. Given the fact that GCaMP6m signal was relatively stable, I calculated the average normalised GCaMP6m intensity over the entire period of imaging as the Ca^{2+} level for a NB. Since the GCaMP6m intensity was also relatively consistent between NBs, I took the average Ca^{2+} level of 4-5 randomly-selected NBs each brain as the average Ca^{2+} level of the brain. Comparison between brains at 0h ALH and 72h ALH shows very significant difference in average NB Ca^{2+} levels [Figure 4.3 (e)]. Although the Ca^{2+} level was relatively stable in most NBs I recorded, I did find Ca^{2+} spikes in about 10% of quiescent NBs (14 out of 141 NBs) [Figure 4.4]. The reason of these spikes were not explored due to their rarity and time limit.

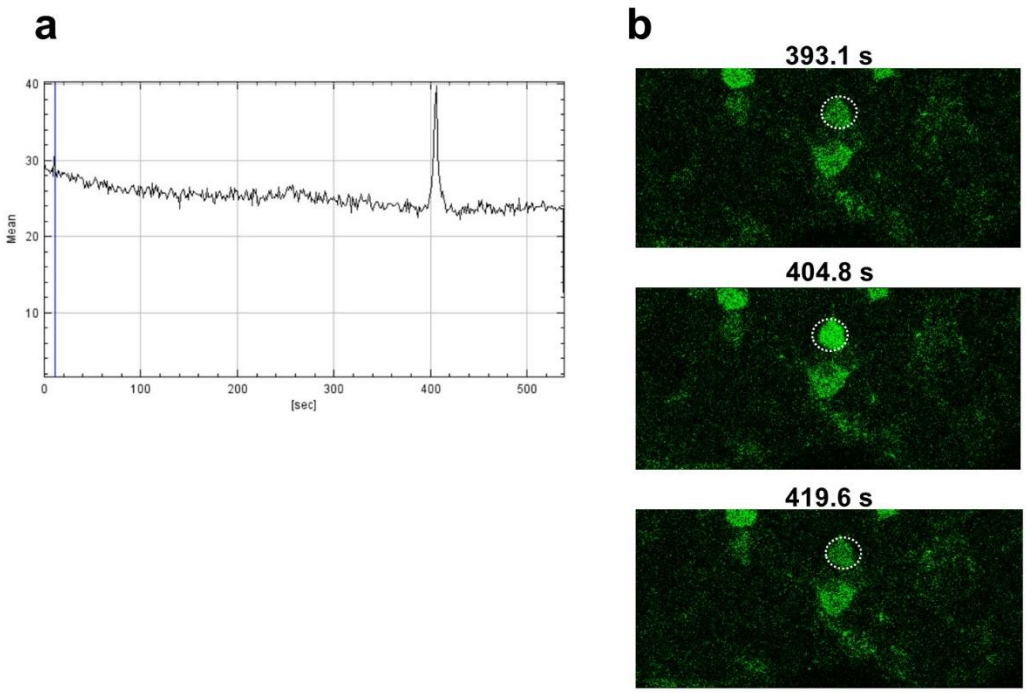

Figure 4.4 Ca^{2+} spikes in a quiescent NB (a) GCaMP6m signal intensity of a quiescent NB. A Ca^{2+} influx occurs at around 400s **(b)** A quiescent NB before, during and after a Ca^{2+} spike.

The GCaMP6m results showed that the $[Ca^{2+}]_{cyto}$ of quiescent NBs was higher than reactivated NBs. However, there are several caveats in my imaging method that need to be addressed. First, at 0 hour ALH, the *mlt*>mRFP signal was very weak, which made it difficult to mark the cell boundary. If part of the membrane-targeted RFP signal was missed in the measurement, the GFP/RFP ratios could be biased towards values that were higher than real. Also, it is possible that the weaker gCaMP6m signal in reactivated NBs is due to the enlarged cell volume that dilutes the gCaMP6m protein. These two problems could be addressed by introducing a ratiometric Ca^{2+} indicator [Cho, J.H *et al*, 2017]. In brief, the ratiometric Ca^{2+} indicator is a tandem construct of calcium-dependent GCaMP and calcium-independent mCherry fluorescent proteins linked by peptide linker [Cho, J.H *et al*, 2017]. This design ensures equimolar expression of GCaMP and mCherry proteins and is ideal for quantitive Ca^{2+} measurements.

One naïve hypothesis at this stage is that Ca^{2+} signalling is required for *Drosophila* NB quiescence. As discussed previously, loss of Slo is likely to increase $[Ca^{2+}]_{cyto}$ in NBs. Interestingly, I also showed in Chapter 4 that loss of Slo strongly prolonged quiescence. Therefore, one possible mechanism for Slo in regulating NB quiescence could be via the Ca^{2+} signalling. In quiescent NBs, high $[Ca^{2+}]_{cyto}$ maintains quiescence and Slo is either not sufficiently expressed or inhibited. As Slo becomes functional, high $[Ca^{2+}]_{cyto}$ activates Slo and Ca^{2+} influx is restricted possibly due to the VGCCs. NBs then reactivate as a result of lower $[Ca^{2+}]_{cyto}$ [Figure 4.5].

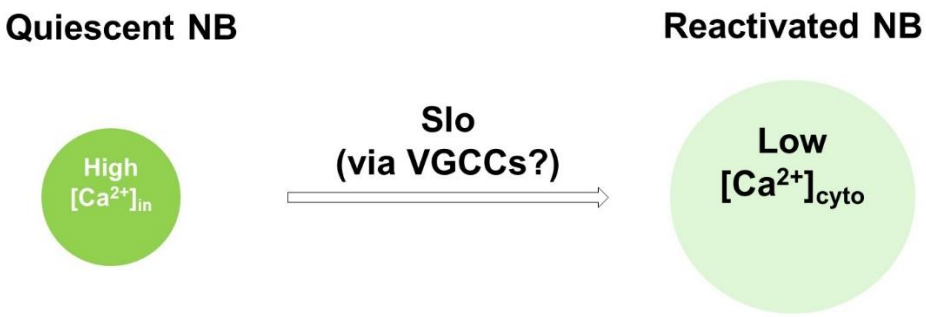

Figure 4.5 Working model of Slo regulating NB quiescence via the Ca^{2+} signalling

4.3 Increasing intracellular Ca^{2+} is sufficient to block NB reactivation

Many things need to be tested to support my working model. One question that can be easily answered is whether increasing intracellular Ca^{2+} is sufficient to block reactivation. I expressed dTprA1 as well as the Orai/Stim complex in neuroblasts using *wor*-GAL4 as the driver. Both tools have been shown to increase $[Ca^{2+}]_{cyto}$ in *Drosophila* cells [Deng, HS et al, 2015][Xu, C et al, 2017]. As shown in Figure 4.6, overexpressing two Ca^{2+} channels significantly reduced brain size and mitosis in early L3 brains. One caveat is that cellular Ca^{2+} overload could interfere with the mitosis machinery. However, expression of these two Ca^{2+} channels in *Drosophila* intestine stem cells actually causes over-proliferation [Deng, HS et al, 2015][Xu, C et al, 2017]. Therefore, it is more likely that high $[Ca^{2+}]_{cyto}$ blocks reactivation rather than mitosis *per se*.

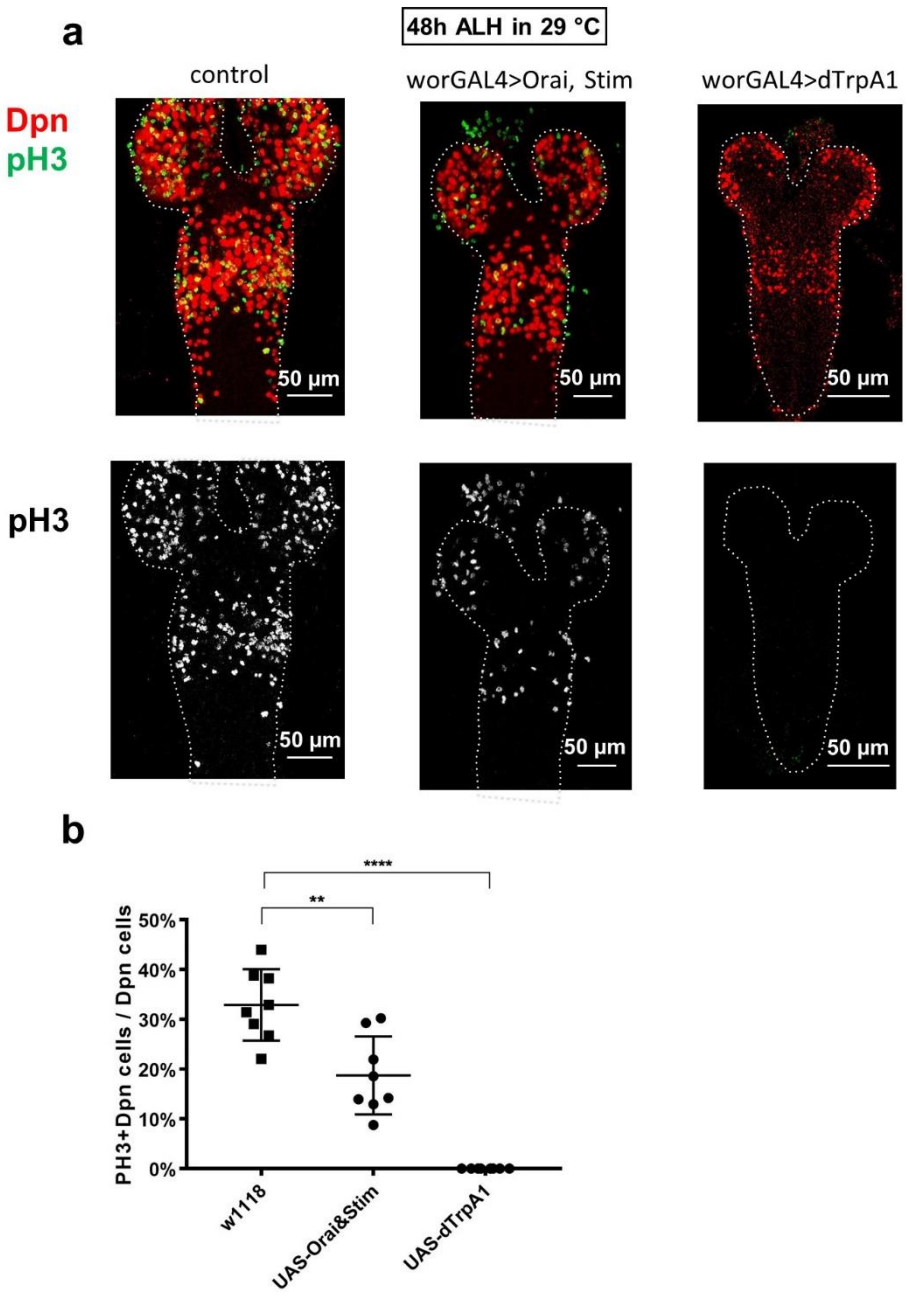

Figure 4.6 Increasing intracellular Ca^{2+} is sufficient to block NB reactivation (a) Overexpression Orai/Stim complex and TrpA1 significantly reduces NB division at 48h ALH **(b)** Quantification of the mitotic index in each genotype. N=7-8 brains per genotype. **: p<0.01, ****: p<0.0001, Student's T-test, error bars indicate SD.

4.4 Exploring the interaction between Slo and Ca^{2+} signalling

So far I have demonstrated that $[Ca^{2+}]_{cyto}$ is higher in quiescent NBs. Also, upregulating $[Ca^{2+}]_{cyto}$ is sufficient to prolong NB quiescence. These results suggest that Ca^{2+} signalling is a positive regulator of NB quiescence. I have also shown that loss of Slo

strongly blocks reactivation. Interestingly, Slo is known to negatively feedback onto Ca^{2+} signalling in neurons and muscles via VGCCs. In *Drosophila* NBs, these is evidence suggesting VGCCs are substantially expressed [Berger, C et al, 2012]. Although I do not have any data on how Slo regulates cellular Ca^{2+} in NBs, it is reasonable to speculate that Slo acts as a negative regulator.

One way of testing if Slo acts via the Ca^{2+} signalling to regulate NB quiescence is epistasis analysis between Slo and components of Ca^{2+} signalling. I first tested if knocking down the central Ca^{2+} sensor, *calmodulin*, is sufficient to rescue the reactivation deficiency caused by knocking down *slo*. As shown in Figure 4.7, knocking down *cam* did not activate NBs that remained quiescent due to loss of Slo. However, this is only a very preliminary result. More live imaging and epistasis experiments are needed to conclude if Slo affects NB activation via the Ca^{2+} signalling pathway.

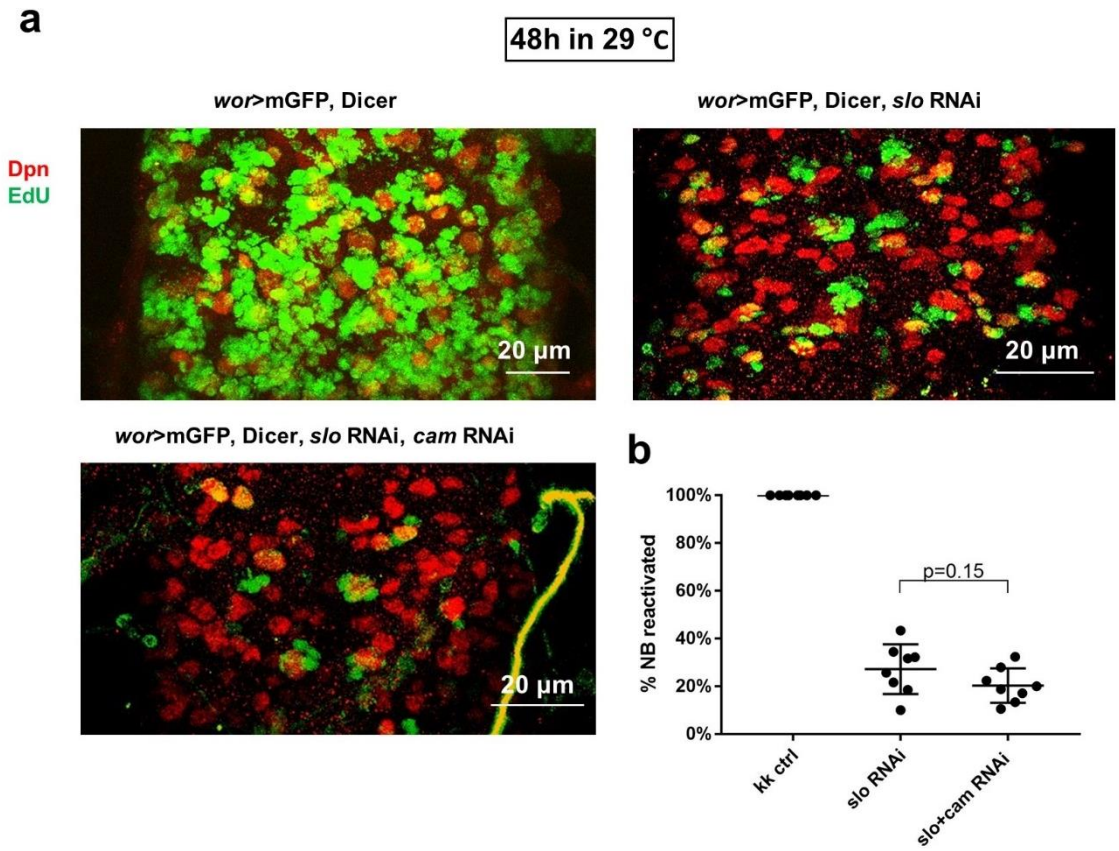

Figure 4.7 Knocking down *calmodulin* in NBs does not rescue the *slo* KD phenotype (a) Epistasis experiment between *slo* KD and *cam* KD. The *wor*-GAL4 driver was used to drive expression of indicated transgenes in NBs throughout development. Reactivation was assayed by EdU (green) incorporation in NB nuclei (red). **(b)** Quantification of reactivated NBs

in each genotype. N=6-8 brains per genotype. Student's T-test, error bars indicate SD. Horizontal bar indicates mean.

4.5 Chapter summary and discussion

In this chapter, I investigated neuroblast Ca^{2+} signalling as one possible downstream effector of Slowpoke. I have found that $[Ca^{2+}]_{cyto}$ is higher in quiescent NBs compared to reactivated NBs. Also, increasing $[Ca^{2+}]_{cyto}$ in NBs is sufficient to impair reactivation. Since Slo could down-regulate cellular Ca^{2+}, my hypothesis is that Slo promotes NB reactivation by suppressing the Ca^{2+} signalling via lowering $[Ca^{2+}]_{cyto}$. Here I will propose some future experiments to test this model.

First, it is important to confirm the difference in $[Ca^{2+}]_{cyto}$ between quiescent and cycling NBs using a ratiometric Ca^{2+} sensor. Once this is established, it would be interesting to apply live Ca^{2+} imaging in embryonic cycling NBs. According to my working model, $[Ca^{2+}]_{cyto}$ should be low in cycling NBs. Although very interestingly, *calmodulin* is not expressed in embryonic cycling NBs but highly expressed in quiescent NBs [Janina Ander and Andrea Brand, unpublished]. So it is also possible that $[Ca^{2+}]_{cyto}$ is high in embryonic cycling NBs but Ca^{2+} signalling is not activated due to lack of Calmodulin. Another important experiment is to monitor changes in $[Ca^{2+}]_{cyto}$ during the period leading up to reactivation. Does $[Ca^{2+}]_{cyto}$ gradually decease as the larvae start feeding? Or does $[Ca^{2+}]_{cyto}$ increase first then decrease before reactivation? Getting these information would help us to further understand the role of Ca^{2+} in NBs.

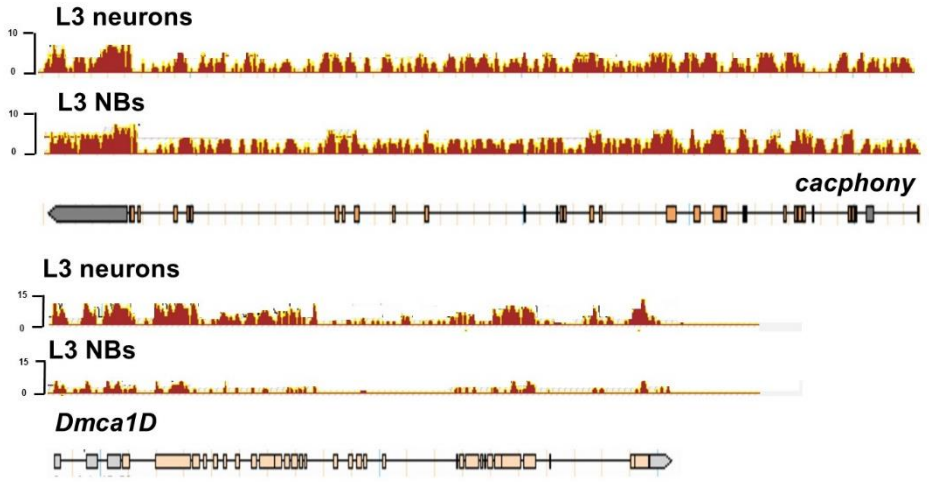

Figure 4.8 Expression of two VGCCs (*cacophony* and *Dcma1D*) in NBs (mRNA-seq tracks of two VGCCs, *cac* and *Dcam1D* in L3 NBs. Expression levels in neurons are used as references. Tracks are copied from Flybase GBrowse [Berger, C et al, 2012].

It is normally difficult to downregulate $[Ca^{2+}]_{cyto}$ as cells actively extrude Ca^{2+} from the cytoplasm. However, in quiescent NBs where $[Ca^{2+}]_{cyto}$ is high, we can overexpress Ca^{2+} pumps including SERCA, PMCA to see if they indeed reduce $[Ca^{2+}]_{cyto}$ and lead the NBs to reactivate prematurely. On the other hand, investigating how high $[Ca^{2+}]_{cyto}$ maintains quiescence is another important aspect of the project. Performing a small RNAi screening on major Ca^{2+} signalling pathway components (PKCs, Calmodulin-dependant kinases, Calcineurin, etc) would be a doable assay.

Alongside investigating the role of Ca^{2+} signalling in NB quiescence, it is also important to establish the link between Slowpoke and Ca^{2+}. First, Slo mostly likely regulates cellular Ca^{2+} by the inhibiting the VGCCs, which are expressed in reactivated NBs [Figure 4.8]. Knock down of VGCCs could rescue the prolonged quiescence phenotype caused by KD of Slo. Second, we can also test if knocking down major Ca^{2+} signalling pathway components could rescue the Slo KD phenotype.

Recently, more and more evidence suggest Ca^{2+} signalling plays important roles in NSC quiescence. Using *Drosophila* neuroblasts as model, I have shown that high $[Ca^{2+}]_{cyto}$ promotes quiescence. In mammalian NSCs, store-operated Ca^{2+} entry

promotes symmetrical division, while the resting $[Ca^{2+}]_{cyto}$ in quiescent and cycling NSCs are unknown [Domenichini, F et al, 2018]. In glioblastoma stem-like cells (GSLC), a cell type that share many similarities with NSCs, SOCE is also found to be present and required for proliferation [Galli, R *et al*, 2004][Aulestia, FJ *et al*, 2018]. Interestingly, Aulestia, FJ and colleagues observed that resting $[Ca^{2+}]_{cyto}$ is lower in proliferating GSLC cells compared to quiescent ones, which is consistent with my results. These results have laid the foundation for further investigation on Ca^{2+} signalling in NSC quiescence using *Drosophila* as the model.

5. Analysis of *mulet*: a highly quiescence-specific microtubule regulator

5.1 Introduction

5.1.1 Neuroblast reactivation is associated with retraction of the quiescence projection

As described in 3.1, one major characteristic of quiescent neuroblasts is the basal projection, which is completely lost in fully reactivated neuroblasts [Figure 5.1]. Although no live imaging was performed to record the behaviour of this projection during reactivation, neuroblasts with shorter projection were frequently observed during this time window [Figure 5.1]. Therefore, it is reasonable to assume that as reactivation happens, neuroblasts gradually retract their basal projection. However, how this major morphology change is regulated and whether it is important for reactivation remain to be explored.

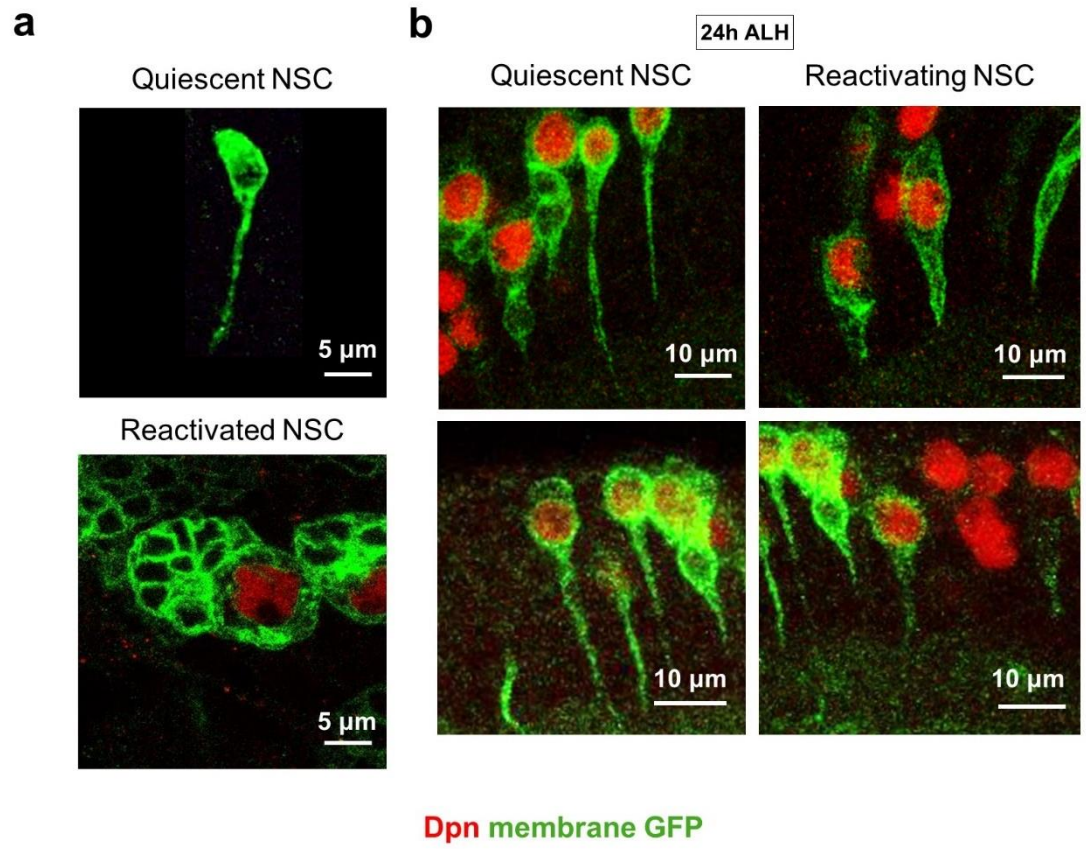

Figure 5.1 Neuroblast reactivation is associated with retraction of the quiescent projection (a) Top: A quiescent neuroblast labelled by membrane GFP (green). Bottom: A

reactivated neuroblast (red) labelled by membrane GFP (green) **(b)** Left column: quiescent neuroblasts (red) with long projections. Right column: reactivating neuroblasts (red) with shrinking projections.

5.1.2 The quiescence-specific projection is rich in microtubules

As shown in 3.1, the quiescence projection in neuroblasts is very similar to axons in neurons. A major component of axonal structures are microtubules (MT) [Dent, EW *et al*, 2011]. To test if microtubules are also present in the quiescent projection, I used a GFP-tagged MT associated protein, Zeus::GFP to visualise MT [Morin, X *et al*, 2001]. As expected, quiescent neuroblast projections labelled with membrane RFP overlap with intense Zeus::GFP signal [Figure 5.2], which suggests MT are very abundant in this projection.

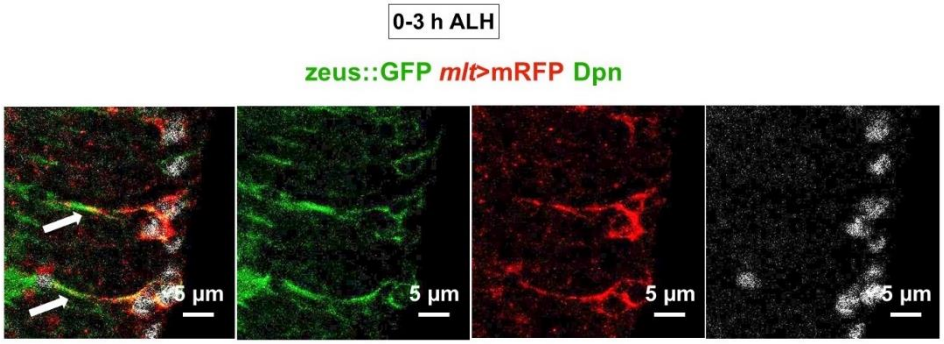

Figure 5.2 Quiescence-specific projections are rich in microtubule. White arrows mark the projections of quiescent neuroblasts.

5.1.3 Microtubule dynamics are partly controlled by tubulin-specific cofactors

Microtubules consist of polymerised α/β tubulin heterodimers and undergo constant growth and destruction [Weisenberg *et al*, 1976][Desai & Mitchison, 1994]. In *vivo*, this highly dynamic system is regulated by a large number of factors that can be broadly categorised into two families by their working mode. One mode is directly interacting with MTs. Factors with this working mode include MT-associated proteins (MAPs), katanins [Hirokawa, N, 1994][Quarmby, L, 2000]. Another mode is controlling the availability of free tubulin heterodimers. In order to be incorporated into the growing MT, α and β tubulin subunits need to be correctly folded and joined together, which requires a series of tubulin specific co-factors named tubulin cofactor A-E (TBCA-E) [reviewed in Lewis, SA *et al*, 1997]. Due to their ability to bind to and process tubulin subunits, tubulin cofactors are found to have significant impact on MT stability. For

instance, loss of TBCA leads to loss of MT in cells while loss of TBCC leads to increase of MT [Nolasco, S *et al*, 2005][[Hage-Sleiman, R *et al*, 2011].

Since tubulin cofactors regulate the stability of MT, which is a major component of axon, it is not surprising that TBCs are involved in axonal growth and maintenance. For instance, KD of TBCB in mouse neurons has been reported to enhance axon growth while overexpression of TBCB caused growth cone retraction [Lopez-Fanarraga, M *et al*, 2007]. In *Drosophila*, loss of TBCE causes the axon bundles in embryos to be grossly interrupted [Shan, J *et al*, 2009]. As shown in Figure 5.1 and 5.2, the quiescence projection is morphologically very similar to axons and is also abundant in MT. Therefore, it would be interesting to explore if TBCs are involved in the behaviour of the quiescence projection and whether that affects reactivation.

5.2 *mulet*, a tubulin cofactor that is expressed in quiescent neuroblasts

While comparing the Targeted DamID data sets generated from quiescent and cycling neuroblasts (described in 3.2), I found *mulet*, a tubulin cofactor gene to be one of the top quiescent specific genes. *mulet* is the *Drosophila* homolog of tubulin cofactor E like (TBCEL) and has been shown to affect cell shape remodelling during spermatid maturation in flies [Nuwal, T *et al*, 2012][Fabrizio, JJ *et al*, 2012]. Therefore, it is interesting to investigate its function in quiescence as well as in the behaviour of the quiescent basal projection.

5.2.1 Structure and known function of *mulet*

The *mulet* locus is nested in a very large intron of the KCNQ gene (a potassium channel) on chromosome 2R. It has three transcripts and only one exon [Figure 5.3 (a)]. The sequence of the Mulet protein shows significant homology to mammalian TBCEL, with two leucine-rich repeats (LRR) for protein-protein interaction and one ubiquitin-like domain (UBL) [Figure 5.3 (c)]. This structure supports the function of TBCEL elucidated in mammalian cells. Bartolini *et al*, 2005 showed TBCEL destabilised MT *in vivo* by targeting tubulin to the proteasome for degradation. The *Drosophila* Mulet shares very high amino acid identity (39%) with the human TBCEL [Figure 5.3 (b)]. In *Drosophila*, the role of Mulet/TBCEL on MT regulation has not been

shown directly. It has been shown, however, to be essential for the investment cone to move along MT during spermatid maturation [Nuwal, T *et al*, 2012]. Based on the sequence homology and implied function, it is reasonable to hypothesise that Mulet/TBCEL is involved in MT dynamics in *Drosophila*.

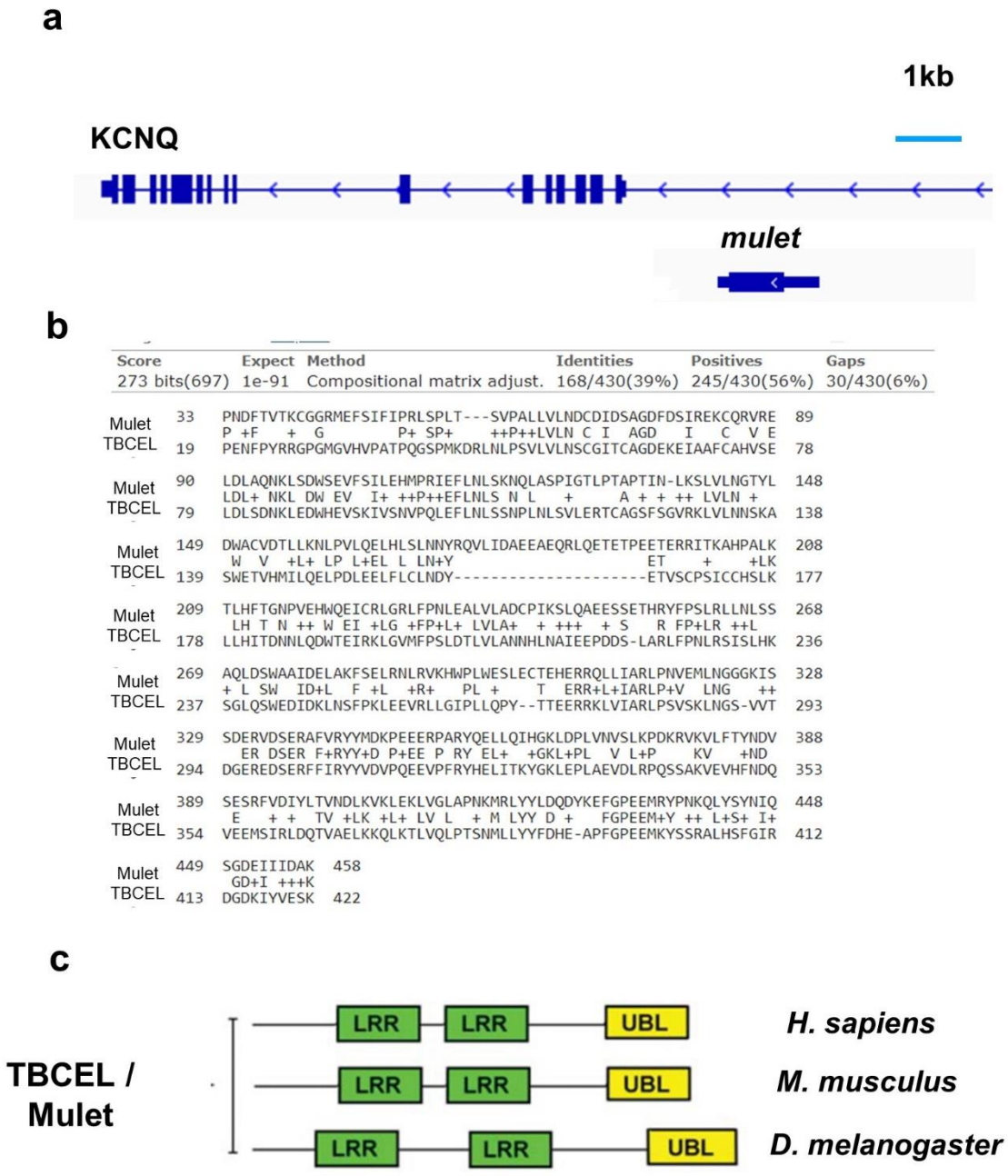

Figure 5.3 Structure of *mulet* gene and protein (a) the *mulet* gene is located in a very large intron of KCNQ gene (KCNQ locus is cropped to fit on the page) **(b)(c)** Structure and sequence homology of Mulet protein. LRR: leucine-rich-repeat. UBL: Ubiquitin-like domain. Adapted from Tulip.N *et al*, 2012.

5.2.2 In neuroblasts, *mulet* only expressed during quiescence

Targeted DamID data generated by Janina Ander and Leo Otsuki suggest *mulet* is absent in embryonic cycling neuroblasts but expressed in quiescent neuroblasts [Figure 5.4 (b)]. In order to confirm the expression pattern of *mulet*, I used RNA *in situ* and antibody staining. There is also a GAL4 insertion line at the endogenous locus of *mulet* (termed *mlt*-GAL4) available from the NP enhancer trap collection. Combined with an UAS-fluorescent protein line, It is used to reflect *mulet* expression at the transcriptional level. Previous RNA *in situs* (BDGP *in situ* database) showed no signal of *mulet* in the CNS at stage 14, a pre-quiescence stage. This result was reproduced by my own *in situ* experiments. As shown in Figure 5.4 (a), *mulet* expression in the CNS initiated at stage 16. At stage 17, three stripes of cells in the thoracic segment of the VNC clearly expressed *mulet* [Figure 5.4 (a)]. The location and pattern of these cells closely resembled neuroblasts, however, the exact identity of the cells could not be determined using this method.

In order to confirm *mulet* expression at the protein level, I co-stained the embryos with a published antibody against Mulet and a neuroblast marker (Tulip, N *et al*, 2012). The Mulet antibody was raised in the same species as the anti-Dpn antibody I regularly used. Therefore, I used the alternative neuroblast marker Miranda. As shown in Figure 5.4 (c), Mulet was expressed in many although not all quiescent neuroblasts. This could either be attributed to the quality of the Mulet antibody or low level of *mulet* expression at this developmental stage, as the signal-noise ratio was rather low in most samples I imaged.

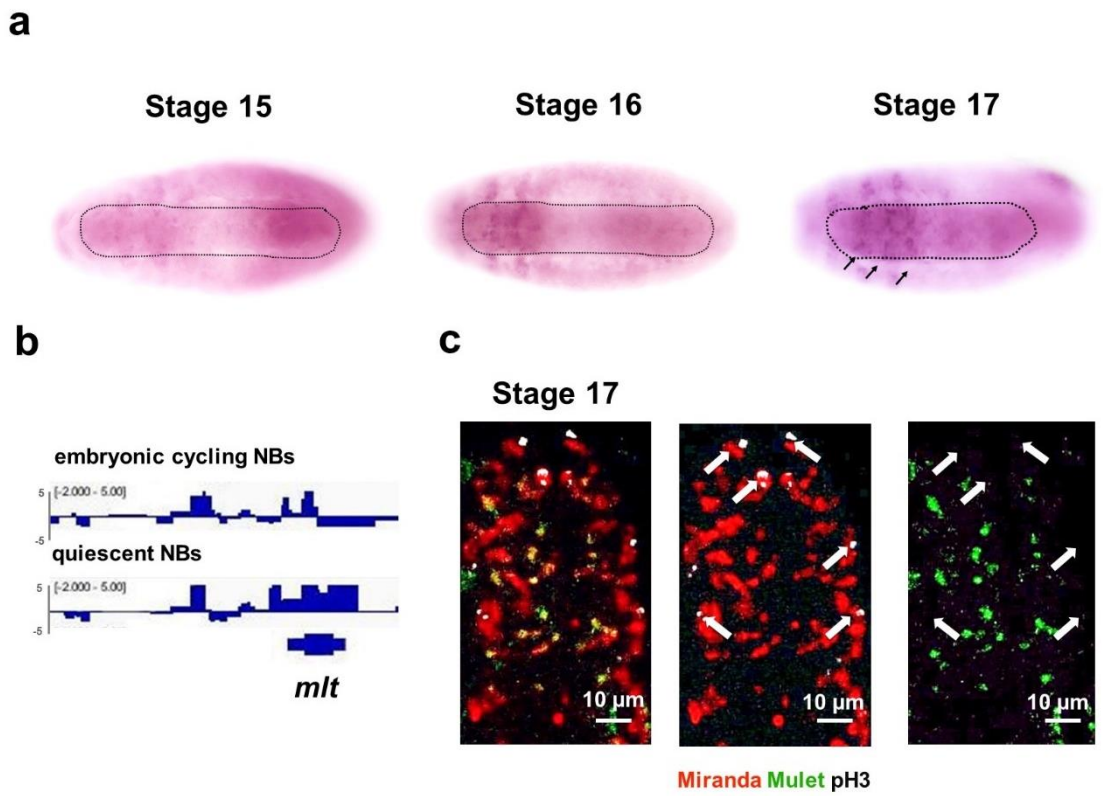

Figure 5.4 *mulet* is expressed in quiescent neuroblasts. (a) RNA *in situ* hybridisation against *mulet* in stage 15, 16,17 embryos. Black dash: outline of CNS; Black arrows: stripes of cell clusters that could be quiescent NBs.**(b)** Pol II occupancy of *mulet* locus revealed by Targeted DamID before and during quiescence (Janina Ander and Andrea Brand, unpublished). **(c)** Immunostaining against Mulet (green) and Miranda in stage 17 embryos. Notice neuroblasts (red) that were cycling (white, white arrow) were all negative for Mulet.

As the only available antibody against Mulet yielded poor-quality staining, I searched for other tools to profile *mulet* expression in neuroblasts throughout development. I used a GAL4 insertion line at the endogenous locus of *mulet* (termed *mlt*-GAL4) and therefore could be used to reflect *mulet* expression with an UAS-reporter. *mlt*-GAL4 starts to express at stage 17, when NBs are mostly quiescent [Figure 5.5 (a)]. At the time of larval hatching, *mlt*-GAL4 is expressed in ~80% of neuroblasts in the VNC, when all neuroblasts are supposed to be quiescent [Figure 5.5 (c)]. In the brain lobes, there are 8 mushroom body NBs and 2 lateral NBs that do not undergo quiescence. Consistently, *mlt*-GAL4 is never found to be expressed in those NBs at larval hatching [Figure 5.5 (b)]. Moreover, the expression of *mlt*-GAL4 in NBs is restricted during quiescence. In both embryonic and larval cycling NBs, *mlt*-GAL4 is not expressed [Figure 5.5 (a)].

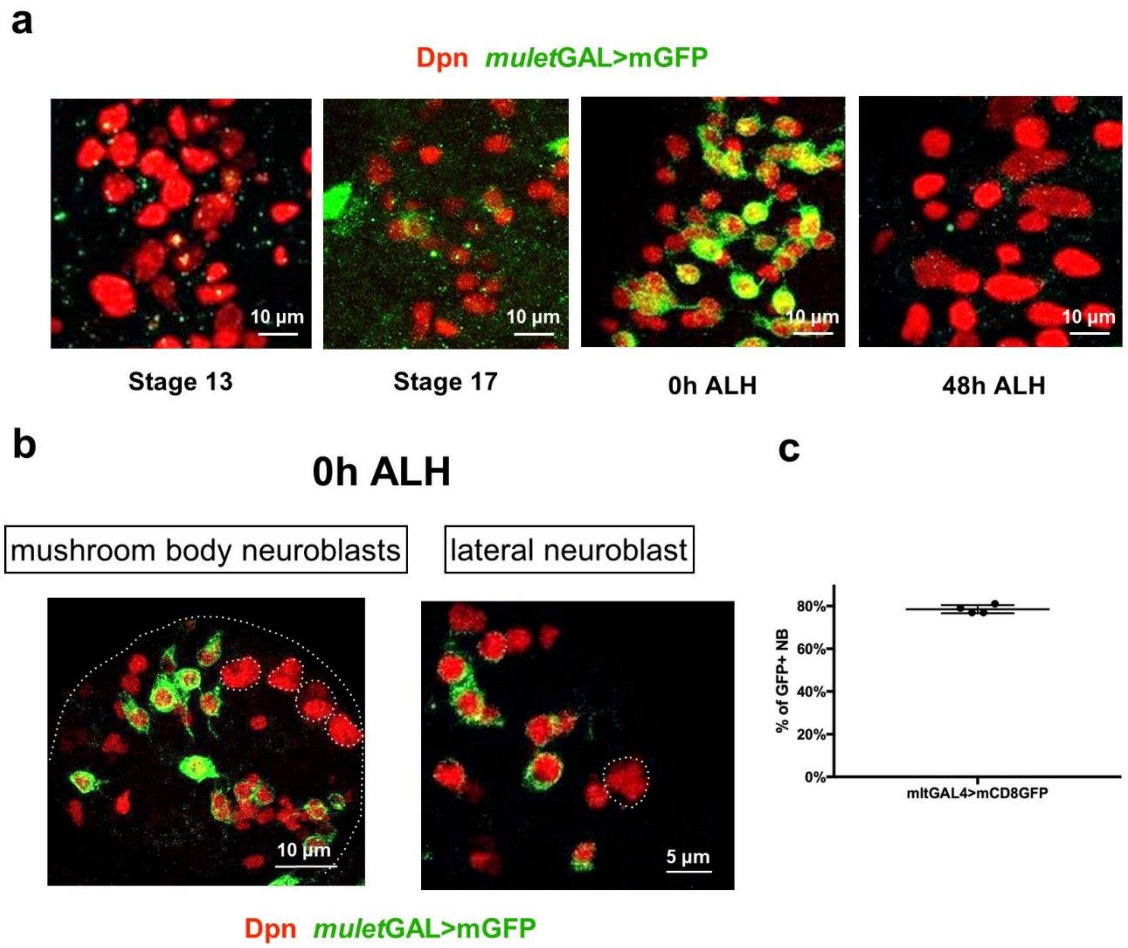

Figure 5.5: *mulet* is not expressed in non-quiescent neuroblasts (a) *mlt*-GAL4 (green) expression in NBs (red) at different developmental stages.**(b)** *mlt*-GAL4 (green) is not expressed in the non-quiescent mushroom body and lateral NBs (red). White dash cycle: mushroom body NBs and lateral NBs **(c)** Percentage of NBs in the VNC that expressed *mlt*-GAL4. Horizontal bar indicated mean. Error bar indicates SD.

The profiling of *mlt*-GAL4 revealed it to be a very good driver for quiescent neuroblasts. Two GAL4 drivers regularly used to drive expression in NBs are *grainyhead* GAL4 (*grh*-GAL4) and *worniu* GAL4(*wor*-GAL4). However, at the time of larval hatching, both drivers are expressed in a great number of non-NB cells, mostly in neurons [Figure 5.6 (a)]. In comparison, apart from a group of midline cells, *mlt*-GAL4 is expressed almost exclusively in quiescent NBs [Figure 5.6 (a)]. Those *mlt*-GAL4+ midline cells are neither positive for Repo nor Elav and their identity is not known. However, judged by their location, morphology and molecular identity, they are likely to be the Repo negative midline glia [Figure 5.6 (b)][Halter, D *et al*, 1995] Therefore, *mlt*-GAL4 is a superior driver for profiling quiescent neuroblasts, as it is expressed in neither non-

quiescent NBs nor neurons. This property of *mlt*-GAL4 makes it particularly useful for Targeted DamID analysis of quiescent NBs, as neurons and non-quiescent NB are the main sources of contamination for this type of experiment.

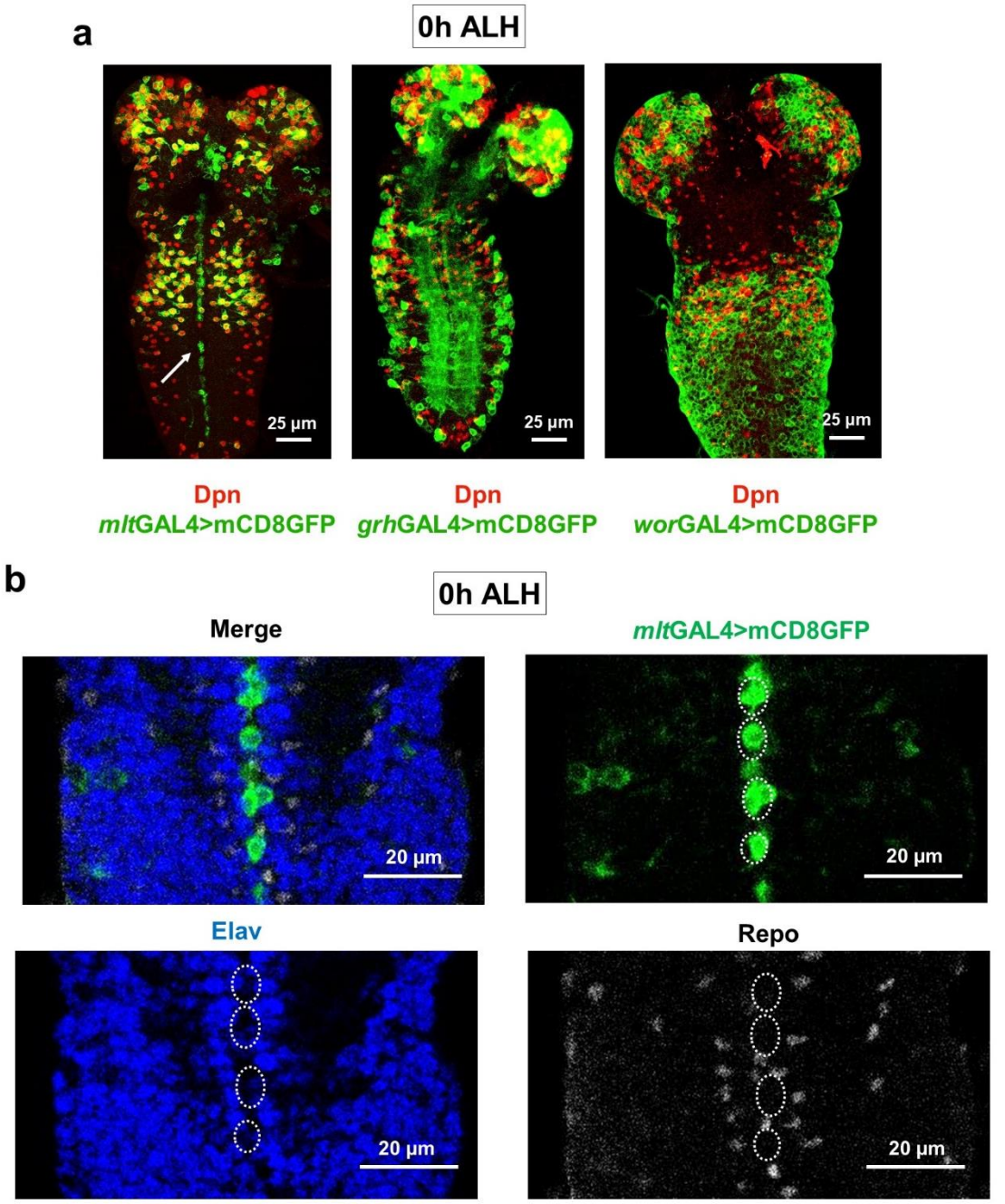

Figure 5.6: *mlt*-GAL4 is so far the best driver for quiescent neuroblasts (a) Expression pattern of *mlt*-GAL4 (left), *grh*-GAL4 (middle) and *wor*-GAL4 (right) at the time of larval hatching. Red: neuroblasts; Green: reporter of GAL4 expression. White arrow: non-neuroblast midline expression of *mlt*-GAL4 **(b)** *mlt*-GAL4 midline cells (green) were double negative for Elav (blue) and Repo (white). White circle: nuclei of *mlt*-GAL4+ midline cells.

5.3 Analysis of *mulet* mutants, RNAi knockdown and overexpression

The analysis of *mulet* expression revealed it to be highly specific during neuroblasts quiescence. The next question is, does it have a role in neuroblast quiescence and/or reactivation?

5.3.1 *mulet* mutant neuroblasts show no defect in quiescence entry

mulet^{G18151} was generated by a P-element insertion in the *mulet* exon. Western blot analysis of *mulet*^{G18151} showed it to be a protein null mutant of *mulet* [Tulip, N *et al*, 2012]. The mutant is homozygous viable, although slightly developmentally delayed compared to *w*^{1118} controls (described in 5.3.2).

To determine if *mulet*^{G18151} neuroblasts enter quiescence normally, I immunostained *mulet*^{G18151} animals and *w*^{1118} controls for Dpn and the M-phase marker phosphorylated H3 (pH3). At both stage 17 and the time of larval hatching, I observed no difference in dividing neuroblasts between the mutants and controls [Figure 5.7]. Therefore, loss of *mulet* does not affect NB quiescence entry. This result is not surprising given that *mulet* expression initiates at stage 16, which is later than the quiescence entry time late stage 14 [Tsuji, T *et al*, 2008].

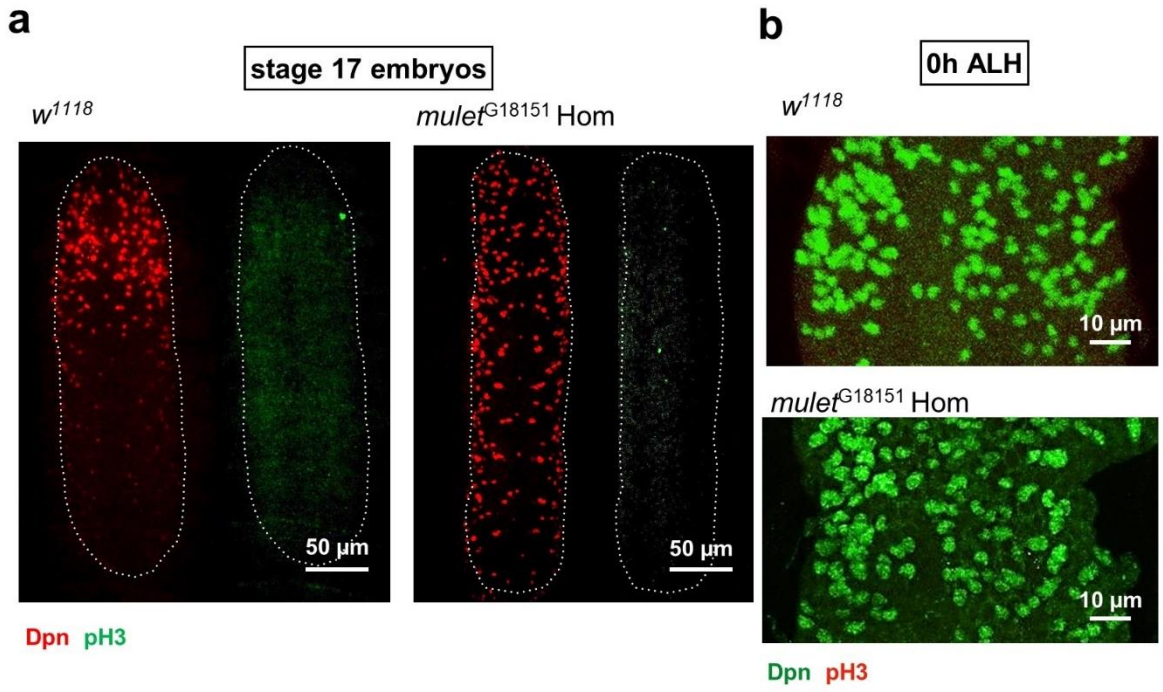

Figure 5.7 *mulet*^{G18151} mutant neuroblasts enter quiescence normally (a) *w*^{1118} controls (left) and *mulet*^{G18151} mutant embryos (right) at stage 17. Red: neuroblasts; Green: pH3; White

dash: outline of CNS **(b)** *w*^{1118} controls (upper) and *mulet*^{G18151} mutant animals (lower) at larval hatching. Green: neuroblasts; Red: pH3.

5.3.2 *mulet* mutants show defects in reactivation and growth

As I have demonstrated using RNA *in situ*, GAL4 expression and antibody staining, the expression of *mulet* initiates not long after quiescence entry and is downregulated in reactivated neuroblasts. This expression pattern suggests two possible functions of *mulet*, maintaining quiescence and/or preparing for reactivation. I therefore assayed neuroblasts in *mulet* mutants at the time of reactivation. I used a different mutant line of *mulet*, *mulet*^{EY02157} together with *mulet*^{G18151} to make sure any phenotype would be the result of the mutation rather than unknown changes in the genetic background. *mulet*^{EY02157} was generated by a P-element construct inserted in the DNA region corresponding to the 5'-UTR of *mulet* mRNA. The P-element construct in *mulet*^{EY02157} carries UAS binding sites and therefore acts both as a mutant and an UAS-Mulet line, which will be discussed later in this chapter.

At the time of NB reactivation (24h ALH in 25°C), *mulet*^{G18151} homozygous brains showed less cell division (marked by pH3) than *mulet*^{G18151} heterozygous controls. Thus, loss of *mulet* causes defect in reactivation rather than quiescence maintenance [Data not shown]. This defect was still seen at 48h ALH in 25°C and was reproduced in *mulet*^{EY02157} homozygous animals as well as *mulet*^{EY02157}/ *mulet*^{G18151} trans-heterozygous mutants [Figure 5.8 (a),(b)]. However, at this stage, it became obvious that the size of *mulet* mutant larvae was smaller than the controls. Moreover, at 72h ALH, NBs in *mulet*^{G18151} were proliferating at the same rate as controls [Figure 5.8 (c)(d)], although the average diameter was significantly smaller [Figure 5.8 (e)]. These results suggest *mulet* could be required for the growth of NBs and the whole larvae.

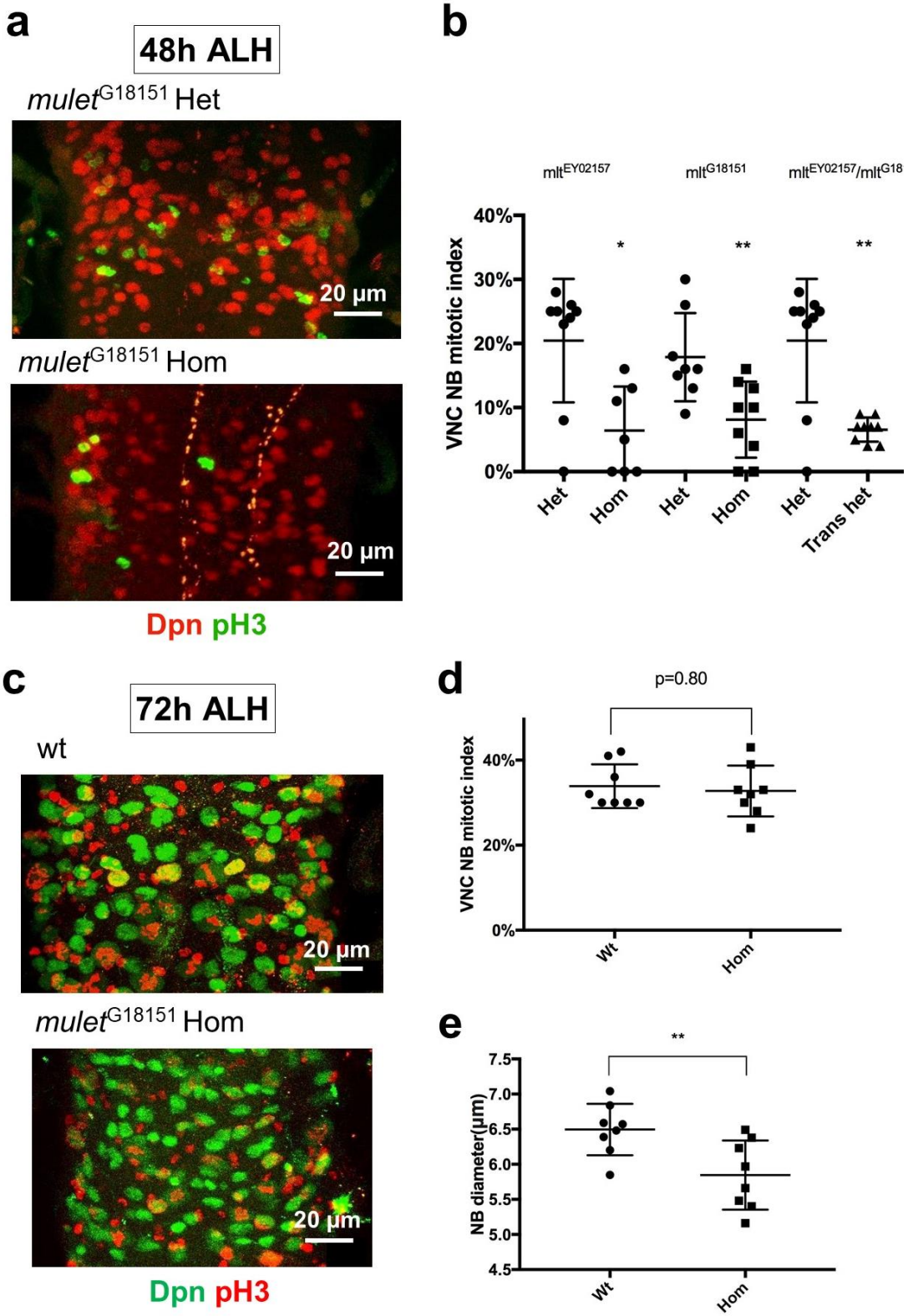

Figure 5.8 *mulet* mutants show reactivation delay (a) There were less dividing neuroblasts (red, green) in *mulet*^{G18151} mutants at 48ALH **(b)** Quantification of neuroblast reactivation at 48h ALH in *mulet* homozygous mutants and heterozygous controls. Mitotic index was defined as the percentage of dividing neuroblasts (marked by pH3) in the total number of neuroblasts

in the VNC, n=7-9 brains, Mann-Whitney non-parametric test. *: p<0.05, **: p<0.01. Error bar indicates SD. **(c)** Neuroblasts in *mulet*^{G18151} mutant proliferated at the same rate as controls at 72h ALH **(d)** Quantification of neuroblast reactivation at 72h ALH in *mulet* ^{G18151} homozygous mutant and controls. n=8 brains, p=0.80, parametric Student t-test. Error bar indicates SD. **(e)** Quantification of the average diameter of *mulet*^{G18151} hom mutant neuroblasts and white controls. n=8 brains, at least 100 neuroblasts were measured in each brain. p<0.01, parametric Student t-test.

5.3.3 *mulet*^{G18151} MARCM clones have no defect in reactivation

I generated MARCM clones of *mulet*^{G18151} to test if loss of *mulet* had an effect on reactivation in a cell-autonomous manner [see Material and Methods]. The heat shock was done at 10 hours after egg laying to induce recombination in proliferating NBs [Figure 5.9 (a)]. At 24h ALH, the expression of GFP was still below detectable levels. Therefore, I dissected the larvae at 48h ALH when GFP+ *mulet*^{G18151} homozygous clones could be clearly identified [Figure 5.9 (a)]. As shown in Figure 5.9 (b), the numbers of GFP+ NB clones (*mulet*^{G18151} homozygous) are comparable in control and test brains at 48 ALH. Without heat shock, the number of GFP+ NB clones were negligible in both control and test, which suggested very little leakiness of the heat shock promoter [Figure 5.9 (b)].

An EdU incorporation assay revealed no difference in reactivation between control and *mulet*^{G18151} mutant clones [Figure 5.9 (c)(d)]. Since all *mulet* mutants showed growth delays, it was also possible that loss of *mulet* would slow down mitosis. Therefore, I analysed the number of progeny generated by mutant and control NBs by measuring the number of EdU+ cells in each clone. Once again, no difference was observed, which suggested *mulet*^{G18151} mutants and control NB proliferated at the same rate in the 3 hour EdU feeding window [Figure 5.9 (e)].

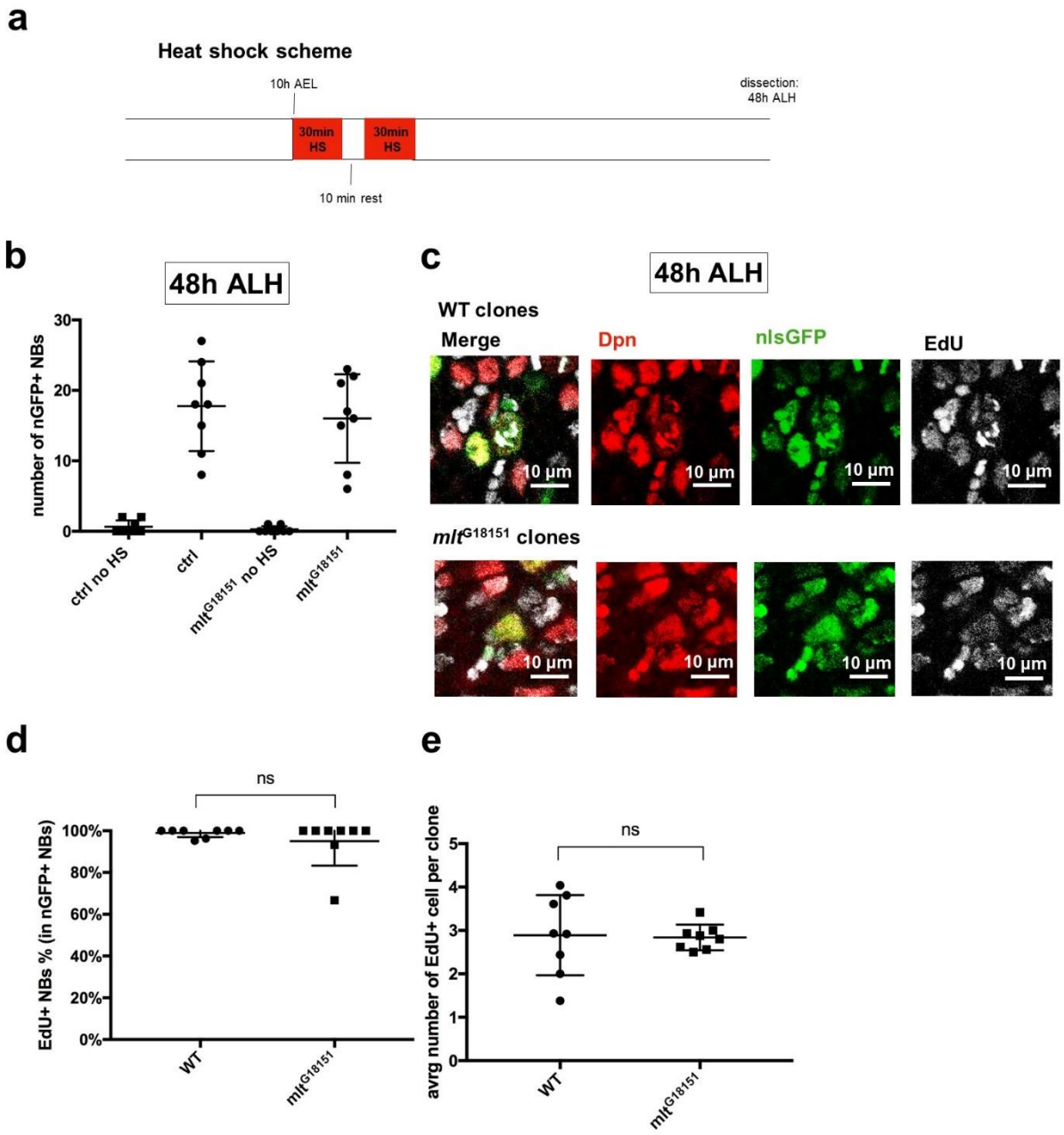

Figure 5.9 *mulet*^{G18151} mutant neuroblast clones do not have defects in reactivation and cell division (a) Heat shock scheme of inducing neuroblast MARCM clones **(b)** Quantification of GFP+ NBs in controls and test brains, with and without heat shock. **(c)** Examples of GFP+ (green) NB (red) in control and test brains. Both control and *mulet*^{G18151} mutant NBs had incorporated EdU (white). **(d)** Quantification of EdU incorporation in control and *mulet*^{G18151} mutant NBs. p>0.05, Mann-Whitney non-parametric test. Each dot represents a brain, n= 8 brains per group, 10-30 NBs per brain **(e)** Quantification of average progeny number generated by control and *mulet*^{G18151} mutant NBs. p>0.05, Mann-Whitney non-parametric test. Each dot represents a brain, n= 8 brains per group, 10-30 NBs per brain. Error bar indicates SD.

5.3.4 Neither *mulet* knockdown nor overexpression affect reactivation

In parallel to the mutant clone analysis, I also tested knockdown and overexpression of *mulet* in neuroblasts. It had been previously shown that overexpression of *mulet* in wing discs resulted in enlarged wings in adults [Raisin, S *et al*, 2003]. However, the published line carrying UAS-Mulet was no longer available. Instead, I used *mulet*^{EY02157}, which also serves as an UAS-Mulet line (thereafter named UAS-Mulet ^{EY02157}).

I tested the function of UAS-Mulet ^{EY02157} by overexpressing it in the posterior compartment of the wing disc using *engrailed*-GAL4 as driver. According to R Raisin, S *et al*, 2003, overexpression of *mulet* caused enlargement of the posterior compartment in adult wings (test area) (normalized to the anterior compartment (control area)) [Figure 5.10 (a)]. Indeed, overexpression of Mulet lead to a small albeit significant increase in size in the test area, which indicates Mulet overexpression using UAS-Mulet ^{EY02157} is functional [Figure 5.10 (b)(c)]. In parallel, I tested the UAS-*mulet* RNAi line in the same system. Knocking down *mulet* in the posterior compartment led to significant reduction in size [Figure 5.10 (b)(c)], which is consistent with the overexpression result. Therefore, UAS-Mulet ^{EY02157} and UAS-*mulet* RNAi are likely to be functional *mulet* overexpression and knockdown tools.

The changes in the size of adult wings could be attributed to two causes. Either there were less/more cells, or the size of cells changed. Each cell in the wing extends a single trichome [Wong, L.L. and Adler, P.N., 1993]. Therefore, the density of trichomes can be used as a proxy for cell size. I compared the trichome density between the anterior and posterior compartment in *mlt* KD, *mlt* OE wings. I selected two squares (0.1mm x 0.1mm) near the A/P boundary and counted the trichome density manually [Figure 5.10 (d)]. No differences were observed [Figure 5.10 (e)]. Therefore, the changes in wing sizes were induced by the increase/decrease of cell numbers rather than cell size.

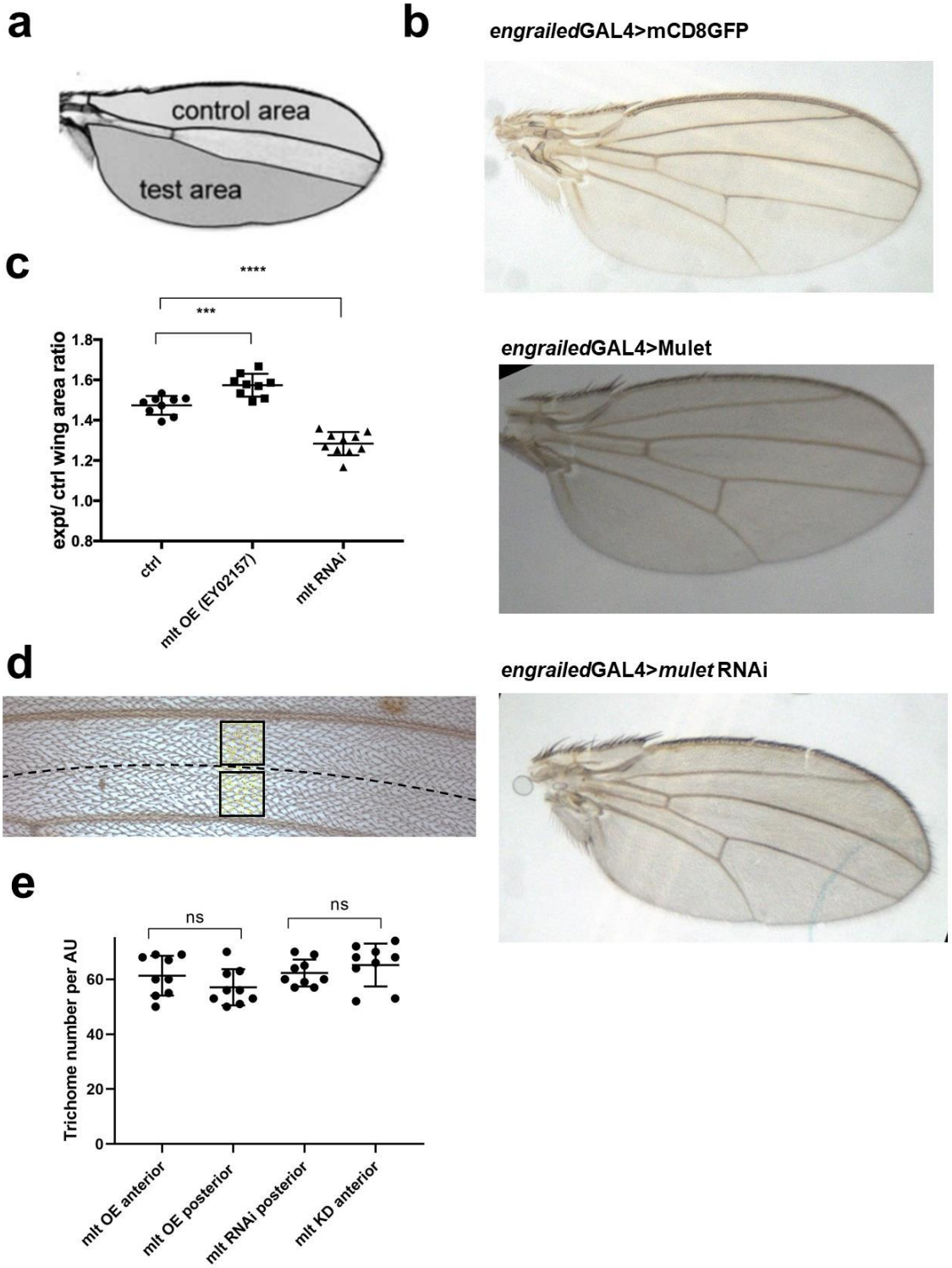

Figure 5.10: Verification of UAS-Mulet ^{EY02157} and UAS-*mulet* RNAi (a) Diagram of anterior compartment (control area) and posterior compartment (test area) in adult wings (from Raisin, S *et al*, 2003). **(b)** From top to bottom: photos of control, *mulet* overexpression and *mulet* knockdown adults wings **(c)** Quantification of relative size of the posterior compartment in control, *mulet* overexpression and *mulet* knockdown adult wings. n=8-10 wings per group,

Student t-test. ***: p<0.001, ****: p<0.0001. Error bar indicates SD. Horizontal bar indicated mean. (d)(e)

I first used the verified UAS-*mulet* RNAi line to test if knocking down *mulet* had any effect on neuroblasts reactivation. I used *grh*-GAL4, a driver that expresses in about 50% of quiescent neuroblasts [Chell, J and Brand, A, 2010] and compared EdU incorporation between *grh*-GAL4+ (labelled by membrane GFP) and *grh*-GAL4- neuroblasts. No difference in EdU incorporation was observed between NBs with and without *mulet* RNAi at 24 h ALH [Figure 5.11]. Therefore, consistent with *mulet*^{G18151} mutant clonal analysis, loss of *mulet* in NBs did not cause any defect in reactivation.

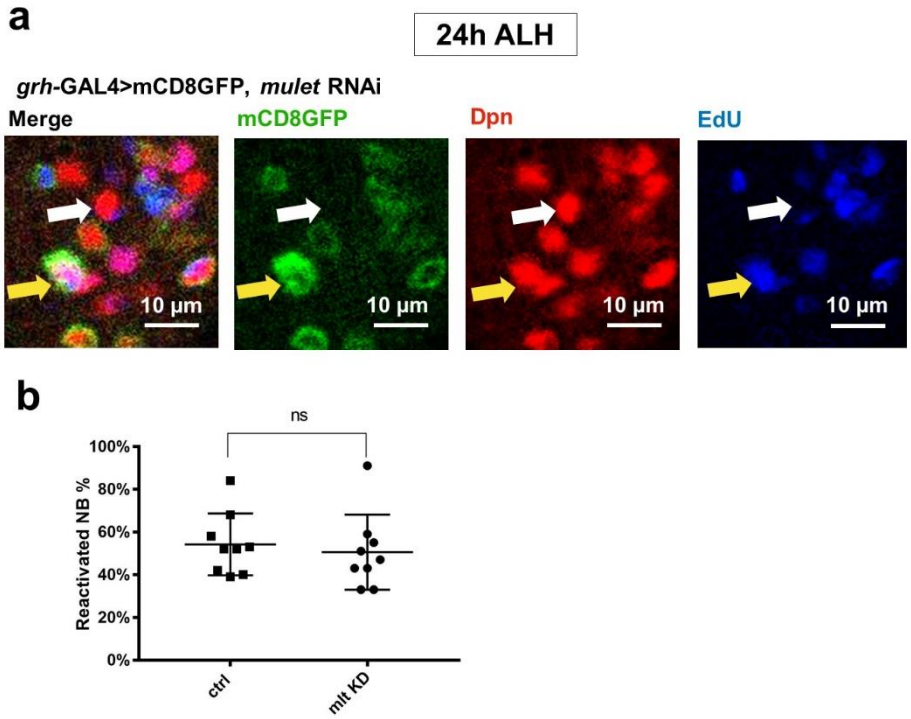

Figure 5.11: Knockdown of *mulet* does not affect reactivation (a) *mulet* knockdown using *grh*-GAL4. Yellow arrow: NB (red) expressing *mulet* RNAi incorporated EdU (blue). White arrow: NB (red) without *mulet* RNAi that had not incorporated EdU. **(b)** Quantification of reactivated NBs in (a), n=9 brains per group, p>0.05, paired Student t-test. Error bar indicates SD. Horizontal bar indicates mean.

Next, I used UAS-Mulet ^{EY02157} to overexpress *mulet* in NBs, again using *grh*-GAL4 as the driver. Antibody staining against Mulet protein confirmed the overexpression of *mulet* in neuroblasts [Figure 5.12 (a)]. However, the overexpression of *mulet* caused neither premature nor delayed neuroblast reactivation [Figure 5.12 (b)(c)].

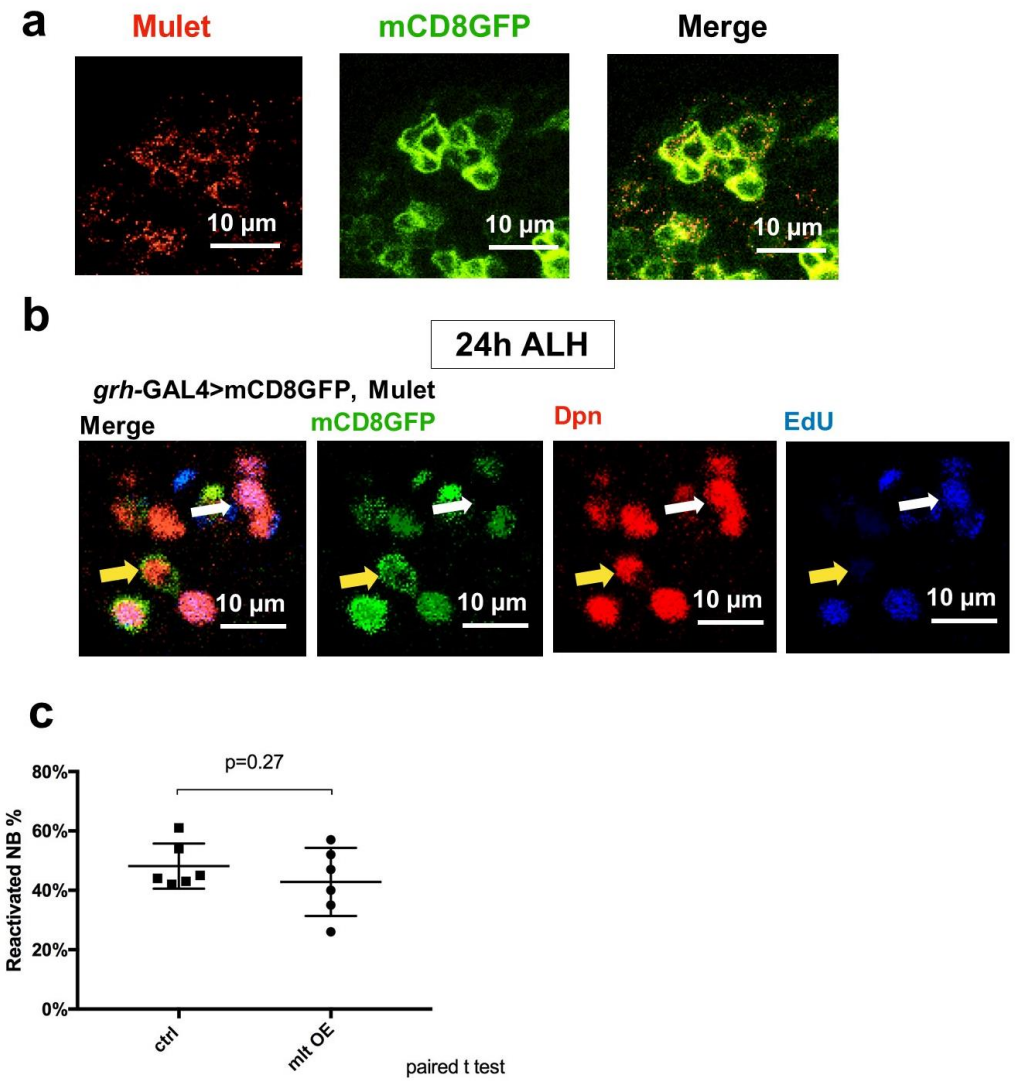

Figure 5.12 : Overexpression of *mulet* does not affect reactivation. (a) Overexpression of *mulet* using UAS-mulet^{EY02157}. Green: *grh*-GAL4>mCD8GFP. Red: Mulet **(b)** *mulet* overexpression using *grh*-GAL4. Yellow arrow: NB (red) with *mulet* overexpression that had not incorporated EdU (blue). White arrow: NB (red) without *mulet* overexpression that had incorporated EdU. **(c)** Quantification of reactivated NBs in (a), n=6 brains per group, p>0.05, paired Student t-test. Error bar indicates SD. Horizontal bar indicates mean.

In summary, all functional analyses I performed so far suggested that despite being a highly quiescence-specific gene, *mulet* does not regulate quiescence entry or reactivation. This result led me to explore another hypothesis based on the function of *mulet*. As described at the beginning of this chapter, *mulet* is necessary for cell shape remodelling and is sufficient for microtubule destruction. Therefore, it would be interesting to test if it is required for neuroblasts to retract their quiescence projections.

5.3.5 *mulet*^{G18151} mutant neuroblasts do not have defects in retracting their quiescence projection

In order to test the role of *mulet* in projection retraction, I generated MARCM clones of the null mutant *mulet* ^{G18151}[see Material and Methods]. The embryos were heat-shocked at 10 hours after egg laying to mark neuroblasts with a membrane-targeted RFP [Figure 5.13 (a)]. Without heat shock, almost no neuroblasts were labelled at 24h ALH, suggesting almost no leakiness of the heat shock system [Figure 5.13 (b)]. In heat-shocked brains, the outline of RFP labelled neuroblasts could be clearly seen at 24h ALH, including the quiescence projection if there was one [Figure 5.13 (c)]. I therefore quantified the percentage of neuroblasts with quiescence-projections in the total number of RFP-labelled neuroblasts [Figure 5.13 (d)]. However, *mulet* ^{G18151} mutant neuroblasts did not show any defects in retracting their projections. Therefore, *mulet* is not required for neuroblasts to remodel their cytoskeleton during reactivation.

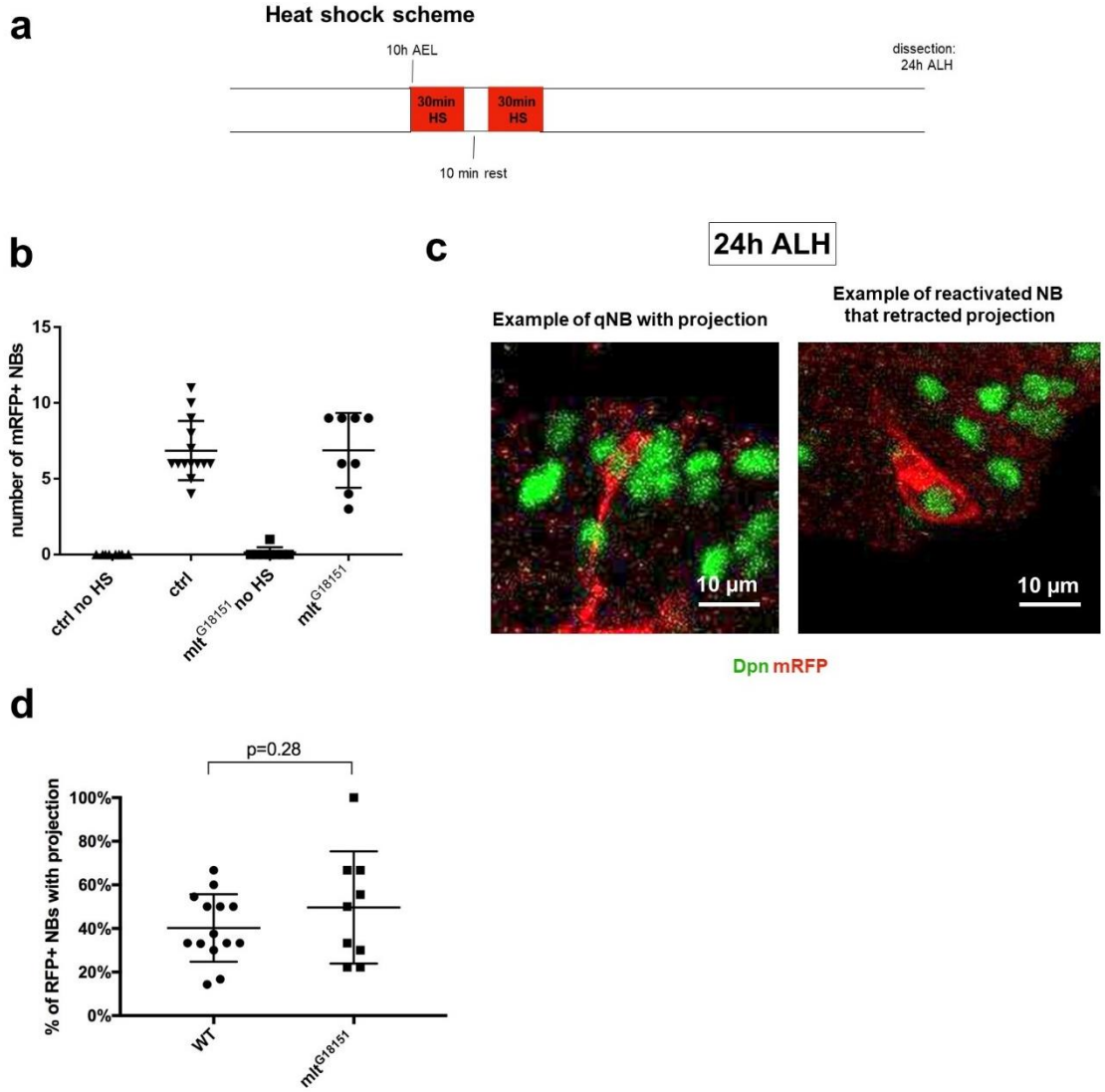

Figure 5.13 *mulet*^{G18151} mutant neuroblast clones do not have defects in projection retraction (a) Heat shock scheme to induce neuroblasts MARCM clones **(b)** Quantification of membrane RFP+ NBs in controls and test brains, with and without heat shock. Error bar indicates SD. **(c)** Example of a quiescent NB (green) with long projection (left) and a reactivated NB that had retracted its projection. **(d)** Percentage of neuroblasts with a quiescence-projection in total RFP-labelled neuroblasts at 24h ALH. p>0.05, Mann-Whitney non-parametric test. Each dot represents a brain, n= 8-12 brains per group, 4-12 labelled NBs per brain. Error bar indicates SD.

5.4 Chapter summary and discussion

Drosophila neural stem cells extend a primary projection during quiescence which is retracted as the cells become reactivated. Although very little is known about this projection, it is tempting to speculate that it is required for the proper transition from

proliferation to quiescence transition. In this chapter, I have investigated a quiescence-specific gene, *mulet*, which has been shown to affect cellular skeleton remodelling in both *Drosophila* and mammals [Bartolini *et al*, 2005][Nuwal, T *et al*, 2012].

mulet was identified as a quiescence-specific gene using Targeted DamID [Janina Ander and Andrea Brand]. Using a combination of RNA *in situ* hybridisation, antibody staining and GAL4 reporter, I have confirmed that the expression of *mulet* is indeed highly specific to quiescent neuroblasts. NBs of whole animal mutants of *mulet* showed no defects in entering quiescence but reactivation was significantly delayed. However, this effect is not cell antunomous. *mulet* mutant MARCM clones reactivated normally. Knocking down or overexpressing *mulet* in neuroblasts also did not alter the timing of reactivation. My interpretation of these seemingly contracdictory results is that the reactivation defects observed in whole animal mutants is an artifect caused by delayed development. There are two pieces of evidence that back up this hypothesis. First, at 48 hours ALH, *mulet* mutant animals were significantly smaller compared to w^{1118} controls. Second, NBs of whole animal *mulet* mutants eventually reactivated at 72h ALH. The direct way to prove this is a stage-matched experiment using molting as reference points.

mulet has been shown to destabilise microtubules and affect cytoskeleton remodelling *in vivo*. Therefore, I moved to the second hypothesis that *mulet* is required for quiescent neuroblasts to retract their microtubule-rich projections. However, *mulet* mutant neuroblasts showed no defect in retracting projections during reactivation.

Although the function of *mulet* in quiescent neuroblasts was not found in this study, there are a few interesting findings. First, among all GAL4 drivers we have tested in the lab, *mulet*-GAL4 is by far the most specific for quiescent neuroblasts. Spatially, this GAL4 driver is expressed in about 80% of quiescent neuroblasts and also in midline glia. In non-quiescent neuroblasts, neurons and most glia, its expression is undetectable (assayed in 0h ALH larval brains). Temporally, the expression window of *mulet*-GAL4 in neuroblasts strictly overlaps with the quiescence window, which makes it a great tool for quiescence-specific misexpressions. Identification of such a driver overcomes one major issue in transcriptionally profiling quiescent neuroblasts, which is contamination from neurons and non-quiescent neuroblasts. As shown in

Figure 4.6, two GAL4 drivers commonly used to drive in neuroblasts, *wor*-GAL4 and *grh*-GAL4 are both expressed in neurons and mushroom body neuroblasts. Moreover, Mulet shares a 39% sequence identity with human TBCEL protein [Figure 4.3]. The specificity and conservation of Mulet protein makes it tempting to speculate that it can be used as a marker for quiescence beyond *Drosophila* neural stem cells.

It has been reported that overexpression of *mulet* is sufficient to induce overgrowth in wing discs [Raisin, S *et al*, 2003]. While testing the *mulet* overexpression line, I recapitulated this result and also showed knockdown of *mulet* caused undergrowth in wing discs. I then assayed the size of adult wing epithelial cells represented by the density of trichomes in the affected area (each cell has one trichome). Interestingly, the size of wing epithelial cells was not altered when *mulet* was overexpressed or knocked down. These results suggest *mulet* promotes the progression of the cell cycle rather than cell size. This interpretation is also supported by my observation of *mulet* mutant larvae, whose growth was significantly slower but eventually reached wildtype size at the time of pupation.

From spindle assembly to separation of sister chromatids, proper microtubule dynamics are fundamental for mitosis. However, in contrast to a plethora of literature about mitosis, there have been very few studies looking into the roles of tubulin binding cofactors in the cell cycle progression. Knockdown of TBCA in mammalian cell culture is reported to arrest cell cycle at G1 phase [Nolasco, S *et al*, 2005]. Similarly, orthologs of TBCs in Arabidopsis are required for cell division but not cell growth [Steinborn, K *et al*, 2002]. More intriguingly, a yeast ortholog of *mulet*, Sto1p, is found to play an essential role in mitosis [Grishchuk, E. L., & McIntosh, J. R, 1999]. These studies, together with my results, strongly suggest an important role of TBCs in cell cycle regulation which is well-conserved across the entire eukaryote kingdom. Also, the fact that overexpressing *mulet* increased the speed of cell division suggests it plays a more ‘active’ role than just being a necessity for mitosis. Although the mechanism of this phenotype is beyond the scope of this study, it would be of interest for people who work on cell cycle regulation.

Based on the fact that *mulet* controls the length of cell cycle in wing discs, I made a third hypothesis on why it is specifically expressed during neuroblast quiescence. The

neuroblasts might express high levels of *mulet* during quiescence to prepare for the very fast post-reactivation cell cycle (1-1.5 hours). Although EdU labelling did not show fewer progeny from *mulet* mutant neuroblasts in 3 hours time [Figure 4.9 (e)], it is still tempting to speculate that over a longer period, the difference in progeny number will be significant, like in the wing discs. However, this is less relevant to our original question about neuroblast quiescence and reactivation.

6. Conclusion and future directions

Quiescence is an innate trait of adult stem cells. The balance between quiescence and activation is key to the maintenance of the tissue as well as the stem cells *per se*. From a therapeutic point of view, understanding stem cell quiescence is essential for regenerative therapies. For instance, loss of quiescence impairs the proliferative capacity of hematopoietic stem cell after bone marrow transplantation [Iriuchishima, H *et al*, 2010]. Also, stem-like cells have been isolated from various types of tumour [Chen, W *et al*, 2016][Aulestia, FJ *et al*, 2018]. These cells are in a relatively quiescent state to evade killing and often lead to treatment failure [Chen, W *et al*, 2016][Aulestia, FJ *et al*, 2018]. Therefore, being able to identify, target and manipulate quiescent cells would be valuable for both stem cell therapy and cancer treatment.

Like other stem cells, neural stem cells occupy unique niches that closely regulate their quiescent state [Berg, DA *et al*, 2013][Ottone, C *et al*, 2014][Otsuki, L and Brand, AH 2017]. Understanding the NSC niche signals is particularly important, as potential NSC therapies are likely to require *in situ* manipulation to ensure correct neuronal circuit. Among the well-established niche signals are neurotransmitters [Banasr, M *et al*, 2004][Song *et al*, 2012][Berg, DA *et al*, 2013][Yeh, CY *et al*, 2018]. It is an elegant mechanism that the activity of neurons regulate the activity of neural stem cells. However, although many neurotransmitters have been shown to affect NSC quiescence, the downstream mechanisms are still poorly understood [Berg, DA *et al*, 2013].

My PhD research uses *Drosophila* as the model for the ease of genetic manipulation and relative simplicity of the CNS. The main objective of my project is to identify novel mechanisms governing neural stem cell quiescence. In particular, I am interested in whether neuronal activities regulate *Drosophila* NSC quiescence and the possible downstream mechanisms. I have addressed this question from two angles. First, I tried to activate potential “quiescent neural progenitors” in adults by hyperactivating the brain [Chapter 2]. Second, I investigated genes enriched in quiescent NBs with a special focus on genes involved in neuronal functions (data generated and analysed by Leo Otsuki, Janina Ander and Andrea Brand) [Chapter 3, 4, 5].

6.1 Triggering cell cycle re-entry in adult brains by hyperactivating neurons and glia

Cell division in the adult *Drosophila* brain is extremely limited and the existence of adult NSC remains a controversy [von Trotha, J *et al*, 2009][Kato, K *et al*, 2009] [Fernandez-Hernandez, I *et al*, 2013]. We found that a subset of adult astrocytes expressed *dpn-GAL4,* which could indicate the expression of the *deadpan* gene. Astrocytes function as NSCs in mammals and neuronal hyperactivity triggers them to overproliferate [Segi-Nishida, E *et al*, 2007][Covolan, L *et al*, 2000][Lugert, S, 2010][Sierra, A *et al*, 2015]. By hyperactivating neurons and subtypes of glia respectively, I found that neuronal hyperactivation *per se* was not sufficient to trigger any cell proliferation in the adult fly brain. On the other hand, hyperactivating astrocytes caused large number of cells (mostly glia) to incorporate the S phase marker EdU. Also, stimulating glia caused more severe damage to the animals. These results fit with the emerging theory that epilepsy originates and propagates via glia, in particular astrocytes, rather than neurons [Haydon, PG and Carmignoto, G, 2006][Carmignoto, G. and Haydon, PG, 2012]. This is also the first example in free behaving animals that hyperactivating astrocytes is sufficient to trigger seizures. However, although some adult fly astrocytes reacted to seizures by incorporating EdU, I could not find any evidence for new neurons. Therefore, unlike their mammalian counterparts, astrocytes in the adult fly brain seem to lack the neurogenic potential and is not a good model for studying NSC quiescence.

6.2 Investigating neuronal genes in neuroblasts

Using the cell-type specific profiling technique Targeted DamID [Southall, TD *et al*, 2013], our lab elucidated the transcriptomes of quiescent and cycling neuroblasts (data generated and analysed by Leo Otsuki, Janina Ander, Seth Cheetam, Owen Marshall and Andrea Brand). Analysis of the quiescent transcriptome shows many neurotransmitter signalling and neuronal differentiation genes are expressed [Janina Ander and Andrea Brand, unpublished]. More interestingly, quiescent NBs extend a conspicuous basal projection which resembles the axon [Figure 3.1][Leo Otsuki, Stephanie Norwood and Andrea Brand, unpublished]. A subset of quiescent NBs send the projection towards the neuropil and makes physical contacts with neurons

[Stephanie Norwood and Andrea Brand, unpublished]. These results suggest that quiescent NBs may receive signals from neurons and possibly react in a neuron-like bioelectric manner.

Transcriptome analysis suggests *slowpoke* as one of the neuronal genes expressed in quiescent but not embryonic cycling NBs. Slowpoke is the pore-forming subunit of the Ca^{2+} activated K^{+} channel. It is critical for neuronal function as it repolarises the membrane potential after firing. The expression and function of Slo had never been described in NSCs before. In human glioma cells, the Slo homolog is highly expressed and inhibition of Slo prevents growth [Liu, X *et al*, 2002][Weaver, AK *et al*, 2004]. This is very interesting as glioma cells share many markers with normal NSCs including Nestin, Musashi and Sox2 [Strojnik, T *et al*, 2007][Garros-Regulez, L *et al*, 2016].

There was no *Drosophila* anti-Slo antibody available at the time so I tested a commercially available antibody against the mammalian homolog of Slo (Abcam 2586), which did not produce reliable staining. RNA *in situ* data show that the *slo* starts to express in the CNS after NBs become quiescent and the expression continues after the NBs reactivate. This completely correlates with the POLII occupancy and RNA-seq data in NBs, although it is not possible to confirm the expression of *slo* in NBs using regular RNA *in situ* due to its pan-CNS expression [Figure 3.3][Janina Ander and Andrea Brand, unpublished][Berger, C *et al*, 2012]. In the future, generating an antibody against Slo or performing fluorescent RNA *in situ* or tagging the Slo protein endogenously would be necessary to confirm *slo* expression in NBs.

Loss of Slo prevents *Drosophila* NBs to reactivate. Likewise, inhibition of Slo in human glioma cells prevents cell division [Liu, X *et al*, 2002][Weaver, AK *et al*, 2004]. How does Slo regulate stem cell division? My epistasis results indicate Slo acts largely independent of the insulin pathway. Another possible downstream effector of Slo is Ca^{2+}, as Slo negatively feeds back onto Ca^{2+}-elicited events in neurons. I investigate Ca^{2+} signalling in the context of NB quiescence and find that reactivated NBs downregulate $[Ca^{2+}]_{cyto}$. Upregulation of Ca^{2+} signalling phenocopies loss of Slo. These results indicate Ca^{2+} signalling indeed affects NB quiescence, which I will discuss in 6.3.

The canonical description of Slo is a plasma membrane-located ion channel. But as a gene with many different isoforms, it also acts in non-canonical ways. For instance, *Drosophila* Slo can bind simultaneously to the Src tyrosine kinase and to the catalytic subunit of the cAMP-dependent protein kinase (PKAc) [Wang, J *et al*, 1999]. This indicates Slo might act as a scaffold for membrane-bound enzymes, which could regulate the behaviour of NBs. Also, Slo has been found to locate on the inner membrane of mitochondria in human glioma cells and affects mitochondrial Ca^{2+} uptake [Siemen, D *et al*, 1999][Balderas, E *et al*, 2015]. More interestingly, Slo is expressed on the nuclear envelop of rodent hippocampal neurons [Li, B *et al*, 2014]. Blockage of nuclear envelop-targeted Slo leads to elevation of nucleoplastic Ca^{2+}, which regulates Ca^{2+} dependent gene expression [Li, B *et al*, 2014]. These results indicate profound links between Slo activity and Ca^{2+} signalling.

6.3 Investigating Ca^{2+} signalling in neuroblasts

Ca^{2+} signalling has a dual role in regulating stem cell quiescence [see Chapter 4]. Its role in neural stem cells is particularly interesting as Ca^{2+} influx is downstream of many neurotransmitters which are known to regulate NSC quiescence [Berg, DA *et al*, 2013]. Very recently, store-operated Ca^{2+} entry is found to be functional in both NSCs and glioma cells [Aulestia, FJ *et al*, 2018][Domenichini, F *et al*, 2018][also see Chapter 4]. Blockage of SOCE in NSCs promotes asymmetrical differentiative division at the cost of symmetrical cell division, while blockage of SOCE in glioma cells drives them into quiescence.

My results show that cytoplasmic Ca^{2+} in quiescent NBs is significantly higher compared to reactivated NBs. Increasing cytoplasmic Ca^{2+} by overexpressing Ca^{2+} channels blocks reactivation. These results are very significant and mostly consistent with the mammalian results. First, the cytoplasmic Ca^{2+} levels in quiescent and active mammalian NSCs are not known, but glioma cells also upregulate cytoplasmic Ca^{2+} during quiescence [Aulestia, FJ *et al*, 2018][Domenichini, F *et al*, 2018]. Second, SOCE in mammalian NSCs favours symmetrical self-renewal division [Kraft, A *et al*, 2017][Domenichini, F *et al*, 2018]. For differentiative asymmetric division, SOCE is

either inhibitory (reported by Domenichini, F and colleagues) or does not have any effect (reported by Kraft, A and colleagues) [Kraft, A *et al*, 2017][Domenichini, F *et al*, 2018]. This could explain why increased Ca^{2+} entry impairs *Drosophila* NB division which is always asymmetric during larval stage [Chia, W *et al*, 2008].

How does Ca^{2+} signalling regulate NB quiescence? Targeted DamID data show that two key components of the Ca^{2+} signalling transduction, *calmodulin* and the regulatory subunit of Calcineurin, *canB* are enriched in quiescent NBs [data generated and analysed by Leo Otsuki, Tony Southall and Andrea Brand, not shown here]. Very interestingly, the Calcineurin-dependant transcription factor NFAT is required by the mammalian follicle stem cells for maintaining quiescence [Horsley, V *et al*, 2008]. Given that the Calmodulin-Calcineurin-NFAT pathway is conserved in *Drosophila*, it should be investigated as a candidate pathway downstream of Ca^{2+} in maintaining NB quiescence [Gwack, Y *et al*, 2006].

How is Ca^{2+} signalling regulated in NBs? My results show that Slowpoke might be responsible for downregulation of Ca^{2+} in reactivated NBs for the following reasons. First, in excitable cells Slo limits Ca^{2+} influx by closing the VGCCs, which are expressed in reactivated NBs [Figure 4.7]. It would be interesting to investigate the expression and role of VGCCs in NBs. Second, KD of Slo phenocopies upregulation of cellular Ca^{2+}. Whether loss of Slo directly results in upregulation of cellular Ca^{2+} in NBs should be tested.

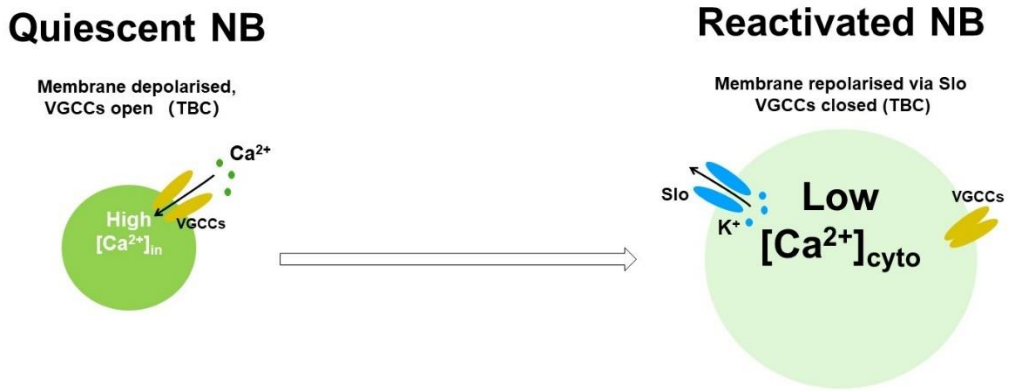

Figure 6.1 Proposed model of Slo regulates NB reactivation via the Ca^{2+} signalling

Store-operated Ca^{2+} entry has been shown to affect mammalian NSC quiescence, is it also functional in *Drosophila* NBs? My live imaging recorded Ca^{2+} oscillations in about 10% of quiescent NBs (14 out of 141 NBs) [Figure 4.4]. It is possible to record more oscillations by extending the imaging time and imaging more brains. Whether this oscillation is SOCE could be tested by adding reagents that empty the ER Ca^{2+} store, such as thapsigargin [Paschen, W *et al*, 1996]. If SOCE is operational in NBs, its role can be investigated by disrupting the Orai/Stim complex [Domenichini, F *et al*, 2018].

Ca^{2+} influx depolarises the membrane potential and is also closely regulated by the membrane potential. Changes in the membrane potential of NSCs have been shown to affect proliferation and differentiation. For instance, in cultured rat adult NSCs, depolarising the membrane by high K^+ in the medium is sufficient to promote neurogenesis [Deisseroth, K *et al*, 2004]. Also, the proliferation pattern of embryonic mouse NSCs is controlled by their membrane potential [Vitali, I *et al*, 2018]. Hyperpolarised NSCs produce late-born neurons via intermediate progenitors while depolarised NSCs produce early-born neurons directly [Vitali, I *et al*, 2018]. Genetically-encoded voltage indicators (GEVI) can be used to visualise the membrane potential of living *Drosophila* NBs. A fly line carrying an UAS-controlled version of GEVI is available and has been verified in adult fly neurons [Gong, Y *et al*, 2015].

In summary, Ca^{2+} signalling has recently emerged as a regulator of NSC quiescence in mammals, but the dynamics of Ca^{2+} level and the downstream mechanism remain largely unknown [Kraft, A *et al*, 2017][Aulestia, FJ *et al*, 2018][Domenichini, F *et al*, 2018]. In the mammalian brain, quiescent and active NSCs co-exist [Codega, C *et al*, 2014]. Thus it is technically very challenging to measure and manipulate Ca^{2+} levels in each cell type *in vivo*. Also, without presenting certain stimuli, it is also nearly impossible to monitor changes in Ca^{2+} levels as NSCs transiting into quiescence or activation. Moreover, mammalian adult NSCs proliferate symmetrically to expand the NSC pool as well as asymmetrically to generate neurons, which further complicates the issue [Piccin, D. and Morshead, CM, 2011]. The *Drosophila* neuroblasts enter and exit quiescence in synchronised patterns. They also completely lack symmetrical cell division. Therefore, *Drosophila* NBs overcome all the abovementioned issues and

provide an excellent model for investigating Ca^{2+} signalling in neural stem cell quiescence.

Following my initial investigation, there are several experiments I propose to further investigate the role of Ca^{2+} signalling in *Drosophila* NBs. First, my current method of normalising the cytoplasmic GCaMP signal against the membrane-targeted RFP signal may provide inaccurate results. A cytoplasmic, ratiometric Ca^{2+} indicator should be used to quantify Ca2+ level in NBs. Once the method is established, investigating the Ca^{2+} level in embryonic cycling NBs would be the next step. It would also be very interesting to monitor the changes in Ca^{2+} levels as the NBs reactivate. For the more mechanistic investigation, I suggest to investigate the role of key Ca^{2+} signalling protein in NB quiescence and activation, including CAMKs, Calceneurin as well as their downstream effectors. The role of voltage-gated Ca^{2+} channels should also be tested as they might be the link between Slo and the Ca^{2+} signalling pathway.

7. Material and methods

7.1 Statement of collaboration

Data and analysis generated by collaborators are underlined and specified in the text.

7.2 Fly husbandry and stocks

7.2.1 Fly husbandry

All *Drosophila melanogaster* stocks were reared on the standard cornmeal food at 25°C unless stated otherwise. For all adult experiments, adults were collected 0-24 hours post eclosion from the original vial to a fresh vial, with no more than 50 flies per vial. For all embryonic and larval experiments, embryos were collected onto apple juice plates with yeast paste. Newly hatched larvae were collected onto fresh food plates with yeast paste and reared until desired stage.

7.2.2 Fly stocks

Table 7.1 List of fly stocks used in this thesis

genotype	source / reference	comments
control line		
w^{1118}	BDRC	
GAL4 Driver lines		
;*alrm*-GAL4	Doherty *et al*, 2009	GAL4 driver that drives in the astrocytes
;*dpn*-GAL4 (GMR13C02)	BDRC	GAL4 driver that drives in the larval neuroblasts and a subset of adult astrocytes
elav-GAL4;;	Luo *et al*, 1994	GAL4 driver that drives in the neurons and neuroblasts

genotype	source / reference	comments
;*en*-GAL4(e16e)	Fietz *et al*., 1995	GAL4 driver that drives in the wing disc and in the posterior compartment only
;*grh*-GAL4	Brand Group (Chell and Brand, 2010)	GAL4 driver that drives in a subset of neuroblasts and neurons
;*mlt*-GAL4(*mulet*^{NP4786})	Eric Buchner Group (Nuwal, *et al*. 2012)	a P element insertion in the 5' UTR of *mulet* with GAL4 driver sequence, verified as a functional *mulet*-GAL4 and *mulet* mutant
;*moody*-GAL4-RFP ;*mdr65*--GAL4	Brand Group	GAL4 driver that drives in subperineurial glia
;GAL4-NP6293	DGRC	GAL4 driver that drives in perineurial glia
;*nSyb*-GAL4	Pauli *et al*, 2008	GAL4 driver that drives in mature neurons
;;*repo*-GAL4	Sepp *et al*, 2001	GAL4 driver that drives in all glia.
;*wor*-GAL4	Albertson *et al*, 2004	GAL4 driver that drives in almost all neuroblasts and a small subset of neurons
RNAi knockdown lines		
;UAS-*mulet*-RNAi	VDRC	KK library
;;UAS-*slo*-RNAi (v6723)	VDRC	GD library
;UAS-*slo*-RNAi (v104421)	VDRC	KK library
;UAS-*slo*-RNAi (JF02146)	BDRC	TRIP

genotype	source / reference	comments
;UAS-cam-RNAi	BDRC	BL-34609
UAS misexpression lines		
;*mulet*^{EY02157}	BDRC	a P element insertion in the 5' UTR of *mulet* with UAS binding sites, verified as a functional UAS-*mulet* and *mulet* mutant
;UAS-dTrpA1	BDRC	a P element insertion with UAS binding sites drive the expression of dTrpA1
;;UAS-NaChBac	BDRC	a P element insertion with UAS binding sites drive the expression of NaChBac
;UAS-Stim; UAS-Orai	Henri Jasper Group (Deng *et al*, 2015)	two P element insertions with UAS binding sites drive the expression of Stim and Orai.
Mutant lines		
;*mulet*^{G18151}	BDRC (Nuwal, *et al*. 2012)	a P element insertion in the ORF of *mulet*
;*mulet*^{EY02157}	BDRC	a P element insertion in the 5' UTR of *mulet* with UAS binding sites, verified as a functional UAS-*mulet* and *mulet* mutant
;*mulet*^{NP4786}	Eric Buchner Group (Nuwal, *et al*. 2012)	a P element insertion in the 5' UTR of *mulet* with GAL4 driver sequence, verified as

genotype	source / reference	comments
		a functional *mulet*-GAL4 and *mulet* mutant
Fluorescent indicator lines		
;UAS-mCD8GFP	BDRC	Membrane-targeted GFP used to profile GAL4 expression
;UAS-myr-RFP	BDRC	Membrane-targeted RFP used to profile GAL4 expression
;;zeus::GFP	BDRC (Morin, *et al*. 2001)	GFP labelled microtubule binding factor
;UAS-gCAMP6m	BDRC (Chen, TW *et al*, 2013)	Fluorescent Ca^{2+} sensor with medium kinetics
;LexAop-CD8-GFP-2A-CD8-GFP; UAS-mLexA-VP16-NFAT, lexAop-rCD2-GFP	BDRC (Masuyama, K *et al*, 2012)	A transcriptional reporter of Ca^{2+} activity
MARCM lines		
yw;FRT42D	BDRC (Xu and Rubin, 1993)	FLP-recombinase recognition target site located in the proximal 2R, marked by a neomycin resistance cassette
;FRT42D *mulet*^{G18151}	Brand Group	FRT42D site followed by *mulet*^{G18151} mutant
yw,hsFLP,tub-GAL4,UAS-GFPnls; FRT42D, tubGal80	Brand Group (Xu and Rubin, 1993)	a ready-made line to generate MARCM clones in

genotype	source / reference	comments
		any tissue labelled by nuclear GFP
yw,hsFLP,tub-GAL4,UAS-mRFP; FRT42D, tubGal80	Brand Group (Xu and Rubin, 1993)	a ready-made line to generate MARCM clones in any tissue labelled by membrane RFP

7.3 Immunohistochemistry

7.3.1 Adult brain dissection, fixation and antibody staining protocol

Adult brains were dissected in PBS with sharp forcets to tear the body wall and remove the attached tissue. The and then fixed in 2% paraformaldehyde (PFA) in PBL (*) for 40 min at RT. After fixation, the brains were washed 3 x 10min in PBST.

- If no ClickIT@ EdU assay (described in 7.4) was required, the samples were then blocked with 10% NGS in PBST for 15 min. Primary antibodies were also diluted in 10% NGS and incubated with the samples overnight at 4°C. (For better penetration, incubation with primary antibodies can be increased to two nights.) The samples were then washed 3 x 10 min in PBST and incubated with secondary antibodies diluted in PBST for 2-3 hours at RT.
- If ClickIT@ EdU assay was required, the samples were then blocked with 3% BSA in PBST for 30 minute RT. The ClickIT@ EdU assay was performed after blocking and before primary antibody incubation. Primary antibodies were also diluted in 3% BSA and incubated with the samples overnight at 4°C. The samples were then washed 3 x 10min in PBST and incubated with secondary antibodies and 3% BSA in PBST for 2-3 hours at RT.

For both protocols, after secondary antibody incubation, the brains were washed 5 x 10 min in PBST at RT before mounted in Vectashield (Vector Laboratories). All fixation, washing and incubation were done on a shaker.

*PBL: Dissolve 3.6 g Lysin-HCL in 100 mL H_2O. Add about 22 mL of 0.1 M Na_2HPO_4 until pH7.4. Adjust volume to 200 mL by adding sodium phosphate buffer.(**).

**Sodium phosphate buffer: Take 200 mL of 0.1 M Na_2HPO_4, add about 220 mL 0.1M NaH_2PO_4 until pH7.4.

7.3.2 Larval brain dissection, fixation and antibody staining protocol

Larval brains were dissected in PBS and then fixed in 4% formaldehyde for 30 min at RT. The rest of protocol was performed the same as described in the “adult brain dissection, fixation and antibody staining” protocol.

7.3.3 Embryonic, fixation and antibody staining protocol

Embryos collected on apple juice plates with yeast paste were transferred into a cell strainer and washed until free of yeast. They were then dechorionated in 50% bleach/water for 3 minutes. After being carefully washed until bleach was completely removed, embryos were transferred into a vial with 3 mL 4% formaldehyde/PBS and 3 mL heptane for fixation on a roller for 20 min. The 4% formaldehyde was then removed and replaced by 3 mL methanol. The vial was shaken vigorously and sunken embryos were collected and washed 3 times with methanol. Fixed embryos were then washed 3 x 5 min in PBST at RT and the immunostaining was performed as described for adult brains without EdU essay protocol. After secondary antibody incubation and wash, the embryos were transferred into 50% PBS/glycerol until sank. The embryos were then mounted in the 50% PBS/glycerol for imaging.

Table 7.2: Primary antibodies used in the thesis

antigen	source/reference	host species	comments
Broad Complex (Br-C)	DSHB	mouse	used 1:100
Chinmo		rat	used 1:500
Cyclin A	Y. Kimata Group (Whitfield et al., 1990)	rabbit	used 1:500
Deadpan	Brand Group	guinea pig	used 1:10000
Dig-AP	Roche	sheep	used 1:2000

antigen	source/reference	host species	comments
Elav	DHSB	rat	used 1:100
GFP	Abcam (ab13870)	chicken	used 1:1000
Miranda	Chris Doe Group	rat	used 1:500
Mulet	Eric Buchner Group (Nuwal, *et al*. 2012)	guinea pig	used 1:100
phosphorylated Histone 3 Ser 10	Millipore (06-570)	rabbit	used 1:100
phosphorylated Histone 3 Ser 10	Abcam (ab10543)	rat	used 1:100
Repo	DHSB	mouse	used 1:70
Repo	B.Altenhein	rabbit	used 1:10000
RFP	Abcam (ab62341)	rabbit	used 1:1000

Secondary antibodies:
All secondaries antibodies used were Alexa Fluor® conjugated antibodies, diluted 1: 250.

7.4 EdU incorporation and detection

Preparation of EdU food

For larval experiments, EdU-containing food plates were prepared by mixing EdU (Abcam) with melted standard cornmeal food. The final concentration of EdU was 50 µg/mL.

For adult experiments, EdU-containing food vials were prepared by mixing EdU (Abcam) with melted standard cornmeal food. The final concentration of EdU was 2 mg/mL.

*Because of the instability of EdU at a high temperature, EdU was only added when the temperature of the food was lower than 55°C.
**Food colour was also added to visualise the food intake of animals.

Experimental conditions of EdU feeding in larvae and adults

For adult experiments, 0-24 h post eclosion adults were collected and transferred to fresh food vials for 24 hours, with no more than 50 animals per vial. The adults were then transferred into food vials containing 2 mg/mL EdU and reared until desired stage. Brains were dissected and fixed according to the aforementioned “adult brain dissection, fixation and antibody staining protocol”.

For larval experiments, embryos were collected and reared as normal until 3 hours before the desired time point for dissection. The larvae were then transferred into food plates containing 50 µg/mL EdU until dissection. Brains were dissected and fixed according to the aforementioned “larval brain dissection, fixation and antibody staining protocol”.

For both adult and larval experiments, EdU incorporation was detected by Click-iT EdU Alexa Fluor 647 detection kit (Molecular Probes) according to manufacturer’s instructions.

7.5 Seizures induction in adult *Drosophila*

7.5.1 Seizures induced by misexpression of dTrpA1

Adult flies reared at 25°C were transferred into an empty vial with no more than 50 animals per vial. The vials were shifted to 31°C for 2 hours before shifted back to 25°C. After the animals regained mobility, they were transferred back to vials with food.

7.5.2 Seizures induced by misexpression of NachBac and Orai/Stim

Newly eclosed flies reared at 18°C were transferred into a fresh vial with no more than 50 animals per vial. The vials were shifted to 29°C for the desired length of time before dissection.

7.6 RNA *in situ* hybridization

Primer design

Primers were designed to amplify unique regions of *slo* and *mulet* from a cDNA library (Oregon R strain, 1:1 mixture of 0-4h and 4-17h embryos, 50 ng/μL). Primers were designed using Primer3 (Rozen and Skaletsky, 2000) with an optimum length of 24bp and optimum Tm of 60°C. The reverse primer included the T7 RNA polymerase sequence, which is wrriten in red. Product sizes were 928 bp for *mulet* and 746 bp for *slo*.

slo FWD:

GAGAAGACCGAAATGAAGTACGAC

slo REV:

CAGTAATACGACTCACTATTAAAGGCGTTTTGATTGAAGTAAGTC

mulet FWD:

CTCAACGACTGTGACATCGATTC

mulet REV:

CAGTAATACGACTCACTATTAGTTTCAGGCTCACATTGACCAAG

PCR amplification

PCR amplification was performed using the Q5 High-fidelity kit (NEB).

PCR reaction mix:		98°C for 10 secs
Q5 buffer (5x):	10 μL	60°C for 30 secs
dNTP:	1 μL	72°C for 2 min 15secs
cDNA:	1.3 μL	——— 35 cycles
Q5 High-fidelity polymerase:	0.5 μL	72°C for 10 min
water:	37.2 μL	
total:	50 μL	

PCR cycle

Heated lid: 110°C

———

98°C for 30 secs

Visualisation of PCR products

PCR products of amplified *mulet* sequence were visualised by gel electrophoresis on a 1% agarose gel. Agarose gels were prepared by dissolving 1 g ultrapure agarose (Invitrogen) in 100 mL of TBE buffer (220mM Tris, 100mM Borate, 5mM EDTA), added 10 µL ethidium bromide (100ng/mL). 2 µL of PCR products were mixed with loading dye (NEB) and run on gel together with 1 kb+ DNA ladder (Thermo Fisher). The gels were visualised by a UV imager (Biorad). The rest of PCR products was then purified using Qiaquick PCR purification kit (Qiagen).

***In vitro* transcription**

Purified PCR products were used to perform *in vitro* transcription using T7 RNA polymerase (NEB) and DIG-labeled UTP (Roche). The reaction was left at 18°C for 48-96 hours.

In vitro transcription mix

Purified PCR product	1 µg
DIG-label UTP	2 µL
10x RNA polymerase buffer (NEB)	2 µL
T7 RNA polymerase	2 µL
RNase inhibitors (NEB)	0.2 µL
DEPC water	up to 20 µL

Probe preparation

After the *in vitro* transcription, the DNA template was removed by adding 1 µL of DNase I (NEB) and incubating at 37°C for 20 min. The probes were then degraded to an average size of 500 bp by adding 40 µL carbonate buffer (60 mM Na_2CO_3, 40mM $NaHCO_3$, pH10.2)and 40 µL DPEC water and incubating at 60°C. The length of incubation was decided according to the length of RNA probes (Cox *et al*, 1984). *mulet* probes were degraded for 8 min. The reaction was then stopped by adding 3.5 µL of acetic acid and 6.5 µL of NaAcetate by pipetting the mix vigoursly. The probes were precipitated by adding 250 µL of ice cold ethanol absolute and left at -20°C for 30min. The mix was then centrifuged at >=13,000 rpm at 4°C for 15 min and the resulted pellet was washed in 70% ethanol. The pallet was then centrifuged again, the ethanol was removed and pellet was left to air dry for 10 min. The precipitated probes were

then resuspended in 10 µL of DPEC water with 0.2µL RNase inhibitor (NEB) and can be stored in -20°C indefinitely. For use, the probes were diluted 1:500 in hybridisation buffer and can be used for up to 4 times.

Hybridisation buffer

Deionised formamide (Sigma-Aldrich)	50%
5X SSC (0.75M NaCl, 0.075M Na3C6H5O7)	
Tween20 (Sigma-Aldrich)	0.1%
E. coli tRNA (Sigma-Aldrich)	100 µg/mL
Heparin (Sigma-Aldrich)	50 µg/mL

In situ hybridisation

Samples were fixed as described in 7.3 and washed 5 x 5 times with PBSW and then 10 min in 50% PBSW / hybridisation buffer. Samples were then pre-hybridised in hybridisation buffer for at least 1 hour at 65°C. The probes were then added and incubated with the samples at 65°C overnight.

Antibody incubation and chromogenic reaction

After the overnight incubation, probes were removed and saved for future use. The samples were then washed for 30 min in hybridisation buffer, 30 min in 50% PBSW / hybridisation buffer and 4 x 30 min in PBSW. All the washed were performed at 65°C without agitation. After the final wash, anti-Dig AP antibody was added 1:2000 in PBSW and incubated for at least 2 hour at RT. The antibody was then removed and the samples were washed 3 x 20 min in PBSW. The samples were then rinsed once in freshly prepared alkaline phosphatase buffer and and washed in alkaline phosphatase buffer for 5 min.

Alkaline phosphatase buffer

Tris, pH9.5	100 mM
NaCl	100 mM
$MgCl_2$	50 mM
Tween20	0.1%

The chromogenic reaction was carried out by washing the samples with 300 µL alkaline phosphatase buffer + 1.5 µL NBT (Roche) for 5 min. The samples were then

placed in a 4-well tissue culture plate (Nunc) and the solution was replaced with 300 µL alkaline phosphatase buffer + 1.5 µL NBT (Roche)+ 1µL BCIT (Roche). The chromogenic reaction was carried out and checked under dissection scope every 10 min until clear signals were visible. To terminate the reaction, the samples were washed 3 x 5 min in PBSW and mounted in 50% PBS/glycerol for imaging.

7.7 Imaging and data analysis

7.7.1 Image acquisition and processing

All non-live fluorescent images used this thesis were acquired using an upright Leica SP8 confocal microscope. All images were processed for brightness and contrast using ImageJ.

All live fluroscent images used this thesis were acquired using an inverted Leica SP8 confocal microscope.

All non-luorescent images used in this thesis were acquired using a Leica dissection scope.

7.7.2 Image data analysis

7.7.2.1 Quantification of NB reactivation

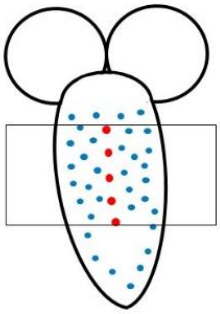

Figure 7.1 Diagram of the tVNC area for NB counting Red: midline NBs. Blue: NBs. All NBs within the black square were counted as the total NB

Larvae: Entire tVNCs immunostained with Dpn and pH3 antibodies were imaged. All Dpn+ nuclei between the first and last midline glia were manually counted as ‘total

NBs' [Figure 7.1]. All Dpn+ plus EdU+ and/or pH3+ (reactivated NBs) were also manually counted and the number was divided by total NBs to yield the reactivation percentage.

Stage 17 embryos: whole embryos immunostained with Dpn and pH3 antibodies were imaged to cover the entire brain from the ventral side. All pH3+ plus Dpn+ NBs were counted manually.

7.7.2.2 Quantification of adult wing size

Intact wings were mounted in Hoyer's medium and images were taken by a Leica dissecting scope with camera. Areas of interest were selected manually and the numbers of pixels were measured using the image processing software Volocity.

7.7.2.3 Quantification of adult wing trichome density

Intact wings were mounted in Hoyer's medium and images were taken by a Leica dissecting scope with built-in camera. The area of interest were defined as two squares (0.1 mm x 0.1 mm) next to the boundary of the anterior/posterior compartment [Figure 5.10]. The trichome density was manually counted.

7.7.2.4 Processing live Ca^{2+} imaging data

All live Ca^{2+} imaging data were processed by ImageJ and Excel. Neuroblasts were selected as the region of interest (ROI) in ImageJ. The average florescence intensity of the ROI in each frame was measured and plotted by the ImageJ plug-in 'Plot Z-axis profile'. The average Ca^{2+} levels were calculated for each cell as the average GCaMP6m:mRFP fluorescence emission ratio for the entire timeline of the experiment using Excel.

7.7.2.5 Statistical analysis

All statistical analysis was done using built-in functions in the data processing software Prism7 and Excel.

For comparisons between two sets of data: All data were subjected to Levene's test for equality of variances and the Shapiro-Wilk test for normality. The type of statistical tests were determined accordingly (see below).

Table 7.3 Statistical test for comparisons between two sets of data

Test	Normal distribution?	Equal variances?
Student t-test	yes	yes
Welch t-test	yes	no
Mann–Whitney U test	no	yes
Kolmogorov-Smirnov test	no	no

For comparisons between more than two sets of data: All data were subjected to Levene's test for equality of variances and the Shapiro-Wilk test for normality. The type of statistical tests were determined accordingly (see below). For data sets with non-equal variances, each data set were compared to the control using Welch t-test or Kolmogorov-Smirnov test.

Table 7.4 Statistical test for comparisons between more than two sets of data

Test	Normal distribution?	Equal variances?
One-way ANOVA	yes	yes
Kruskal–Wallis H test	no	yes

7.8 Ca^{2+} live imaging

Two different conditions were analyzed: quiescent stage (0h ALH) (genotype ;*mlt*-GAL4; UAS-mCD8-RFP, UAS-GCaMP6m) and reactivated stage (72h ALH) (genotype ;*wor*-GAL4; UAS-mCD8-RFP, UAS-GCaMP6m). Brains were dissected in Schneider insect's medium (Sigma) at room temperature, then immediately mounted in a drop of Schneider insect's medium on a 35mm Ibidi imaging well (µ-Dish with ibiTreat suface) with the VNCs facing down.

Mounted brains were imaged with a 63x oil immersion objective on a Leica SP8 inverted confocal microscope. The focal plane with most GCaMP signal was imaged.

GCaMP and mCD8-RFP were imaged simultaneously with the following settings: resolution: 1024 x 256; 0.769 frame per second, 400 frames in total (8 min 40 sec).

7.9 Other experimental conditions

7.9.1 Heatshock procedure for MARCM clone generation

Embryos were collected on apple juice plates with yeast paste for 2 hours in 25°C. 9 hours after the end of collection, the plates were sealed by Parafilm and submerged in 37°C water bath for 60 minutes, with 10 minute break after the first 30 minutes. After the heatshock, the Parafilm was removed and the plates were returned to 25°C.

7.9.2 Temperature control of GAL4 activity using temperature sensitive GAL80 ($GAL80^{TS}$)

Animals with GAL4 and $GAL80^{TS}$ in the genetic background were kept in 18°C to suppress GAL4 activity, and 29°C to activate GAL4 activity.

Reference

Abdullaev, I.F., Rudkouskaya, A., Mongin, A.A. and Kuo, Y.H., 2010. Calcium-activated potassium channels BK and IK1 are functionally expressed in human gliomas but do not regulate cell proliferation. *PloS one*, 5(8), p.e12304.

Adelman, J. P., Shen, K.-Z., Kavanaugh, M. P., Warren, R. A., Wu, Y.-N., Lagrutta, A., … Alan North, R. (1992). Calcium-activated potassium channels expressed from cloned complementary DNAs. *Neuron*, 9(2), 209–216.

Agarwal, M. L., Agarwal, A., Taylor, W. R., & Stark, G. R. (1995). p53 controls both the G2/M and the G1 cell cycle checkpoints and mediates reversible growth arrest in human fibroblasts. *Proceedings of the National Academy of Sciences,* 92(18), 8493–8497.

Ahn, S. and Joyner, A.L., 2005. In vivo analysis of quiescent adult neural stem cells responding to Sonic hedgehog. *Nature*, 437(7060), p.894.

Allen, N.J. and Eroglu, C., 2017. Cell biology of astrocyte-synapse interactions. *Neuron*, 96(3), pp.697-708.

Anderson, C.M. and Swanson, R.A., 2000. Astrocyte glutamate transport: review of properties, regulation, and physiological functions. *Glia*, *32*(1), pp.1-14.

Andersen, J., Urbán, N., Achimastou, A., Ito, A., Simic, M., Ullom, K., Martynoga, B., Lebel, M., Göritz, C., Frisén, J. and Nakafuku, M., 2014. A transcriptional mechanism integrating inputs from extracellular signals to activate hippocampal stem cells. *Neuron,* 83(5), pp.1085-1097.

Atkinson, N.S., Brenner, R., Bohm, R.A., Yu, J.Y. and Wilbur, J.L., 1998. Behavioral and Electrophysiological Analysis of Ca-activated K-channel Transgenes in Drosophila. *Annals of the New York Academy of Sciences,* 860(1), pp.296-305.

Atkinson, N.S., Brenner, R., Chang, W.M., Wilbur, J., Larimer, J.L. and Yu, J., 2000. Molecular separation of two behavioral phenotypes by a mutation affecting the promoters of a Ca-activated K channel. *Journal of Neuroscience*, *20*(8), pp.2988-2993.

Atkinson, N.S., Robertson, G.A., & Ganetzky, B. (1991). A component of calcium-activated potassium channels encoded by the *Drosophila* slo locus. *Science*, (5019), 551-555.

Albertson, R., Chabu, C., Sheehan, A. and Doe, C. Q. (2004). Scribble protein domain mapping reveals a multistep localization mechanism and domains necessary for establishing cortical polarity. *J. Cell. Sci*. 117, 6061–6070.

Altman, J.(1962) Are New Neurons Formed in the Brains of Adult Mammals? *Science*. 135,3509, 1127-1128

Altman, J.(1963) Autoradiographic investigation of cell proliferation in the brains of rats and cats. *The Anatomical Record*.1454, 573-591

Altman, J., and Das, G.D. (1965). Autoradiographic and histological evidence of postnatal hippocampal neurogenesis in rats. *J. Comp. Neurol*. 124, 319–335.

Altman J(1969) Autoradiographic and histological studies of postnatal neurogenesis. IV. Cell proliferation and migration in the anterior forebrain, with special reference to persisting neurogenesis in the olfactory bulb. *J Comp Neurol* 137:433–458

Allen, N. J., & Eroglu, C. (2017). Cell Biology of Astrocyte-Synapse Interactions. *Neuron*, 96(3), 697–708.

Aulestia, F.J., Néant, I., Dong, J., Haiech, J., Kilhoffer, M.C., Moreau, M. and Leclerc, C., 2018. Quiescence status of glioblastoma stem-like cells involves remodelling of Ca 2+ signalling and mitochondrial shape. *Scientific reports*, 8(1), p.9731.

Awasaki, T., Lai, S.L., Ito, K., and Lee, T. (2008). Organization and postembryonic development of glial cells in the adult central brain of *Drosophila*. *J. Neurosci*. 28, 13742–13753.

Balderas, E., Zhang, J., Stefani, E. and Toro, L., 2015. Mitochondrial BKCa channel. *Frontiers in* physiology, 6, p.104.

Banasr, M., Hery, M., Printemps, R. and Daszuta, A., 2004. Serotonin-induced increases in adult cell proliferation and neurogenesis are mediated through different and common 5-HT receptor subtypes in the dentate gyrus and the subventricular zone. *Neuropsychopharmacology*, 29(3), p.450.

Bao, H., Asrican, B., Li, W., Gu, B., Wen, Z., Lim, S.A., Haniff, I., Ramakrishnan, C., Deisseroth, K., Philpot, B. and Song, J., 2017. Long-range GABAergic inputs regulate neural stem cell quiescence and control adult hippocampal neurogenesis. *Cell stem cell*, 21(5), pp.604-617.

Barnett, L.M., Hughes, T.E. and Drobizhev, M., 2017. Deciphering the molecular mechanism responsible for GCaMP6m's Ca2+-dependent change in fluorescence. *PloS one*, 12(2), p.e0170934.

Bartolini, F., Tian, G., Piehl, M., Cassimeris, L., Lewis, S. a, & Cowan, N. J. (2005). Identification of a novel tubulin-destabilizing protein related to the chaperone cofactor E. *Journal of Cell Science,* 118(Pt 6), 1197–1207.

Bayraktar, O.A., Boone, J.Q., Drummond, M.L. and Doe, C.Q., 2010. *Drosophila* type II neuroblast lineages keep Prospero levels low to generate large clones that contribute to the adult brain central complex. *Neural development,* 5(1), p.26.

Baumgardt, M., Karlsson, D., Salmani, B.Y., Bivik, C., MacDonald, R.B., Gunnar, E. and Thor, S., 2014. Global programmed switch in neural daughter cell proliferation mode triggered by a temporal gene cascade. *Developmental cell*, *30*(2), pp.192-208.

Basak, O., Krieger, T.G., Muraro, M.J., Wiebrands, K., Stange, D.E., Frias-Aldeguer, J., Rivron, N.C., van de Wetering, M., van Es, J.H., van Oudenaarden, A. and Simons, B.D., 2018. Troy+ brain stem cells cycle through quiescence and regulate their number by sensing niche occupancy. *Proceedings of the National Academy of Sciences*, p.201715911.

Basrai, D., Kraft, R., Bollensdorff, C., Liebmann, L., Benndorf, K. and Patt, S., 2002. BK channel blockers inhibit potassium-induced proliferation of human astrocytoma cells. *Neuroreport*, 13(4), pp.403-407.

Becker, M. N., Brenner, R., & Atkinson, N. S. (1995). Tissue-specific expression of a *Drosophila* calcium-activated potassium channel. *J Neurosci*, *15*(9), 6250–6259.

Bello, B. C., Hirth, F., & Gould, A. P. (2003). A pulse of the *Drosophila* Hox protein Abdominal-A schedules the end of neural proliferation via neuroblast apoptosis. *Neuron*, *37*(2), 209–219.

Ben-Ari, Y. (1985). Limbic seizure and brain damage produced by kainic acid: Mechanisms and relevance to human temporal lobe epilepsy*. Neuroscience,* 14(2), 375–403.

Berchtold, M.W. and Villalobo, A., 2014. The many faces of calmodulin in cell proliferation, programmed cell death, autophagy, and cancer. *Biochimica et Biophysica Acta (BBA)-Molecular Cell Research*, *1843*(2), pp.398-435.

Berg, D.A., Belnoue, L., Song, H. and Simon, A., 2013. Neurotransmitter-mediated control of neurogenesis in the adult vertebrate brain. *Development*, *140*(12), pp.2548-2561.

Berger, C., Harzer, H., Burkard, T.R., Steinmann, J., van der Horst, S., Laurenson, A.S., Novatchkova, M., Reichert, H. and Knoblich, J.A., 2012. FACS purification and transcriptome analysis of *Drosophila* neural stem cells reveals a role for Klumpfuss in self-renewal. *Cell reports*, *2*(2), pp.407-418.

Berni, J., Muldal, A. M., & Pulver, S. R. (2010). Using Neurogenetics and the Warmth-Gated Ion Channel TRPA1 to Study the Neural Basis of Behavior in *Drosophila*. *Journal of Undergraduate Neuroscience Education*, 9(1), 5–14.

Bidaye, S.S., Machacek, C., Wu, Y., & Dickso, B.J. (2014). Neuronal Control of *Drosophila* Walking Direction. *Science*, 344(April), 97–101

Boddum, K., Jensen, T. P., Magloire, V., Kristiansen, U., Rusakov, D. A., Pavlov, I., & Walker, M. C. (2016). Astrocytic GABA transporter activity modulates excitatory neurotransmission. *Nature Communications*, 7, 1–10.

Bollag, G.E., Roth, R.A., Beaudoin, J., Mochly-Rosen, D. and Koshland, D.E., 1986. Protein kinase C directly phosphorylates the insulin receptor in vitro and reduces its protein-tyrosine kinase activity. *Proceedings of the National Academy of Sciences*, *83*(16), pp.5822-5824.

Boldrini, M., Fulmore, C.A., Tartt, A.N., Simeon, L.R., Pavlova, I., Poposka, V., Rosoklija, G.B., Stankov, A., Arango, V., Dwork, A.J. and Hen, R., 2018. Human hippocampal neurogenesis persists throughout aging. *Cell Stem Cell*, *22*(4), pp.589-599.

Bonaguidi, M.A., Wheeler, M.A., Shapiro, J.S., Stadel, R.P., Sun, G.J., Ming, G.L. and Song, H., 2011. In vivo clonal analysis reveals self-renewing and multipotent adult neural stem cell characteristics. *Cell*, *145*(7), pp.1142-1155.

Boone, J.Q. and Doe, C.Q., 2008. Identification of *Drosophila* type II neuroblast lineages containing transit amplifying ganglion mother cells. *Developmental neurobiology*, *68*(9), pp.1185-1195.

Bracko, O., Singer, T., Aigner, S., Knobloch, M., Winner, B., Ray, J., Clemenson, G.D., Suh, H., Couillard-Despres, S., Aigner, L. and Gage, F.H., 2012. Gene expression profiling of neural stem cells and their neuronal progeny reveals IGF2 as a regulator of adult hippocampal neurogenesis. *Journal of Neuroscience*, 32(10), pp.3376-3387.

Brand, A. H., & Perrimon, N. (1993). Targeted gene expression as a means of altering cell fates and generating dominant phenotypes. *Development*, 118(2), 401–415.

Brand, A.H. and Livesey, F.J., 2011. Neural stem cell biology in vertebrates and invertebrates: more alike than different? *Neuron*, *70*(4), pp.719-729.

Britton, J.S. and Edgar, B.A., 1998. Environmental control of the cell cycle in *Drosophila*: nutrition activates mitotic and endoreplicative cells by distinct mechanisms. *Development*, 125(11), pp.2149-2158.

Britton, J.S., Lockwood, W.K., Li, L., Cohen, S.M. and Edgar, B.A., 2002. *Drosophila*'s insulin/PI3-kinase pathway coordinates cellular metabolism with nutritional conditions. *Developmental cell*, *2*(2), pp.239-249.

Broadus, J., Fuerstenberg, S. and Doe, C.Q., 1998. Staufen-dependent localization of prospero mRNA contributes to neuroblast daughter-cell fate. *Nature*, 391(6669), p.792.

Brown J, Cooper-Kuhn CM, Kempermann G, Van Praag H, Winkler J, *et al*. 2003. Enriched environment and physical activity stimulate hippocampal but not olfactory bulb neurogenesis. *Eur. J. Neurosci*. 17: 2042–46

Cabernard, C. and Doe, C.Q., 2009. Apical/basal spindle orientation is required for neuroblast homeostasis and neuronal differentiation in *Drosophila*. *Developmental cell,* 17(1), pp.134-141.

Cabrera, C.V., 1990. Lateral inhibition and cell fate during neurogenesis in *Drosophila*: the interactions between scute, Notch and Delta. *Development*, *109*(3), pp.733-742.

Carmignoto, G. and Haydon, P.G., 2012. Astrocyte calcium signaling and epilepsy. *Glia*, *60*(8), pp.1227-1233.

Campos-Ortega, J.A., 1993. Mechanisms of early neurogenesis in *Drosophila* melanogaster. *Developmental Neurobiology*, *24*(10), pp.1305-1327.

Carre-Pierrat, M., *et* (2006). The SLO-1 BK Channel of Caenorhabditis elegans is Critical for Muscle Function and is Involved in Dystrophin-dependent Muscle Dystrophy. *Journal of Molecular Biology*, 358(2), 387–395.

Castilho, R.M., Squarize, C.H., Chodosh, L.A., Williams, B.O. and Gutkind, J.S., 2009. mTOR mediates Wnt-induced epidermal stem cell exhaustion and aging. *Cell stem cell*, 5(3), pp.279-289.

Campos-Ortega, J.A. and Hartenstein, V., 1997. *The embryonic development of Drosophila melanogaster*. Springer Science & Business Media.

Carney, T.D., Miller, M.R., Robinson, K.J., Bayraktar, O.A., Osterhout, J.A. and Doe, C.Q., 2012. Functional genomics identifies neural stem cell sub-type expression profiles and genes regulating neuroblast homeostasis. *Developmental biology*, 361(1), pp.137-146.

Cenci, C. and Gould, A.P., 2005. *Drosophila* Grainyhead specifies late programmes of neural proliferation by regulating the mitotic activity and Hox-dependent apoptosis of neuroblasts. *Development*, *132*(17), pp.3835-3845.

Ceron, J., Gonzalez, C. and Tejedor, F.J., 2001. Patterns of cell division and expression of asymmetric cell fate determinants in postembryonic neuroblast lineages of Drosophila. *Developmental biology*, 230(2), pp.125-138.

Chai, P.C., Liu, Z., Chia, W. and Cai, Y., 2013. Hedgehog signalling acts with the temporal cascade to promote neuroblast cell cycle exit. *PLoS biology*, *11*(2), p.e1001494.

Chakkalakal, J.V., Jones, K.M., Basson, M.A. and Brack, A.S., 2012. The aged niche disrupts muscle stem cell quiescence. *Nature*, *490*(7420), p.355.

Charalambous, K., & Wallace, B. A. (2011). NaChBac: The long lost sodium channel ancestor. *Biochemistry*, 50(32), 6742–6752.

Chell and Brand,(2010). Nutrition-responsive glia control exit of neural stem cells from quiescence. *Cell*, 143(7), 1161–1173.

Chen, C. T., Shih, Y. R., Kuo, T. K., Lee, O. K. & Wei, Y. H. Coordinated changes of mitochondrial biogenesis and antioxidant enzymes during osteogenic differentiation of human mesenchymal stem cells. *Stem Cells* **26**, 960–968 (2008).

Chen, T.W., Wardill, T.J., Sun, Y., Pulver, S.R., Renninger, S.L., Baohan, A., Schreiter, E.R., Kerr, R.A., Orger, M.B., Jayaraman, V. and Looger, L.L., 2013. Ultrasensitive fluorescent proteins for imaging neuronal activity. *Nature*, *499*(7458), p.295.

Chen, W., Dong, J., Haiech, J., Kilhoffer, M.C. and Zeniou, M., 2016. Cancer stem cell quiescence and plasticity as major challenges in cancer therapy. *Stem cells international*, 2016.

Chever, O., Dossi, E., Pannasch, U., Derangeon, M., & Rouach, N. (2016). Astroglial networks promote neuronal coordination. *Science Signalling*, 9(410), 1–9.

Cheung, T.H. and Rando, T.A., 2013. Molecular regulation of stem cell quiescence. *Nature reviews Molecular cell biology*, *14*(6), p.329.

Choksi, S.P., Southall, T.D., Bossing, T., Edoff, K., de Wit, E., Fischer, B.E., van Steensel, B., Micklem, G. and Brand, A.H., 2006. Prospero acts as a binary switch between self-renewal and differentiation in *Drosophila* neural stem cells. *Developmental cell*, *11*(6), pp.775-789.

Clapham, D.E., 2007. Calcium signaling. *Cell*, *131*(6), pp.1047-1058.

Clapham, D.E., Runnels, L.W. and Strübing, C., 2001. The TRP ion channel family. Nature Reviews Neuroscience, 2(6), p.387.

Codega, P., Silva-Vargas, V., Paul, A., Maldonado-Soto, A.R., DeLeo, A.M., Pastrana, E. and Doetsch, F., 2014. Prospective identification and purification of quiescent adult neural stem cells from their in vivo niche. *Neuron*, *82*(3), pp.545-559.

Cotsarelis, G., Sun, T.T. and Lavker, R.M., 1990. Label-retaining cells reside in the bulge area of pilosebaceous unit: implications for follicular stem cells, hair cycle, and skin carcinogenesis. *Cell*, *61*(7), pp.1329-1337.

Covolan, L., Ribeiro, L., Longo, B., & Mello, L. (2000). Cell damage and neurogenesis in the dentate granule cell layer of adult rats after pilocarpine- or kainate-induced status epilepticus. *Hippocampus*, 10(2), 169-80.

Cox, *et al*, (1984). Detection of mRNAs in sea urchin embryos by in situ hybridization using asymmetric RNA probes. *Developmental Biology*, 101(2), 485-502.

Cui, J., Yang, H., & Lee, U. S. (2009). Molecular mechanisms of BK channel activation. *Cellular and Molecular Life Sciences*, *66*(5), 852–875.

Deisseroth, K., Singla, S., Toda, H., Monje, M., Palmer, T. D., & Malenka, R. C. (2004). Excitation-Neurogenesis Coupling in Adult Neural Stem/Progenitor Cells. *Neuron*, *42*(4), 535–552.

Del Bigio, M.R., 1995. The ependyma: a protective barrier between brain and cerebrospinal fluid. *Glia*, 14(1), pp.1-13.

Delgado, A.C., Ferrón, S.R., Vicente, D., Porlan, E., Perez-Villalba, A., Trujillo, C.M., Pilar, D. and Fariñas, I., 2014. Endothelial NT-3 delivered by vasculature and CSF promotes quiescence of subependymal neural stem cells through nitric oxide induction. *Neuron*, 83(3), pp.572-585.

Deng, H., Gerencser, A. A., & Jasper, H. (2015). Signal integration by Ca2+ regulates intestinal stem-cell activity. *Nature*, 528(7581), 212–217.

Dent, E. W., Gupton, S. L., & Gertler, F. B. (2011). The Growth Cone Cytoskeleton in Axon outgrowth and guidance.pdf. *Cold Spring Harbor Perspectives in Biology*, 1–40.

Desai, A., & Mitchison, T. J. (1997). Microtubule Polymerization Dynamics. *Annual Review of Cell and Developmental Biology*, 13(1), 83–117.

Desalvo, M.K., Mayer, N., Mayer, F. and Bainton, R.J., 2011. Physiologic and anatomic characterization of the brain surface glia barrier of *Drosophila*. *Glia*, 59(9), pp.1322-1340.

Di Giovanni, Simone, Vilen Movsesyan, Farid Ahmed, Ibolja Cernak, Sergio Schinelli, Bogdan Stoica, and Alan I. Faden. "Cell cycle inhibition provides neuroprotection and reduces glial proliferation and scar formation after traumatic brain injury." *Proceedings of the National Academy of Sciences* 102, no. 23 (2005): 8333-8338.

Ding, R., Weynans, K., Bossing, T., Barros, C.S. and Berger, C., 2016. The Hippo signalling pathway maintains quiescence in *Drosophila* neural stem cells. *Nature communications*, 7, p.10510.

Dodson, MV., Allen, RE. and Hossner, KL., 1985. Ovine somatomedin, multiplication-stimulating activity, and insulin promote skeletal muscle satellite cell proliferation in vitro. *Endocrinology*, *117*(6), pp.2357-2363.

Doe, C. Q. (1992). Molecular markers for identified neuroblasts and ganglion mother cells in the *Drosophila*central nervous system. *Development* **116**,855 -863

Doe, C.Q., Fuerstenberg, S. and Peng, C.Y., 1998. Neural stem cells: from fly to vertebrates. *Developmental Neurobiology*, *36*(2), pp.111-127.

Doe, C.Q., 2017. Temporal patterning in the *Drosophila* CNS. *Annual review of cell and developmental biology*, *33*, pp.219-240.

Doetsch, F., García-Verdugo, J. M., & Alvarez-Buylla, A. (1997). Cellular Composition and Three-Dimensional Organization of the Subventricular Germinal Zone in the Adult Mammalian Brain. *The Journal of Neuroscience*, *17*(13), 5046 LP-5061. Retrieved from

Doetsch, F., García-Verdugo, J.M. and Alvarez-Buylla, A., 1999. Regeneration of a germinal layer in the adult mammalian brain. *Proceedings of the National Academy of Sciences*, 96(20), pp.11619-11624.

Doetsch, F., Caille, I., Lim, D. A., Garcı, J. M., & Alvarez-buylla, A. (1999). Subventricular Zone Astrocytes Are Neural Stem Cells in the Adult Mammalian Brain. *Cell*, 97, 703–716.

Doherty, J., Logan, M. a, Taşdemir, O. E., & Freeman, M. R. (2009). Ensheathing glia function as phagocytes in the adult *Drosophila* brain. *The Journal of Neuroscience*, 29(15)

Domenichini, F., Terrié, E., Arnault, P., Harnois, T., Magaud, C., Bois, P., Constantin, B. and Coronas, V., 2018. Store-Operated Calcium Entries Control Neural Stem Cell Self-Renewal in the Adult Brain Subventricular Zone. *Stem Cells*, 36(5), pp.761-774.

Donlea,JM, Matthew S. Thimgan, Yasuko Suzuki, Laura Gottschalk, P. J. S. (2011). Inducing Sleep by Remote Control Facilitates Memory Consolidation in *Drosophila*. *Science*, 332(June), 1571–1576.

Du, K., Herzig, S., Kulkarni, R.N. and Montminy, M., 2003. TRB3: a tribbles homolog that inhibits Akt/PKB activation by insulin in liver. *Science*, *300*(5625), pp.1574-1577.

Duman RS, Malberg J, Nakagawa S. 2001. Regulation of adult neurogenesis by psychotropic drugs and stress. *J. Pharmacol. Exp. Ther*. 299: 401–7

Eisch AJ, Barrot M, Schad CA, Self DW, Nestler EJ. 2000. Opiates inhibit neurogenesis in the adult rat hippocampus. *Proc. Natl. Acad. Sci. USA* 97: 7579–84

Ehaideb, S. N., Iyengar, A., Ueda, A., Iacobucci, G. J., Cranston, C., Bassuk, A. G., … Manak, J. R. (2014). Prickle Modulates Microtubule Polarity and Axonal Transport To Ameliorate Seizures in Flies. *Proceedings of the National Academy of Sciences*, 111(30), 11187–11192.

Egger, B., Chell, J.M. and Brand, A.H., 2008. Insights into neural stem cell biology from flies. *Philosophical Transactions of the Royal Society B: Biological Sciences*, *363*(1489), pp.39-56.

Egger, B., Leemans, R., Loop, T., Kammermeier, L., Fan, Y., Radimerski, T., Strahm, M.C., Certa, U. and Reichert, H., 2002. Gliogenesis in *Drosophila*: genome-wide analysis of downstream genes of glial cells missing in the embryonic nervous system. *Development*, *129*(14), pp.3295-3309.

Egger, B., Gold, K.S. and Brand, A.H., 2010. Notch regulates the switch from symmetric to asymmetric neural stem cell division in the Drosophila optic lobe. *Development*, pp.dev-051250.

Elliott, J., Jolicoeur, C., Ramamurthy, V. and Cayouette, M., 2008. Ikaros confers early temporal competence to mouse retinal progenitor cells. *Neuron*, *60*(1), pp.26-39.

Elkins, T., Ganetzky, B., & Wu, C. F. (1986). A *Drosophila* mutation that eliminates a calcium-dependent potassium current. *Proceedings of the National Academy of Sciences*, *83*(21), 8415–9.

Encinas, J.M., Michurina, T.V., Peunova, N., Park, J.H., Tordo, J., Peterson, D.A., Fishell, G., Koulakov, A. and Enikolopov, G., 2011. Division-coupled astrocytic differentiation and age-related depletion of neural stem cells in the adult hippocampus. *Cell stem cell*, *8*(5), pp.566-579.

Eriksson, P. S., Perfilieva, E., Bjork-Eriksson, T., Alborn, A. M., Nordborg, C., Peterson, D. A., & Gage, F. H. (1998). Neurogenesis in the adult human hippocampus. *Nat Med*, 4(11), 1313–1317.

Eyers, P.A., Keeshan, K. and Kannan, N., 2017. Tribbles in the 21st century: the evolving roles of tribbles pseudokinases in biology and disease. *Trends in cell biology*, *27*(4), pp.284-298.

Fabrizio, J.J., Aqeel, N., Cote, J., Estevez, J., Jongoy, M., Mangal, V., Tema, W., Rivera, A., Wnukowski, J. and Bencosme, Y., 2012. mulet (mlt) encodes a tubulin-binding cofactor E-like homolog required for spermatid individualization in *Drosophila* melanogaster. *Fly*, *6*(4), pp.261-272.

Favaro, R., Valotta, M., Ferri, A.L., Latorre, E., Mariani, J., Giachino, C., Lancini, C., Tosetti, V., Ottolenghi, S., Taylor, V. and Nicolis, S.K., 2009. Hippocampal development and neural stem cell maintenance require Sox2-dependent regulation of Shh. *Nature neuroscience*, 12(10), p.1248.

Failli, P. Ruocco, R.. De Franco, A.. Caligiuri, A. Gentilini, A.. Giotti, P. Gentilini, and M.M. O. Pinzani. "The mitogenic effect of platelet-derived growth factor in human hepatic stellate cells requires calcium influx." *American Journal of Physiology-Cell Physiology* 269, no. 5 (1995): C1133-C1139.

Fernández-Hernández, I., Rhiner, C., & Moreno, E. (2013). Adult Neurogenesis in *Drosophila*. *Cell Reports*, 3(6), 1857–1865.

Fettiplace, R., & Fuchs, P. A. (1999). MECHANISMS OF HAIR CELL TUNING. *Annual Review of Physiology*, *61*(1), 809–834.

Fietz, M. J., Jacinto, A., Taylor, A. M., Alexandre, C. and Ingham, P. W. (1995). Secretion of the amino-terminal fragment of the hedgehog protein is necessary and sufficient for hedgehog signalling in *Drosophila*. *Current Biology* 5, 643–650.

Fleming, H.E., Janzen, V., Celso, C.L., Guo, J., Leahy, K.M., Kronenberg, H.M. and Scadden, D.T., 2008. Wnt signalling in the niche enforces hematopoietic stem cell quiescence and is necessary to preserve self-renewal in vivo. *Cell stem cell*, *2*(3), pp.274-283.

Ford, K.J. and Davis, G.W., 2014. Archaerhodopsin voltage imaging: synaptic calcium and BK channels stabilize action potential repolarization at the *Drosophila* neuromuscular junction. *Journal of Neuroscience*, *34*(44), pp.14517-14525.

Forsberg, E. C. *et al.* Molecular signatures of quiescent, mobilized and leukemia-initiating hematopoietic stem cells. *PLoS ONE* **5**, e8785 (2010)

Freeman, M.R., 2015. *Drosophila* central nervous system glia. *Cold Spring Harbor perspectives in biology*, *7*(11), p.a020552.

Freeman, M.R. and Doherty, J., 2006. Glial cell biology in *Drosophila* and vertebrates. *Trends in neurosciences*, *29*(2), pp.82-90.

Frisén, J. (2016). Neurogenesis and Gliogenesis in Nervous System Plasticity and Repair. *Annual Review of Cell and Developmental Biology*, 32(1), 127–141.

Fukuda S, Kato F, Tozuka Y, Yamaguchi M, Miyamoto Y, Hisatsune T. (2003)Two distinct subpopulations of nestin-positive cells in adult mouse dentate gyrus. *J Neurosci*. 23:9357–66

Fukada, S. *et al.* Molecular signature of quiescent satellite cells in adult skeletal muscle. *Stem Cells*

Furutachi, S., Miya, H., Watanabe, T., Kawai, H., Yamasaki, N., Harada, Y., Imayoshi, I., Nelson, M., Nakayama, K.I., Hirabayashi, Y. and Gotoh, Y., 2015. Slowly dividing neural progenitors are an embryonic origin of adult neural stem cells. *Nature neuroscience*, 18(5), p.657.

Galli, R., Binda, E., Orfanelli, U., Cipelletti, B., Gritti, A., De Vitis, S., Fiocco, R., Foroni, C., Dimeco, F. and Vescovi, A., 2004. Isolation and characterization of tumorigenic, stem-like neural precursors from human glioblastoma. *Cancer research*, *64*(19), pp.7011-7021.

Galvin, K. E., Ye, H., Erstad, D. J., Feddersen, R., & Wetmore, C. (2008). Gli1 Induces G2/M Arrest and Apoptosis in Hippocampal but Not Tumor-Derived Neural Stem Cells. *Stem Cells*, 26(4), 1027–1036.

Garros-Regulez, L., Garcia, I., Carrasco-Garcia, E., Lantero, A., Aldaz, P., Moreno-Cugnon, L., Arrizabalaga, O., Undabeitia, J., Torres-Bayona, S., Villanua, J. and Ruiz, I., 2016. Targeting SOX2 as a therapeutic strategy in glioblastoma. *Frontiers in oncology*, *6*, p.222.

Gao, X.J., Riabinina, O., Li, J., Potter, C.J., Clandinin, T.R. and Luo, L., 2015. A transcriptional reporter of intracellular Ca^{2+} in Drosophila. *Nature neuroscience*, *18*(6), p.917.

Goldman, S. A., & Nottebohm, F. (1983). Neuronal production, migration, and differentiation in a vocal control nucleus of the adult female canary brain. *Proceedings of the National Academy of Sciences*, 80(8), 2390–2394.

Goldstein, B. and Macara, I.G., 2007. The PAR proteins: fundamental players in animal cell polarization. *Developmental cell*, *13*(5), pp.609-622.

Gomez-Gonzalo, M., Losi, G., Chiavegato, A., Zonta, M., Cammarota, M., Brondi, M., … Carmignoto, G. (2010). An excitatory loop with astrocytes contributes to drive neurons to seizure threshold. *PLoS Biology*, 8(4)

Gonçalves, J.T., Schafer, S.T. and Gage, F.H., 2016. Adult neurogenesis in the hippocampus: from stem cells to behavior. *Cell*, 167(4), pp.897-914.

Gong, Y., Huang, C., Li, J.Z., Grewe, B.F., Zhang, Y., Eismann, S. and Schnitzer, M.J., 2015. High-speed recording of neural spikes in awake mice and flies with a fluorescent voltage sensor. *Science*, 350(6266), pp.1361-1366.

Goodell, M.A., Brose, K., Paradis, G., Conner, A.S. and Mulligan, R.C., 1996. Isolation and functional properties of murine hematopoietic stem cells that are replicating in vivo. *Journal of Experimental Medicine*, *183*(4), pp.1797-1806.

Gebremedhin, D., Yamaura, K., Zhang, C., Bylund, J., Koehler, R.C. and Harder, D.R., 2003. Metabotropic glutamate receptor activation enhances the activities of two types of Ca2+-activated K+ channels in rat hippocampal astrocytes. *Journal of Neuroscience*, *23*(5), pp.1678-1687.

Gómez-Gaviro, M.V., Scott, C.E., Sesay, A.K., Matheu, A., Booth, S., Galichet, C. and Lovell-Badge, R., 2012. Betacellulin promotes cell proliferation in the neural stem cell niche and stimulates neurogenesis. *Proceedings of the National Academy of Sciences,* 109(4), pp.1317-1322.

Götz, M. and Huttner, W.B., 2005. Developmental cell biology: The cell biology of neurogenesis. *Nature reviews Molecular cell biology*, *6*(10), p.777.

Grishchuk, E. L., & McIntosh, J. R. (1999). Sto1p, a fission yeast protein similar to tubulin folding cofactor E, plays an essential role in mitotic microtubule assembly. *Journal of Cell Science*, *112 Pt 1*, 1979–88.

Guillemot, F., 2007. Spatial and temporal specification of neural fates by transcription factor codes. *Development*, *134*(21), pp.3771-3780.

Gwack, Y., Sharma, S., Nardone, J., Tanasa, B., Iuga, A., Srikanth, S., Okamura, H., Bolton, D., Feske, S., Hogan, P.G. and Rao, A., 2006. A genome-wide Drosophila RNAi screen identifies DYRK-family kinases as regulators of NFAT. *Nature*, *441*(7093), p.646.

Hage-Sleiman, R., Herveau, S., Matera, E.-L., Laurier, J.-F., & Dumontet, C. (2011). Silencing of Tubulin Binding Cofactor C Modifies Microtubule Dynamics and Cell Cycle Distribution and Enhances Sensitivity to Gemcitabine in Breast Cancer Cells. *Molecular Cancer Therapeutics*, 10(2), 303–312.

Halter, D. A., Urban, J., Rickert, C., Ner, S. S., Ito, K., Travers, A. A., & Technau, G. M. (1995). The homeobox gene repo is required for the differentiation and maintenance of glia function in the embryonic nervous system of *Drosophila* melanogaster. *Development*, 121(2), 317–332.

Hara, M., Tabata, K., Suzuki, T., Do, M.K.Q., Mizunoya, W., Nakamura, M., Nishimura, S., Tabata, S., Ikeuchi, Y., Sunagawa, K. and Anderson, J.E., 2012. Calcium influx through a possible coupling of cation channels impacts skeletal muscle satellite cell activation in response to mechanical stretch. *American Journal of Physiology-Cell Physiology*, *302*(12), pp.C1741-C1750.

Hartenstein, V. and Campos-Ortega, J.A., 1984. Early neurogenesis in wild-type *Drosophila* melanogaster. *Wilhelm Roux's archives of developmental biology*, *193*(5), pp.308-325.

Hartenstein, V., Younossi-Hartenstein, A. and Lekven, A., 1994. Delamination and division in the Drosophila neurectoderm: spatiotemporal pattern, cytoskeletal dynamics, and common control by neurogenic and segment polarity genes. *Developmental biology*, 165(2), pp.480-499.

Hayashi, Y., Jinnou, H., Sawamoto, K. and Hitoshi, S., 2018. Adult neurogenesis and its role in brain injury and psychiatric diseases. *Journal of neurochemistry*, 147(5), pp.584-594.

Haydon, P. G., & Carmignoto, G. (2006). Astrocyte control of synaptic transmission and neurovascular coupling. *Physiol Rev*, 86(3), 1009–1031.

He, L., Si, G., Huang, J., Samuel, A.D. and Perrimon, N., 2018. Mechanical regulation of stem-cell differentiation by the stretch-activated Piezo channel. *Nature*, *555*(7694), p.103.

Hedlund, E., Belnoue, L., Theofilopoulos, S., Salto, C., Bye, C., Parish, C., Deng, Q., Kadkhodaei, B., Ericson, J., Arenas, E. and Perlmann, T., 2016. Dopamine receptor antagonists enhance proliferation and neurogenesis of midbrain Lmx1a-expressing progenitors. *Scientific reports*, 6, p.26448.

Hewavitharana, T., Deng, X., Soboloff, J., & Gill, D. L. (2007). Role of STIM and Orai proteins in the store-operated calcium signalling pathway. *Cell Calcium,* 42(2), 173–182.

Hirata, J., Nakagoshi, H., Nabeshima, Y.I. and Matsuzaki, F., 1995. Asymmetric segregation of the homeodomain protein Prospero during*Drosophila* development. *Nature*, 377(6550), p.627.

Hirokawa, N. (1994). Microtubule organization and dynamics dependent on microtubule-associated proteins. *Current Opinion in Cell Biology*, 6(1), 74–81.

Hirth, F., Hartmann, B. and Reichert, H., 1998. Homeotic gene action in embryonic brain development of *Drosophila*. *Development*, *125*(9), pp.1579-1589.

Hayashi, S. and Yamaguchi, M., 1999. Kinase-independent activity of Cdc2/Cyclin A prevents the S phase in the Drosophila cell cycle. *Genes to Cells*, 4(2), pp.111-122.

Hoglinger G.U, Rizk P, Muriel M.P, Duyckaerts C, Oertel W.H, Caille I, Hirsch E.C (2004) Dopamine depletion impairs precursor cell proliferation in Parkinson disease. *Nat. Neurosci*. 7, 726–735

Homem, C.C. and Knoblich, J.A., 2012. *Drosophila* neuroblasts: a model for stem cell biology. *Development*, *139*(23), pp.4297-4310.

Homem, C.C., Steinmann, V., Burkard, T.R., Jais, A., Esterbauer, H. and Knoblich, J.A., 2014. Ecdysone and mediator change energy metabolism to terminate proliferation in *Drosophila* neural stem cells. *Cell*, *158*(4), pp.874-888.

Hope, K. A., LeDoux, M. S., & Reiter, L. T. (2017). Glial overexpression of Dube3a causes seizures and synaptic impairments in *Drosophila* concomitant with down regulation of the Na+/K+pump ATPα. *Neurobiology of Disease*, 108(September), 238–248.

Horsley, V., Aliprantis, A.O., Polak, L., Glimcher, L.H. and Fuchs, E., 2008. NFATc1 balances quiescence and proliferation of skin stem cells. *Cell*, *132*(2), pp.299-310.

Hu, H., Shao, L. R., Chavoshy, S., Gu, N., Trieb, M., Behrens, R., … Storm, J. F. (2001). Presynaptic Ca2+-activated K+ channels in glutamatergic hippocampal terminals and their role in spike repolarization and regulation of transmitter release. *The Journal of Neuroscience*, *21*(24), 9585–9597.

Huang, J., Wu, S., Barrera, J., Matthews, K. and Pan, D., 2005. The Hippo signalling pathway coordinately regulates cell proliferation and apoptosis by inactivating Yorkie, the *Drosophila* Homolog of YAP. *Cell*, *122*(3), pp.421-434.

Ikeshima-Kataoka, H., Skeath, J.B., Nabeshima, Y.I., Doe, C.Q. and Matsuzaki, F., 1997. Miranda directs Prospero to a daughter cell during *Drosophila* asymmetric divisions. *Nature,* 390(6660), p.625.

Ishibashi, M., Ang, S.L., Shiota, K., Nakanishi, S., Kageyama, R. and Guillemot, F., 1995. Targeted disruption of mammalian hairy and Enhancer of split homolog-1 (HES-1) leads to up-regulation of neural helix-loop-helix factors, premature neurogenesis, and severe neural tube defects. *Genes & development*, *9*(24), pp.3136-3148.

Isshiki, T., Pearson, B., Holbrook, S. and Doe, C.Q., 2001. *Drosophila* neuroblasts sequentially express transcription factors which specify the temporal identity of their neuronal progeny. *Cell*, *106*(4), pp.511-521.

Ito, K. and Hotta, Y., 1992. Proliferation pattern of postembryonic neuroblasts in the brain of *Drosophila* melanogaster. *Developmental biology*, *149*(1), pp.134-148.

Ito, K., Hirao, A., Arai, F., Takubo, K., Matsuoka, S., Miyamoto, K., Ohmura, M., Naka, K., Hosokawa, K., Ikeda, Y. and Suda, T., 2006. Reactive oxygen species act through p38 MAPK to limit the lifespan of hematopoietic stem cells. *Nature medicine*, *12*(4), p.446.

Ito, K. and Suda, T., 2014. Metabolic requirements for the maintenance of self-renewing stem cells. *Nature reviews Molecular cell biology*, *15*(4), pp.243-256.

Iriuchishima, H., Takubo, K., Matsuoka, S., Onoyama, I., Nakayama, K.I., Nojima, Y. and Suda, T., 2010. Ex vivo maintenance of hematopoietic stem cells by quiescence induction through Fbxw7α overexpression. *Blood,* pp.blood-2010.

Jacob, J., Maurange, C. and Gould, A.P., 2008. Temporal control of neuronal diversity: common regulatory principles in insects and vertebrates?. *Development*, *135*(21), pp.3481-3489.

Jepson, J.E., Shahidullah, M., Lamaze, A., Peterson, D., Pan, H. and Koh, K., 2012. dyschronic, a *Drosophila* homolog of a deaf-blindness gene, regulates circadian output and Slowpoke channels. *PLoS genetics*, *8*(4), p.e1002671.

Jepson, J.E., Shahidullah, M., Liu, D., Le Marchand, S.J., Liu, S., Wu, M.N., Levitan, I.B., Dalva, M.B. and Koh, K., 2014. Regulation of synaptic development and function by the *Drosophila* PDZ protein Dyschronic. *Development*, *141*(23), pp.4548-4557.

Ji Z, Tian B. Reprogramming of 3′ untranslated regions of mRNAs by alternative polyadenylation in generation of pluripotent stem cells from different cell types. *PLoS ONE*. 2009;4:e8419

Jiang, Y., Lee, A., Chen, J., Cadene, M., & al, e. (2002). Crystal structure and mechanism of a calcium-gated potassium channel. *Nature, 417*(6888), 515-22

Jin K, Galvan V, Xie L, Mao XO, Gorostiza OF, *et al*. 2004. Enhanced neurogenesis in Alzheimer's disease transgenic (PDGF-APPSw,Ind) mice. *Proc. Natl. Acad. Sci. USA* 101:13363–67

Jin, S., Pan, L., Liu, Z., Wang, Q., Xu, Z., & Zhang, Y. Q. (2009). *Drosophila* Tubulin-specific chaperone E functions at neuromuscular synapses and is required for microtubule network formation. *Development,* 136, 1571–1581.

Jinnou, H., Sawada, M., Kawase, K., Kaneko, N., Herranz-Pérez, V., Miyamoto, T., Kawaue, T., Miyata, T., Tabata, Y., Akaike, T. and García-Verdugo, J.M., 2018. Radial glial fibers promote neuronal migration and functional recovery after neonatal brain injury. *Cell stem cell*, 22(1), pp.128-137.

Jones, K.M., Sarić, N., Russell, J.P., Andoniadou, C.L., Scambler, P.J. and Basson, M.A., 2015. CHD7 maintains neural stem cell quiescence and prevents premature stem cell depletion in the adult hippocampus. *Stem Cells*, 33(1), pp.196-210.

Jowett, J. B. M., Planelles, V., Poon, B., Shah, N. P., Chen, M.-L., & Chen, I. S. Y. (1995). The human immunodeficiency virus type 1 vpr gene arrests infected T cells in the G2 + M phase of the cell cycle. *J. Virol.,* 69(10), 6304–6313.

Kadamur, G. and Ross, E.M., 2013. Mammalian phospholipase C. *Annual review of physiology*, *75*, pp.127-154.

Kadas, D., Ryglewski, S. and Duch, C., 2015. Transient BK outward current enhances motoneurone firing rates during Drosophila larval locomotion. *The Journal of physiology*, *593*(22), pp.4871-4888.

Kanai, M.I., Okabe, M. and Hiromi, Y., 2005. seven-up Controls switching of transcription factors that specify temporal identities of *Drosophila* neuroblasts. *Developmental cell*, *8*(2), pp.203-213.

Kaiser, M., 2015. Neuroanatomy: connectome connects fly and mammalian brain networks. *Current Biology*, *25*(10), pp.R416-R418.

Kato, K., Awasaki, T., & Ito, K. (2009). Neuronal programed cell death induces glial cell division in the adult *Drosophila* brain. *Development*, 136(1), 51–59.

Karashima, Y., Prenen, J., Talavera, K., Janssens, A., Voets, T. and Nilius, B., 2010. Agonist-induced changes in Ca2+ permeation through the nociceptor cation channel TRPA1. *Biophysical journal*, 98(5), pp.773-783.

Karcavich, R. and Doe, C.Q., 2005. *Drosophila* neuroblast 7-3 cell lineage: a model system for studying programmed cell death, Notch/Numb signalling , and sequential specification of ganglion mother cell identity. *Journal of comparative neurology*, *481*(3), pp.240-251.

Katsimpardi, L., Litterman, N.K., Schein, P.A., Miller, C.M., Loffredo, F.S., Wojtkiewicz, G.R., Chen, J.W., Lee, R.T., Wagers, A.J. and Rubin, L.L., 2014. Vascular and neurogenic rejuvenation of the aging mouse brain by young systemic factors. *Science*, 344(6184), pp.630-634.

Kempermann, G. and Gage, F.H., 2002. Genetic determinants of adult hippocampal neurogenesis correlate with acquisition, but not probe trial performance, in the water maze task. *European Journal of Neuroscience*, *16*(1), pp.129-136.

Kimura, K. I., and James W. Truman. "Postmetamorphic cell death in the nervous and muscular systems of *Drosophila* melanogaster." *Journal of Neuroscience* 10.2 (1990): 403-401

Kippin, T.E., Martens, D.J. and van der Kooy, D., 2005. p21 loss compromises the relative quiescence of forebrain stem cell proliferation leading to exhaustion of their proliferation capacity. *Genes & development*, *19*(6), pp.756-767.

Knoblich, J.A., 2008. Mechanisms of asymmetric stem cell division. *Cell*, *132*(4), pp.583-597.

Knoblich, J.A. and Jan, Y.N., 1995. Asymmetric segregation of Numb and Prospero during cell division. *Nature*, 377(6550), p.624.

Kohwi, M. and Doe, C.Q., 2013. Temporal fate specification and neural progenitor competence during development. *Nature Reviews Neuroscience*, *14*(12), p.823.

Kokaia Z, Lindvall O. 2003. Neurogenesis after ischaemic brain insults. *Curr. Opin. Neurobiol.*13:127–32

Kojima, I., Matsunaga, H., Kurokawa, K., Ogata, E. and Nishimoto, I., 1988. Calcium influx: an intracellular message of the mitogenic action of insulin-like growth factor-I. *Journal of Biological Chemistry*, 263(32), pp.16561-16567.

Kraft, A., Jubal, E.R., von Laer, R., Döring, C., Rocha, A., Grebbin, M., Zenke, M., Kettenmann, H., Stroh, A. and Momma, S., 2017. Astrocytic calcium waves signal brain injury to neural stem and progenitor cells. *Stem cell reports*, *8*(3), pp.701-714.

Kriegstein, A., Noctor, S. and Martínez-Cerdeño, V., 2006. Patterns of neural stem and progenitor cell division may underlie evolutionary cortical expansion. *Nature Reviews Neuroscience*, *7*(11), p.883.

Kriegstein, A., & Alvarez-buylla, A. (2011). The Glial Nature of Embryonic and Adult Neural Stem Cells. *Annual Reviews of Neuroscience*, 149–184.

Kuhn HG, Dickinson-Anson H, Gage FH. 1996. Neurogenesis in the dentate gyrus of the adult rat: age-related decrease of neuronal progenitor proliferation. *J. Neurosci.* 16:2027–33

Lacin, H. and Truman, J.W., 2016. Lineage mapping identifies molecular and architectural similarities between the larval and adult *Drosophila* central nervous system. *Elife*, *5*.

Lai, K., Kaspar, B.K., Gage, F.H. and Schaffer, D.V., 2003. Sonic hedgehog regulates adult neural progenitor proliferation in vitro and in vivo. *Nature neuroscience*, 6(1), p.21.

Lai, S.L. and Doe, C.Q., 2014. Transient nuclear Prospero induces neural progenitor quiescence. *Elife*, *3*.

Latorre, R., & Brauchi, S. (2006). Large conductance Ca2+-activated K+ (BK) channel: Activation by Ca2+ and voltage. *Biological Research*, *39*(3), 385–401.

Lay, K., Kume, T. and Fuchs, E., 2016. FOXC1 maintains the hair follicle stem cell niche and governs stem cell quiescence to preserve long-term tissue-regenerating potential. *Proceedings of the National Academy of Sciences*, *113*(11), pp.E1506-E1515.

Laywell, E.D., Rakic, P., Kukekov, V.G., Holland, E.C. and Steindler, D.A., 2000. Identification of a multipotent astrocytic stem cell in the immature and adult mouse brain. *Proceedings of the National Academy of Sciences*, *97*(25), pp.13883-13888.

Le Belle, J.E., Orozco, N.M., Paucar, A.A., Saxe, J.P., Mottahedeh, J., Pyle, A.D., Wu, H. and Kornblum, H.I., 2011. Proliferative neural stem cells have high endogenous ROS levels that regulate self-renewal and neurogenesis in a PI3K/Akt-dependant manner. *Cell stem cell*, *8*(1), pp.59-71.

Lee, Jihye, and Chun-Fang Wu. "Orchestration of stepwise synaptic growth by K+ and Ca2+ channels in *Drosophila*." *Journal of Neuroscience*30.47 (2010): 15821-15833.

Lee, Jihye, Atsushi Ueda, and C-F. Wu. "Pre-and post-synaptic mechanisms of synaptic strength homeostasis revealed by slowpoke and shaker K+ channel mutations in *Drosophila*." *Neuroscience*154.4 (2008): 1283-1296.

Leventhal, C., Rafii, S., Rafii, D., Shahar, A. and Goldman, S.A., 1999. Endothelial trophic support of neuronal production and recruitment from the adult mammalian subependyma. *Molecular and Cellular Neuroscience,* 13(6), pp.450-464.

Lewis, S. a, Tian, G., & Cowan, N. J. (1997). The alpha- and beta-tubulin folding pathways. *Trends in Cell Biology*, 7(12), 479–484.

Li, B., Jie, W., Huang, L., Wei, P., Li, S., Luo, Z., Friedman, A.K., Meredith, A.L., Han, M.H., Zhu, X.H. and Gao, T.M., 2014. Nuclear BK channels regulate gene expression via the control of nuclear calcium signaling. *Nature neuroscience*, *17*(8), p.1055.

Li, S., Koe, C.T., Tay, S.T., Tan, A.L.K., Zhang, S., Zhang, Y., Tan, P., Sung, W.K. and Wang, H., 2017. An intrinsic mechanism controls reactivation of neural stem cells by spindle matrix proteins. *Nature communications*, *8*(1), p.122.

Lie, D.C., Dziewczapolski, G., Willhoite, A.R., Kaspar, B.K., Shults, C.W. and Gage, F.H., 2002. The adult substantia nigra contains progenitor cells with neurogenic potential. *Journal of Neuroscience*, *22*(15), pp.6639-6649.

Liddelow, S.A. and Barres, B.A., 2017. Reactive astrocytes: production, function, and therapeutic potential. *Immunity*, *46*(6), pp.957-967.

Lien, W.H., Guo, X., Polak, L., Lawton, L.N., Young, R.A., Zheng, D. and Fuchs, E., 2011. Genome-wide maps of histone modifications unwind in vivo chromatin states of the hair follicle lineage. *Cell stem cell*, *9*(3), pp.219-232.

Li, L.H., Tian, X.R., Jiang, Z., Zeng, L.W., He, W.F. and Hu, Z.P., 2013. The Golgi apparatus: panel point of cytosolic Ca2+ regulation. *Neurosignals*, 21(3-4), pp.272-284.

Lim, D.A., Tramontin, A.D., Trevejo, J.M., Herrera, D.G., García-Verdugo, J.M. and Alvarez-Buylla, A., 2000. Noggin antagonizes BMP signalling to create a niche for adult neurogenesis. *Neuron*, 28(3), pp.713-726.

Liu, J., Solway, K., Messing, R.O. and Sharp, F.R., 1998. Increased neurogenesis in the dentate gyrus after transient global ischemia in gerbils. *Journal of Neuroscience*, *18*(19), 7768-7778.

Liu, X., Chang, Y., Reinhart, P.H. and Sontheimer, H., 2002. Cloning and characterization of glioma BK, a novel BK channel isoform highly expressed in human glioma cells. *Journal of Neuroscience*, *22*(5), 1840-1849.

Liu, X., Wang, Q., Haydar, T. F., & Bordey, A. (2005). Nonsynaptic GABA signalling in postnatal subventricular zone controls proliferation of GFAP-expressing progenitors. *Nature Neuroscience*, *8*, 1179.

Liu, Z., Yang, C.P., Sugino, K., Fu, C.C., Liu, L.Y., Yao, X., Lee, L.P. and Lee, T., 2015. Opposing intrinsic temporal gradients guide neural stem cell production of varied neuronal fates. *Science*, *350*(6258), pp.317-320.

Lopez-Fanarraga, M., Carranza, G., Bellido, J., Kortazar, D., Villegas, J. C., & Zabala, J. C. (2007). Tubulin cofactor B plays a role in the neuronal growth cone. *Journal of Neurochemistry*, 100(6), 1680–1687.

Lu, W., Del Castillo, U. and Gelfand, V.I., 2013. Organelle transport in cultured Drosophila cells: S2 cell line and primary neurons. *Journal of visualized experiments: JoVE,* (81).

Lugert, S., Basak, O., Knuckles, P., Haussler, U., Fabel, K., Götz, M., … Giachino, C. (2010). Quiescent and active hippocampal neural stem cells with distinct morphologies respond selectively to physiological and pathological stimuli and aging. *Cell Stem Cell*, 6(5), 445–456.

Luo, L., Liao, Y. J., Jan, L. Y. and Jan, Y. N. (1994). Distinct morphogenetic functions of similar small GTPases: *Drosophila* Drac1 is involved in axonal outgrowth and myoblast fusion. *Genes & Development* 8, 1787–1802.

Luo, Y., Coskun, V., Liang, A., Yu, J., Cheng, L., Ge, W., Shi, Z., Zhang, K., Li, C., Cui, Y. and Lin, H., 2015. Single-cell transcriptome analyses reveal signals to activate dormant neural stem cells. *Cell*, *161*(5), pp.1175-1186.

MacDermott, A.B., Mayer, M.L., Westbrook, G.L., Smith, S.J. and Barker, J.L., 1986. NMDA-receptor activation increases cytoplasmic calcium concentration in cultured spinal cord neurones. *Nature*, *321*(6069), p.519.

Madsen, T. M., Yeh, D. D., Valentine, G. W., & Duman, R. S. (2005). Electroconvulsive seizure treatment increases cell proliferation in rat frontal cortex. *Neuropsychopharmacology,* 30(1), 27–34.

McGuire, S.E., Le, P.T., Osborn, A.J., Matsumoto, K. and Davis, R.L., 2003. Spatiotemporal rescue of memory dysfunction in Drosophila*. Science,* 302(5651), pp.1765-1768.

Magavi, S.S., Leavitt, B.R. and Macklis, J.D., 2000. Induction of neurogenesis in the neocortex of adult mice. *Nature*, *405*(6789), p.951.

Magleby, K. L. (2003). Gating Mechanism of BK (Slo1) Channels: So Near, Yet So Far. *The Journal of General Physiology*, 121(2), 81–96.

Martynoga, B., Mateo, J.L., Zhou, B., Andersen, J., Achimastou, A., Urbán, N., van den Berg, D., Georgopoulou, D., Hadjur, S., Wittbrodt, J. and Ettwiller, L., 2013. Epigenomic enhancer annotation reveals a key role for NFIX in neural stem cell quiescence. *Genes & development*, *27*(16), pp.1769-1786.

Masuyama, K., Zhang, Y., Rao, Y. and Wang, J.W., 2012. Mapping neural circuits with activity-dependent nuclear import of a transcription factor. *Journal of neurogenetics*, *26*(1), pp.89-102.

Mata, J., Curado, S., Ephrussi, A. and Rørth, P., 2000. Tribbles coordinates mitosis and morphogenesis in *Drosophila* by regulating string/CDC25 proteolysis. *Cell*, *101*(5), pp.511-522.

Maugeri-Saccà, M., Di Martino, S. and De Maria, R., 2013. Biological and clinical implications of cancer stem cells in primary brain tumors. *Frontiers in oncology*, *3*, p.6.

Maurange, C., Cheng, L. and Gould, A.P., 2008. Temporal transcription factors and their targets schedule the end of neural proliferation in *Drosophila*. *Cell*, *133*(5), pp.891-902.

McKenzie IA, Ohayon D, Li H, de Faria JP, Emery B, *et al*. 2014. Motor skill learning requires active central myelination. *Science* 346:318–22

Melom, J.E. and Littleton, J.T., 2013. Mutation of a NCKX eliminates glial microdomain calcium oscillations and enhances seizure susceptibility. *Journal of Neuroscience*, *33*(3), pp.1169-1178.

Merkle, F.T., Tramontin, A.D., García-Verdugo, J.M. and Alvarez-Buylla, A., 2004. Radial glia give rise to adult neural stem cells in the subventricular zone. *Proceedings of the National Academy of Sciences*, *101*(50), pp.17528-17532.

Mikoshiba, K., 2007. IP3 receptor/Ca2+ channel: from discovery to new signaling concepts. *Journal of neurochemistry*, *102*(5), pp.1426-1446.

Mira, H., Andreu, Z., Suh, H., Lie, D.C., Jessberger, S., Consiglio, A., San Emeterio, J., Hortigüela, R., Marqués-Torrejón, M.Á., Nakashima, K. and Colak, D., 2010. Signalling through BMPR-IA regulates quiescence and long-term activity of neural stem cells in the adult hippocampus. *Cell stem cell*, 7(1), pp.78-89.

Miller, F.D. and Gauthier, A.S., 2007. Timing is everything: making neurons versus glia in the developing cortex. *Neuron*, 54(3), pp.357-369.

Ming, G.L. and Song, H., 2005. Adult neurogenesis in the mammalian central nervous system. *Annu. Rev. Neurosci.,* 28, pp.223-250.

Mirzadeh, Z., Merkle, F.T., Soriano-Navarro, M., Garcia-Verdugo, J.M. and Alvarez-Buylla, A., 2008. Neural stem cells confer unique pinwheel architecture to the ventricular surface in neurogenic regions of the adult brain. *Cell stem cell*, *3*(3), pp.265-278.

Miyamoto, K., Araki, K.Y., Naka, K., Arai, F., Takubo, K., Yamazaki, S., Matsuoka, S., Miyamoto, T., Ito, K., Ohmura, M. and Chen, C., 2007. Foxo3a is essential for maintenance of the hematopoietic stem cell pool. *Cell stem cell*, *1*(1), pp.101-112.

Mochly-Rosen, D., Das, K. and Grimes, K.V., 2012. Protein kinase C, an elusive therapeutic target?. *Nature reviews Drug discovery*, *11*(12), p.937.

Morin, X., Daneman, R., Zavortink, M. and Chia, W., 2001. A protein trap strategy to detect GFP-tagged proteins expressed from their endogenous loci in *Drosophila*. *Proceedings of the National Academy of Sciences*, *98*(26), pp.15050-15055.

Morshead, C.M., Reynolds, B.A., Craig, C.G., McBurney, M.W., Staines, W.A., Morassutti, D., Weiss, S. and van der Kooy, D., 1994. Neural stem cells in the adult mammalian forebrain: a relatively quiescent subpopulation of subependymal cells. *Neuron*, 13(5), pp.1071-1082.

Mukherjee, S., Tucker-Burden, C., Zhang, C., Moberg, K., Read, R., Hadjipanayis, C. and Brat, D.J., 2016. *Drosophila* Brat and human ortholog TRIM3 maintain stem cell equilibrium and suppress brain tumorigenesis by attenuating Notch nuclear transport. *Cancer research*, 76(8), pp.2443-2452.

Naito, Y., Yamada, T., Matsumiya, T., Ui-Tei, K., Saigo, K., & Morishita, S. (2005). dsCheck: highly sensitive off-target search software for double-stranded RNA-mediated RNA interference. *Nucleic acids research*, 33, W589-W591.

Naka, H., Nakamura, S., Shimazaki, T. and Okano, H., 2008. Requirement for COUP-TFI and II in the temporal specification of neural stem cells in CNS development. *Nature neuroscience*, 11(9), pp.1014-1023.

Nakai, J., Ohkura, M. and Imoto, K., 2001. A high signal-to-noise Ca 2+ probe composed of a single green fluorescent protein. *Nature biotechnology*, 19(2), p.137.

Narbonne-Reveau, K., Lanet, E., Dillard, C., Foppolo, S., Chen, C.H., Parrinello, H., Rialle, S., Sokol, N.S. and Maurange, C., 2016. Neural stem cell-encoded temporal patterning delineates an early window of malignant susceptibility in *Drosophila*. *Elife,* 5.

Neville, K.E., Bosse, T.L., Klekos, M., Mills, J.F., Weicksel, S.E., Waters, J.S. and Tipping, M., 2018. A novel ex vivo method for measuring whole brain metabolism in model systems. *Journal of neuroscience methods*, *296*, pp.32-43.

Nicolaï, L.J., Ramaekers, A., Raemaekers, T., Drozdzecki, A., Mauss, A.S., Yan, J., Landgraf, M., Annaert, W. and Hassan, B.A., 2010. Genetically encoded dendritic marker sheds light on neuronal connectivity in *Drosophila*. *Proceedings of the National Academy of Sciences*, 107(47), pp.20553-20558.

Nishimoto, I., Hata, Y., Ogata, E. and Kojima, I., 1987. Insulin-like growth factor II stimulates calcium influx in competent BALB/c 3T3 cells primed with epidermal growth factor. Characteristics of calcium influx and involvement of GTP-binding protein. *Journal of Biological Chemistry*, 262(25), pp.12120-12126.

Ningaraj, N.S., Rao, M., Hashizume, K., Asotra, K. and Black, K.L., 2002. Regulation of blood-brain tumor barrier permeability by calcium-activated potassium channels. *Journal of Pharmacology and Experimental Therapeutics,* 301(3), pp.838-851.

Noctor, S.C., Martínez-Cerdeño, V., Ivic, L. and Kriegstein, A.R., 2004. Cortical neurons arise in symmetric and asymmetric division zones and migrate through specific phases. *Nature neuroscience*, 7(2), p.136.

Nolasco, S., Bellido, J., Gonçalves, J., Zabala, J. C., & Soares, H. (2005). Tubulin cofactor A gene silencing in mammalian cells induces changes in microtubule cytoskeleton, cell cycle arrest and cell death. *FEBS Letters*, 579(17), 3515–3524.

Nuwal, T., Kropp, M., Wegener, S., Racic, S., Montalban, I., & Buchner, E. (2012). The *Drosophila* homologue of tubulin-specific chaperone E-like protein is required for synchronous sperm individualization and normal male fertility. *Journal of Neurogenetics*, 26(3-4), 374–81

Okano, H. and Temple, S., 2009. Cell types to order: temporal specification of CNS stem cells. *Current opinion in neurobiology*, *19*(2), pp.112-119.

Otsuki, L. and Brand, A.H., 2017. The vasculature as a neural stem cell niche. *Neurobiology of disease,* 107, pp.4-14.

Otsuki, L. and Brand, A.H., 2018. Cell cycle heterogeneity directs the timing of neural stem cell activation from quiescence. *Science*, *360*(6384), pp.99-102.

Ottone, C., Krusche, B., Whitby, A., Clements, M., Quadrato, G., Pitulescu, M.E., Adams, R.H. and Parrinello, S., 2014. Direct cell–cell contact with the vascular niche maintains quiescent neural stem cells. *Nature cell biology*, *16*(11), p.1045.

Ou, J.W., Kumar, Y., Alioua, A., Sailer, C., Stefani, E. and Toro, L., 2009. Ca^{2+}-and thromboxane-dependent distribution of MaxiK channels in cultured astrocytes: From microtubules to the plasma membrane. *Glia*, *57*(12), pp.1280-1295.

Palmer, T. D., Takahashi, J., & Gage, F. H. (1997). The adult rat hippocampus contains primordial neural stem cells. *Molecular and Cellular Neurosciences*, 8(6), 389–404.

Pallanck, L. and Ganetzky, B., 1994. Cloning and characterization of human and mouse homologs of the *Drosophila* calcium-activated potassium channel gene, *slowpoke. Human Molecular Genetics*, 3(8), pp.1239-1243.

Parent, J. M., Yu, T. W., Leibowitz, R. T., Geschwind, D. H., Sloviter, R. S., & Lowenstein, D. H. (1997). Dentate granule cell neurogenesis is increased by seizures and contributes to aberrant network reorganization in the adult rat hippocampus. *The Journal of Neuroscience*, 17(10), 3727–3738.

Parent JM. 2003. Injury-induced neurogenesis in the adult mammalian brain. *Neuroscientist* 9:261–72

Parpura, V, Trent A. Basarsky, Fang Liu, Ksenija Jeftinija, Srdija Jeftinija, & Philip G. Haydon. (1994). Glutamate-mediated astrocyte–neuron signalling. *Nature*, 369(6483), 744-7.

Paschen, W., Doutheil, J., Gissel, C. and Treiman, M., 1996. Depletion of neuronal endoplasmic reticulum calcium stores by thapsigargin: effect on protein synthesis. *Journal of neurochemistry*, *67*(4), pp.1735-1743.

Pauli, A., Althoff, F., Oliveira, R. A., Heidmann, S., Schuldiner, O., Lehner, C. F., Dickson, B. J. and Nasmyth, K. (2008). Cell-Type-Specific TEV Protease Cleavage Reveals Cohesin Functions in *Drosophila* Neurons. *Developmental Cell* 14, 239-251.

Pearce, B., Albrecht, J., Morrow, C. and Murphy, S., 1986. Astrocyte glutamate receptor activation promotes inositol phospholipid turnover and calcium flux. *Neuroscience letters*, *72*(3), pp.335-340.

Pekny, M., Wilhelmsson, U. and Pekna, M., 2014. The dual role of astrocyte activation and reactive gliosis. *Neuroscience letters*, *565*, pp.30-38.

Pereanu, W., Shy, D. and Hartenstein, V., 2005. Morphogenesis and proliferation of the larval brain glia in *Drosophila*. *Developmental biology,* 283(1), pp.191-203.

Peterson, C., Carney, G.E., Taylor, B.J. and White, K., 2002. reaper is required for neuroblast apoptosis during *Drosophila* development. *Development*, *129*(6), pp.1467-1476.

Petrik, D., Myoga, M.H., Grade, S., Gerkau, N.J., Pusch, M., Rose, C.R., Grothe, B. and Götz, M., 2018. Epithelial sodium channel regulates adult neural stem cell proliferation in a flow-dependent manner. *Cell stem cell*, 22(6), pp.865-878.

Pilz, G.A., Bottes, S., Betizeau, M., Jörg, D.J., Carta, S., Simons, B.D., Helmchen, F. and Jessberger, S., 2018. Live imaging of neurogenesis in the adult mouse hippocampus. *Science*, 359(6376), pp.658-662.

Pollak, M., 2008. Insulin and insulin-like growth factor signalling in neoplasia. *Nature Reviews Cancer,* 8(12), p.915.

Poon, C.L., Mitchell, K.A., Kondo, S., Cheng, L.Y. and Harvey, K.F., 2016. The Hippo pathway regulates neuroblasts and brain size in *Drosophila* melanogaster. *Current Biology*, 26(8), pp.1034-1042.

Prakriya, M., Feske, S., Gwack, Y., Srikanth, S., Rao, A. and Hogan, P.G., 2006. Orai1 is an essential pore subunit of the CRAC channel. *Nature*, 443(7108), p.230.

Postiglione, M.P., Jüschke, C., Xie, Y., Haas, G.A., Charalambous, C. and Knoblich, J.A., 2011. Mouse inscuteable induces apical-basal spindle orientation to facilitate intermediate progenitor generation in the developing neocortex. *Neuron*, *72*(2), pp.269-284.

Prokop AN, Technau GM, 1991. The origin of postembryonic neuroblasts in the ventral nerve cord of *Drosophila* melanogaster. *Development*. 1;111(1):79-88.

Petrik, D., Myoga, M. H., Grade, S., Rose, C. R., Grothe, B., Go, M., … Rose, C. R. (2018). Epithelial Sodium Channel Regulates Adult Neural Stem Cell Proliferation in a Flow-Dependent Manner. *Cell Stem Cell*, 1–14.

Piccin, D. and Morshead, C.M., 2011. Wnt signaling regulates symmetry of division of neural stem cells in the adult brain and in response to injury. *Stem Cells*, *29*(3), pp.528-538.

Pineda, J.R., Daynac, M., Chicheportiche, A., Cebrian-Silla, A., Felice, K.S., Garcia-Verdugo, J.M., Boussin, F.D. and Mouthon, M.A., 2013. Vascular-derived TGF-β increases in the stem cell niche and perturbs neurogenesis during aging and following irradiation in the adult mouse brain. E*MBO molecular medicine,* 5(4), pp.548-562.

Pulver, S.R., Pashkovski, S.L., Hornstein, N.J., Garrity, P.A. and Griffith, L.C., 2009. Temporal dynamics of neuronal activation by Channelrhodopsin-2 and TRPA1 determine behavioral output in *Drosophila* larvae. *Journal of neurophysiology*, *101*(6), pp.3075-3088.

Putney, J.W., 2012. Calcium signaling: deciphering the calcium–NFAT pathway. *Current Biology*, *22*(3), pp.R87-R89.

Qu, Q., Sun, G., Li, W., Yang, S., Ye, P., Zhao, C., Ruth, T.Y., Gage, F.H., Evans, R.M. and Shi, Y., 2010. Orphan nuclear receptor TLX activates Wnt/β-catenin signalling to stimulate neural stem cell proliferation and self-renewal. *Nature cell biology*, 12(1), p.31.

Quarmby, L. (2000). Cellular Samurai: katanin and the severing of microtubules. *J. Cell Sci*. 113, 2821-2827

Raisin, S., Pantalacci, S., Breittmayer, J. P., & Léopold, P. (2003). A new genetic locus controlling growth and proliferation in *Drosophila* melanogaster. *Genetics*, 164(3), 1015–1025.

Raffaelli, G., Saviane, C., Mohajerani, M.H., Pedarzani, P. and Cherubini, E., 2004. BK potassium channels control transmitter release at CA3–CA3 synapses in the rat hippocampus. *The Journal of physiology*, *557*(1), pp.147-157.

Ramalho-Santos, M. and Willenbring, H., 2007. On the origin of the term “stem cell”. *Cell stem cell*, 1(1), pp.35-38.

Ramírez-Castillejo, C., Sánchez-Sánchez, F., Andreu-Agulló, C., Ferrón, S.R., Aroca-Aguilar, J.D., Sánchez, P., Mira, H., Escribano, J. and Farinas, I., 2006. Pigment epithelium–derived factor is a niche signal for neural stem cell renewal. *Nature neuroscience*, 9(3), p.331.

Rath, U., Wang, D., Ding, Y., Xu, Y.Z., Qi, H., Blacketer, M.J., Girton, J., Johansen, J. and Johansen, K.M., 2004. Chromator, a novel and essential chromodomain protein interacts

directly with the putative spindle matrix protein skeletor. *Journal of cellular biochemistry*, 93(5), pp.1033-1047.

Reichert, H., 2009. Evolutionary conservation of mechanisms for neural regionalization, proliferation and interconnection in brain development. *Biology letters*, *5*(1), pp.112-116.

Renault, V.M., Rafalski, V.A., Morgan, A.A., Salih, D.A., Brett, J.O., Webb, A.E., Villeda, S.A., Thekkat, P.U., Guillerey, C., Denko, N.C. and Palmer, T.D., 2009. FoxO3 regulates neural stem cell homeostasis*. Cell stem cell*, 5(5), pp.527-539.

Riquelme, P. A., Drapeau, E., & Doetsch, F. (2008). Brain micro-ecologies: neural stem cell niches in the adult mammalian brain. *Philosophical Transactions of the Royal Society B: Biological Sciences*, *363*(1489), 123–137.

Robel, S., & Sontheimer, H. (2015). Glia as drivers of abnormal neuronal activity. *Nature Neuroscience*, 19(1), 28–33.

Robinow, Steven, *et al*. "Programmed cell death in the *Drosophila* CNS is ecdysone-regulated and coupled with a specific ecdysone receptor isoform." *Development* 119.4 (1993): 1251-1259.

Robitaille, R., Garcia, M.L., Kaczorowski, G.J. and Chariton, M.P., 1993. Functional colocalization of calcium and calcium-gated potassium channels in control of transmitter release. *Neuron*, *11*(4), pp.645-655.

Rochat, A., Kobayashi, K. and Barrandon, Y., 1994. Location of stem cells of human hair follicles by clonal analysis. *Cell*, *76*(6), pp.1063-1073.

Rochefort C, Gheusi G, Vincent JD, Lledo PM. 2002. Enriched odor exposure increases the number of newborn neurons in the adult olfactory bulb and improves odor memory. *J. Neurosci*. 22: 2679–89

Rogulja-Ortmann, A., Lüer, K., Seibert, J., Rickert, C. and Technau, G.M., 2007. Programmed cell death in the embryonic central nervous system of *Drosophila* melanogaster. *Development*, 134(1), pp.105-116.

Rozen S, Skaletsky H. (2000) Primer3 on the WWW for general users and for biologist programmers. *Methods Mol Biol* ;132:365-86

Rusan, Z. M., Kingsford, O. A., & Tanouye, M. A. (2014). Modeling glial contributions to seizures and epileptogenesis: Cation-chloride cotransporters in *Drosophila* melanogaster. *PLoS ONE*, 9(6), 1–10.

Saka, V.R., Hall, K., Von Holtz, H., Humbel, R., Sjören, B. and Wetterberg, L., 1982. Evidence for the presence of specific receptors for insulin-like growth factors 1 (IGF-1) and 2 (IGF-2) and insulin throughout the adult human brain. *Neuroscience letters,* 34(1), pp.39-44.

Santo-Domingo, J. and Demaurex, N., 2010. Calcium uptake mechanisms of mitochondria. *Biochimica et Biophysica Acta (BBA)-Bioenergetics,* 1797(6-7), pp.907-912.

Sampath, S.C., Sampath, S.C., Ho, A.T., Corbel, S.Y., Millstone, J.D., Lamb, J., Walker, J., Kinzel, B., Schmedt, C. and Blau, H.M., 2018. Induction of muscle stem cell quiescence by the secreted niche factor Oncostatin M. *Nature communications*, *9*(1), p.1531.

Sato, Y., Uchida, Y., Hu, J., Young-Pearse, T.L., Niikura, T. and Mukouyama, Y.S., 2017. Soluble APP functions as a vascular niche signal that controls adult neural stem cell number. *Development*, pp.dev-143370.

Sausbier, M., Arntz, C., Bucurenciu, I., Zhao, H., Zhou, X.-B., Sausbier, U., … Ruth, P. (2005). Elevated Blood Pressure Linked to Primary Hyperaldosteronism and Impaired Vasodilation in BK Channel–Deficient Mice. *Circulation*, *112*(1), 60 LP-68.

Scheckel (2011) Scheckel K. Potassium channel expression in the larval Drosophila melanogaster CNS; *Annual meeting of the American Association for the advancement of science*; Washington, D.C. 2011. Feb. 17–21

Schreiber, M., & Salkoff, L. (1997). A novel calcium-sensing domain in the BK channel. *Biophysical Journal*, *73*(3), 1355–1363.

Schuldt, A.J., Adams, J.H., Davidson, C.M., Micklem, D.R., Haseloff, J., St Johnston, D. and Brand, A.H., 1998. Miranda mediates asymmetric protein and RNA localization in the developing nervous system. *Genes & development*, 12(12), pp.1847-1857.

Schultz, E., Gibson, M.C. and Champion, T., 1978. Satellite cells are mitotically quiescent in mature mouse muscle: an EM and radioautographic study. *Journal of Experimental Zoology Part A: Ecological Genetics and Physiology*, *206*(3), pp.451-456.

Schultz, E., Jaryszak, D.L. and Valliere, C.R., 1985. Response of satellite cells to focal skeletal muscle injury. *Muscle & nerve*, *8*(3), pp.217-222.

Schweizer, N., Weiss, M. and Maiato, H., 2014. The dynamic spindle matrix. *Current opinion in cell biology,* 28, pp.1-7

Scott, B.W., Wojtowicz, J.M. and Burnham, W.M., 2000. Neurogenesis in the dentate gyrus of the rat following electroconvulsive shock seizures. *Experimental neurology*, *165*(2), pp.231-236.

Siegrist, S.E., Haque, N.S., Chen, C.H., Hay, B.A. and Hariharan, I.K., 2010. Inactivation of both Foxo and reaper promotes long-term adult neurogenesis in *Drosophila*. *Current Biology*, *20*(7), pp.643-648.

Sierra, A., Martín-Suárez, S., Valcárcel-Martín, R., Pascual-Brazo, J., Aelvoet, S.A., Abiega, O., Deudero, J.J., Brewster, A.L., Bernales, I., Anderson, A.E. and Baekelandt, V., 2015. Neuronal hyperactivity accelerates depletion of neural stem cells and impairs hippocampal neurogenesis. *Cell stem cell*, *16*(5), pp.488-503.

Segi-Nishida, E., Warner-Schmidt, J.L. and Duman, R.S., 2008. Electroconvulsive seizure and VEGF increase the proliferation of neural stem-like cells in rat hippocampus. *Proceedings of the National Academy of Sciences*.

Sepp, K. J., Schulte, J., & Auld, V. J. (2001). Peripheral glia direct axon guidance across the CNS/PNS transition zone. *Developmental Biology*, 238(1), 47-63.

Seri, B., Garcıa-Verdugo, J.M., McEwen, B.S. and Alvarez-Buylla, A., 2001. Astrocytes give rise to new neurons in the adult mammalian hippocampus. *Journal of Neuroscience*, *21*(18), pp.7153-7160.

Silva-Vargas, V., Maldonado-Soto, A.R., Mizrak, D., Codega, P. and Doetsch, F., 2016. Age-dependent niche signals from the choroid plexus regulate adult neural stem cells. *Cell Stem Cell*, 19(5), pp.643-652.

Silva-Vargas, V., Delgado, A.C. and Doetsch, F., 2018. Symmetric Stem Cell Division at the Heart of Adult Neurogenesis. *Neuron*, 98(2), pp.246-248.

Shen, Q., Wang, Y., Kokovay, E., Lin, G., Chuang, S.M., Goderie, S.K., Roysam, B. and Temple, S., 2008. Adult SVZ stem cells lie in a vascular niche: a quantitative analysis of niche cell-cell interactions. *Cell stem cell*, 3(3), pp.289-300.

Shigetomi, E., Tong, X., Kwan, K. Y., Corey, D. P., & Khakh, B. S. (2012). TRPA1 channels regulate astrocyte resting calcium and inhibitory synapse efficacy through GAT-3. *Nature Neuroscience*, 15(1), 70–80.

Shimozaki, K., Zhang, C.L., Suh, H., Denli, A.M., Evans, R.M. and Gage, F.H., 2011. Sex determining region Y-box 2 (SOX2) regulation of nuclear receptor tailless (TLX) transcription in adult neural stem cells. *Journal of Biological Chemistry,* pp.jbc-M111.

Slusarski, D.C. and Pelegri, F., 2007. Calcium signaling in vertebrate embryonic patterning and morphogenesis. *Developmental biology*, 307(1), pp.1-13.

Song, J., Zhong, C., Bonaguidi, M. A., Sun, G. J., Hsu, D., Gu, Y., … Song, H. (2012). Neuronal circuitry mechanism regulating adult quiescent neural stem-cell fate decision. *Nature*, *489*(7414), 150–154.

Sorrells, S.F., Paredes, M.F., Cebrian-Silla, A., Sandoval, K., Qi, D., Kelley, K.W., James, D., Mayer, S., Chang, J., Auguste, K.I. and Chang, E.F., 2018. Human hippocampal neurogenesis drops sharply in children to undetectable levels in adults. *Nature*, 555(7696), p.377.

Spalding, K.L., Bergmann, O., Alkass, K., Bernard, S., Salehpour, M., Huttner, H.B., Boström, E., Westerlund, I., Vial, C., Buchholz, B.A. and Possnert, G., 2013. Dynamics of hippocampal neurogenesis in adult humans. *Cell,* 153(6), pp.1219-1227.

Spéder, P. and Brand, A.H., 2014. Gap junction proteins in the blood-brain barrier control nutrient-dependent reactivation of *Drosophila* neural stem cells. *Developmental cell*, *30*(3), pp.309-321.

Spéder, P. and Brand, A.H., 2018. Systemic and local cues drive neural stem cell niche remodelling during neurogenesis in *Drosophila*. *eLife*, *7*.

Spana, E.P. and Doe, C.Q., 1995. The prospero transcription factor is asymmetrically localized to the cell cortex during neuroblast mitosis in *Drosophila*. *Development*, *121*(10), pp.3187-3195.

Rodgers, J.T., King, K.Y., Brett, J.O., Cromie, M.J., Charville, G.W., Maguire, K.K., Brunson, C., Mastey, N., Liu, L., Tsai, C.R. and Goodell, M.A., 2014. mTORC1 controls the adaptive transition of quiescent stem cells from G 0 to G Alert. *Nature*, *510*(7505), p.393.

Stevens, C. F. (2002). Astroglia induce neurogenesis from adult neural stem cells. *Nature*, *417*(6884), 39–44.

Steinborn, K., Maulbetsch, C., Priester, B., Trautmann, S., Pacher, T., Geiges, B., … Mayer, U. (2002). The Arabidopsis PILZ group genes encode tubulin-folding cofactor\orthologs required for cell division but not cell growth. *Genes & Development*, *16*(8), 959–971.

Strojnik, T., Røsland, G.V., Sakariassen, P.O., Kavalar, R. and Lah, T., 2007. Neural stem cell markers, nestin and musashi proteins, in the progression of human glioma: correlation of nestin with prognosis of patient survival. *Surgical neurology*, *68*(2), pp.133-143.

Stork, T., Sheehan, A., Tasdemir-Yilmaz, O. E., & Freeman, M. R. (2014). Neuron-Glia interactions through the heartless fgf receptor signalling pathway mediate morphogenesis of *Drosophila* astrocytes. *Neuron*, 83(2), 388–403.

Sofroniew, M.V., 2014. Astrogliosis. *Cold Spring Harbor perspectives in biology,* p.a020420.

Søndergaard, L., 1993. Homology between the mammalian liver and the *Drosophila* fat body. *Trends in Genetics*, 9(6), p.193.

Sousa-Nunes, R., Yee, L.L. and Gould, A.P., 2011. Fat cells reactivate quiescent neuroblasts via TOR and glial insulin relays in *Drosophila*. *Nature*, *471*(7339), p.508.

Strausfeld, N.J. and Hirth, F., 2013. Deep homology of arthropod central complex and vertebrate basal ganglia. *Science*, *340*(6129), pp.157-161.

Suda, T., Takubo, K. & Semenza, G. L. Metabolic regulation of hematopoietic stem cells in the hypoxic niche. *Cell Stem Cell* **9**, 298–310 (2011)

Suh, H., Consiglio, A., Ray, J., Sawai, T., D'Amour, K. A., & Gage, F. H. (2007). In Vivo Fate Analysis Reveals the Multipotent and Self-Renewal Capacities of Sox2+ Neural Stem Cells in the Adult Hippocampus. *Cell Stem Cell*, 1(5), 515–528.

Sullivan, J.M., Benton, J.L., Sandeman, D.C. and Beltz, B.S., 2007. Adult neurogenesis: a common strategy across diverse species. *Journal of Comparative Neurology*, *500*(3), pp.574-584.

Syed, M. H., Mark, B., & Doe, C. Q. (2017). Steroid hormone induction of temporal gene expression in *Drosophila* brain neuroblasts generates neuronal and glial diversity. *ELife*, *6*.

Sullivan, J.M., Benton, J.L., Sandeman, D.C. and Beltz, B.S., 2007. Adult neurogenesis: a common strategy across diverse species. *Journal of Comparative Neurology*, *500*(3), pp.574-584.

Takemoto-Kimura, S., Suzuki, K., Horigane, S.I., Kamijo, S., Inoue, M., Sakamoto, M., Fujii, H. and Bito, H., 2017. Calmodulin kinases: essential regulators in health and disease. *Journal of neurochemistry*, *141*(6), pp.808-818.

Takubo, K., Nagamatsu, G., Kobayashi, C.I., Nakamura-Ishizu, A., Kobayashi, H., Ikeda, E., Goda, N., Rahimi, Y., Johnson, R.S., Soga, T. and Hirao, A., 2013. Regulation of glycolysis by Pdk functions as a metabolic checkpoint for cell cycle quiescence in hematopoietic stem cells. *Cell stem cell*, *12*(1), pp.49-61.

Tatsumi, R., Wuollet, A.L., Tabata, K., Nishimura, S., Tabata, S., Mizunoya, W., Ikeuchi, Y. and Allen, R.E., 2009. A role for calcium-calmodulin in regulating nitric oxide production during skeletal muscle satellite cell activation. *American Journal of Physiology-Cell Physiology*, 296(4), pp.C922-C929.

Tavares, R.G., Tasca, C.I., Santos, C.E., Alves, L.B., Porciúncula, L.O., Emanuelli, T. and Souza, D.O., 2002. Quinolinic acid stimulates synaptosomal glutamate release and inhibits glutamate uptake into astrocytes. *Neurochemistry international*, 40(7), pp.621-627.

Tavazoie, M., Van der Veken, L., Silva-Vargas, V., Louissaint, M., Colonna, L., Zaidi, B., … Doetsch, F. (2008). A Specialized Vascular Niche for Adult Neural Stem Cells. *Cell Stem Cell*, *3*(3), 279–288.

Temple, S., 2001. The development of neural stem cells. *Nature*, *414*(6859), p.112.

Theodore, W.H., Porter, R.J., Albert, P., Kelley, K., Bromfield, E., Devinsky, O. and Sato, S., 1994. The secondarily generalized tonic-clonic seizure: a videotape analysis. *Neurology*, *44*(8), pp.1403-1403.

Tian, G.F., Azmi, H., Takano, T., Xu, Q., Peng, W., Lin, J., Oberheim, N., Lou, N., Wang, X., Zielke, H.R. and Kang, J., 2005. An astrocytic basis of epilepsy. *Nature medicine*, *11*(9), p.973. Thomas, T., Wang, B., Brenner, R., & Atkinson, N. S. (1997). Novel embryonic regulation of Ca2+-activated K+ channel expression in *Drosophila*. *Invertebrate Neuroscience*, *2*(4), 283–291.

Tong, C.K., Chen, J., Cebrián-Silla, A., Mirzadeh, Z., Obernier, K., Guinto, C.D., Tecott, L.H., García-Verdugo, J.M., Kriegstein, A. and Alvarez-Buylla, A., 2014. Axonal control of the adult neural stem cell niche. *Cell stem cell*, 14(4), pp.500-511.

Torii, M., Matsuzaki, F., Osumi, N., Kaibuchi, K., Nakamura, S., Casarosa, S., Guillemot, F. and Nakafuku, M., 1999. Transcription factors Mash-1 and Prox-1 delineate early steps in differentiation of neural stem cells in the developing central nervous system. *Development*, *126*(3), pp.443-456.

Tozuka, Y., Fukuda, S., Namba, T., Seki, T., & Hisatsune, T. (2005). GABAergic excitation promotes neuronal differentiation in adult hippocampal progenitor cells. *Neuron*, *47*(6), 803–815.

Truman, J.W. and Bate, M., (1988). Spatial and temporal patterns of neurogenesis in the central nervous system of *Drosophila* melanogaster. *Developmental biology*, *125*(1), pp.145-157.

Tsao, C.K., Ku, H.Y., Lee, Y.M., Huang, Y.F. and Sun, Y.H., 2016. Long term ex vivo culture and live imaging of Drosophila larval imaginal discs. *PloS one*, *11*(9), p.e0163744.

Tsuji, T., Hasegawa, E. and Isshiki, T., 2008. Neuroblast entry into quiescence is regulated intrinsically by the combined action of spatial Hox proteins and temporal identity factors. *Development*, *135*(23), pp.3859-3869.

Umemoto, T., Hashimoto, M., Matsumura, T., Nakamura-Ishizu, A. and Suda, T., 2018. Ca2+–mitochondria axis drives cell division in hematopoietic stem cells*. Journal of Experimental Medicine*, 215(8), pp.2097-2113.

Unhavaithaya, Y., & Orr-weaver, T. L. (2012). Polyploidization of glia in neural development links tissue growth to blood – brain barrier integrity. *Genes & Development*, 31–36.

Urbán, N., van den Berg, D.L., Forget, A., Andersen, J., Demmers, J.A., Hunt, C., Ayrault, O. and Guillemot, F., 2016. Return to quiescence of mouse neural stem cells by degradation of a proactivation protein. *Science*, 353(6296), pp.292-295.

Vaidya, V. A., Siuciak, J. A., Du, F., & Duman, R. S. (1999). Hippocampal mossy fiber sprouting induced by chronic electroconvulsive seizures. *Neuroscience*, 89(1), 157–166.

Van Petegem, F., 2012. Ryanodine receptors: structure and function. *Journal of Biological Chemistry*, 287(38), pp.31624-31632.

van Praag H, Kempermann G, Gage FH. 1999b. Running increases cell proliferation and neurogenesis in the adult mouse dentate gyrus. *Nat. Neurosci*. 2: 266–70

Velíšková, J. and DeSantis, K.A., 2013. Sex and hormonal influences on seizures and epilepsy. *Hormones and behavior*, 63(2), pp.267-277.

Venere, M., Han, Y.G., Song, J.S., Bell, R., Alvarez-Buylla, A. and Blelloch, R., 2012. Sox1 marks an activated neural stem/progenitor cell in the hippocampus. *Development*, pp.dev-081133.

Venken, K.J., Simpson, J.H. and Bellen, H.J., 2011. Genetic manipulation of genes and cells in the nervous system of the fruit fly. Neuron, 72(2), pp.202-230.

Venkatachalam, K., van Rossum, D.B., Patterson, R.L., Ma, H.T. and Gill, D.L., 2002. The cellular and molecular basis of store-operated calcium entry. *Nature cell biology*, 4(11), p.E263.

Venkiteswaran, G. and Hasan, G., 2009. Intracellular Ca2+ signaling and store-operated Ca2+ entry are required in Drosophila neurons for flight. *Proceedings of the National Academy of Sciences*, 106(25), pp.10326-10331.

Vergara C, Latorre R, Marrion NV & Adelman JP (1998). Calcium-activated potassium channels. *Curr Opin Neurobiol* **8**, 321–329.

Villeda, S.A., Luo, J., Mosher, K.I., Zou, B., Britschgi, M., Bieri, G., Stan, T.M., Fainberg, N., Ding, Z., Eggel, A. and Lucin, K.M., 2011. The ageing systemic milieu negatively regulates neurogenesis and cognitive function. *Nature*, 477(7362), p.90.

Vissers, J.H., Manning, S.A., Kulkarni, A. and Harvey, K.F., 2016. A *Drosophila* RNAi library modulates Hippo pathway-dependent tissue growth. *Nature communications*, *7*, p.10368.

Vitali, I., Fièvre, S., Telley, L., Oberst, P., Bariselli, S., Frangeul, L., Baumann, N., McMahon, J.J., Klingler, E., Bocchi, R. and Kiss, J.Z., 2018. Progenitor Hyperpolarization Regulates the Sequential Generation of Neuronal Subtypes in the Developing Neocortex. *Cell*.

von Trotha, J. W., Egger, B., & Brand, A. H. (2009). Cell proliferation in the *Drosophila* adult brain revealed by clonal analysis and bromodeoxyuridine labelling. *Neural Development*, 4, 9.

Wakeham, A., Correia, K.M., Samper, E., Brown, S., Aguilera, R.J., Nakano, T., Honjo, T., Mak, T.W., Rossant, J. and Conlon, R.A., 1997. Conservation of the Notch signalling pathway in mammalian neurogenesis. *Development*, *124*(6), pp.1139-1148.

Wang, G., Zhu, H., Situ, C., Han, L., Yu, Y., Cheung, T.H., Liu, K. and Wu, Z., 2018. p110α of PI3K is necessary and sufficient for quiescence exit in adult muscle satellite cells. *The EMBO journal*, 37(8), p.e98239.

Wang, J., Zhou, Y., Wen, H. and Levitan, I.B., 1999. Simultaneous binding of two protein kinases to a calcium-dependent potassium channel. *Journal of Neuroscience*, *19*(10), pp.RC4-RC4.

Wang, L., & Sigworth, F. J. (2009). Cryo-EM structure of the BK potassium channel in a lipid membrane. *Nature*, *461*(7261), 292–295.

Wang, Z. *et al* (2001). SLO-1 potassium channels control quantal content of neurotransmitter r elease at the C. elegans neuromuscular junction. *Neuron*, 32(5), 867–881.

Weaver, A.K., Liu, X. and Sontheimer, H., 2004. Role for calcium-activated potassium channels (BK) in growth control of human malignant glioma cells. *Journal of neuroscience research*, *78*(2), pp.224-234.

Weaver, A.K., Olsen, M.L., McFerrin, M.B. and Sontheimer, H., 2007. BK Channels Are Linked to Inositol 1, 4, 5-Triphosphate Receptors via Lipid Rafts: A Novel Mechanism for coupling $[Ca^{2+}]_i$ to ion channel activation. *Journal of Biological Chemistry*, *282*(43), pp.31558-31568.

Weisenberg RC, Deery WJ, Dickinson PJ. 1976. Tubulin-nucleotide interactions during the polymerization and depolymerization of microtubules. *Biochemistry* 15:4248–54

White, K. and Kankel, D.R., 1978. Patterns of cell division and cell movement in the formation of the imaginal nervous system in *Drosophila* melanogaster. *Developmental biology*, *65*(2), pp.296-321.

White, K., Grether, M.E., Abrams, J.M., Young, L., Farrell, K. and Steller, H., 1994. Genetic control of programmed cell death in *Drosophila*. *Science*, *264*(5159), pp.677-683.

Wong, L.L. and Adler, P.N., 1993. Tissue polarity genes of *Drosophila* regulate the subcellular location for prehair initiation in pupal wing cells. *The Journal of cell biology*, 123(1), pp.209-221.

Wu and Luo. (2006) A protocol for mosaic analysis with a repressible cell marker (MARCM) in *Drosophila*. *Nature Protocols* 1, 2583-2589.

Xu, C., Luo, J., He, L., Montell, C. and Perrimon, N., 2017. Oxidative stress induces stem cell proliferation via TRPA1/RyR-mediated Ca2+ signalling in the *Drosophila* midgut. *Elife*, *6*.

Xu and Rubin. (1993) Analysis of genetic mosaics in developing and adult *Drosophila* tissues. *Development* 117, 1223-1237.

Yap, K.L., Ames, J.B., Swindells, M.B. and Ikura, M., 1999. Diversity of conformational states and changes within the EF-hand protein superfamily. *Proteins: Structure, Function, and Bioinformatics*, *37*(3), pp.499-507.

Ye, L., Haroon, M.A., Salinas, A. and Paukert, M., 2017. Comparison of GCaMP3 and GCaMP6f for studying astrocyte Ca2+ dynamics in the awake mouse brain. *PloS one*, *12*(7), p.e0181113.

Yu, F., Morin, X., Kaushik, R., Bahri, S., Yang, X. and Chia, W., 2003. A mouse homologue of *Drosophila* pins can asymmetrically localize and substitute for pins function in *Drosophila* neuroblasts. *Journal of Cell Science*, *116*(5), pp.887-896.

Yuan, P., Leonetti, M.D., Pico, A.R., Hsiung, Y. and MacKinnon, R., 2010. Structure of the human BK channel Ca2+-activation apparatus at 3.0 Å resolution. *Science*, *329*(5988), pp.182-186.

Zahradnikova, A. and Zahradnik, I., 1992. Single potassium channels of human glioma cells. *Physiological research*, *41*(4), pp.299-305.

Zhang, S.L., Yu, Y., Roos, J., Kozak, J.A., Deerinck, T.J., Ellisman, M.H., Stauderman, K.A. and Cahalan, M.D., 2005. STIM1 is a Ca 2+ sensor that activates CRAC channels and migrates from the Ca 2+ store to the plasma membrane. *Nature*, 437(7060), p.902.

Zhang, S.L., Yeromin, A.V., Zhang, X.H.F., Yu, Y., Safrina, O., Penna, A., Roos, J., Stauderman, K.A. and Cahalan, M.D., 2006. Genome-wide RNAi screen of Ca2+ influx identifies genes that regulate Ca2+ release-activated Ca2+ channel activity. *Proceedings of the National Academy of Sciences*, 103(24), pp.9357-9362.

Zhang, Y. Q., Rodesch, C. K. and Broadie, K. (2002). Living synaptic vesicle marker: synaptotagmin-GFP. *Genesis* 34, 142–145.

Zhao, B., Tumaneng, K. and Guan, K.L., 2011. The Hippo pathway in organ size control, tissue regeneration and stem cell self-renewal. *Nature cell biology*, *13*(8), p.877.

Zheng, Y., 2010. A membranous spindle matrix orchestrates cell division. *Nature reviews Molecular cell biology*, 11(7), p.529.

Zhong, W. and Chia, W., 2008. Neurogenesis and asymmetric cell division. *Current opinion in neurobiology*, *18*(1), pp.4-11.

Zhou, C., Wen, Z.X., Shi, D.M. and Xie, Z.P., 2004. Muscarinic acetylcholine receptors involved in the regulation of neural stem cell proliferation and differentiation in vitro. *Cell biology international*, 28(1), pp.63-67.